

⁴⁰Ar/³⁹Ar Investigations of the Ocate Volcanic Field,

North-Central New Mexico

by

Brian W. Olmsted

NMIMT
LIBRARY
SOCORRO, NM

Submitted in partial fulfillment of the requirements for the degree of

Masters of Science in Geochemistry

August 2000

Department of Earth and Environmental Science

New Mexico Institute of Mining and Technology

Socorro, New Mexico

Acknowledgements

This thesis would not have been possible without the help of the Bureau of Mines and Mineral Resources, the New Mexico Geochronology Research Laboratory and the members of my Committee: Bill McIntosh, Phil Kyle, Chuck Chapin and Matt Heizler.

A special thanks goes out to my advisor, Bill McIntosh, for his continued help and guidance throughout the research. In addition, I would like to thank Nelia Dunbar for her time and patience with the electron microprobe analyses, Lisa Peters and Rich Esser for their expertise and help in the argon lab, O.B. and Bailey Rose for their field assistance and my girlfriend, Carisa Tremayne, for her support throughout my stay at Tech.

Finally, I would like to thank all of the landowners throughout the Ocate area for their permission to collect samples from their respective properties, especially the Mora, UU Bar, Fort Union and Philmont Ranches. Without their permission none of this would have ever been possible.

Table of Contents

Acknowledgements	i
Table of Contents	ii
List of Figures	iv
List of Tables	v
List of Appendices	v
Abstract	vi
1. Introduction	1
2. Methods	5
2.1. Field Methods	5
2.2. Analytical Methods	5
3. Interpretation of Basaltic $^{40}\text{Ar}/^{39}\text{Ar}$ Age Spectra and Implications for Sample Collection	9
3.1. Results	12
3.1.1. Sample Characteristics	12
3.1.2. $^{40}\text{Ar}/^{39}\text{Ar}$ Results	12
3.2. Discussion	19
3.2.1. Recoil	19
3.2.2. Modeling the Degassing Behavior	22
3.2.3. Relating the Degassing Behavior to the Sample Characteristics	28
3.2.4. Relating the Degassing Behavior to the Age Spectrum	30
3.2.5. Sampling Strategy for Obtaining Precise Eruption Ages	32

3.2.6. General Criteria for Age Assignment in Basaltic Samples	33
4. $^{40}\text{Ar}/^{39}\text{Ar}$ Experiment: Phenocryst Concentrate Analyses	38
4.1. Results	39
4.2. Discussion	39
5. $^{40}\text{Ar}/^{39}\text{Ar}$ Experiment: Laser vs. Furnace Step-Heating Analyses	50
5.1. Results	50
5.2. Discussion	59
6. Geologic Interpretations	63
6.1. Results	63
6.2. Discussion	71
6.2.1. Maxson Crater	74
6.2.2. Spatial Distribution of Ages	74
6.2.3. Minimum Erosion Rates	76
6.2.4. Vent Locations and Alignments	78
6.2.5. Flow Directions	80
6.2.6. Timing of Tectonic and Geomorphic Events	80
6.2.7. Evolution of the Ocate Volcanic Field	83
6.2.8. Regional Relationships	85
7. Conclusions	87
8. References	89

List of Figures

Figure 1. Shaded relief map of the Ocate Volcanic field area.	2
Figure 2. Late Cenozoic volcanic fields of northern New Mexico.	3
Figure 3. Sample location map.	6
Figure 4. BSE and K-maps of representative samples.	14
Figure 5. Age and degassing spectra of representative samples.	16
Figure 6. Graph of volume depleted by recoil versus a-b length for a rhombic prism.	21
Figure 7. Modeling results: graphs of the effect of recoil on K/Ca and degassing spectra for the representative samples.	23
Figure 8. Geologic comparison between “plateau” and new approach eruption ages for samples collected from the same flow unit.	36
Figure 9. Comparison between phenocryst and groundmass concentrate age spectra.	40
Figure 10. Comparison between laser and furnace age spectra.	51
Figure 11. Comparison of replicate analyses.	66
Figure 12. Comparison of analyses of multiple samples from the same flow unit.	67
Figure 13. Graph of samples collected in stratigraphic order from Maxson Crater.	68
Figure 14. Histogram of absolute and percent error for all analyses.	69
Figure 15. Graph comparing previously published K-Ar ages and the new $^{40}\text{Ar}/^{39}\text{Ar}$ ages for samples from the same flow unit.	70
Figure 16. Histogram comparing the precision of the $^{40}\text{Ar}/^{39}\text{Ar}$ results from	73

studies of the Taos, Raton-Clayton and Ocate volcanic fields.	
Figure 17. Geochronologic map of the Ocate Volcanic field.	75
Figure 18. Map illustrating the calculated minimum erosion rates throughout the field.	77
Figure 19. Vent alignment map.	79
Figure 20. Flow direction map.	81
Figure 21. Timeline of events.	84
Figure 22. Ideogram of the Ocate, Raton-Clayton and Taos volcanic fields.	86

List of Tables

Table 1. Sample characterization of representative samples.	13
Table 2. Data tables for representative samples.	17
Table 3. Data tables for phenocryst and corresponding groundmass concentrates.	43
Table 4. Sample characterization of phenocryst concentrates.	45
Table 5. Data tables for laser and corresponding furnace analyses.	56
Table 6. Locations and eruption ages for all analyses.	64

List of Appendices

Appendix A: Data Tables	A-1
Appendix B: Age Spectra	B-1
Appendix C: Values used in the calculation of volumes erupted	C-1
Appendix D: Values used in the erosion rate calculations	D-1

Abstract.

Eighty-two $^{40}\text{Ar}/^{39}\text{Ar}$ analyses from seventy basaltic samples from the Ocate Volcanic field reveal that the field was episodically erupted in approximately sixteen pulses between 8.2 and 0.8 Ma. In general, a north-to-south time progression of volcanism occurred during the evolution of the field. Two major eruptive episodes, 5.13-4.35 and 3.36-2.85 Ma, produced approximately 32 and 40 vol. % (28 and 36 km³) of the field (90 km³ total), respectively. Between 8.2 and 4.4 Ma a period of erosion without tectonic activity occurred which supplied sediment for the Ogallala Formation. After the 5.13-4.35 Ma eruptions, a period of tectonic activity with extensive down-to-the-west faulting took place within the western portion of the field. Following the 3.36-2.85 Ma eruptions, a period of decreased eruptive activity with small localized eruptive centers ensued within the central and southern portions of the field. Regionally, the Ocate, Taos and Raton-Clayton volcanic fields all experienced eruptive activity near 5.7, 5.1, 4.7, 3.5, 3.0 and 2.3 Ma with each field displaying an overall peak in eruptive activity between 5.1 and 2.3 Ma.

Modeling and comparing the mineral chemistry and petrographic characteristics of five basaltic groundmass samples from the Ocate Volcanic field with the corresponding age, K/Ca and $^{37}\text{Ar}_{\text{Ca}}$, $^{38}\text{Ar}_{\text{Cl}}$ and $^{39}\text{Ar}_{\text{K}}$ release spectra show that the styles of argon release in a basalt sample are dependent on the crystallinity, chemistry and modal abundance of the phases present. From first to last, the phases degas in the following order: interstitial phases, feldspar rim, feldspar core, olivine/oxide, and pyroxene. Flow interior samples in which the majority of potassium is contained within the feldspar rim display convex upward $^{39}\text{Ar}_{\text{K}}$ release patterns. In contrast, flow surface

samples in which the majority of the potassium is contained within the interstitial phases display descending $^{39}\text{Ar}_\text{K}$ release patterns. Convex upward shaped K/Ca spectra reflect high degrees of recoil redistribution and are dominantly seen in flow interior samples whereas descending K/Ca spectra seen dominantly in flow surface samples reflect low degrees of recoil redistribution. Flow interior samples are concluded to yield more precise ages with heating steps comprising a greater percentage of the total $^{39}\text{Ar}_\text{K}$ released than flow surface samples.

Analysis of plagioclase, pyroxene and olivine phenocryst concentrates, along with the corresponding groundmass analyses, confirms previous findings that phenocryst phases degas at temperatures higher than $\sim 1025^\circ\text{C}$. In addition, for the samples studied here, apparent ages associated with the degassing of the olivine and pyroxene phenocryst phases are found to yield geologically inaccurate ages whereas the plagioclase separate yielded apparent ages in agreement with the corresponding groundmass analysis. Excess ^{40}Ar found within the olivine and plagioclase phenocryst concentrates are calculated to be at most 9.58×10^{-14} and 1.64×10^{-13} moles/g, respectively, suggesting that excess ^{40}Ar is minor effect within these samples.

Comparison of basalt samples step-heated with both the furnace and CO₂ laser show that the laser technique reproduces the radiogenic yields, K/Ca, Cl/K and age gradients seen in the furnace analyses. Based on this, the CO₂ laser step-heating technique is concluded to be an effective alternative approach to dating basalt samples using the $^{40}\text{Ar}/^{39}\text{Ar}$ dating method.

1. Introduction

The Ocate Volcanic field is located in north-central New Mexico within the transition zone between the Great Plains and Rocky Mountain physiographic provinces, just east of the Rio Grande rift (Figure 1). The field is one of several dominantly basaltic late Miocene-Pleistocene eruptive complexes that define the Jemez lineament in northern New Mexico (Figure 2). Northeast of the Ocate field lies the Raton-Clayton volcanic field and to the northwest lies the Taos Plateau volcanic field. The Ocate field is bounded to the west by the southern Sangre de Cristo Mountains, to the east by the Canadian River, to the north by the Cimarron Range and to the south by the Mora River. The eruptive products range in composition from alkali olivine basalt to dacite and were erupted out of shield volcanoes, composite cones, fissures and cinder cones (Nielsen and Dungan, 1985; O'Neill and Mehnert, 1988).

Based on eighteen K-Ar analyses, previous workers found that at least 16 lavas ranging from 8.3-0.8 Ma are present within the field (O'Neill and Mehnert, 1988). The field exhibits inverted topography where the oldest flows cap the highest mesas and younger flows cap lower mesas. Based on the physiographic evolution of the field it was suggested by O'Neill and Mehnert (1988) that volcanism in the Ocate area was coeval with the epeirogenic rise of the Sangre de Cristo Mountains and the adjacent Great Plains.

The petrogenesis of the Ocate field was investigated by Nielsen and Dungan (1985) and was integrated with previous geochemical studies of the Raton-Clayton and Taos fields. They concluded that for all three fields the most voluminous period of volcanism was between 4.5 and 2.0 Ma and that the pattern of volcanism present within

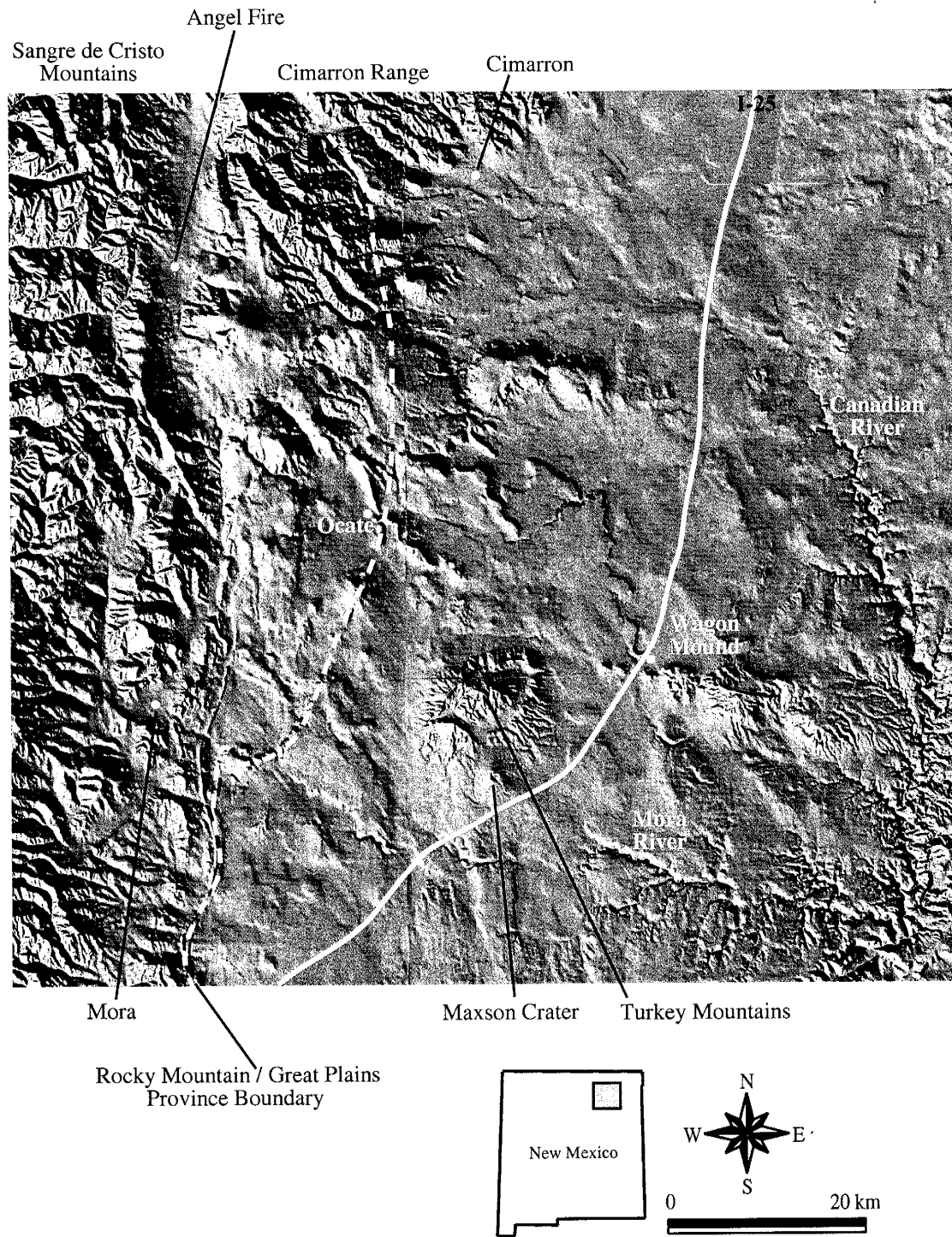


Figure 1. Shaded relief map of the Ocate Volcanic field.

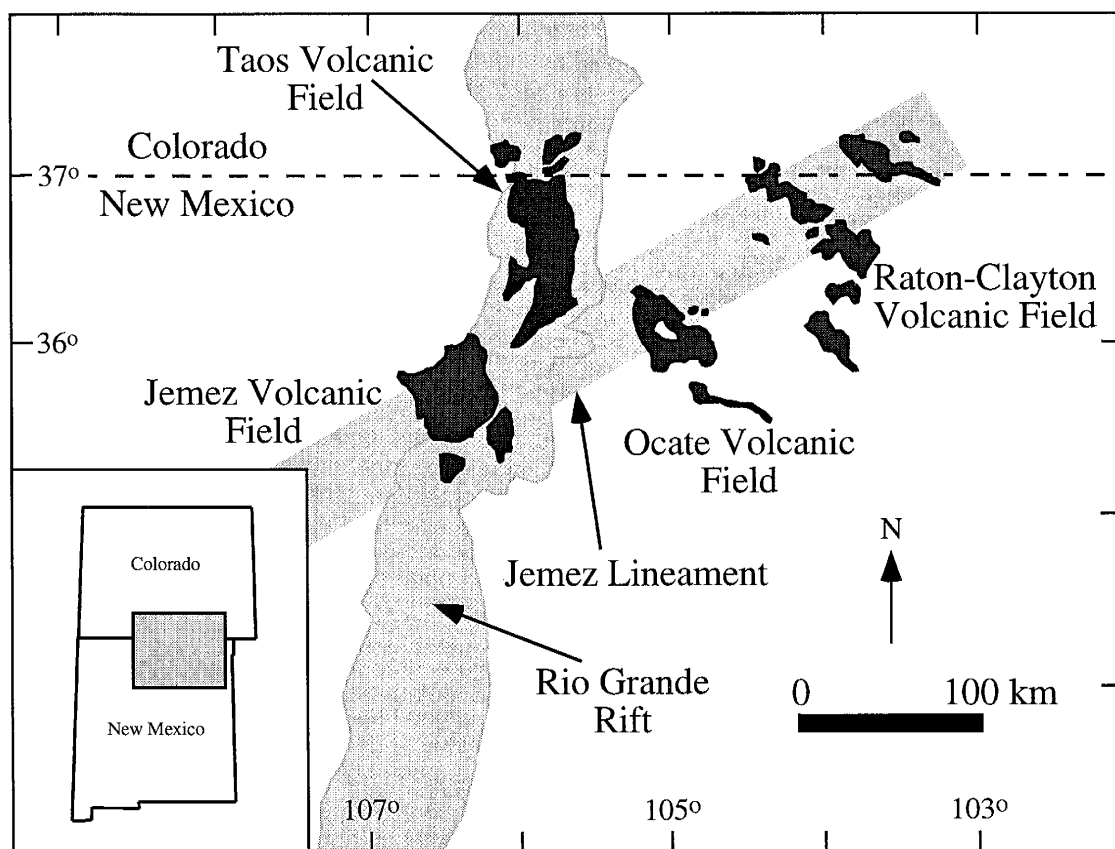


Figure 2. Late Cenozoic Volcanic fields of northern New Mexico and southern Colorado.

the Ocate field is consistent with a systematic increase in upper mantle heat flux from 8.1-3.2 Ma followed by a cooling trend that continues today.

The primary purpose of this study was to obtain a precise record of the eruptive episodes that have occurred within the Ocate Volcanic field. The $^{40}\text{Ar}/^{39}\text{Ar}$ technique was used because of its high precision and potential ability to detect and correct for extraneous ^{40}Ar , $^{40}\text{Ar}^*$ loss and xenocrystic contamination (McDougall and Harrison, 1999).

In an effort to understand and properly interpret the results, several experiments were performed. These included replicate analyses of seven samples, analyses of multiple samples from eight flow units, chemical and petrographic analyses of five representative samples, both CO₂ laser and furnace analyses for five samples and the individual analysis of olivine, plagioclase and pyroxene phenocryst concentrates from three separate samples. The conclusions generated from the chemical and petrographic analyses were then applied to all of the samples to interpret each sample's eruption age.

The eruption ages determined in this study are used to reconstruct the eruptive history, both spatially and temporally, and to constrain the landscape evolution of the Ocate field. In addition, the ages are compared with those of the neighboring Raton-Clayton and Taos volcanic fields to evaluate the temporal relationships present within all three fields.

2. Methods

2.1. Field Methods

Samples were collected from eighty-three locations throughout the field. Of these, seventy were analyzed. Figure 3 displays the locations of the samples analyzed. Approximately ten percent of the field could not be sampled because permission was denied to access the privately owned Ojo Feliz Ranch located within the central portion of the field. Because of this, one K-Ar age from O'Neill and Mehnert's (1988) study is used along with the new $^{40}\text{Ar}/^{39}\text{Ar}$ data (Figure 3).

Wherever possible, non-vesicular, well-crystallized and non-weathered samples were collected. Sample locations were measured with a hand-held GPS unit.

2.2. Analytical Methods

Samples were crushed and sieved to 20-48 mesh ($300\text{-}850\mu\text{m}$), ultrasonically cleaned with dilute HCl and ultrasonically washed with deionized water. Using a binocular microscope, care was taken to remove all visible phenocryst/xenocryst phases from the groundmass concentrates. In addition, phenocryst concentrates of olivine, plagioclase and pyroxene were hand-picked from three different samples. The groundmass phases adhered to the rims of the phenocrysts were not removed, resulting in the olivine and pyroxene phenocryst concentrates each containing 1% groundmass phases and the plagioclase phenocryst concentrate containing 42% groundmass phases (Percentages based on mass balance calculations, see Section 4 for further details).

The groundmass and phenocryst concentrates were packaged in machined Al discs and irradiated with Fish Canyon sanidine flux monitors (assigned age of 27.84 Ma

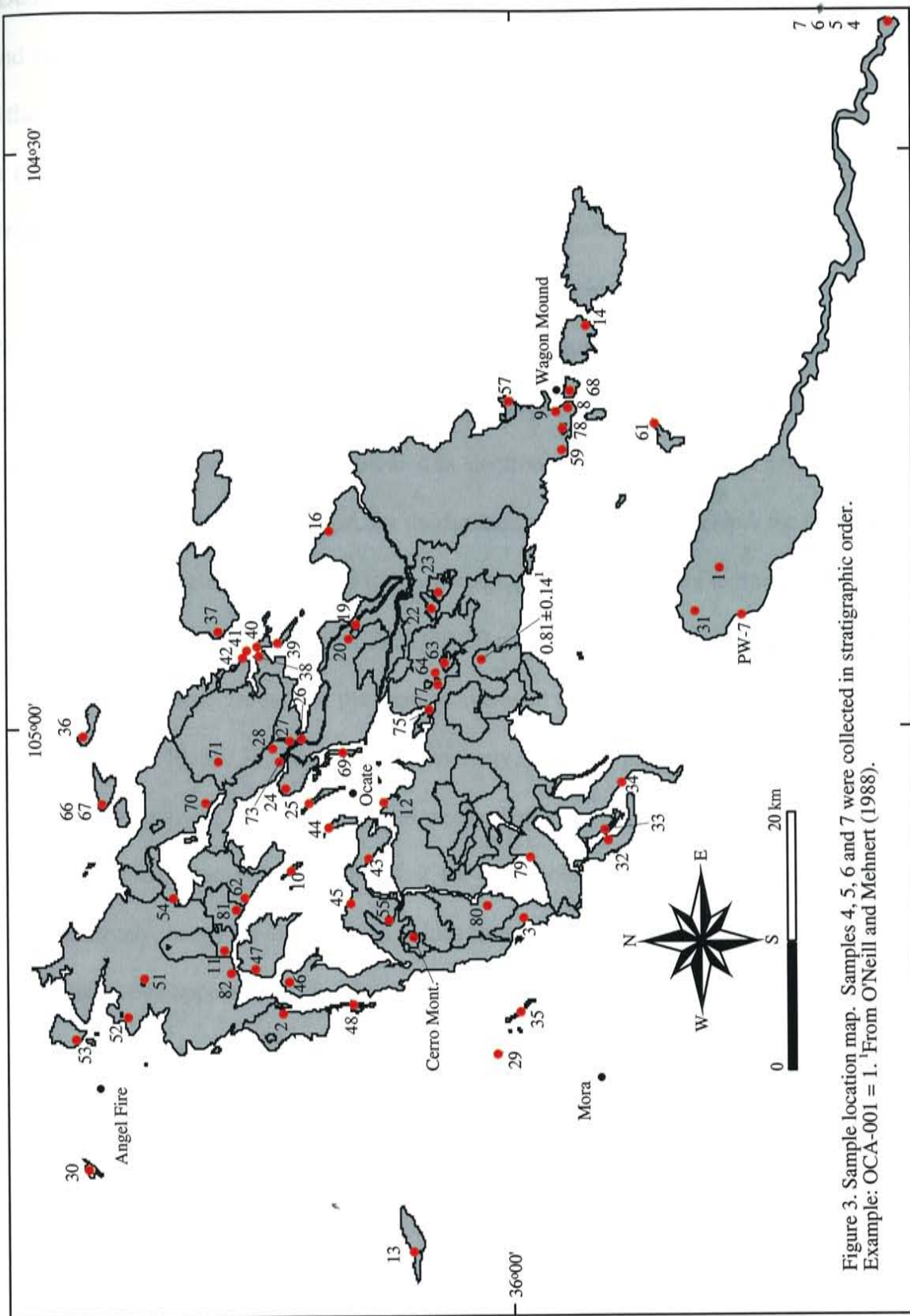


Figure 3. Sample location map. Samples 4, 5, 6 and 7 were collected in stratigraphic order.
Example: OCA-001 = 1. [From O'Neill and Mehrt (1988).

(Deino and Potts, 1990) relative to Mmhb-1 at 520.4 Ma (Samson and Alexander, 1987)) and potassium and calcium salts. Samples were irradiated between one to seven hours in either the D-3 position at the Texas A & M reactor or the L-6 position at the Ford reactor at the University of Michigan. $^{38}\text{Ar}_{\text{Cl}}$ values were unable to be measured for samples irradiated at Texas because of shielding of low-energy neutrons.

All $^{40}\text{Ar}/^{39}\text{Ar}$ analyses were performed in the New Mexico Geochronological Research Laboratory (NMGRL) at the New Mexico Institute of Mining and Technology, Socorro, New Mexico. Isotopic ratios were measured by a Mass Analyzer Products (MAP) 215-50 mass spectrometer operated in electron multiplier mode at a net sensitivity of approximately 2×10^{-16} moles/pA for the furnace and 1×10^{-16} moles/pA for the laser. The mass spectrometer is connected to a two-stage, all-metal, vacuum extraction line. The first and second stages contain SAES GP-50 getters to remove reactive gases. Total system blank and background for the furnace averaged 640, 4.8, 0.7, 2.0, 2.6×10^{-18} moles at masses 40, 39, 38, 37 and 36, respectively, based on four or more values from each group of analyses ran during a given week. Total system blank and background for the CO₂ laser averaged 327, 4.2, 0.6, 2.1, 2.4×10^{-18} moles at masses 40, 39, 38, 37 and 36, respectively, based on four or more values from each group of analyses ran during a given week. See appendix A for J-factor precision, discrimination values and the correction factors used for the interfering nuclear reactions.

All samples were step-heated in a standard double-vacuum Mo resistance furnace with a heating duration of seven minutes per step. In addition, six samples were also step-heated using a defocused CO₂ laser beam with a heating duration of thirteen minutes per step. Samples for laser analyses were loaded into wells in copper sample trays to a

thickness of approximately one grain size. Mass spectrometer operation and age calculation was facilitated by the program "Mass Spec v.4.92" written by A. Deino at the Berkeley Geochronology Center.

All $^{40}\text{Ar}/^{39}\text{Ar}$ ages were determined using the decay constants recommended by Steiger and Jager (1977). Uncertainties in eruption ages are reported at the 2σ confidence level and include errors in J-value, system blank, isotope peak height regression and mass discrimination. Eruption ages are weighted by the inverse of the variance for the steps selected and uncertainties are calculated using the method of Samson and Alexander (1987).

Five representative samples were examined on a Cameca SX-100 microprobe at the New Mexico Bureau of Mines and Mineral Resources. For each representative sample more than fifty, 20-48 mesh ($300\text{-}850\mu\text{m}$), sample chips were viewed. The back scatter electron (BSE) images, X-ray maps and the chemical composition of the phases were obtained with a probe current of 20nA and an accelerating voltage of 15kV. The K-maps were used to estimate the modal percentages of the potassium bearing phases (See Section 3.1.1. for further explanation of the phases present). A histogram of the pixel colors for three or more BSE images were averaged and used to estimate the modal percentages of the non-potassium phases.

3. Interpretation of Basaltic $^{40}\text{Ar}/^{39}\text{Ar}$ Age Spectra and Implications for Sample Collection

The dating of basalts using the $^{40}\text{Ar}/^{39}\text{Ar}$ technique has been widely used to investigate such processes as sea floor spreading rates, the timing of geomagnetic reversal events, the eruption age of major flood basalt provinces, and the eruptive history of volcanic fields (e.g. Foland et al., 1993; Lo et al., 1994; Singer and Pringle, 1996; Baski and Archibald, 1997). Considering the major applications for dating basalts, little attention has been given to understanding the link between the petrology and chemistry of a sample and the $^{40}\text{Ar}/^{39}\text{Ar}$ data.

One major problem facing the interpretation of whole rock age spectra that contain multiple phases is determining the contribution and behavior of the individual phases upon the overall spectrum. The differential thermal release of Ar isotopes from each of the phases during a step-heating analysis has been semi-quantitatively shown in mafic volcanic whole rock samples. Glass has been shown to degas at relatively low temperatures followed by the groundmass crystallized phases and lastly the phenocrystic phases (Foland et al., 1993; Lo et.al, 1994).

Discordance of basaltic age spectra has been shown to be due to three factors: $^{40}\text{Ar}^*$ loss, excess ^{40}Ar and recoil redistribution (Turner and Cadogan, 1974; Huenke and Smith, 1976; Foland et al., 1993; Koppers et al., 2000). $^{40}\text{Ar}^*$ loss causes the apparent age to be less than the eruption age whereas excess ^{40}Ar causes the apparent age to be greater than the eruption age. Recoil redistribution between different phases of the irradiation generated $^{39}\text{Ar}_\text{K}$ isotope can cause the apparent ages associated with the degassing of the individual phases to be greater or less than the eruption age. The

magnitude that this effect has on the age spectrum depends on the amount lost or gained between the phases.

In addition, two other factors have been inferred to cause discordance in basaltic age spectra: inaccurate Ca-correction and inherited argon (Turner and Cadogan, 1974; Heizler et al., 1999). For Ca-rich samples, the Ca-correction becomes an increasing factor that may overestimate or underestimate the step's apparent age. Inherited argon from xenocryst contamination may cause the apparent age associated with the degassing of the xenocryst phase to be greater than the eruption age if the argon within the xenocryst phase has not been lost.

Research done on the effects that recoil and alteration have on age spectra has greatly benefited the interpretation of $^{40}\text{Ar}/^{39}\text{Ar}$ age spectra for basaltic samples (Turner and Cadogan, 1974; Huenke and Smith, 1976; Foland et al., 1993; Lo et al., 1994). However, some questions remain unanswered. Are the groundmass crystal dimensions at the same scale as the recoil distance? At what relative temperatures do each of the phases degas? What effect does the crystallinity and the location of the potassium have on the argon release patterns?

Based on their differing age spectra shapes and argon release patterns, five of the seventy samples analyzed in this study were selected for detailed petrographic and chemical study. In general, the representative samples contain the same phases as those seen in all other samples dated in this study and exemplify the extreme sample types (i.e. a poorly crystallized sample, a well crystallized sample, a pyroxene-rich sample). Eight percent of the samples were collected from the surface of flows, thirteen percent proximal to eruptive vents and the remaining seventy-nine percent were collected from the flow

interiors. Two of the five representative samples were collected from the surface of the flows and three from the flow interiors. The representative samples were analyzed petrographically and chemically to help understand the degassing behavior of the different phases and how this relates to the discordance found in their age spectra. Similar heating schedules were used for all five representative samples so that comparison of the $^{37}\text{Ar}_{\text{Ca}}$, $^{38}\text{Ar}_{\text{Cl}}$ and $^{39}\text{Ar}_{\text{K}}$ release patterns could be made.

3.1. Results

3.1.1. Sample Characteristics

Table 1 lists the samples studied with the weight percent of K₂O, CaO and Cl obtained from microprobe analyses for the phases present along with petrographic comments. Figure 4 displays the potassium X-ray maps taken of the samples. The term “interstitial phases” is used to describe the sub-micron scale intergrown mixture of glass, K-feldspar and oxides present within the space between groundmass crystallized phases (phases smaller than 1 µm could not be resolved with the microprobe). In all samples the groundmass feldspar was found to be progressively zoned from a Ca-rich, K-poor core to a K-rich, Ca-poor rim. Of the phases present, the interstitial phases and feldspar rims were found to contain the greatest amount of K₂O, whereas the feldspar core and pyroxene contain the greatest amount of CaO. Concentrations of Cl were only detected in the interstitial phases. All phases were found to be free of low-temperature alteration products such as clays, zeolites or palagonite. Because bulk sample chemistries were not performed, a level of uncertainty exists for the estimated modal percentages.

3.1.2. $^{40}\text{Ar}/^{39}\text{Ar}$ Results

Analyses of representative samples, including replicates of OCA-073, are given in Figure 5 and Table 2. Three different K/Ca spectra shapes are seen: descending, convex upward and descending/convex upward, where the first two or three steps are descending followed by a convex upward K/Ca. In all samples, the lowest K/Ca value is present at the two highest-temperature steps. The flow surface samples (OCA-073 and OCA-079) display a descending K/Ca with steps 550-675 containing approximately fifty percent of

Table 1: Chemical and Petrographic Characterization of Representative Samples

Sample ID	Phases	K ₂ O (wt.%)	CaO (wt.%)	Cl (wt.%)	K/Ca	Est. Modal %	K ₂ O (%) ³	CaO (%)	size (um) ⁴	Comments
OCA-025 interstitial phases ¹	feldspar ² :	1.75-8.61	0.23-5.34	≤ 0.06	0.4-4.5	4	12	1	≤ 25 5-70	Feldspar supported matrix. Majority of K resides within the K-rich rim of feldspar.
	K-rich rim	1-6.34	1.67-9	< 0.01	0.1-4.5	31	68	19		
	Ca-rich core	0.37-1	9-11.77	< 0.01	0.03-0.1	48	20	58		
	pyroxene	≤ 0.03	18.73-19.48	< 0.01	≤ 0.002	10	≤ 0.2	22	4-55	Interstitial phases occur in isolated pockets.
	olivine	≤ 0.02	0.12-0.26	< 0.01	≤ 0.2	3	≤ 0.04	0.06	6-80	Sample collected from core of flow.
	oxide	≤ 0.01	0.06-0.09	< 0.01	≤ 0.2	4	≤ 0.02	0.04	1-40	
OCA-030 interstitial phases ¹	feldspar ² :	3.89-7.76	1.19-3.54	≤ 0.08	1.3-7.8	3	18	0.7	≤ 7 3-55	Feldspar supported matrix. Majority of K resides within the K-rich rim of feldspar.
	K-rich rim	1-3.43	3.41-9	< 0.01	0.1-1.2	24	56	14		
	Ca-rich core	0.27-1	9-12.50	< 0.01	0.03-0.1	36	24	36		
	pyroxene	≤ 0.07	20.27-21.24	< 0.01	≤ 0.004	25	≤ 2	49	3-55	Interstitial phases occur between feldspar grains.
	olivine	≤ 0.03	0.35-0.57	< 0.01	≤ 0.1	8	≤ 0.3	0.5	7-55	Sample collected from core of flow.
	oxide	≤ 0.04	0.22-0.28	< 0.01	≤ 0.2	4	≤ 0.2	0.09	2-22	
OCA-073 interstitial phases ¹	feldspar ² :	3.88-5.87	0.43-4.51	0.09-0.15	1.0-16	37	83	12	≤ 55 4-55	Interstitial supported matrix. Majority of K resides within the interstitial matrix.
	K-rich rim	1-3.08	2.77-9	< 0.01	0.1-1.3	3	3	2		
	Ca-rich core	0.35-1	9-12.05	< 0.01	0.03-0.1	44	14	63		
	pyroxene	≤ 0.01	20.04-20.50	< 0.01	≤ 0.0006	8	≤ 0.04	22	5-40	Interstitial phases occur between feldspar grains.
	olivine	≤ 0.03	0.36-0.66	< 0.01	≤ 0.1	8	≤ 0.1	0.6	5-80	Sample collected from flow surface.
OCA-077 interstitial phases ¹	feldspar ² :	2.87-6.09	1.74-5.06	≤ 0.06	0.7-4.2	3	13	1	≤ 7 3-30	Feldspar supported matrix. Majority of K resides within the K-rich rim of feldspar.
	K-rich rim	1-4.34	3.04-9	< 0.01	0.1-1.7	18	46	11		
	Ca-rich core	0.35-1	9-11.97	< 0.01	0.03-0.1	62	40	68		
	pyroxene	≤ 0.09	18.66-19.53	< 0.01	≤ 0.006	10	≤ 0.9	20	2-20	Interstitial phases occur between feldspar grains.
	olivine	≤ 0.04	0.10-0.37	< 0.01	≤ 0.5	4	≤ 0.2	0.1	9-45	Sample collected from vent.
	oxide	≤ 0.04	0.18	< 0.01	≤ 0.3	3	≤ 0.1	0.06	2-20	
OCA-079 interstitial phases ¹	feldspar ² :	1.90-3.30	0.46-5.59	0.21-0.38	0.4-8.5	23	66	6	≤ 25 2-40	Interstitial/feldspar supported matrix. Majority of K resides within the interstitial matrix.
	K-rich rim	1-2.12	7.85-9	< 0.01	0.1-0.3	2	3	2		
	Ca-rich core	0.21-1	9-13.68	< 0.01	0.02-0.1	43	29	43		
	pyroxene	≤ 0.06	21.29-21.43	< 0.01	≤ 0.003	26	≤ 2	49	1-30	Interstitial phases occur between feldspar grains.
	olivine	≤ 0.01	0.22-0.65	< 0.01	≤ 0.05	1	≤ 0.01	0.04	30-70	Sample collected from flow surface.
	oxide	≤ 0.01	0.32	< 0.01	≤ 0.04	5	≤ 0.04	0.1	1-25	

¹ interstitial phases describes a micron scale intergrown mixture of glass, K-feldspar, and oxides.² feldspars are progressively zoned with K-rich, Ca-poor rims grading into K-poor, Ca-rich cores over approximately 1-10 um.1 and 9 are arbitrarily chosen for the limits of K₂O and CaO between the K-rich rim and Ca-rich core of feldspar, respectively.³% K₂O represents the percentage of K₂O each phase contains; calculation uses median K₂O and CaO content.⁴shortest width reported

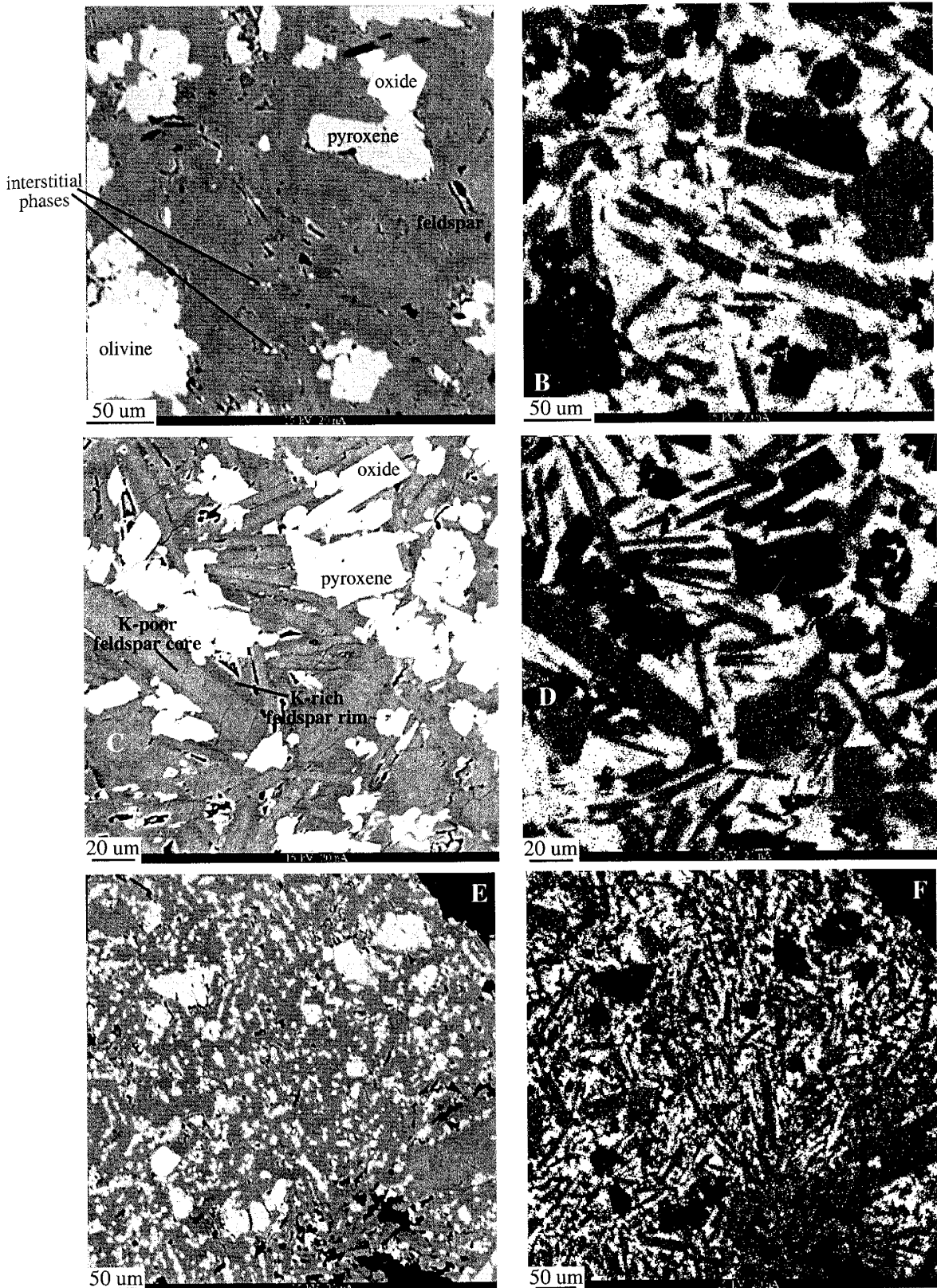


Figure 4 A-L. Back scatter images and corresponding K-maps for samples OCA-025 (A-B), OCA-030 (C-D), OCA-077 (E-F), OCA-073 (G-H, I-J) and OCA-079 (K-L). For K-maps, white areas represent high K regions while black areas represent low K regions. For back scatter images, oxides are white, olivine and pyroxene are light gray, plagioclase is medium gray and interstitial groundmass is dark gray.

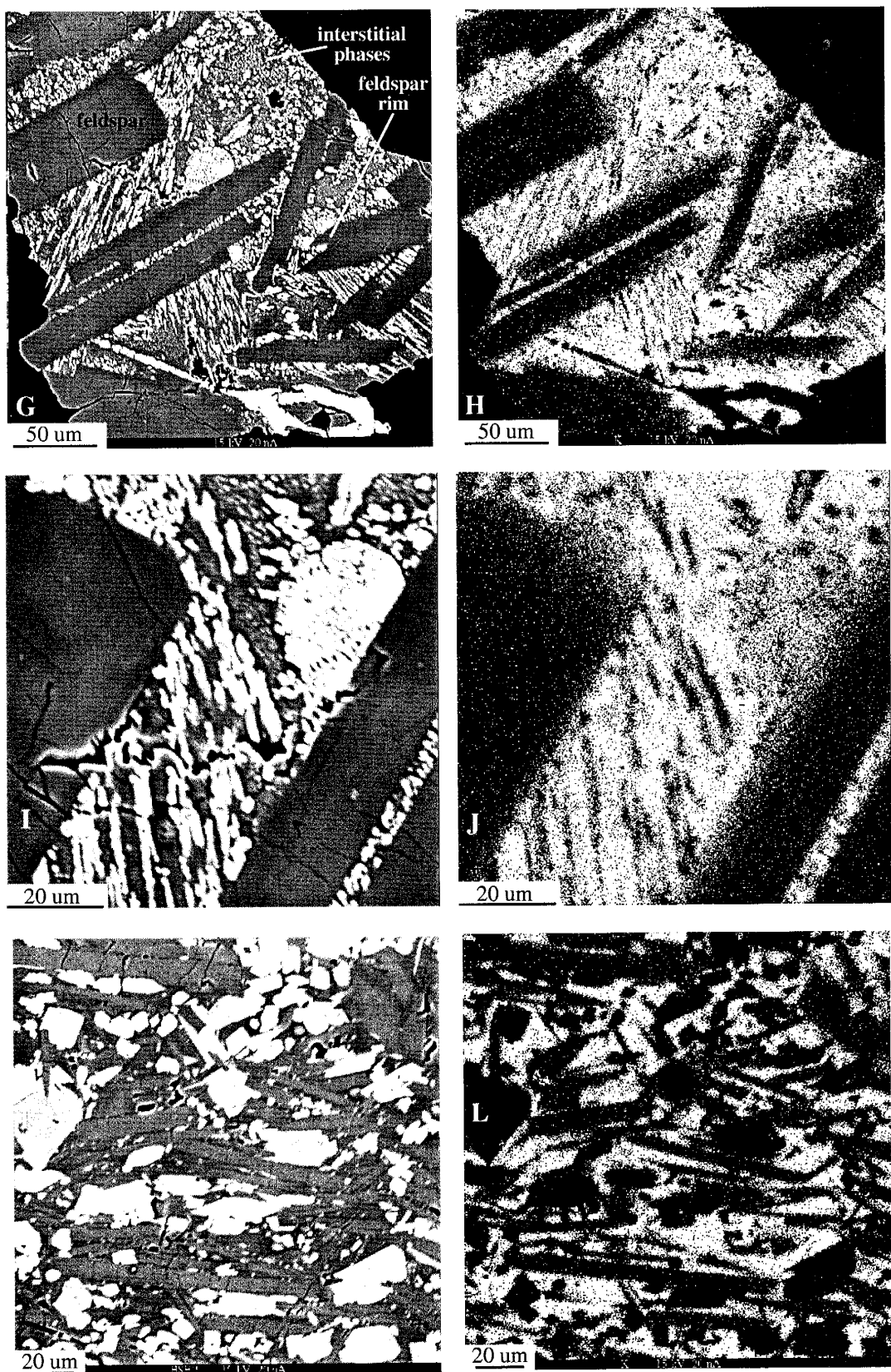


Figure 4 A-L. Continued.

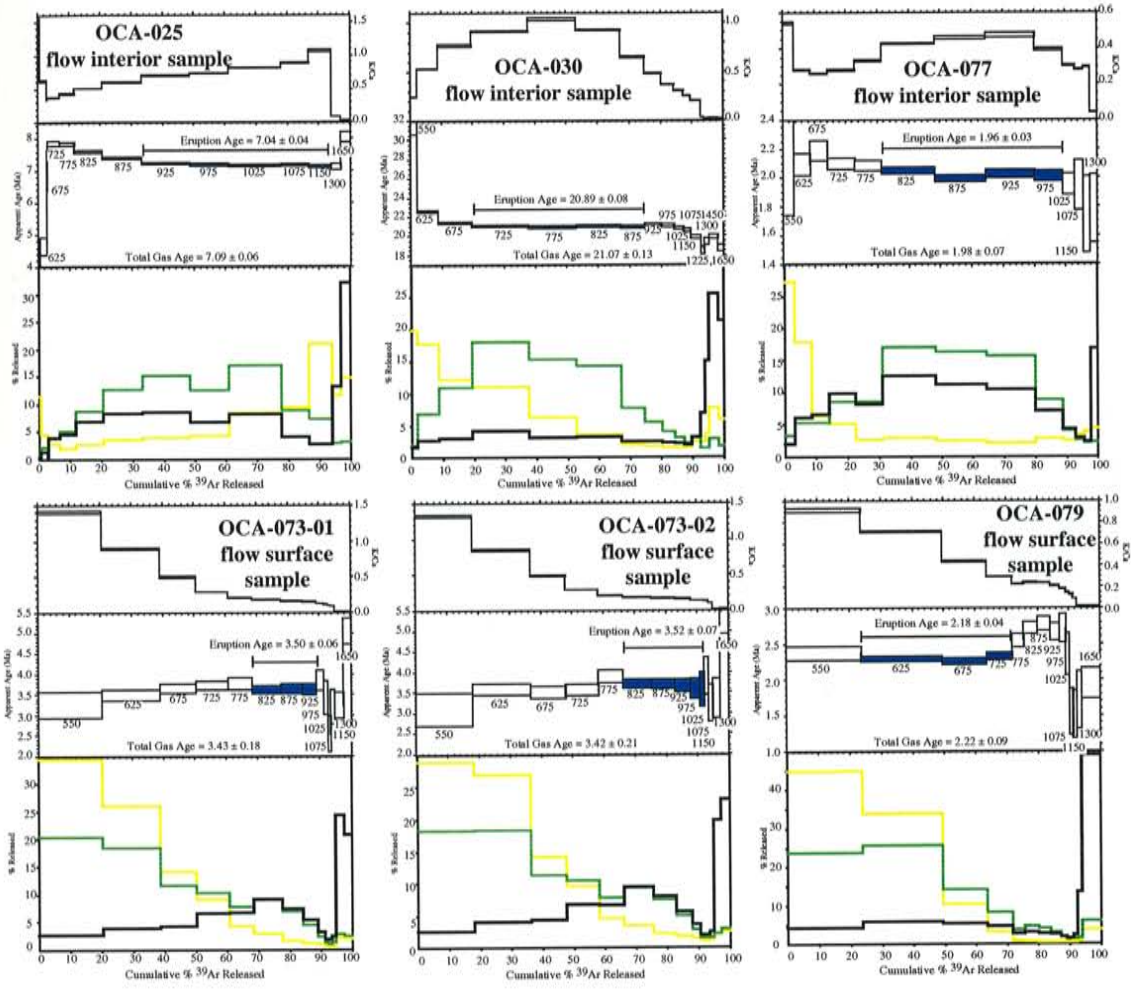


Figure 5. K/Ca, age spectrum and degassing spectrum plots for representative samples studied by electron microprobe. For the degassing graphs, black represents $^{37}\text{ArCa}$, yellow represents $^{38}\text{ArCl}$ and green represents ^{39}ArK .

Table 2: Argon Data Tables for Representative Samples

ID	Temp (°C)	$^{40}\text{Ar}/^{39}\text{Ar}$	$^{37}\text{Ar}/^{39}\text{Ar}$	$^{36}\text{Ar}/^{39}\text{Ar}$	$^{39}\text{Ar}_K$ (mol)	K/Ca	Cl/K	$^{37}\text{Ar}_{\text{Ca}}$ (%)	$^{38}\text{Ar}_{\text{Cl}}$ (%)	$^{39}\text{Ar}_K$ (%)	$^{40}\text{Ar}^*$ (%)	^{39}Ar (%)	Age (Ma)	$\pm 2\sigma$ (Ma)	
OCA-025; Z5:120, groundmass concentrate, 88.00mg, J=0.000793±0.10%, D=1.00644±0.00091, NM-120, Lab#=51027-01															
A	550	5.81E+01	3.33E-01	1.93E-01	3.3E-15	1.5E+00	3.3E-02	0.2	11.4	0.7	2.1	0.7	1.73	1.12	
B	625	1.24E+01	8.18E-01	3.14E-02	1.0E-14	6.2E-01	4.3E-03	1.3	4.5	2.1	25.6	2.8	4.56	0.28	
C	675	7.88E+00	1.50E+00	1.06E-02	1.1E-15	3.4E-01	3.2E-03	0.3	0.4	0.2	61.2	3.0	6.89	0.60	
D	725	6.39E+00	1.37E+00	3.64E-03	1.8E-14	3.7E-01	1.6E-03	3.9	2.8	3.7	84.4	6.7	7.70	0.06	
E	775	5.71E+00	1.18E+00	1.36E-03	2.4E-14	4.3E-01	8.1E-04	4.5	2.0	5.0	94.1	11.8	7.68	0.05	
F	825	5.42E+00	1.00E+00	8.94E-04	4.2E-14	5.1E-01	6.2E-04	6.7	2.7	8.8	96.1	20.6	7.44	0.04	
G	875	5.22E+00	8.55E-01	6.60E-04	6.0E-14	6.0E-01	5.6E-04	8.2	3.4	12.6	97.0	33.2	7.24	0.03	
H	925	5.09E+00	7.33E-01	5.64E-04	7.2E-14	7.0E-01	5.1E-04	8.5	3.8	15.2	97.3	48.4	7.08	0.03	
I	975	5.01E+00	6.99E-01	3.46E-04	5.9E-14	7.3E-01	6.9E-04	6.6	4.2	12.5	98.5	60.9	7.06	0.03	
J	1025	5.02E+00	6.29E-01	4.37E-04	8.0E-14	8.1E-01	1.0E-03	8.1	8.4	17.0	97.9	77.8	7.01	0.03	
K	1075	5.05E+00	5.78E-01	4.56E-04	4.2E-14	8.8E-01	2.1E-03	3.9	9.3	8.9	97.7	86.8	7.05	0.04	
L	1150	5.10E+00	4.80E-01	7.33E-04	3.5E-14	1.1E+00	5.9E-03	2.7	20.9	7.3	96.0	94.0	6.99	0.04	
M	1300	6.55E+00	6.00E+00	7.18E-03	1.4E-14	8.5E-02	8.3E-03	13.1	11.6	2.9	74.3	96.9	6.98	0.10	
N	1650	9.68E+00	1.36E+01	1.77E-02	1.5E-14	3.8E-02	9.8E-03	32.0	14.8	3.1	56.4	100.0	7.88	0.14	
total gas age		n=14				4.7E-13	6.7E-01						7.09	0.06	
Eruption Age		n=5	steps H-L		2.9E-13	8.1E-01							60.9	7.04	0.04
OCA-030; A2:117, groundmass concentrate, 81.08mg, J=0.001072496±0.10%, D=1.00644±0.00091, NM-117, Lab#=50832-01															
A	550	5.04E+01	2.03E+00	1.16E-01	1.1E-14	2.5E-01	3.9E-02	1.6	19.8	1.9	32.1	1.9	31.15	0.75	
B	625	1.24E+01	9.52E-01	2.53E-03	3.7E-14	5.4E-01	9.8E-03	2.6	17.7	6.8	94.4	8.7	22.48	0.09	
C	675	1.12E+01	6.60E-01	5.85E-04	6.0E-14	7.7E-01	4.2E-03	2.9	12.2	10.9	98.7	19.6	21.32	0.10	
D	725	1.10E+01	5.55E-01	4.79E-04	9.9E-14	9.2E-01	2.3E-03	4.1	10.9	18.0	98.9	37.6	20.94	0.07	
E	775	1.09E+01	4.89E-01	3.74E-04	8.4E-14	1.0E+00	1.5E-03	3.1	6.1	15.3	99.1	52.9	20.82	0.09	
F	825	1.10E+01	5.48E-01	4.34E-04	7.9E-14	9.3E-01	9.4E-04	3.2	3.5	14.2	99.0	67.1	20.92	0.10	
G	875	1.10E+01	7.84E-01	6.69E-04	4.2E-14	6.5E-01	9.5E-04	2.5	1.9	7.6	98.6	74.8	20.84	0.09	
H	925	1.11E+01	1.05E+00	9.31E-04	3.1E-14	4.9E-01	1.1E-03	2.4	1.7	5.6	98.1	80.3	21.03	0.09	
I	975	1.12E+01	1.36E+00	1.38E-03	2.2E-14	3.7E-01	1.5E-03	2.2	1.5	4.0	97.1	84.3	20.93	0.11	
J	1025	1.12E+01	1.66E+00	1.95E-03	1.7E-14	3.1E-01	1.7E-03	2.1	1.3	3.0	95.9	87.4	20.65	0.13	
K	1075	1.12E+01	2.02E+00	2.65E-03	1.3E-14	2.5E-01	2.5E-03	1.9	1.5	2.3	94.3	89.6	20.44	0.18	
L	1150	1.13E+01	2.46E+00	4.10E-03	1.7E-14	2.1E-01	3.0E-03	3.1	2.4	3.0	90.9	92.7	19.74	0.15	
M	1225	1.27E+01	1.24E+01	1.45E-02	7.4E-15	4.1E-02	6.5E-03	6.8	2.3	1.3	74.3	94.0	18.35	0.33	
N	1300	1.27E+01	2.53E+01	1.68E-02	8.0E-15	2.0E-02	9.7E-03	14.9	3.7	1.4	77.3	95.4	19.31	0.34	
O	1450	1.24E+01	2.18E+01	1.39E-02	1.6E-14	2.3E-02	1.0E-02	25.4	7.7	2.9	81.3	98.3	19.77	0.20	
P	1650	1.50E+01	3.02E+01	2.73E-02	9.5E-15	1.7E-02	1.3E-02	21.2	5.7	1.7	62.8	100.0	18.61	0.34	
total gas age		n=16			5.5E-13	7.0E-01							21.07	0.13	
Eruption Age		n=4	steps D-G		3.0E-13	9.2E-01							55.2	20.89	0.08
OCA-073-01; V1:117, groundmass concentrate, 55.79mg, J=0.001038789±0.11%, D=1.00644±0.00091, NM-117, Lab#=50879-01															
A	550	2.08E+01	3.61E-01	6.49E-02	6.3E-14	1.4E+00	3.5E-02	2.7	34.3	20.4	8.0	20.4	3.14	0.31	
B	625	6.07E+00	5.69E-01	1.46E-02	5.7E-14	9.0E-01	2.9E-02	3.8	25.9	18.5	29.6	38.8	3.36	0.12	
C	675	4.98E+00	1.02E+00	1.07E-02	3.6E-14	5.0E-01	2.5E-02	4.3	14.1	11.6	37.7	50.5	3.52	0.11	
D	725	4.14E+00	1.76E+00	7.93E-03	3.2E-14	2.9E-01	1.8E-02	6.5	9.0	10.2	46.3	60.7	3.59	0.10	
E	775	3.47E+00	2.38E+00	5.79E-03	2.4E-14	2.1E-01	1.2E-02	6.6	4.3	7.7	55.7	68.4	3.63	0.14	
F	825	2.94E+00	2.74E+00	4.33E-03	2.8E-14	1.9E-01	6.7E-03	9.1	2.9	9.2	63.4	77.6	3.49	0.08	
G	875	2.78E+00	3.02E+00	3.84E-03	2.1E-14	1.7E-01	4.9E-03	7.5	1.6	6.9	67.3	84.5	3.51	0.11	
H	925	2.87E+00	3.26E+00	4.25E-03	1.4E-14	1.6E-01	5.4E-03	5.3	1.2	4.5	64.8	89.0	3.49	0.12	
I	975	3.15E+00	3.79E+00	4.95E-03	7.3E-15	1.3E-01	8.2E-03	3.2	0.9	2.3	62.7	91.3	3.71	0.24	
J	1025	3.21E+00	4.34E+00	6.05E-03	3.7E-15	1.2E-01	9.9E-03	1.9	0.6	1.2	54.7	92.5	3.30	0.39	
K	1075	3.31E+00	4.71E+00	8.03E-03	3.3E-15	1.1E-01	1.1E-02	1.8	0.6	1.1	39.3	93.5	2.44	0.42	
L	1150	3.79E+00	5.09E+00	8.60E-03	4.0E-15	1.0E-01	9.9E-03	2.4	0.6	1.3	43.4	94.8	3.09	0.40	
M	1300	5.67E+00	2.41E+01	2.03E-02	8.6E-15	2.1E-02	1.5E-02	24.2	2.0	2.8	28.8	97.6	3.11	0.31	
N	1650	8.10E+00	2.41E+01	2.55E-02	7.4E-15	2.1E-02	1.8E-02	20.8	2.0	2.4	31.5	100.0	4.86	0.31	
total gas age		n=14			3.1E-13	6.0E-01							3.43	0.18	
Eruption Age		n=3	steps F-H		6.4E-14	1.7E-01							20.5	3.50	0.06

Table 2 continued

ID	Temp (°C)	^{40}Ar	^{39}Ar	^{37}Ar	$^{39}\text{Ar}/^{36}\text{Ar}$	^{39}Ar	$^{39}\text{Ar}_K$	K/Ca (mol)	Cl/K	$^{37}\text{Ar}_{\text{Ca}}$ (%)	$^{38}\text{Ar}_{\text{Cl}}$ (%)	$^{39}\text{Ar}_K$ (%)	$^{40}\text{Ar}^*$ (%)	^{39}Ar (%)	Age (Ma)	$\pm 2\sigma$ (Ma)
OCA-073-02; V3:117, groundmass concentrate, 55.73mg, J=0.001031232±0.11%, D=1.00644±0.00091, NM-117, Lab#=50881-01																
A	550	1.92E+01	3.86E-01	5.96E-02	4.3E-14	1.3E+00	3.1E-02	2.6	28.8	18.2	8.3	18.2	2.96	0.38		
B	625	6.19E+00	6.01E-01	1.48E-02	4.4E-14	8.5E-01	2.9E-02	4.0	26.9	18.3	29.7	36.5	3.42	0.13		
C	675	5.18E+00	1.05E+00	1.16E-02	2.7E-14	4.9E-01	2.5E-02	4.3	14.0	11.3	34.8	47.8	3.35	0.14		
D	725	4.34E+00	1.75E+00	8.90E-03	2.5E-14	2.9E-01	1.8E-02	6.7	9.5	10.5	42.2	58.3	3.40	0.13		
E	775	3.66E+00	2.34E+00	6.19E-03	1.9E-14	2.2E-01	1.2E-02	6.7	4.5	7.8	54.6	66.1	3.72	0.14		
F	825	3.16E+00	2.75E+00	4.93E-03	2.2E-14	1.9E-01	7.2E-03	9.4	3.4	9.4	60.3	75.5	3.54	0.10		
G	875	3.01E+00	2.90E+00	4.50E-03	1.8E-14	1.8E-01	5.7E-03	7.9	2.1	7.4	63.1	82.9	3.54	0.10		
H	925	3.25E+00	3.08E+00	5.41E-03	1.2E-14	1.7E-01	6.6E-03	5.6	1.7	5.0	57.9	87.9	3.50	0.14		
I	975	3.84E+00	3.59E+00	7.67E-03	6.5E-15	1.4E-01	9.9E-03	3.6	1.4	2.7	48.1	90.7	3.44	0.23		
J	1025	3.87E+00	3.61E+00	7.83E-03	3.5E-15	1.4E-01	1.4E-02	1.9	1.0	1.5	47.4	92.1	3.42	0.40		
K	1075	3.65E+00	3.71E+00	6.54E-03	3.4E-15	1.4E-01	1.3E-02	1.9	1.0	1.4	54.9	93.5	3.74	0.43		
L	1150	3.75E+00	4.73E+00	8.33E-03	3.5E-15	1.1E-01	1.6E-02	2.5	1.2	1.4	44.2	95.0	3.10	0.42		
M	1300	5.27E+00	2.50E+01	1.90E-02	5.2E-15	2.0E-02	1.8E-02	19.8	2.0	2.2	32.1	97.2	3.21	0.47		
N	1650	7.43E+00	2.21E+01	2.22E-02	6.8E-15	2.3E-02	1.7E-02	23.1	2.5	2.8	35.9	100.0	5.04	0.33		
total gas age		n=14												3.42	0.21	
Eruption Age		n=5	steps F-J	6.2E-14	1.7E-01								26.0	3.52	0.07	
OCA-077; I4:118, groundmass concentrate, 122.10mg, J=0.000156553±0.11%, D=1.00644±0.00091, NM-118, Lab#=50910-01																
A	550	2.29E+02	9.36E-01	7.45E-01	2.9E-15	5.5E-01	6.1E-02	1.9	27.3	3.3	3.7	3.3	2.40	0.71		
B	625	1.48E+01	1.82E+00	2.61E-02	4.7E-15	2.8E-01	2.5E-02	6.1	17.8	5.4	48.6	8.7	2.03	0.07		
C	675	1.09E+01	1.97E+00	1.18E-02	4.7E-15	2.6E-01	8.9E-03	6.6	6.4	5.4	69.0	14.1	2.12	0.07		
D	725	9.59E+00	1.83E+00	8.55E-03	7.5E-15	2.8E-01	4.5E-03	9.7	5.1	8.6	74.9	22.7	2.03	0.04		
E	775	9.04E+00	1.54E+00	6.75E-03	7.4E-15	3.3E-01	2.2E-03	8.2	2.5	8.5	79.0	31.2	2.02	0.03		
F	825	8.47E+00	1.19E+00	5.16E-03	1.5E-14	4.3E-01	1.3E-03	12.6	3.0	17.0	82.8	48.2	1.98	0.02		
G	875	8.43E+00	1.11E+00	5.63E-03	1.4E-14	4.6E-01	1.1E-03	11.2	2.4	16.2	81.0	64.4	1.93	0.02		
H	925	8.72E+00	1.07E+00	6.20E-03	1.4E-14	4.8E-01	1.0E-03	10.4	2.1	15.6	79.6	80.0	1.96	0.03		
I	975	9.77E+00	1.30E+00	1.00E-02	7.7E-15	3.9E-01	2.3E-03	7.1	2.8	8.9	70.5	88.9	1.95	0.04		
J	1025	1.29E+01	1.68E+00	2.13E-02	3.6E-15	3.0E-01	4.6E-03	4.3	2.5	4.1	52.0	93.0	1.89	0.07		
K	1075	2.14E+01	1.82E+00	5.01E-02	2.2E-15	2.8E-01	9.6E-03	2.9	3.3	2.6	31.2	95.6	1.88	0.17		
L	1150	2.86E+01	1.72E+00	7.71E-02	1.9E-15	3.0E-01	1.4E-02	2.3	3.9	2.2	20.8	97.7	1.69	0.25		
M	1300	3.69E+01	1.18E+01	1.07E-01	2.0E-15	4.3E-02	1.4E-02	16.8	4.3	2.3	16.4	100.0	1.73	0.23		
N	1650	1.65E+02	0.00E+00	3.63E-01	-1.8E-17	-	-6.0E+00	0.0	16.5	0.0	34.9	100.0	16.14	20.38		
total gas age		n=14				8.7E-14	3.8E-01						1.98	0.07		
Eruption Age		n=4	steps F-I	5.0E-14	4.4E-01								57.7	1.96	0.03	
OCA-079; K2:118, groundmass concentrate, 97.00mg, J=0.000154005±0.12%, D=1.00644±0.00091, NM-118, Lab#=50920-01																
A	550	3.70E+01	5.58E-01	9.78E-02	1.8E-14	9.1E-01	9.9E-02	4.2	44.8	23.8	22.0	23.8	2.26	0.09		
B	625	1.51E+01	7.13E-01	2.47E-02	1.9E-14	7.2E-01	7.0E-02	5.8	33.8	25.7	51.9	49.4	2.18	0.03		
C	675	1.32E+01	1.17E+00	1.86E-02	1.1E-14	4.4E-01	3.8E-02	5.3	10.2	14.1	58.6	63.6	2.14	0.04		
D	725	1.33E+01	1.75E+00	1.85E-02	6.1E-15	2.9E-01	1.9E-02	4.5	2.9	8.2	59.8	71.8	2.22	0.05		
E	775	1.52E+01	2.28E+00	2.26E-02	2.8E-15	2.2E-01	9.8E-03	2.7	0.7	3.7	57.3	75.5	2.43	0.09		
F	825	1.58E+01	2.15E+00	2.22E-02	3.4E-15	2.4E-01	6.3E-03	3.1	0.5	4.5	59.2	79.9	2.59	0.08		
G	875	1.59E+01	2.17E+00	2.20E-02	3.0E-15	2.4E-01	4.9E-03	2.7	0.4	3.9	59.9	83.9	2.64	0.09		
H	925	1.70E+01	2.46E+00	2.72E-02	2.3E-15	2.1E-01	7.5E-03	2.4	0.4	3.1	53.7	87.0	2.54	0.12		
I	975	1.90E+01	2.88E+00	3.35E-02	1.5E-15	1.8E-01	1.1E-02	1.8	0.4	1.9	48.9	89.0	2.58	0.19		
J	1025	1.97E+01	3.47E+00	4.01E-02	8.6E-16	1.5E-01	1.7E-02	1.3	0.4	1.1	40.9	90.1	2.24	0.28		
K	1075	2.42E+01	4.07E+00	6.51E-02	8.7E-16	1.3E-01	2.5E-02	1.5	0.6	1.2	21.8	91.3	1.47	0.30		
L	1150	3.31E+01	5.68E+00	9.58E-02	9.5E-16	9.0E-02	1.9E-02	2.3	0.5	1.3	15.6	92.5	1.44	0.31		
M	1300	5.14E+01	3.01E+01	1.62E-01	1.1E-15	1.7E-02	2.5E-02	13.5	0.7	1.4	11.2	93.9	1.63	0.38		
N	1650	5.66E+01	2.54E+01	1.76E-01	4.6E-15	2.0E-02	3.3E-02	49.0	3.8	6.1	11.6	100.0	1.86	0.20		
total gas age		n=14				7.5E-14	5.3E-01						2.22	0.09		
Eruption Age		n=3	steps B-D	3.6E-14	5.6E-01								48.0	2.18	0.04	

the $^{39}\text{Ar}_\text{K}$ released, whereas the flow interior samples display a convex upward (OCA-030) and descending/convex upward K/Ca (OCA-025, OCA-077) with steps 550-675 containing less than twenty percent of the $^{39}\text{Ar}_\text{K}$ released.

In all samples, the $^{37}\text{Ar}_\text{Ca}$ release spectra displays a convex upward shape over the first ~90% of the $^{39}\text{Ar}_\text{K}$ released then ascends over the last ~10% of the $^{39}\text{Ar}_\text{K}$ released. For the samples displaying a descending K/Ca (flow surface samples), the % $^{39}\text{Ar}_\text{K}$ released per step shows an overall descending shape, whereas samples that display a convex upward and descending/convex upward K/Ca (flow interior samples) show an overall convex upward shaped $^{39}\text{Ar}_\text{K}$ release spectra. All samples show an overall descending shaped $^{38}\text{Ar}_\text{Cl}$ release spectra, except for OCA-030 and OCA-025 which display a descending/convex upward shaped $^{38}\text{Ar}_\text{Cl}$ release spectrum.

Varying degrees of discordance exist for all age spectra. All samples display discordance associated with the low- and high-temperature steps whereas the mid-temperature steps, except for OCA-079, do not display significant discordance. For sample OCA-079, discordance is associated with the mid-temperature steps. Plateau approaches such as that used by Fleck et al., (1977) or Singer and Pringle (1996) were not used to determine the steps used in the eruption age calculation. Instead, a new approach was used that will be discussed in the upcoming Section 3.2.6.

3.2. Discussion

3.2.1. Recoil

Recoil of the $^{39}\text{Ar}_\text{K}$ isotope has long been considered one of the major reasons for discordant age spectra in fine-grained volcanic whole rock samples (Turner and Cadogan,

1974; Huenke and Smith, 1976; Foland et al., 1993; Lo et al., 1994). However, no studies have examined the crystal sizes of the phases present in basaltic samples to see if they are at the same scale at which recoil occurs. In order to get a rough idea of the scale at which $^{37}\text{Ar}_{\text{Ca}}$, $^{38}\text{Ar}_{\text{Cl}}$ and $^{39}\text{Ar}_{\text{K}}$ recoil occurs, loss of the isotopes were modeled against the a and b crystallographic lengths based on the geometry of a rhombic prism. Figure 6 displays the modeled results for the percent volume depleted by recoil of $^{37}\text{Ar}_{\text{Ca}}$, $^{38}\text{Ar}_{\text{Cl}}$ and $^{39}\text{Ar}_{\text{K}}$ versus the a-b length for a rhombic prism. Values for recoil depletion are based on Onstott et al., (1995), where the recoil distance for ^{39}K (n, p) ^{39}Ar is 0.162 μm , ^{40}Ca (n, α) ^{37}Ar is 0.378 μm and ^{37}Cl (n, γ) ^{38}Cl (β) ^{38}Ar is 0.0011 μm .

Because of the small recoil distance for the production of $^{38}\text{Ar}_{\text{Cl}}$ and because the majority of chlorine is contained within the interstitial phases, the percent $^{38}\text{Ar}_{\text{Cl}}$ released per step allows the degassing of the interstitial phases to be identified (Foland et al., 1993). Applying this identification criteria to the basaltic samples studied, the interstitial phases are found to degas first. This conclusion agrees with that of Foland et al., (1993) and Lo et al., (1994).

Although the recoil distance for the production of $^{37}\text{Ar}_{\text{Ca}}$ and $^{39}\text{Ar}_{\text{K}}$ is 0.378 and 0.162 μm , respectively, recoil can still greatly effect the apparent age of a micron size crystal (Figure 6). For example, a 5 μm K-rich crystal within a potassium poor matrix with an age of 20 Ma will have ~5% of its $^{39}\text{Ar}_{\text{K}}$ depleted yielding an apparent age of ~22 Ma. However, the younger the sample is, the less discordance will exist in terms of years between the recoil affected apparent ages and the actual cooling ages.

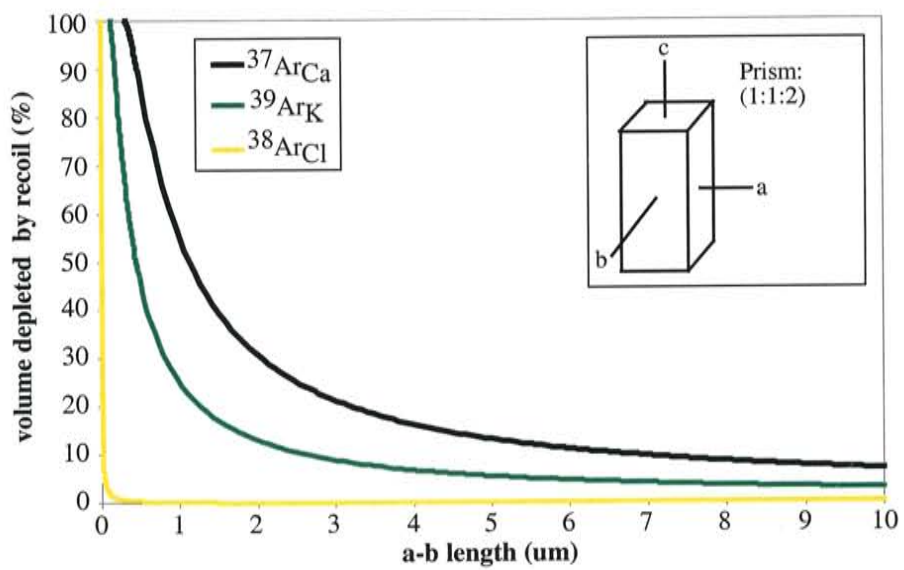


Figure 6. Relationship between grain size and recoil for a 1:1:2 prism. Assuming a mean depletion length of 0.2, 0.08 and 0.0006 μm for $^{37}\text{ArCa}$, ^{39}ArK and $^{38}\text{ArCl}$, respectively. Mean depletion length is half of the recoil length.

3.2.2. Modeling the Degassing Behavior

Modeling of the K/Ca and degassing spectra based on the electron microprobe data presented in Table 1 was performed in an attempt to reproduce the overall shapes of the release patterns seen in the Ar data. It is assumed that the interstitial phases degas first and as one phase followed by feldspar rim, feldspar core, olivine/oxide and lastly by pyroxene. For simplicity, it is assumed that each phase degasses completely in one step and that no phenocryst phases are present. Olivine and opaque oxides were grouped together due to their similar K₂O, CaO and Cl concentrations. Because the lowest K/Ca value occurs in the two highest-temperature steps, pyroxene is interpreted to degas last. Because a range of K₂O and CaO values exists for each phase, the median values were used in the calculations and because chlorine concentrations were only detected in the interstitial phases, the modeled results assume the interstitial phases contain all of the percent ³⁸Ar_{Cl} released.

Figure 7 displays the results of the modeling. Three figures for each sample are shown. The first assumes no recoil of ³⁹Ar_K or ³⁷Ar_{Ca} has happened and is simply the values calculated from Table 1 displayed graphically. The second figure assumes 5% of the ³⁹Ar_K from the interstitial phases and feldspar rim is recoiled into feldspar core, olivine/oxide and pyroxene equally (i.e. a third of the ³⁹Ar_K lost from both interstitial phases and feldspar rim is implanted into each feldspar core, olivine/oxide and pyroxene) and 10% of the ³⁷Ar_{Ca} is recoiled from pyroxene and feldspar core into interstitial phases, feldspar rim and olivine/oxide equally. For the third figure 30% ³⁹Ar_K and 60% ³⁷Ar_{Ca} is recoiled. The percent of ³⁷Ar_{Ca} recoiled is double that of ³⁹Ar_K because the recoil distance of ³⁷Ar_{Ca} is roughly double that of ³⁹Ar_K (Onstott, et al., 1995).

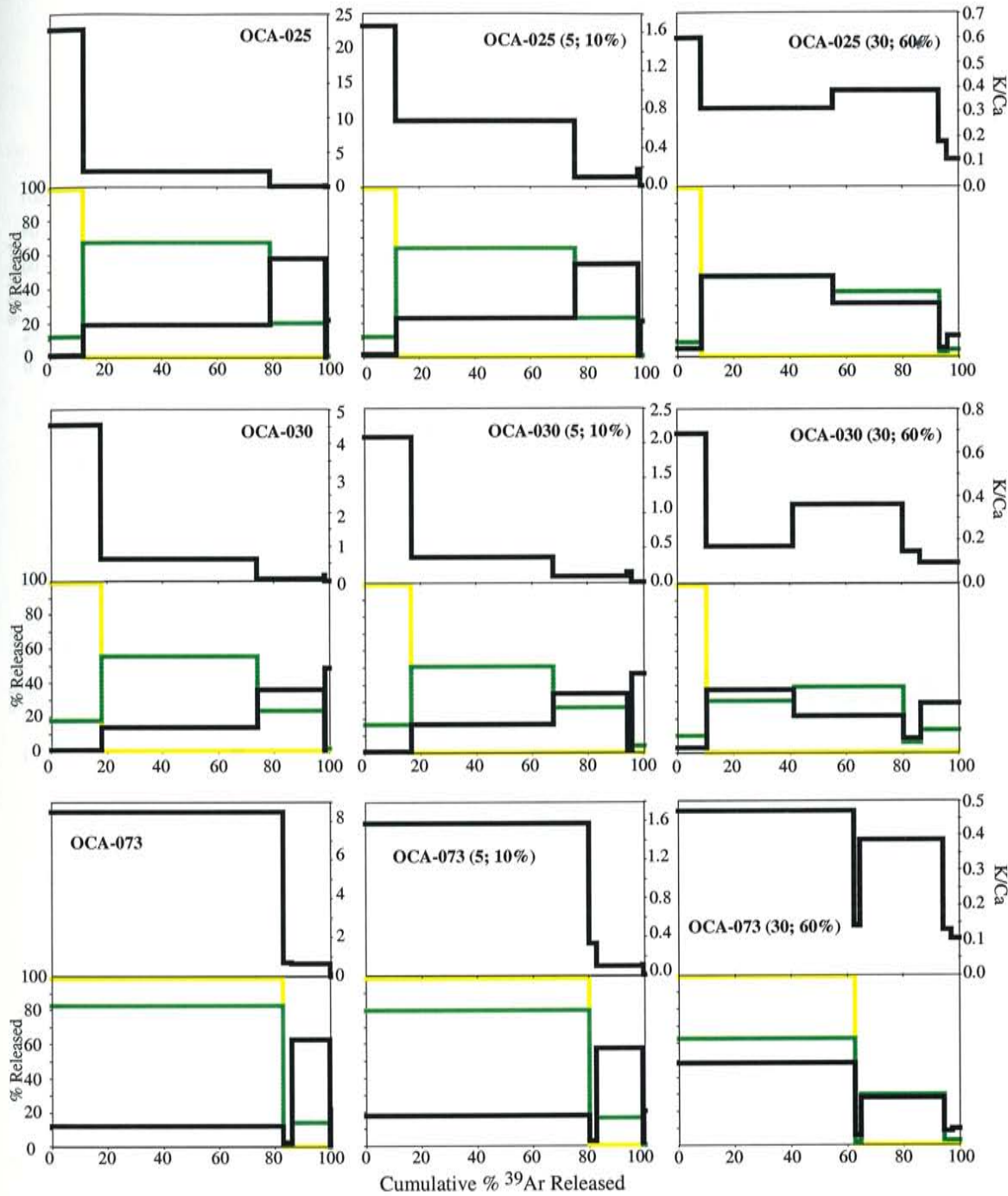


Figure 7. Effect of recoil on K/Ca and the release spectra. For the release spectra, black represents $^{37}\text{Ar}_{\text{Ca}}$, yellow represents $^{38}\text{Ar}_{\text{Cl}}$ and green represents $^{39}\text{Ar}_{\text{K}}$. First step represents complete degassing of interstitial phases, second step represents complete degassing of K-rich feldspar rim, third step represents complete degassing of Ca-rich feldspar core, fourth step represents complete degassing of both olivine and oxide, and fifth step represents complete degassing of pyroxene. First graph assumes no recoil has occurred while the following graphs represent increasing degrees of recoil where the first number in parentheses represents the percent of recoil occurring from $^{39}\text{Ar}_{\text{K}}$ and the second number represents the percent of recoil occurring from $^{37}\text{Ar}_{\text{Ca}}$. Calculations were made assuming $^{39}\text{Ar}_{\text{K}}$ recoiled from both interstitial and K-rich feldspar rim into remaining phases equally, while $^{37}\text{Ar}_{\text{Ca}}$ recoiled from pyroxene and Ca-rich feldspar core into the remaining phases equally.

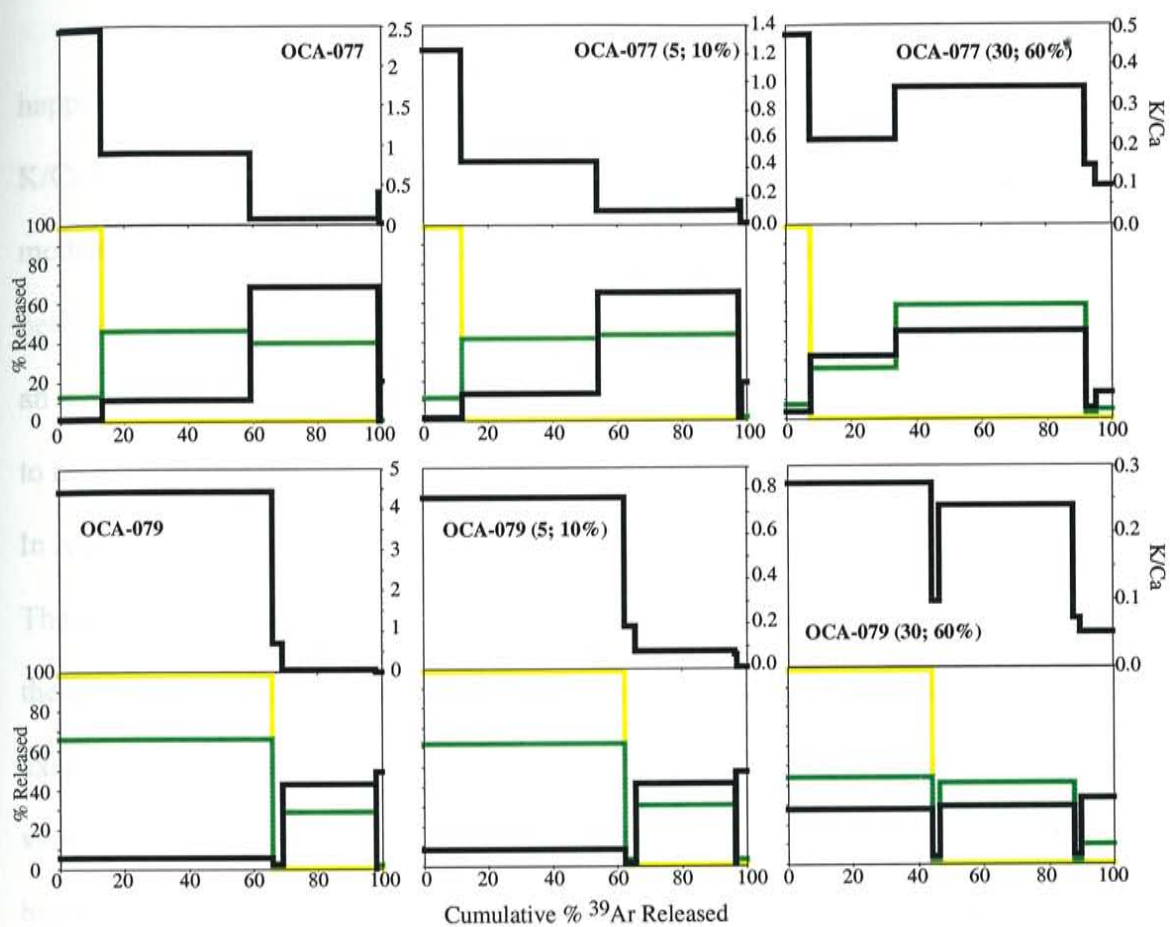


Figure 7 continued.

Several observations can be made based on Figure 7. First, if no recoil has happened the overall shape of the K/Ca should be descending. Second, the maximum K/Ca values for the Ar results is at least an order of magnitude less than that seen in the modeled K/Ca values if no recoil has happened. Third, increased levels of recoil causes a peak in $^{37}\text{Ar}_{\text{Ca}}$ to correspond to a peak in $^{39}\text{Ar}_{\text{K}}$. Fourth, with increasing degrees of recoil, an initially descending K/Ca spectra can become convex upward in shape. It is important to note that the modeled results assume that each phase degasses completely in one step. In reality, all heating steps are going to be a mixture of gasses from two or more phases. Therefore, when comparing the modeled results with the argon results, a mixture between the extreme values (i.e. each step in the modeled results) needs to be envisioned. For example, in the modeled results of OCA-073, the small decrease in $^{37}\text{Ar}_{\text{Ca}}$ and $^{39}\text{Ar}_{\text{K}}$ values associated with the feldspar rim would probably never be resolved by step-heating. Instead, a mixture between the interstitial phases, feldspar rim and feldspar core would result in a steady increase in $^{37}\text{Ar}_{\text{Ca}}$ and $^{39}\text{Ar}_{\text{K}}$ values, thus erasing the low $^{37}\text{Ar}_{\text{Ca}}$ and $^{39}\text{Ar}_{\text{K}}$ values seen in the modeled results.

In general, considering the many assumptions associated with the modeled results, the results fit some of the overall patterns seen in the real K/Ca, $^{37}\text{Ar}_{\text{Ca}}$, $^{38}\text{Ar}_{\text{Cl}}$ and $^{39}\text{Ar}_{\text{K}}$ values. However, there are three aspects of the modeled data that disagree with the argon data. First, in the modeled results, no substantial peak in $^{37}\text{Ar}_{\text{Ca}}$ is seen for the high-temperature steps. Instead, in order for recoil to produce the K/Ca, $^{37}\text{Ar}_{\text{Ca}}$, $^{38}\text{Ar}_{\text{Cl}}$ and $^{39}\text{Ar}_{\text{K}}$ variations seen in the argon results, the modeled $^{37}\text{Ar}_{\text{Ca}}$ peak associated with pyroxene needs to be subdued. Second, the high-temperature $^{38}\text{Ar}_{\text{Cl}}$ peak seen in OCA-025 and OCA-030 can not be reproduced in the modeled results. Third, the increasing

K/Ca values seen in low-temperature steps of OCA-030 are not seen in the modeled results. The lack of a high-temperature $^{37}\text{Ar}_{\text{Ca}}$ peak may be due to not incorporating any phenocryst phases into the modeled results (as will be shown in Section 4, plagioclase and pyroxene phenocryst phases are rich in calcium and degas at high temperatures). Although phenocryst phases were removed during sample preparation, inevitably some phenocryst phases were incorporated in the groundmass concentrate. The high-temperature $^{38}\text{Ar}_{\text{Cl}}$ peak seen in OCA-025 and OCA-030 may be due to the presence of melt inclusions within phenocrysts of pyroxene and/or olivine. Melt inclusions within groundmass phases were not seen during probe analysis. The inability of the OCA-030 modeling results in replicating the overall convex upward K/Ca pattern, may be due to incomplete degassing of the interstitial phases (i.e. the low-temperature step represents about half interstitial phases and half feldspar rim) and/or an overestimate of the amount of interstitial phases present within the sample.

The above observations raise an important paradox. As seen in Table 1, the average size of the phases present is an order of magnitude greater than that of the recoil distance, suggesting that recoil of $^{37}\text{Ar}_{\text{Ca}}$ and $^{39}\text{Ar}_{\text{K}}$ should be negligible. However, in order to generate the convex upward shaped K/Ca and the overall degassing spectra shapes of $^{37}\text{Ar}_{\text{Ca}}$ and $^{39}\text{Ar}_{\text{K}}$ seen in the argon results, it appears that recoil redistribution from interstitial areas into other phases is a significant factor affecting some of the samples studied here.

The above paradox suggests that either one or more of the assumptions used in the modeling are incorrect or that another explanation besides recoil may exist to explain the discrepancy between the argon and probe results. Heizler et al., (1999) suggested an

alternative explanation to account for basaltic samples that initially display old apparent ages followed by younger ages associated with the low-temperature steps. Heizler et al., (1999) suggested that “the old apparent ages and complex age spectra pattern could be related to excess or inherited argon”. Because the old apparent ages are positively correlated to degassing of the interstitial phases and feldspar rim, the phases that crystallize during flow (i.e. they have the greatest likelihood of equilibrating with atmospheric argon), excess argon is inferred not to be a viable explanation. In addition, excess argon would not produce the convex upward shaped K/Ca pattern seen.

Inherited argon from xenocryst contamination has the potential to produce discordance in the age spectrum and alter the K/Ca spectrum. Furthermore, in a study of the petrology and geochemistry of the Ocate Volcanic field, Nielsen and Dungan (1985) found xenocrysts of plagioclase and quartz in some of the rocks they examined. However, great care was taken to remove all visible xenocrysts and phenocrysts during sample preparation and, in the 50+ chips of each sample viewed on the microprobe, no xenocrysts were found. In addition, in order for inherited argon to produce the old apparent ages seen in the low-temperature steps, the xenocrysts would need to degas at low temperatures. Lo et al., (1994) and Koppers et al., (2000) found that phenocryst phases dominate the high-temperature steps and that groundmass phases dominate the low-temperature steps. Therefore, assuming that plagioclase and quartz xenocrysts degas similar to phenocrysts, old apparent ages associated with inherited argon from xenocryst contamination should produce an increase in apparent age with increasing temperature. In addition, xenocrysts should be at least partially degassed in the lava. All other things

being equal, this would result in inherited argon being released during high-temperature steps.

Another possible explanation to resolve the discrepancy between the argon and probe results is that the interstitial phases may not degas together as one phase, as assumed in the modeling. The interstitial phases are generally smaller than 1 μm , therefore, recoil will strongly affect the interstitial phases (Figure 6). Whether or not the interstitial phases will become completely homogenized with respect to $^{39}\text{Ar}_\text{K}$ and $^{37}\text{Ar}_\text{Ca}$ is not known. Assuming that the recoil does not completely homogenize the interstitial phases, if the glass and K-feldspar phases within the interstitial phases degas at low temperatures, and the oxides within the interstitial phases degas at high temperatures along with the pyroxenes, olivine and phenocrysts, then this could account for the convex upward-shaped K/Ca patterns seen within samples OCA-025, OCA-030 and OCA-077 as well as the discordance seen within the age spectra.

3.2.3. Relating the Degassing Behavior to the Sample Characteristics

Now that the degassing behavior of the phases has been addressed, a discussion of how this relates to the sample characteristics is presented. For samples that were collected from the surface of flows (OCA-073 and OCA-079) the majority of potassium resides within the interstitial phases, whereas for samples collected from the core of the flow (OCA-025, OCA-030 and OCA-077) the majority of potassium resides within feldspar rims. These potassium distributions are interpreted to be due to the cooling history of the sample. Flow surface samples cool quickly resulting in K-rich interstitial

phases whereas flow core samples cool relatively slowly resulting in a higher percentage of K-bearing feldspar (Dalrymple and Moore, 1968).

As noted earlier, samples OCA-073 and OCA-079 have descending K/Ca values and approximately fifty percent of the $^{39}\text{Ar}_\text{K}$ is released in the first three heating steps. Also, in these samples, more than half of the total potassium present is concentrated within the interstitial phases. From Figure 7, it appears that only a small degree of recoil has happened within these samples during irradiation. Based on these observations it is interpreted that the relatively large size of zones of interstitial phases results in a smaller degree of recoil redistribution to low-K bearing phases, although recoil probably does homogenize the $^{39}\text{Ar}_\text{K}$ and $^{37}\text{Ar}_\text{Ca}$ within these zones to some extent.

As noted earlier, samples OCA-025 and OCA-077 have initially descending K/Ca values followed by a convex upward shaped K/Ca whereas OCA-030 has a convex upward K/Ca without the initial descending portion. Based on Figure 7, approximately thirty percent recoil is necessary to mimic the overall degassing spectrum and K/Ca pattern seen in the samples. Based on these observations it is interpreted that for samples where the majority of potassium resides within the feldspar rim, recoil redistribution between the feldspar rim and core can significantly affect the argon release patterns. For samples OCA-025 and OCA-077, the $^{39}\text{Ar}_\text{K}$ within the interstitial phases is inferred not to have redistributed significantly, thus retaining the initial high K/Ca values. For sample OCA-030, no initially decreasing K/Ca values are observed, instead, increasing K/Ca values are seen in the low-temperature steps. The modeled results do not reproduce this aspect of the K/Ca spectrum for OCA-030. As discussed earlier, the inability of the OCA-030 modeling results in replicating the overall convex upward K/Ca pattern, may

be due to incomplete degassing of the interstitial phases (i.e. the low-temperature step represents about half interstitial phases and half feldspar rim) and/or an overestimate of the amount of interstitial phases present within the sample.

In summary, flow surface samples are poorly crystallized, the majority of potassium is contained within the interstitial phases and are the least affected by recoil redistribution between low- and high-K phases. In contrast, samples collected from the core of a flow are well crystallized with the majority of potassium contained within the feldspar rim and are the most affected by recoil redistribution between low- and high-K phases.

3.2.4. Relating the Degassing Behavior to the Age Spectrum

Now that the degassing behavior has been interpreted, it can be related to the age spectrum so that the step or steps least affected by recoil, $^{40}\text{Ar}^*$ loss, or excess ^{40}Ar can be identified and used to infer the eruption age of the sample. For sample OCA-030, the old apparent ages associated with the first three steps are interpreted to reflect the degassing of the low-temperature interstitial phases and feldspar rim which have undergone recoil loss (Figure 5). Steps 1025-1650 are interpreted to have young apparent ages due to the addition of $^{39}\text{Ar}_\text{K}$ into the pyroxene and olivine/oxide phases. Steps 725-875 are interpreted to represent the degassing of feldspar and are the best estimate of the eruption age of the sample.

For OCA-025, the young apparent ages associated with the first three steps are interpreted to be due to $^{40}\text{Ar}^*$ loss (Figure 5). The old apparent ages associated with steps 725-825 are interpreted to reflect degassing of the recoil affected feldspar rim. The

old apparent age associated with the 1650 step is inferred to be due to excess ^{40}Ar present within the pyroxene phase. The consistent apparent ages associated with steps 925-1150 are interpreted to represent the degassing of feldspar and olivine/oxide and are the best estimate of the eruption age of the sample.

The first five steps of OCA-077 are interpreted to reflect the degassing of recoil affected interstitial phases and feldspar rim (Figure 5). The young apparent ages associated with steps 1025-1650 are interpreted to reflect the degassing of recoil affected pyroxene and olivine/oxides. Steps 725-975 are interpreted to represent the degassing of feldspar and are the best estimate of the eruption age of the sample.

For sample OCA-073, the young apparent ages seen in steps 550-775 are interpreted to be due to $^{40}\text{Ar}^*$ loss within the interstitial phases (Figure 5). Steps 975-1650 in OCA-073-01 and steps 1075-1650 in OCA-073-02 are interpreted to reflect degassing of olivine/oxide and pyroxene. Steps 825-925 are interpreted to represent the degassing of feldspar core and are the best estimate of the eruption age of the sample.

For sample OCA-079 two interpretations are possible. Interpretation 1 is that the young apparent ages associated with steps 550-725 represent the degassing of interstitial phases which have lost $^{40}\text{Ar}^*$ (Figure 5). The young apparent ages associated with steps 1075-1650 represent the degassing of recoil affected pyroxene and olivine/oxides. The old apparent ages associated with steps 825-975 represents the eruption age of the sample. Interpretation 2 differs from interpretation 1 in that no $^{40}\text{Ar}^*$ loss has happened within the interstitial phases and either excess ^{40}Ar is present within the feldspar core or recoil of $^{39}\text{Ar}_K$ out of feldspar core into pyroxene and olivine/oxide has happened. By

this interpretation, steps 625-725 would best reflect the age of eruption. Interpretation 2 is inferred to be a more plausible explanation.

3.2.5. Sampling Strategy for Obtaining Precise Eruption Ages

The conclusions generated from the above discussions have important implications for what type of samples should be dated so that the best possible results can be obtained. There are several advantages and disadvantages to dating either flow surface or flow interior samples. Because flow surface samples contain large areas of potassium-rich interstitial phases, their age spectra are less disturbed by recoil than are well crystallized flow interior samples. However, because of the larger percentage of glass within flow surface samples and the poor argon retention properties of glass, a large percentage of the age spectrum has the potential to be affected by $^{40}\text{Ar}^*$ loss (Foland et al., 1993). Therefore, because the steps that represent the eruption age comprise a small amount of the total $^{39}\text{Ar}_K$ released, unless the sample size is increased, a relatively large error will be associated with the eruption age due to the small signal size. In addition, for flow surface samples there is large amount of atmospheric argon within the sample (resulting in low radiogenic yields and high analytical uncertainty) and a greater potential to choose the wrong steps when interpreting the age spectrum.

For flow interior samples, because the area containing the interstitial phases is small, recoil redistribution between the interstitial phases and the other phases has the potential to produce age spectrum discordance. However, because flow interior samples contain the majority of potassium within the feldspar rim, the portion of the age spectrum used to calculate the eruption age represents a large percentage of the total $^{39}\text{Ar}_K$ released

resulting in a more precise eruption age. In addition, because glass is not an abundant phases and the majority of the $^{40}\text{Ar}^*$ is within crystallized phases, the radiogenic yields are typically greater than flow surface samples leading to a higher level of precision.

In conclusion, if flow interior samples can be obtained, these samples will yield a more precise age than the corresponding flow surface samples. If flow interior samples can not be obtained then a large sample size should be used to help increase the precision of the eruption age.

3.2.6. General Criteria for Age Assignment in Basaltic Samples

Full geochemical analysis of a basaltic sample is typically the exception rather than the norm due to time and money constraints. However, some useful information can be gathered from the samples analyzed here. First, detailed sample characterization is useful in understanding multi-phased samples (i.e. whole rocks). Second, a plot of the % $^{37}\text{Ar}_{\text{Ca}}$, $^{38}\text{Ar}_{\text{Cl}}$ and $^{39}\text{Ar}_{\text{K}}$ released per step can be very beneficial in interpreting which step or steps to chose for calculation of the eruption age of the sample. Third, the overall shape of the K/Ca plot can give insight into whether recoil has significantly effected the sample. The following criteria is used as a guide to age assignment for all the samples dated in the Ocate geochronology study and is found to be helpful for assigning eruption ages to discordant spectra. In choosing the step or steps:

- 1) Find the step or steps with both a $^{37}\text{Ar}_{\text{Ca}}$ and $^{39}\text{Ar}_{\text{K}}$ peak within the mid-temperature steps.
- 2) Avoid choosing low- and high- temperature steps.
- 3) When in doubt, reanalyze the sample with a different heating schedule.

Although reanalysis of a sample with a different heating schedule does not allow direct comparison of the $^{37}\text{Ar}_{\text{Ca}}$, $^{38}\text{Ar}_{\text{Cl}}$ and $^{39}\text{Ar}_{\text{K}}$ values, it can give insight into possible sample inhomogeneities and, if several analyses are preformed, it can allow the analyses to be examined statistically. In addition, the removal of phenocryst phases during sample preparation can greatly simplify interpretations and increase the percentage of K-bearing phases within the sample. Furthermore, the use of high-resolution heating steps can better define the gas reservoirs.

An important aspect of this study that allowed comparison between samples and utilization of the new criteria is the use of consistent heating schedules for all analyses. This is because the $^{37}\text{Ar}_{\text{Ca}}$, $^{38}\text{Ar}_{\text{Cl}}$ and $^{39}\text{Ar}_{\text{K}}$ release spectra are in part a function of the heating schedule used. By utilizing a heating schedule with consistent temperature intervals, the $^{37}\text{Ar}_{\text{Ca}}$, $^{38}\text{Ar}_{\text{Cl}}$ and $^{39}\text{Ar}_{\text{K}}$ release spectra can be properly interpreted and the new criteria can be applied to other basaltic data.

Based on the results given in this study, no advantage is seen in applying a strict “plateau” criteria. Whether or not a sample will display a “plateau” is dependent on the phases present, their chemistry, grain size and modal abundance as well as the crystallinity of the sample and the heating schedule used. Furthermore, a “plateau” criteria is arbitrary. For flow surface samples in which some $^{40}\text{Ar}^*$ loss has occurred within the glass phase, a plateau criteria will typically incorrectly choose the low-temperature steps. For example, if the plateau criteria suggested by Fleck et al., (1977) is used for sample OCA-073-02 (Figure 5), steps 550-725 would have been selected resulting in an underestimate of the eruption age. This is because the low-temperature steps for flow surface samples typically comprise about half of the total $^{39}\text{Ar}_{\text{K}}$ released

and are usually within error of each other due to the large errors associated with their low radiogenic yields.

Seventy-nine percent of the samples analyzed in this study were collected from the interior of flows. For these samples a “plateau” criteria would choose many of the same steps for calculation of the eruption age as that used in this study utilizing the new approach. For flow surface samples, however, the “plateau” approach will yield eruption ages less than or equal to the eruption age calculated using the approach outlined above. An added advantage associated with the use of the new approach is that eruption ages for all dated samples can be calculated. The plateau criteria used by Fleck et al., (1977) and Singer and Pringle (1996) choose three or more steps that are within analytical error at 2σ and comprise greater than fifty percent of the $^{39}\text{Ar}_\text{K}$ released. By applying such a strict criteria, if a sample displays three or more steps that are within error of each other at the 2σ confidence level but comprise only forty percent of the $^{39}\text{Ar}_\text{K}$ released, an eruption age can not be determined unless the criteria is modified.

To illustrate these points, Figure 8 displays the eruption ages calculated by both the Fleck et al., (1977) plateau criteria and the new criteria outlined above for five samples collected from a flow unit located in the Rivera Mesas area of the Ocate Volcanic field (see Section 6 for the rest of the geologic results and Appendix A and B for the data Tables and age spectra). As noted in Figure 8, one sample was collected from the vent (OCA-071), one from the surface of the flow (OCA-073) and three from the flow interior (OCA-039, -040 and -041). Sample OCA-073 was analyzed three times, twice with the furnace and once with the CO₂ laser (See Section 5 for details concerning the laser analyses). Two possible plateau ages exist for OCA-073-01 whereas

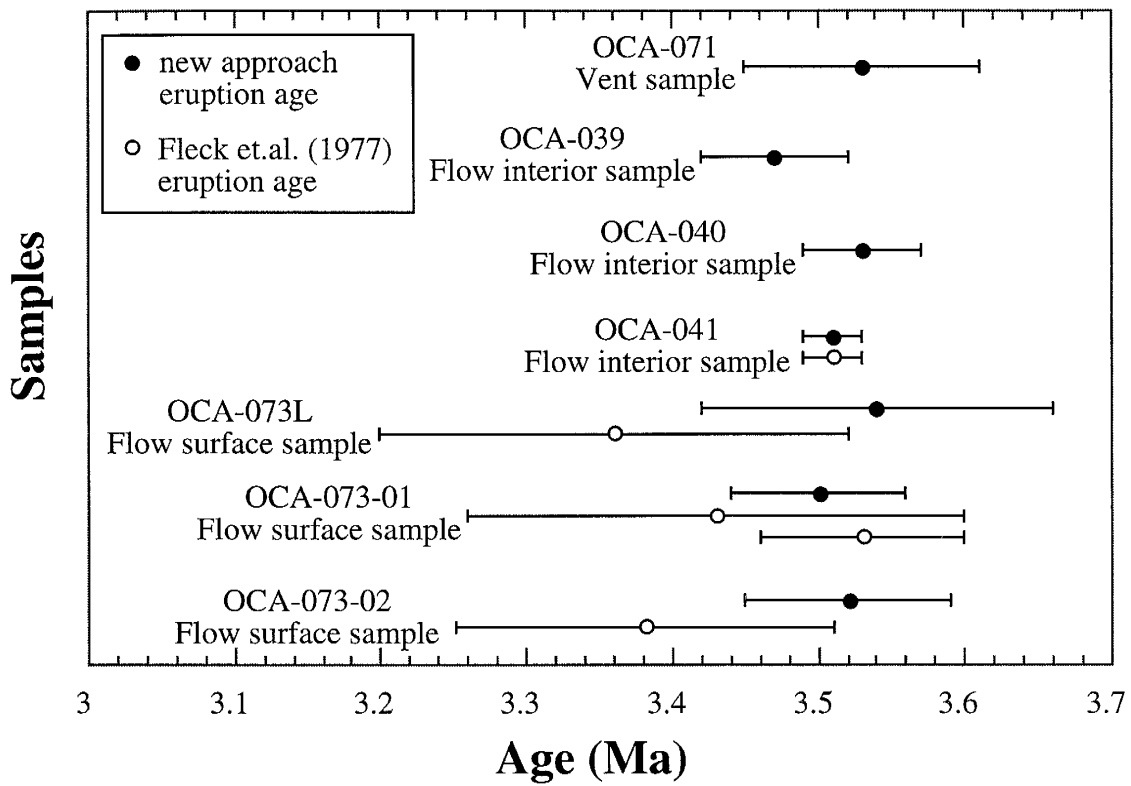


Figure 8. Comparison between Fleck et.al. (1977) plateau criteria and the new approach outlined in the text of eruption age calculations for samples collected from a flow unit in the Rivera Mesas area of the Ocate Volcanic field. Samples OCA-071, -040 and -039 do not meet the "plateau" criteria. Two "plateaus" exist for sample OCA-073-01.

three of the samples do not contain a plateau (OCA-039, -040 and -071). For the flow interior sample OCA-041, the plateau age agrees well with the eruption age calculated with the new approach outlined above. However, for the replicate analyses of the flow surface sample OCA-073, the plateau age underestimates the eruption age in two out of the three replicate analyses as well as yielding eruption ages with a greater level of uncertainty.

4. $^{40}\text{Ar}/^{39}\text{Ar}$ Experiment: Phenocryst Concentrate Analyses

One of the major problems hindering a simple interpretation and age assignment of basaltic age spectra is the differential thermal degassing of the various phases within a groundmass concentrate (Section 3). However, because of the fine-grained texture of a basalt sample, separation and subsequent analysis of the different groundmass phases is not practical. Because of problems associated with interpretation and age assignment of basaltic samples, several workers have analyzed phenocryst concentrates to avoid the problems associated with multiphase samples (Koppers et al., 2000; Singer and Pringle, 1996; Foland et al., 1993; Feraud et al., 1986).

Geologically unrealistic old ages have been noted in the dating of both plutonic and volcanic phenocryst separates due to excess ^{40}Ar incorporated within the crystals (Damon et al., 1967; McDougall and Harrison, 1999). Plagioclase, olivine and pyroxene, all common phenocryst phases in basalt samples, have been shown to contain excess ^{40}Ar (Hart and Dodd, 1962; Burke et al., 1969; Laughlin et al., 1969; McDougall et al., 1969). In an attempt to constrain the degassing behavior of the phenocryst phases, to compare the eruption ages obtained from phenocryst concentrates with ages of their corresponding groundmass concentrates and to evaluate the presence of excess ^{40}Ar within Ocate basalts, three phenocryst concentrates (plagioclase, pyroxene, and olivine) from three different samples were analyzed and compared with the groundmass concentrates from which they were separated. For the geologic context from which these samples were collected, see Section 6.

4.1. Results

Results from the phenocryst concentrates along with their corresponding groundmass concentrates are given in Figure 9 and Table 3. For sample OCA-039plag the two highest-temperature steps contain the greatest percentage of $^{37}\text{Ar}_{\text{Ca}}$, $^{38}\text{Ar}_{\text{Cl}}$ and $^{39}\text{Ar}_{\text{K}}$ released per step. For sample OCA-039CPX the two highest-temperature steps contain the greatest percentage of $^{37}\text{Ar}_{\text{Ca}}$ and $^{38}\text{Ar}_{\text{Cl}}$ released per step whereas the greatest percentage of $^{39}\text{Ar}_{\text{K}}$ released per step exists at the 875°C step. For sample OCA-008oliv the highest-temperature step contains the greatest percentage of $^{37}\text{Ar}_{\text{Ca}}$ and $^{39}\text{Ar}_{\text{K}}$ released per step whereas the greatest percentage of $^{38}\text{Ar}_{\text{Cl}}$ released per step exists at the lowest-temperature step.

Similarities in apparent ages for all pairs of groundmass and phenocryst concentrate analyses are seen in the low- and mid-temperature steps. For OCA-008oliv the apparent ages for steps 1075-1275 are less than the groundmass concentrate eruption age (OCA-008) whereas step 1650 is greater than the groundmass concentrate eruption age (OCA-008). For OCA-038CPX the apparent ages for step 1375-1650 are less than the groundmass concentrate eruption age (OCA-038). For OCA-039plag the apparent age for step 1650 is greater than that of the groundmass concentrate eruption age (OCA-039).

4.2. Discussion

Because groundmass phases adhered to the rims of the phenocryst phases were not removed and due to the low potassium contents of the phenocryst phases, evaluation of each phenocryst's potassium contribution must first be addressed. Table 4 lists the

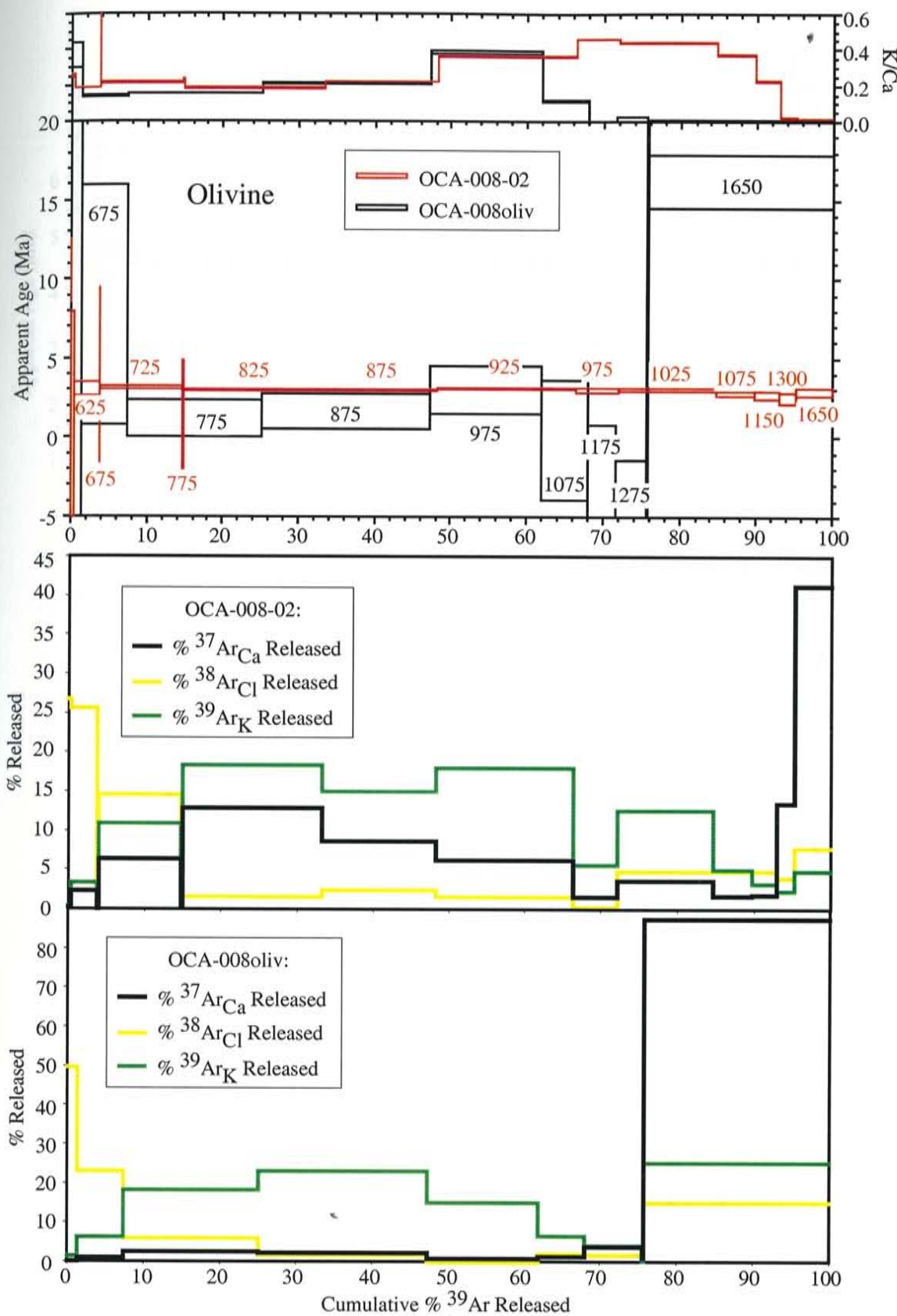


Figure 9. Comparison between phenocryst and groundmass concentrate age spectra.

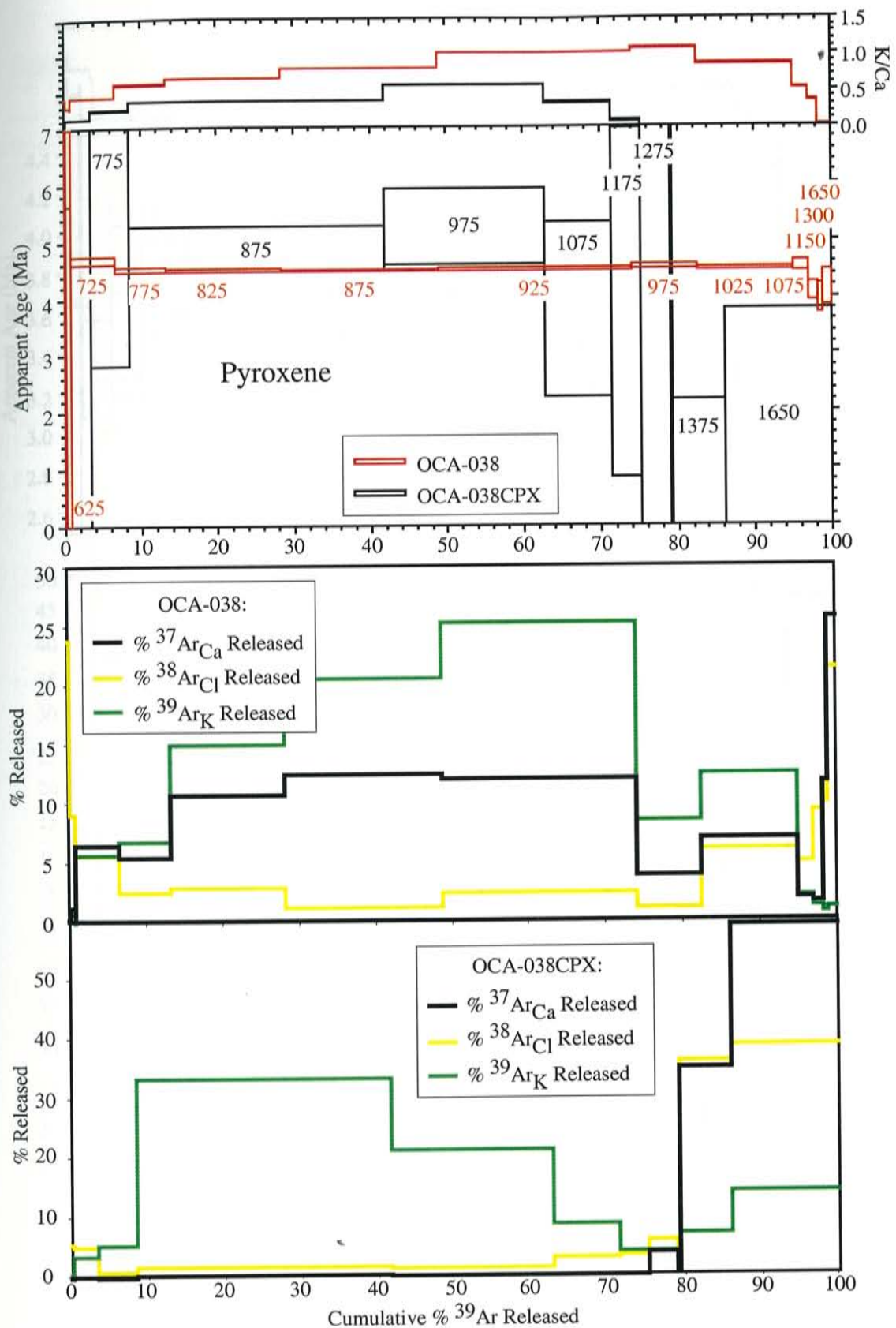


Figure 9 continued.

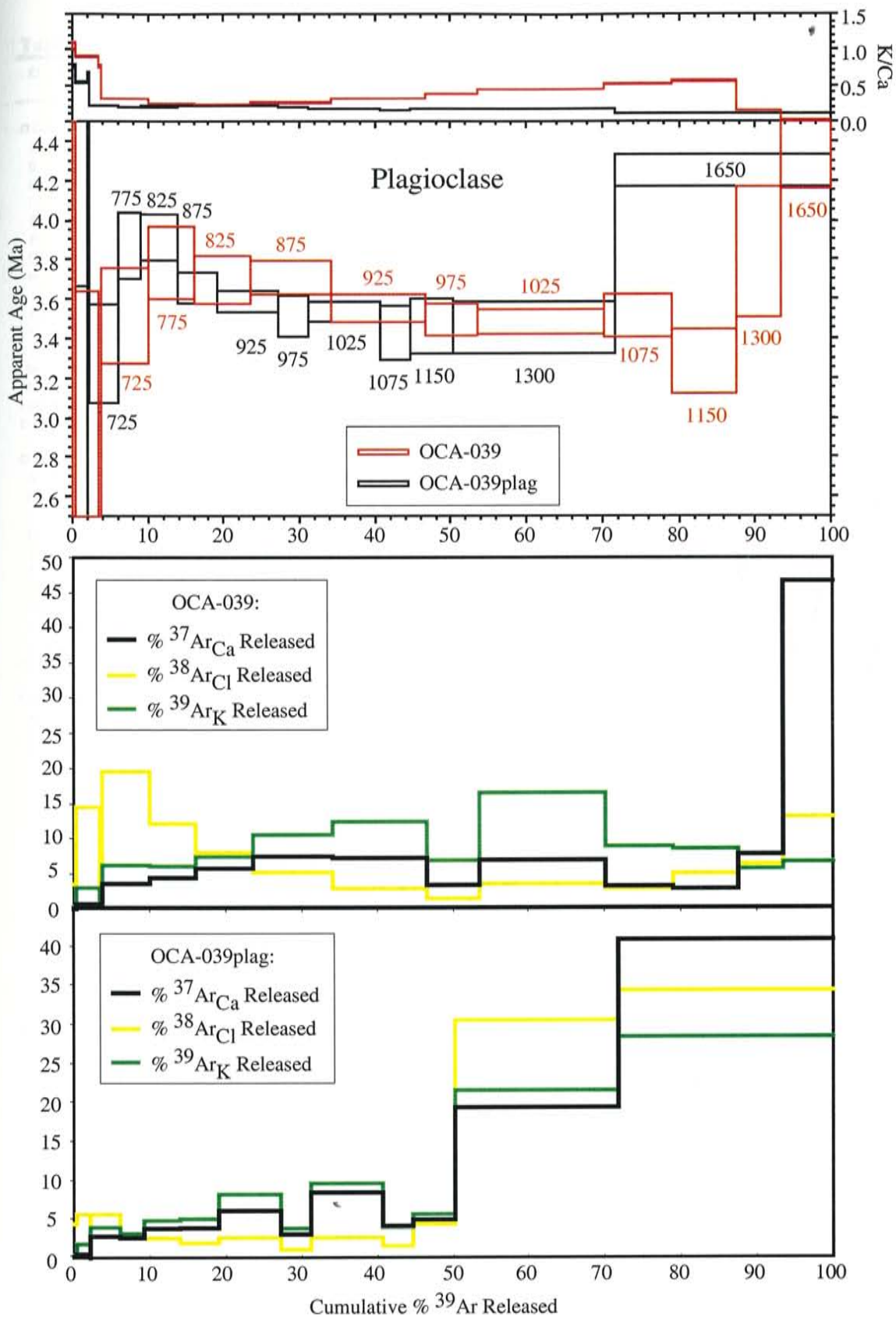


Figure 9 continued.

Table 3: Argon Data Table for Phenocryst Concentrate Analyses

Table 3 continued

ID	Temp (°C)	$^{40}\text{Ar}/^{39}\text{Ar}$	$^{37}\text{Ar}/^{39}\text{Ar}$	$^{36}\text{Ar}/^{39}\text{Ar}$	$^{39}\text{Ar}_K$ (mol)	K/Ca	Cl/K	$^{37}\text{Ar}_{\text{Ca}}$ (%)	$^{38}\text{Ar}_{\text{Cl}}$ (%)	$^{39}\text{Ar}_K$ (%)	$^{40}\text{Ar}^*$ (%)	^{39}Ar (%)	Age (Ma)	$\pm 2\sigma$ (Ma)	
OCA-039; ?2:121, groundmass concentrate, 90.30mg, J=0.000479454±0.10%, D=1.00644±0.00091, NM-121, Lab#=51082-01															
A	550	3.10E+02	4.81E-01	1.04E+00	5.2E-16	1.1E+00	7.6E-02	0.1	3.5	0.3	0.6	0.3	1.74	8.33	
B	625	5.83E+01	5.67E-01	1.86E-01	4.8E-15	9.0E-01	3.4E-02	0.7	14.5	3.1	5.8	3.4	2.94	0.66	
C	675	4.33E+01	6.61E-01	1.41E-01	4.7E-16	7.7E-01	3.3E-02	0.1	1.4	0.3	3.7	3.8	1.37	1.62	
D	725	2.83E+01	1.55E+00	8.27E-02	9.7E-15	3.3E-01	2.3E-02	3.6	19.6	6.3	14.2	10.0	3.47	0.24	
E	775	1.77E+01	1.95E+00	4.58E-02	9.5E-15	2.6E-01	1.5E-02	4.4	12.2	6.1	24.3	16.2	3.74	0.18	
F	825	1.13E+01	2.10E+00	2.43E-02	1.1E-14	2.4E-01	7.9E-03	5.8	8.0	7.4	37.4	23.6	3.65	0.12	
G	875	7.78E+00	1.90E+00	1.24E-02	1.6E-14	2.7E-01	3.6E-03	7.4	5.2	10.6	54.5	34.2	3.66	0.08	
H	925	6.45E+00	1.58E+00	8.41E-03	1.9E-14	3.2E-01	1.8E-03	7.2	3.0	12.4	62.9	46.6	3.51	0.07	
I	975	6.40E+00	1.31E+00	8.40E-03	1.1E-14	3.9E-01	1.5E-03	3.4	1.5	7.0	62.4	53.6	3.45	0.08	
J	1025	7.02E+00	1.13E+00	1.05E-02	2.6E-14	4.5E-01	1.6E-03	6.9	3.6	16.5	56.7	70.1	3.44	0.06	
K	1075	1.07E+01	9.85E-01	2.28E-02	1.4E-14	5.2E-01	2.4E-03	3.2	3.0	8.9	37.6	79.0	3.47	0.11	
L	1150	2.05E+01	9.04E-01	5.67E-02	1.3E-14	5.6E-01	4.3E-03	2.9	5.0	8.5	18.3	87.6	3.25	0.16	
M	1300	3.83E+01	3.63E+00	1.16E-01	8.9E-15	1.4E-01	8.1E-03	7.8	6.4	5.8	11.4	93.4	3.79	0.33	
N	1650	4.49E+01	1.90E+01	1.39E-01	1.0E-14	2.7E-02	1.4E-02	46.7	13.1	6.6	11.5	100.0	4.51	0.40	
total gas age		n=14											3.56	0.19	
Eruption Age		n=4	steps H-K	6.9E-14	4.2E-01								44.8	3.47	0.05
OCA-039plag; ?6:121, phenocryst concentrate, 159.05mg, J=0.000479502±0.10%, D=1.00644±0.00091, NM-121, Lab#=51080-(
A	550	5.96E+02	6.61E-01	2.04E+00	5.7E-16	7.7E-01	1.6E-01	0.1	4.3	0.3	-0.9	0.3	-4.50	18.39	
B	625	8.24E+01	9.25E-01	2.68E-01	3.3E-15	5.5E-01	3.7E-02	0.5	5.7	1.8	3.8	2.1	2.73	0.89	
C	675	2.32E+01	8.00E-01	3.22E-02	1.4E-16	6.4E-01	4.1E-02	0.0	0.3	0.1	59.3	2.1	11.88	3.80	
D	725	1.67E+01	2.35E+00	4.43E-02	7.3E-15	2.2E-01	1.6E-02	2.8	5.6	3.9	22.7	6.1	3.28	0.24	
E	775	8.88E+00	2.63E+00	1.57E-02	5.7E-15	1.9E-01	9.2E-03	2.5	2.5	3.1	49.7	9.1	3.82	0.16	
F	825	6.75E+00	2.54E+00	8.31E-03	9.0E-15	2.0E-01	6.1E-03	3.7	2.6	4.8	66.1	14.0	3.86	0.11	
G	875	5.95E+00	2.45E+00	6.56E-03	9.5E-15	2.1E-01	4.3E-03	3.8	1.9	5.1	70.1	19.0	3.61	0.08	
H	925	5.40E+00	2.42E+00	4.98E-03	1.5E-14	2.1E-01	3.7E-03	6.0	2.6	8.2	75.7	27.2	3.54	0.06	
I	975	5.30E+00	2.58E+00	4.94E-03	7.2E-15	2.0E-01	3.3E-03	3.0	1.1	3.9	75.7	31.1	3.47	0.11	
J	1025	5.87E+00	2.91E+00	6.89E-03	1.8E-14	1.8E-01	3.1E-03	8.5	2.6	9.5	68.7	40.7	3.49	0.05	
K	1075	7.68E+00	3.33E+00	1.36E-02	7.4E-15	1.5E-01	4.6E-03	4.0	1.6	4.0	50.9	44.7	3.38	0.14	
L	1150	1.13E+01	2.91E+00	2.57E-02	1.0E-14	1.8E-01	8.7E-03	5.0	4.3	5.6	34.8	50.3	3.42	0.14	
M	1300	2.09E+01	2.97E+00	5.81E-02	4.0E-14	1.7E-01	1.6E-02	19.4	30.5	21.4	18.8	71.7	3.41	0.13	
N	1650	1.41E+01	4.75E+00	3.24E-02	5.3E-14	1.1E-01	1.4E-02	40.8	34.3	28.3	34.4	100.0	4.20	0.08	
total gas age		n=14											3.66	0.18	

Table 4: Phenocryst Concentrate Data

Sample ID	Phases	K ₂ O (wt.%) ¹	CaO (wt.%)	K/Ca	(moles ³⁹ Ar _K / mg)	calc. modal %	K ₂ O (%) ²	CaO (%) ²	max. excess ⁴⁰ Ar (moles/g)
OCA-008oliv:									
	groundmass	1.5 ¹	10 ¹	0.2	1.02E-15	1	≥ 34	23	
	phenocryst	≤ 0.03	0.18-0.50	≤ 0.2	6.43E-18	99	≤ 66	77	9.58E-14
OCA-038CPX:									
	groundmass	1.5 ¹	10 ¹	0.2	5.84E-15	1	≥ 34	0.5	
	phenocryst	≤ 0.03	20.19-21.59	≤ 0.002	4.02E-19	99	≤ 66	99.5	-
OCA-039plag:									
	groundmass	1.5 ¹	10 ¹	0.2	1.66E-15	42	72	41	
	phenocryst	0.31-0.52	9.30-11.77	0.06-0.03	1.19E-15	58	28	59	1.64E-13

¹ Estimated values for bulk groundmass.² Percent K₂O and CaO within each phase based on median K₂O and CaO values

data and calculation results. A mass balance calculation of the modal percentage of each phenocyst phase relative to their groundmass phases was performed by utilizing the total moles per milligram of $^{39}\text{Ar}_\text{K}$ released for each group of groundmass and phenocryst analyses. Both the OCA-008oliv and OCA-038CPX phenocryst concentrates contain 99% phenocrysts and 1% groundmass and the OCA-039plag phenocryst concentrate contains 58% phenocrysts and 42% groundmass, based on mass balance calculations and supported by microprobe observations. The olivine and pyroxene phases each comprise at most, 66% of the total K_2O within each of the OCA-008oliv and OCA-038CPX phenocryst concentrates analyzed, respectively. The plagioclase separate contains 28% of the total K_2O within the phenocryst concentrate analyzed (Table 4).

The different phenocryst phases are interpreted to degas at temperatures higher than $\sim 1025^\circ\text{C}$. The interpretation is based on the large percentage of $^{37}\text{Ar}_\text{Ca}$, $^{38}\text{Ar}_\text{Cl}$ and $^{39}\text{Ar}_\text{K}$ released per step within the high-temperature steps and agrees with the previous interpretations found by Lo et al., (1994) and Feraud et al., (1986). Because groundmass phases adhered to the rim of the phenocryst concentrates were not completely removed, degassing of these phases is seen in the low- to mid-temperature steps.

The old apparent ages seen in step 1650 of both OCA-008oliv and OCA-039plag are interpreted to be a result of excess ^{40}Ar within the phenocrysts. An alternative explanation would be that the old apparent ages are due to incorrect Ca-correction (Turner and Cadogan, 1974). However, calculations using extreme values for the $^{39}\text{Ar}/^{37}\text{Ar}$ and $^{36}\text{Ar}/^{37}\text{Ar}$ Ca-corrections yield ages within error of the apparent ages reported. Therefore, incorrect Ca-correction is not a valid explanation for the high apparent ages seen in the 1650 steps of the plagioclase and olivine phenocryst

concentrate analyses. For the two high-temperature steps in the pyroxene analysis, varying the $^{39}\text{Ar}/^{37}\text{Ar}$ Ca-correction between 0.00065 and 0.0009, and the $^{36}\text{Ar}/^{37}\text{Ar}$ Ca-correction between 0.00021 and 0.00029, yields changes in the apparent ages of these steps by as much as 50 and 90 Ma years for the 1375 and 1650 steps, respectively. However, the correction factors for the Michigan reactor have been measured extensively by the NMGRRL and although large ranges are possible, the correction factors are precisely known (Appendix A). The apparent age uncertainty associated with the two highest-temperature steps for the pyroxene analyses is assumed to reflect this. Therefore, due to the young apparent ages seen in these steps, significant excess ^{40}Ar within the pyroxene phases probably does not exist. The young apparent ages seen in the high-temperature steps of OCA-008oliv may be a result of the addition of recoiled $^{39}\text{Ar}_\text{K}$ from the groundmass phases into the phenocryst.

For all the analyses, the ages associated with the groundmass analyses are interpreted to be geologically meaningful. The old and young apparent ages associated with the degassing of the olivine and pyroxene phenocrysts (OCA008oliv and OCA-038CPX, respectively) are geologically inaccurate. In contrast, steps 1025-1300 for the plagioclase separate (OCA-039plag) are in agreement with steps 925-1075 of OCA-039, the steps chosen to represent the eruption age of the groundmass concentrate. However, this is in part due to the large percentage of groundmass adhered to the plagioclase grains making the conclusion indefinite (Table 4).

Also listed in Table 4 is the maximum amount (moles/g) of excess ^{40}Ar contained within both the plagioclase and olivine phenocryst concentrate analyses based on the comparison between the old apparent age associated with step 1650 and the eruption age

for each sample. The excess ^{40}Ar contents for OCA-008oliv and OCA-039plag are 9.58×10^{-14} and 1.64×10^{-13} moles/g, respectively (Table 4). These quantities are about an order of magnitude less than that found by Damon et al., (1967) for the volcanic minerals they studied, and several orders of magnitude lower than the amounts found in some minerals found from intrusive rocks, as summarized by Damon et al. In an experiment on an olivine analysis from a sample in the neighboring Raton-Clayton field, Stroud (1997) found a similar amount of excess ^{40}Ar (4.45×10^{-14} moles/g) as that found in this study.

Because the majority of phenocryst phases were removed from all groundmass samples, excess ^{40}Ar is inferred not to be a significant factor affecting the results. Furthermore, from the phenocryst concentrate analyses it has been shown that even if phenocrysts from a given sample do contain appreciable amounts of excess ^{40}Ar , the phenocrysts will degas their excess ^{40}Ar at high temperatures. Therefore, even if excess ^{40}Ar is contained within phenocryst phases, step-heating of the sample will allow the old apparent ages associated with the high-temperature steps to be detected and avoided when calculating the eruption age of the sample. However, if excess ^{40}Ar is incorporated within the groundmass phases, detection will not be possible. Although this may be a potential problem, a precautionary sample collection technique can be made.

In a study comparing the glass content of fresh samples of young submarine basalts to the quantity of excess ^{40}Ar , Funkhouser et al., (1968) found that the presence of excess ^{40}Ar is related to the glass content of the samples: the greater the glass content, the greater the amount of excess ^{40}Ar present, whereas the more crystalline interior portions of the flow showed less or no excess ^{40}Ar present. Funkhouser et al., (1968) attributed

this to the cooling history of the sample, where formation and growth of crystals would tend to force out the ambient rare gases from the solid phases into the intercrystalline "mush" where it can diffuse out of the rock more rapidly, whereas if the magma is rapidly quenched, the ambient gases are more likely to be frozen into the basaltic glass. Therefore, based on the Funkhouser et al., (1968) study, by collecting flow interior samples which contain small amounts of glass (Table 1), the chances of the sample containing excess ^{40}Ar incorporated within the groundmass is minimized. This further supports the conclusion found in Section 3, that flow interior samples yield better $^{40}\text{Ar}/^{39}\text{Ar}$ results than flow surface samples and should be collected whenever possible.

5. $^{40}\text{Ar}/^{39}\text{Ar}$ Experiment: Laser vs. Furnace Step-Heating Analyses

Step-heating analyses of basaltic samples using a CO₂ laser offers a potential advantage to furnace step-heating due to the lower extraction line blank (Section 2.2.). However, differences or similarities in the degassing behavior of a basalt sample or the eruption ages calculated between the two step-heating techniques have not been addressed. Five basaltic samples were step-heated both with the laser and furnace to compare the two techniques.

5.1. Results

The results of the laser and furnace step-heating analyses are given in Table 5 and Figure 10. See Section 3 for the chemical and petrographic characteristics of samples OCA-030, -073, -077 and -079. See Section 6 for the geologic context from which the samples were collected. Replicate laser step-heating analyses were performed for samples OCA-079 and OCA-030.

In all samples except for OCA-030 and OCA-079, no significant difference between the two techniques is seen in the radiogenic yields, K/Ca, Cl/K and apparent age values. For OCA-030 and OCA-079, the laser and furnace radiogenic yields, K/Ca and Cl/K spectra agree with each other. For OCA-030, although the laser reproduces the old and young apparent ages for the low- and high-temperature steps, respectively, the eruption ages between the furnace and two laser analyses are not within 2σ error of each other. For OCA-079, the old apparent ages seen in the mid-temperature steps of the furnace analysis are not reproduced by the two laser analyses. Overall, compared with the furnace technique, the laser technique reproduces the radiogenic yields, K/Ca, Cl/K

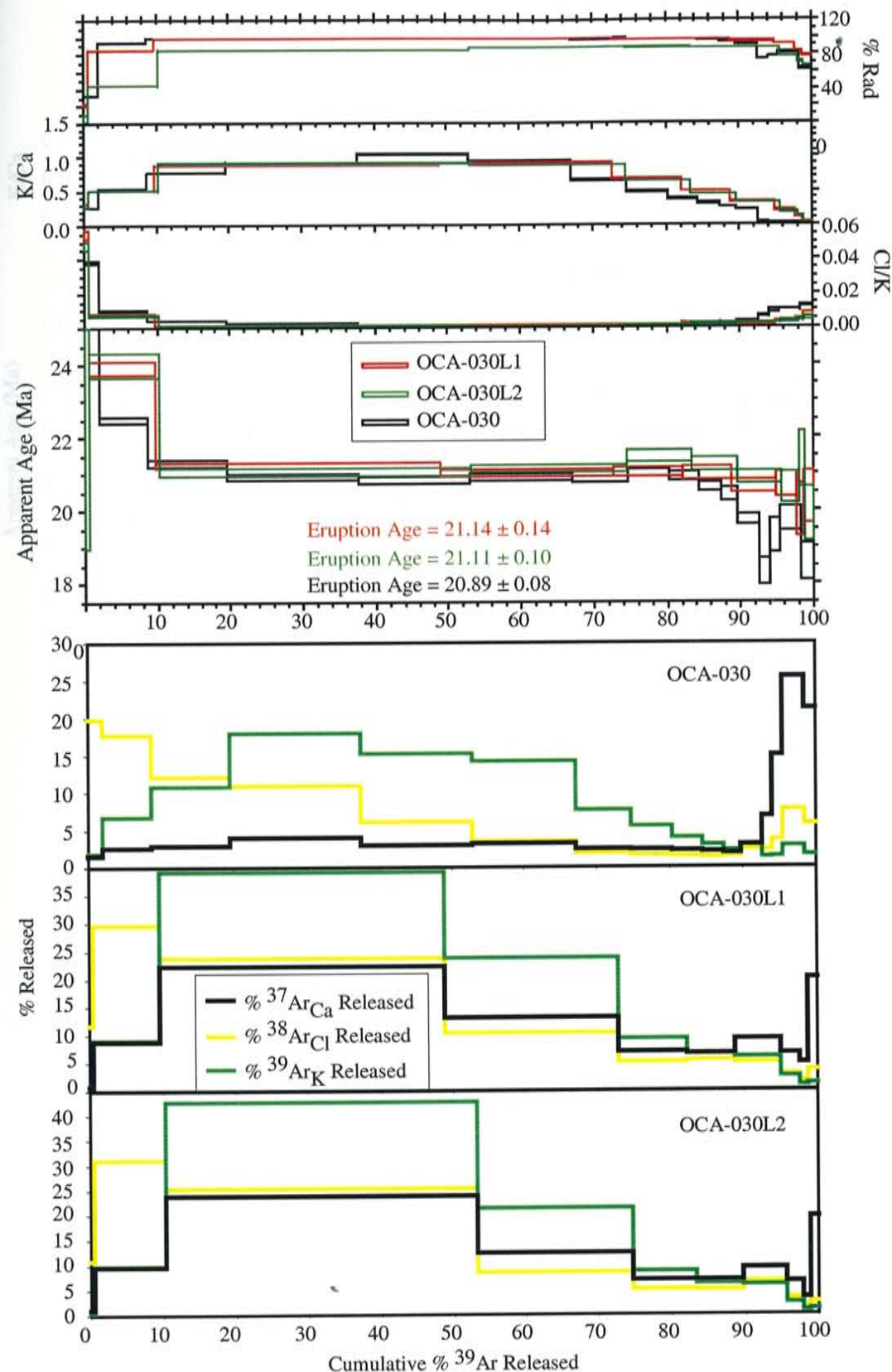


Figure 10. Comparison between laser and furnace age spectra ("L" represents laser).

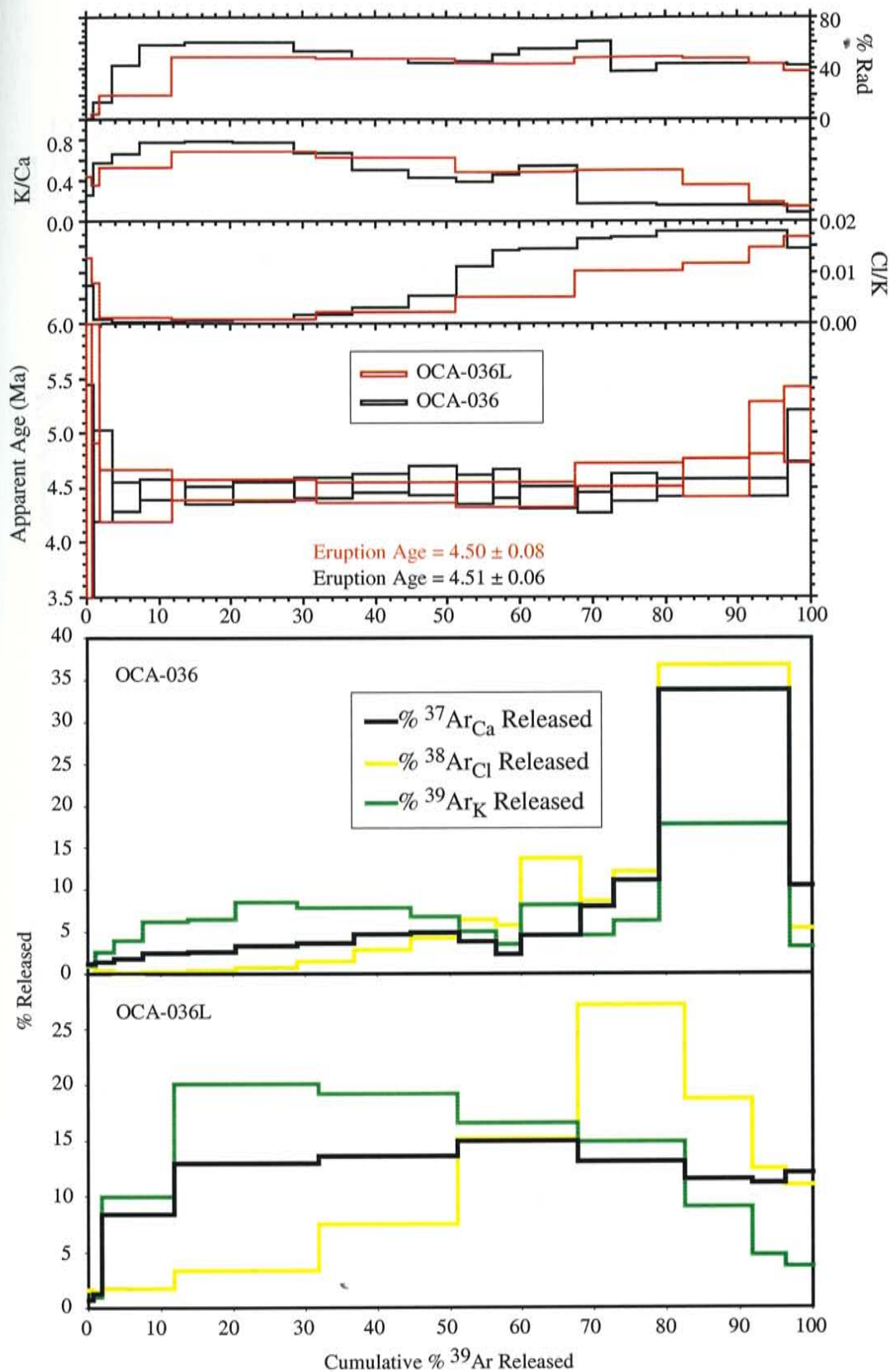


Figure 10 continued.

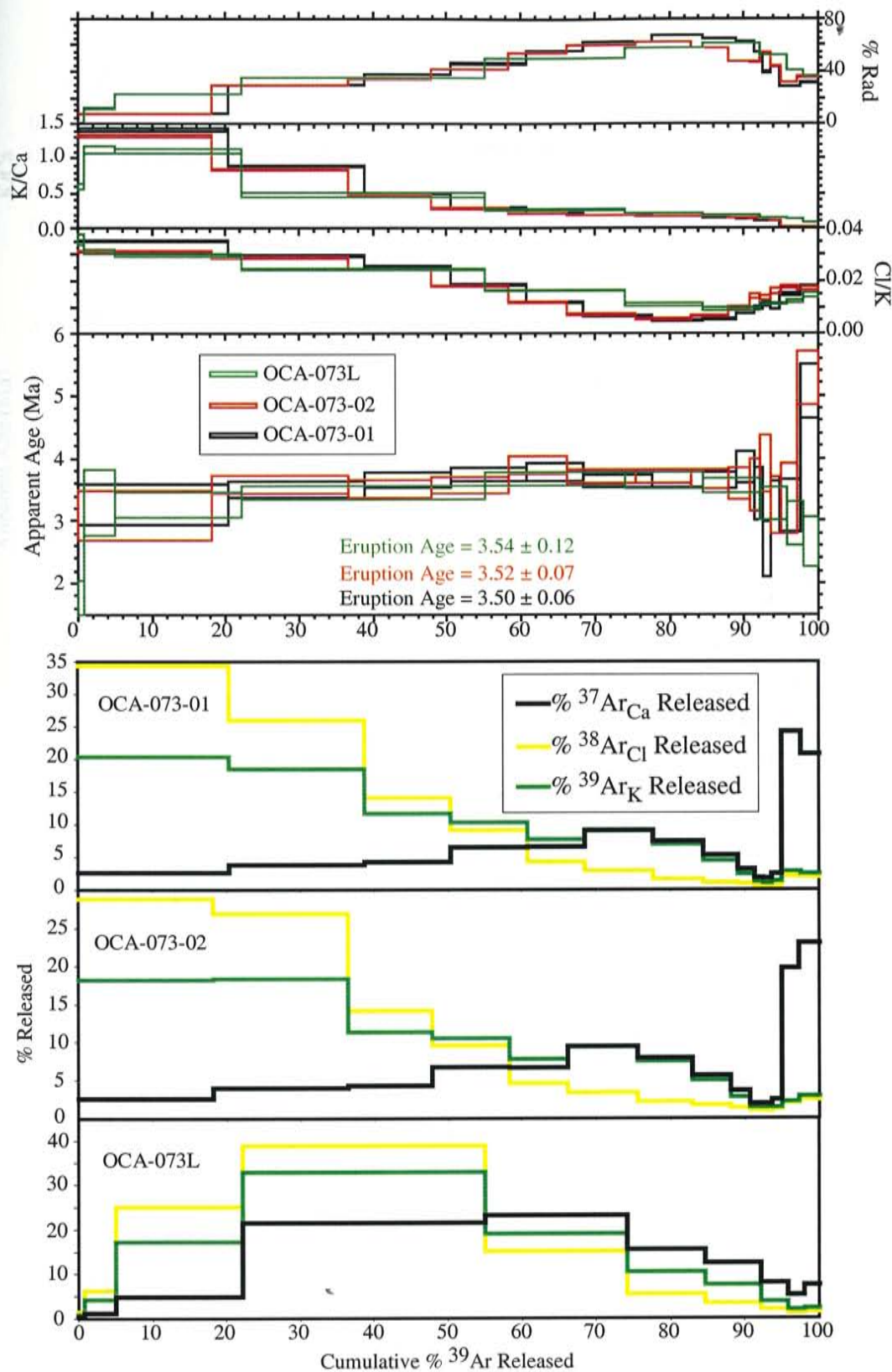


Figure 10 continued.

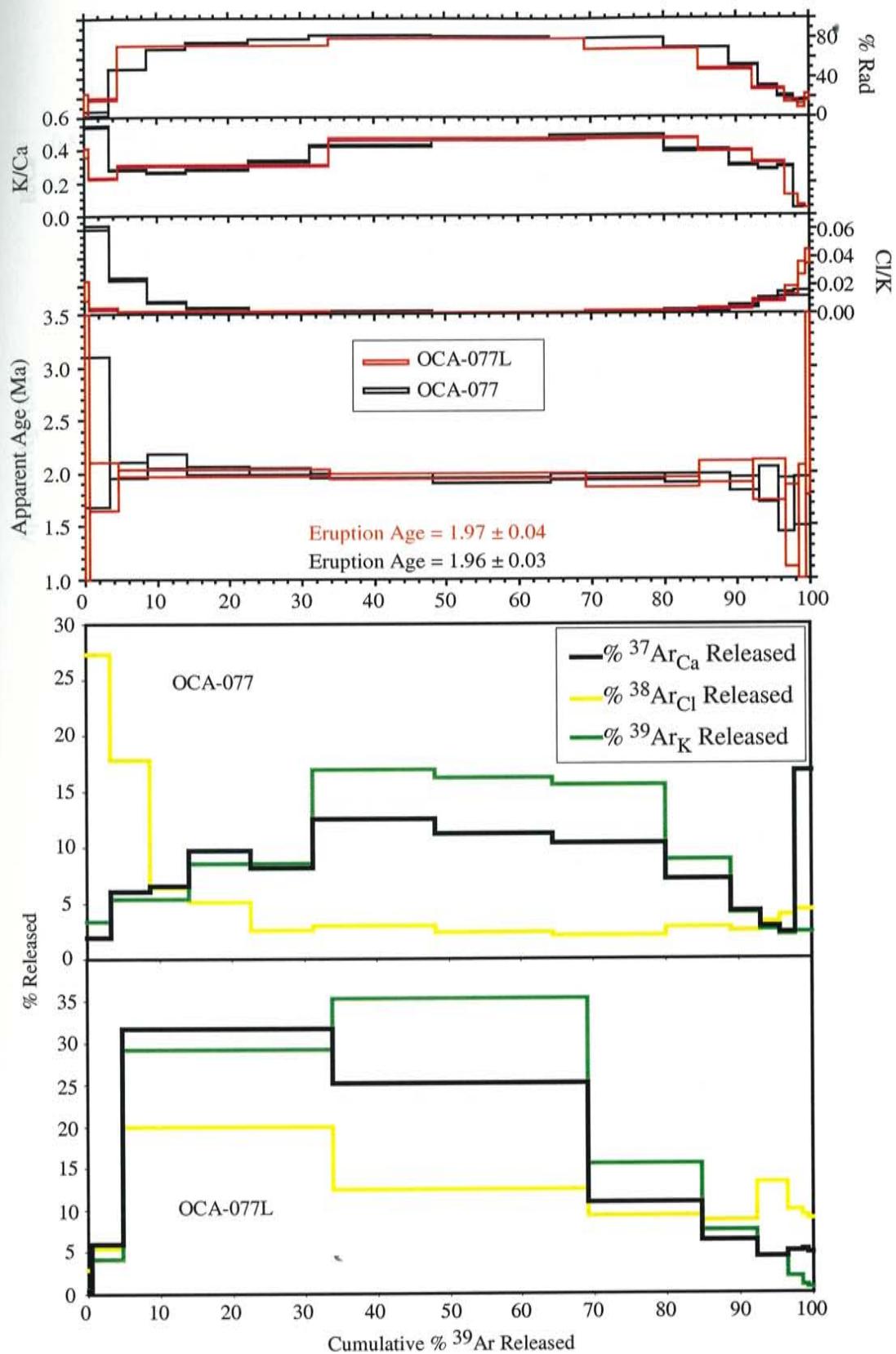


Figure 10 continued.

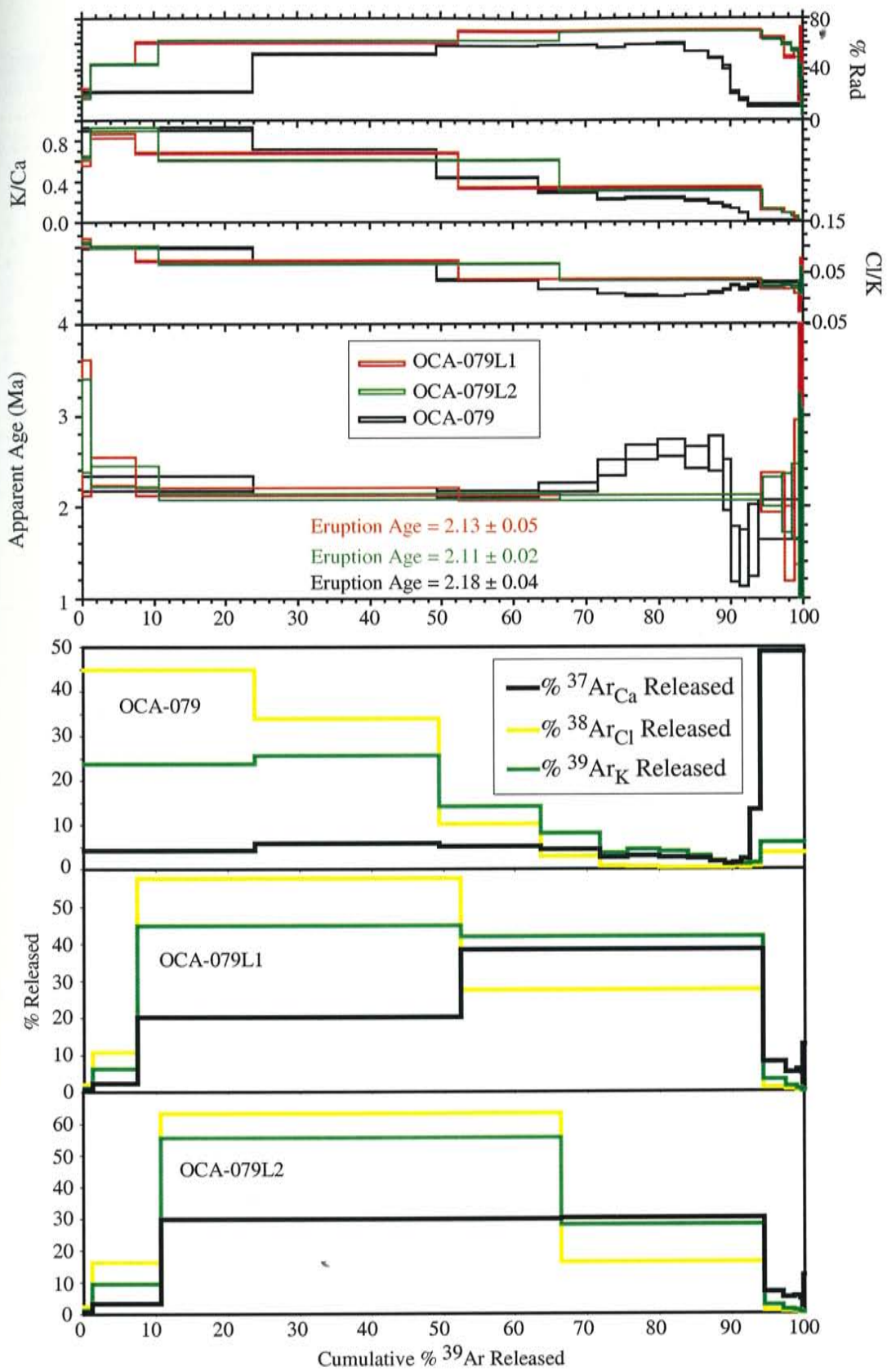


Figure 10 continued.

Table 5: Argon Data Table for Laser and Furnace Analyses

ID	Temp/P (°C/W)	⁴⁰ Ar	³⁹ Ar	³⁷ Ar	³⁸ Ar	⁴⁰ Ar	³⁹ Ar	K/Ca	Cl/K	³⁷ Ar/Ca	³⁸ Ar/Ca	³⁹ Ar/Cl	⁴⁰ Ar/K	⁴⁰ Ar*	³⁹ Ar	Age	±2σ (Ma)
OCA-030; A2;117, groundmass concentrate, 81.08mg, J=0.001072496±0.10%, D=1.00644±0.00091, NM-117, Lab#=50832-01																	
A	550	5.04E+01	2.03E+00	1.16E-01	1.1E-14	2.5E-01	3.9E-02	1.6	19.8	1.9	32.1	1.9	31.15	0.75			
B	625	1.24E+01	9.52E-01	2.53E-03	3.7E-14	5.4E-01	9.8E-03	2.6	17.7	6.8	94.4	8.7	22.48	0.09			
C	675	1.12E+01	6.60E-01	5.85E-04	6.0E-14	7.7E-01	4.2E-03	2.9	12.2	10.9	98.7	19.6	21.32	0.10			
D	725	1.10E+01	5.55E-01	4.79E-04	9.9E-14	9.2E-01	2.3E-03	4.1	10.9	18.0	98.9	37.6	20.94	0.07			
E	775	1.09E+01	4.89E-01	3.74E-04	8.4E-14	1.0E+00	1.5E-03	3.1	6.1	15.3	99.1	52.9	20.82	0.09			
F	825	1.10E+01	5.48E-01	4.34E-04	7.9E-14	9.3E-01	9.4E-04	3.2	3.5	14.2	99.0	67.1	20.92	0.10			
G	875	1.10E+01	7.84E-01	6.69E-04	4.2E-14	6.5E-01	9.5E-04	2.5	1.9	7.6	98.6	74.8	20.84	0.09			
H	925	1.11E+01	1.05E+00	9.31E-04	3.1E-14	4.9E-01	1.1E-03	2.4	1.7	5.6	98.1	80.3	21.03	0.09			
I	975	1.12E+01	1.36E+00	1.38E-03	2.2E-14	3.7E-01	1.5E-03	2.2	1.5	4.0	97.1	84.3	20.93	0.11			
J	1025	1.12E+01	1.66E+00	1.95E-03	1.7E-14	3.1E-01	1.7E-03	2.1	1.3	3.0	95.9	87.4	20.65	0.13			
K	1075	1.12E+01	2.02E+00	2.65E-03	1.3E-14	2.5E-01	2.5E-03	1.9	1.5	2.3	94.3	89.6	20.44	0.18			
L	1150	1.13E+01	2.46E+00	4.10E-03	1.7E-14	2.1E-01	3.0E-03	3.1	2.4	3.0	90.9	92.7	19.74	0.15			
M	1225	1.27E+01	1.24E+01	1.45E-02	7.4E-15	4.1E-02	6.5E-03	6.8	2.3	1.3	74.3	94.0	18.35	0.33			
N	1300	1.27E+01	2.53E+01	1.68E-02	8.0E-15	2.0E-02	9.7E-03	14.9	3.7	1.4	77.3	95.4	19.31	0.34			
O	1450	1.24E+01	2.18E+01	1.39E-02	1.6E-14	2.3E-02	1.0E-02	25.4	7.7	2.9	81.3	98.3	19.77	0.20			
P	1650	1.50E+01	3.02E+01	2.73E-02	9.5E-15	1.7E-02	1.3E-02	21.2	5.7	1.7	62.8	100.0	18.61	0.34			
total gas age		n=16			5.5E-13	7.0E-01								21.07	0.13		
Eruption Age		n=4	steps D-G	3.0E-13	9.2E-01									55.2	20.89	0.08	
OCA-030L1; A3; 117, groundmass concentrate, 17.22mg, J=0.001072496±0.10%, D=1.00644±0.00091, NM-117, Lab#=50832-02																	
A	2	8.92E+01	1.60E+00	2.36E-01	6.2E-16	3.2E-01	3.2E-07	0.9	11.8	0.6	21.8	0.6	37.31	3.45			
B	4	1.44E+01	9.87E-01	6.99E-03	9.9E-15	5.2E-01	5.2E-07	8.9	29.6	9.2	86.1	9.7	23.89	0.17			
C	7	1.12E+01	5.79E-01	5.24E-04	4.2E-14	8.8E-01	8.8E-07	22.3	23.8	39.2	98.8	48.9	21.25	0.07			
D	10	1.11E+01	5.62E-01	5.79E-04	2.6E-14	9.1E-01	9.1E-07	13.1	10.4	23.8	98.7	72.7	21.03	0.10			
E	12	1.12E+01	7.61E-01	1.03E-03	1.0E-14	6.7E-01	6.7E-07	7.0	5.2	9.4	97.6	82.1	21.06	0.13			
F	15	1.12E+01	1.03E+00	1.27E-03	7.2E-15	5.0E-01	5.0E-07	6.7	5.6	6.6	97.2	88.7	21.03	0.17			
G	20	1.13E+01	1.54E+00	2.19E-03	6.6E-15	3.3E-01	3.3E-07	9.3	5.1	6.1	95.2	94.8	20.68	0.17			
H	25	1.15E+01	2.53E+00	3.31E-03	2.9E-15	2.0E-01	2.0E-07	6.7	3.0	2.7	93.1	97.5	20.70	0.34			
I	30	1.23E+01	4.58E+00	7.74E-03	1.2E-15	1.1E-01	1.1E-07	5.0	1.8	1.1	84.3	98.6	20.02	0.72			
J	40	1.34E+01	1.48E+01	1.41E-02	1.5E-15	3.4E-02	3.4E-08	20.1	3.8	1.4	78.0	100.0	20.36	0.70			
total gas age		n=10			1.1E-13	7.3E-01								21.42	0.15		
Eruption Age		n=4	steps C-F	8.5E-14	8.3E-01									79.0	21.14	0.14	
OCA-030L2; A3; 117, groundmass concentrate, 22.74mg, J=0.001072496±0.10%, D=1.00644±0.00091, NM-117, Lab#=50832-02																	
A	2	2.53E+02	1.94E+00	8.07E-01	8.0E-16	2.6E-01	2.6E-07	1.0	10.8	0.5	5.7	0.5	27.95	8.98			
B	4	2.82E+01	9.92E-01	5.36E-02	15.4E-14	5.1E-01	5.1E-07	9.6	31.1	9.8	44.1	10.3	23.97	0.33			
C	7	1.27E+01	5.61E-01	5.86E-03	6.4E-14	9.1E-01	9.1E-07	23.8	25.5	42.8	86.5	53.1	21.08	0.10			
D	10	1.22E+01	5.81E-01	4.29E-03	3.2E-14	8.8E-01	8.8E-07	12.4	8.5	21.4	89.8	74.6	21.14	0.11			
E	12	1.27E+01	8.00E-01	5.18E-03	1.3E-14	6.4E-01	6.4E-07	7.0	5.1	8.8	88.3	83.3	21.51	0.16			
F	15	1.26E+01	1.12E+00	5.41E-03	9.3E-15	4.5E-01	4.5E-07	7.0	5.0	6.3	87.8	89.6	21.26	0.19			
G	20	1.24E+01	1.58E+00	5.64E-03	8.9E-15	3.2E-01	3.2E-07	9.4	6.6	6.0	87.4	95.6	20.91	0.19			
H	25	1.38E+01	2.82E+00	1.1E-02	3.5E-15	1.8E-01	1.8E-07	6.6	3.4	2.4	77.8	97.9	20.64	0.40			
I	30	1.56E+01	3.83E+00	1.63E-02	1.3E-15	1.3E-01	1.3E-07	3.4	1.6	0.9	71.1	98.8	21.41	0.75			
J	40	1.53E+01	1.71E+01	2.18E-02	1.7E-15	3.0E-02	3.0E-08	19.7	2.5	1.2	66.9	100.0	19.91	0.70			
total gas age		n=10			1.5E-13	7.4E-01								21.43	0.21		
Eruption Age		n=2	steps C-D	9.5E-14	9.0E-01									64.2	21.11	0.10	
OCA-036; B6;117, groundmass concentrate, 71.62mg, J=0.001068649±0.10%, D=1.00644±0.00091, NM-117, Lab#=50836-01																	
A	550	1.30E+02	1.95E+00	4.35E-01	6.3E-15	2.6E-01	7.6E-03	1.2	0.9	1.0	1.2	1.0	2.94	2.51			
B	625	1.68E+01	8.88E-01	4.88E-02	1.5E-14	5.7E-01	9.7E-04	1.3	0.3	2.5	14.3	3.6	4.61	0.42			
C	675	5.43E+00	7.75E-01	1.07E-02	2.4E-14	6.6E-01	2.4E-04	1.8	0.1	4.0	42.3	7.5	4.42	0.13			
D	725	4.02E+00	6.65E-01	5.84E-03	3.7E-14	7.7E-01	3.1E-04	2.5	0.2	6.2	57.9	13.8	4.48	0.10			
E	775	3.82E+00	6.55E-01	5.26E-03	3.9E-14	7.8E-01	4.7E-04	2.5	0.3	6.5	60.1	20.3	4.43	0.08			
F	825	3.86E+00	6.59E-01	5.31E-03	5.1E-14	7.7E-01	8.1E-04	3.3	0.8	8.5	60.1	28.8	4.47	0.09			
G	875	4.35E+00	7.61E-01	6.94E-03	4.8E-14	6.7E-01	1.6E-03	3.6	1.5	7.9	53.7	36.8	4.50	0.09			
H	925	4.91E+00	1.01E+00	8.82E-03	4.7E-14	5.1E-01	3.2E-03	4.7	2.9	7.9	48.1	44.6	4.54	0.08			
I	975	5.25E+00	1.20E+00	1.00E-02	4.1E-14	4.5E-01	5.4E-03	4.9	4.2	6.8	45.1	51.4	4.56	0.13			
J	1025	5.04E+00	1.30E+00	9.46E-03	3.0E-14	3.9E-01	1.1E-02	3.9	6.4	5.0	46.2	56.4	4.49	0.13			
K	1075	4.62E+00	1.11E+00	7.89E-03	2.1E-14	4.6E-01	1.4E-02	2.3	5.7	3.5	51.0	59.9	4.54	0.13			
L	1150	4.11E+00	9.30E-01	6.34E-03	4.9E-14	5.5E-01	1.5E-02	4.5	13.7	8.2	55.7	68.1	4.41	0.10			
M	1225	3.65E+00	2.94E+00	5.47E-03	2.8E-14	1.7E-01	1.6E-02	8.0	8.7	4.6	61.8	72.7	4.36	0.09			
N	1300	6.21E+00	2.97E+00	1.39E-02	3.8E-14	1.7E-01	1.7E-02	11.1	12.2	6.3	37.6	79.0	4.51	0.12			
O	1450	5.34E+00	3.19E+00	1.10E-02	1.1E-13	1.6E-01	1.8E-02	33.9	36.8	17.8	43.7	96.8	4.50	0.07			
P	1650	6.05E+00	5.52E+00	1.33E-02	1.9E-14	9.2E-02	1.5E-02	10.5	5.3	3.2	42.4	100.0	4.97	0.22			
total gas age		n=16			6.0E-13	4.6E-01								4.49	0.14		
Eruption Age		n=5	steps F-J	2.2E-13	5.7E-01									36.1	4.51	0.06	
OCA-036L; B6; 117, groundmass concentrate, 22.90mg, J=0.001068649±0.10%, D=1.00644±0.00091, NM-117, Lab#=50836-02																	
A	2	1.88E+02	1.15E+00	6.32E-01	1.1E-15	4.4E-01											

Table 5 continued

ID	Temp/F (°C/W)	$^{40}\text{Ar}/^{39}\text{Ar}$	$^{37}\text{Ar}/^{39}\text{Ar}$	$^{36}\text{Ar}/^{39}\text{Ar}$	$^{39}\text{Ar}_\text{K}$	K/Ca	Cl/K	$^{37}\text{Ar}_\text{Ca}$ (%)	$^{38}\text{Ar}_\text{Cl}$ (%)	$^{39}\text{Ar}_\text{K}$ (%)	$^{40}\text{Ar}^*$ (%)	^{39}Ar (%)	Age (Ma)	$\pm 2\sigma$ (Ma)
OCA-073-01; V1:117, groundmass concentrate, 55.79mg, J=0.001038789±0.11%, D=1.00644±0.00091, NM-117, Lab#=50879-0														
A	550	2.08E+01	3.61E-01	6.49E-02	6.3E-14	1.4E+00	3.5E-02	2.7	34.3	20.4	8.0	20.4	3.14	0.31
B	625	6.07E+00	5.69E-01	1.46E-02	5.7E-14	9.0E-01	2.9E-02	3.8	25.9	18.5	29.6	38.8	3.36	0.12
C	675	4.98E+00	1.02E+00	1.07E-02	3.6E-14	5.0E-01	2.5E-02	4.3	14.1	11.6	37.7	50.5	3.52	0.11
D	725	4.14E+00	1.76E+00	7.93E-03	3.2E-14	2.9E-01	1.8E-02	6.5	9.0	10.2	46.3	60.7	3.59	0.10
E	775	3.47E+00	2.38E+00	5.79E-03	2.4E-14	2.1E-01	1.2E-02	6.6	4.3	7.7	55.7	68.4	3.63	0.14
F	825	2.94E+00	2.74E+00	4.33E-03	2.8E-14	1.9E-01	6.7E-03	9.1	2.9	9.2	63.4	77.6	3.49	0.08
G	875	2.78E+00	3.02E+00	3.84E-03	2.1E-14	1.7E-01	4.9E-03	7.5	1.6	6.9	67.3	84.5	3.51	0.11
H	925	2.87E+00	3.26E+00	4.25E-03	1.4E-14	1.6E-01	5.4E-03	5.3	1.2	4.5	64.8	89.0	3.49	0.12
I	975	3.15E+00	3.79E+00	4.95E-03	7.3E-15	1.3E-01	8.2E-03	3.2	0.9	2.3	62.7	91.3	3.71	0.24
J	1025	3.21E+00	4.34E+00	6.05E-03	3.7E-15	1.2E-01	9.9E-03	1.9	0.6	1.2	54.7	92.5	3.30	0.39
K	1075	3.31E+00	4.71E+00	8.03E-03	3.3E-15	1.1E-01	1.1E-02	1.8	0.6	1.1	39.3	93.5	2.44	0.42
L	1150	3.79E+00	5.09E+00	8.60E-03	4.0E-15	1.0E-01	9.9E-03	2.4	0.6	1.3	43.4	94.8	3.09	0.40
M	1300	5.67E+00	2.41E+01	2.03E-02	8.6E-15	2.1E-02	1.5E-02	24.2	2.0	2.8	28.8	97.6	3.11	0.31
N	1650	8.10E+00	2.41E+01	2.55E-02	7.4E-15	2.1E-02	1.8E-02	20.8	2.0	2.4	31.5	100.0	4.86	0.31
total gas age		n=14			3.1E-13	6.0E-01							3.43	0.18
Eruption Age		n=3	steps F-H	6.4E-14	1.7E-01								20.5	3.50 0.06
OCA-073-02; V3:117, groundmass concentrate, 55.73mg, J=0.001031232±0.11%, D=1.00644±0.00091, NM-117, Lab#=50881-0														
A	550	1.92E+01	3.86E-01	5.96E-02	4.3E-14	1.3E+00	3.1E-02	2.6	28.8	18.2	8.3	18.2	2.96	0.38
B	625	6.19E+00	6.01E-01	1.48E-02	4.4E-14	8.5E-01	2.9E-02	4.0	26.9	18.3	29.7	36.5	3.42	0.13
C	675	5.18E+00	1.05E+00	1.16E-02	2.7E-14	4.9E-01	2.5E-02	4.3	14.0	11.3	34.8	47.8	3.35	0.14
D	725	4.34E+00	1.75E+00	8.90E-03	2.5E-14	2.9E-01	1.8E-02	6.7	9.5	10.5	42.2	58.3	3.40	0.13
E	775	3.66E+00	2.34E+00	6.19E-03	1.9E-14	2.2E-01	1.2E-02	6.7	4.5	7.8	54.6	66.1	3.72	0.14
F	825	3.16E+00	2.75E+00	4.93E-03	2.2E-14	1.9E-01	7.2E-03	9.4	3.4	9.4	60.3	75.5	3.54	0.10
G	875	3.01E+00	2.90E+00	4.50E-03	1.8E-14	1.8E-01	5.7E-03	7.9	2.1	7.4	63.1	82.9	3.54	0.10
H	925	3.25E+00	3.08E+00	5.41E-03	1.2E-14	1.7E-01	6.6E-03	5.6	1.7	5.0	57.9	87.9	3.50	0.14
I	975	3.84E+00	3.59E+00	7.67E-03	6.5E-15	1.4E-01	9.9E-03	3.6	1.4	2.7	48.1	90.7	3.44	0.23
J	1025	3.87E+00	3.61E+00	7.83E-03	3.5E-15	1.4E-01	1.4E-02	1.9	1.0	1.5	47.4	92.1	3.42	0.40
K	1075	3.65E+00	3.71E+00	6.54E-03	3.4E-15	1.4E-01	1.3E-02	1.9	1.0	1.4	54.9	93.5	3.74	0.43
L	1150	3.75E+00	4.73E+00	8.33E-03	3.5E-15	1.1E-01	1.6E-02	2.5	1.2	1.4	44.2	95.0	3.10	0.42
M	1300	5.27E+00	2.50E+01	1.90E-02	5.2E-15	2.0E-02	1.8E-02	19.8	2.0	2.2	32.1	97.2	3.21	0.47
N	1650	7.43E+00	2.21E+01	2.22E-02	6.8E-15	2.3E-02	1.7E-02	23.1	2.5	2.8	35.9	100.0	5.04	0.33
total gas age		n=14			2.4E-13	5.5E-01							3.42	0.21
Eruption Age		n=5	steps F-J	6.2E-14	1.7E-01								26.0	3.52 0.07
OCA-073L; V5; 117, groundmass concentrate, 20.4mg, J=0.0010801±0.10%, D=1.0052±0.00121, NM-117, Lab#=50883-03														
A	2	2.87E+01	8.51E-01	9.77E-02	7.4E-16	6.0E-01	3.6E-02	0.4	1.5	0.8	-0.5	0.8	-0.26	2.05
B	4	1.40E+01	4.53E-01	4.18E-02	3.7E-15	1.1E+00	3.1E-02	1.2	6.2	4.1	11.7	5.0	3.18	0.54
C	7	7.19E+00	4.63E-01	1.88E-02	1.5E-14	1.1E+00	3.0E-02	5.0	25.0	17.2	22.9	22.2	3.20	0.21
D	10	4.91E+00	1.05E+00	1.09E-02	2.9E-14	4.8E-01	2.4E-02	21.5	38.7	32.9	35.6	55.1	3.41	0.11
E	12	3.73E+00	1.96E+00	6.76E-03	1.7E-14	2.6E-01	1.6E-02	23.1	15.1	19.0	50.1	74.1	3.64	0.10
F	15	3.18E+00	2.39E+00	5.08E-03	9.2E-15	2.1E-01	1.1E-02	15.5	5.4	10.5	58.3	84.6	3.62	0.13
G	20	2.97E+00	2.65E+00	4.57E-03	6.7E-15	1.9E-01	9.2E-03	12.5	3.4	7.6	61.2	92.2	3.55	0.12
H	25	3.17E+00	3.54E+00	6.01E-03	3.2E-15	1.4E-01	1.1E-02	8.0	2.0	3.7	52.5	95.8	3.25	0.27
I	30	3.65E+00	4.06E+00	8.37E-03	1.8E-15	1.3E-01	1.2E-02	5.2	1.2	2.1	40.8	97.9	2.92	0.34
J	40	3.73E+00	5.78E+00	9.62E-03	1.9E-15	8.8E-02	1.5E-02	7.6	1.5	2.1	36.0	100.0	2.63	0.39
total gas age		n=10			8.8E-14	5.0E-01							3.38	0.18
Eruption Age		n=5	steps D-H	6.5E-14	3.4E-01								73.6	3.54 0.12

and apparent age remarkably well. Subtle differences are, however, seen in the $^{37}\text{Ar}_{\text{Ca}}$, $^{38}\text{Ar}_{\text{Cl}}$ and $^{39}\text{Ar}_{\text{K}}$ release spectra.

In all samples, the overall release pattern of $^{37}\text{Ar}_{\text{Ca}}$, $^{38}\text{Ar}_{\text{Cl}}$ and $^{39}\text{Ar}_{\text{K}}$ for the laser analyses are convex upward in shape whereas the furnace analyses of OCA-073 and -079 display a descending pattern. For samples OCA-073 and -079, the descending $^{38}\text{Ar}_{\text{Cl}}$ and $^{39}\text{Ar}_{\text{K}}$ seen in the furnace analyses are not seen in the laser analyses, instead, a convex upward shape is seen. For sample OCA-036, a peak of $^{38}\text{Ar}_{\text{Cl}}$ exists in the mid- to high-temperature/power steps. Except for OCA-030, no significant difference between the two techniques is seen for the eruption ages obtained or the precision of the analyses (Eruption ages given in Figure 10 are calculated based on the new approach outlined in Section 3). For OCA-030, the two eruption ages calculated for the laser analyses are greater than the furnace eruption age at the 95% confidence level.

5.2. Discussion

The subtle differences seen in the K/Ca, Cl/K, radiogenic yields and apparent ages between the laser and furnace step-heating analyses for all samples is attributed to differences in heating schedule resolution, differences between furnace temperature and laser power, and heating inhomogeneity. Because the resolution of the furnace-heating schedule was greater than that with the laser, the laser technique homogenized the different gas reservoirs to a greater extent. In addition, step-heating using the furnace allows the entire sample to be heated at a single temperature whereas the laser initially degasses only the surface of the sample. Furthermore, the lower-laser power steps probably reflect the equivalent of a furnace temperature step less than 550°C. Likewise

the highest-furnace-temperature step probably reflects the equivalent of a laser power greater than 40 watts. However, given these differences between the two techniques, the laser technique reproduces the radiogenic yields, K/Ca, Cl/K and age gradients seen in the furnace analyses remarkably well.

The most significant difference seen between the two techniques is the $^{38}\text{Ar}_{\text{Cl}}$ release patterns within the first several steps of OCA-073, -077 and -079, and the $^{39}\text{Ar}_{\text{K}}$ release patterns for the first three steps in OCA-073 and the first two steps in OCA-079 (Figure 10). For the furnace analyses of samples OCA-073 and -079, the $^{38}\text{Ar}_{\text{Cl}}$ and $^{39}\text{Ar}_{\text{K}}$ release patterns display an overall descending shape over the first several steps whereas the furnace analysis of OCA-077 displays only a descending shaped $^{38}\text{Ar}_{\text{Cl}}$ release pattern. At first glance, these results appear to contradict two of the conclusion drawn in Section 3. Namely, that the interstitial phases degas first based on the descending $^{38}\text{Ar}_{\text{Cl}}$ release pattern and that an overall convex-shaped $^{39}\text{Ar}_{\text{K}}$ release pattern is associated with samples in which the majority of potassium is contained within the feldspar rim phase. However, these seemingly contradictory results can be resolved. These differences seen in the $^{38}\text{Ar}_{\text{Cl}}$ and $^{39}\text{Ar}_{\text{K}}$ release patterns between the two techniques are interpreted to be due to differences between the furnace and laser heating schedules. As discussed in Section 3, the $^{37}\text{Ar}_{\text{Ca}}$, $^{38}\text{Ar}_{\text{Cl}}$ and $^{39}\text{Ar}_{\text{K}}$ release spectra are in part a function of the heating schedule used. In addition, other variables can affect the release patterns such as differences in grain sizes, sample inhomogeneity and diffusive verses non-diffusive degassing behavior. For the furnace analyses of the representative samples shown in Section 3, the heating schedule was held constant so that each sample's chemical and petrographic differences could be assessed by use of the $^{37}\text{Ar}_{\text{Ca}}$, $^{38}\text{Ar}_{\text{Cl}}$ and

$^{39}\text{Ar}_\text{K}$ release spectra. However, the heating schedule used in the laser analyses is not the equivalent of that used for the furnace analyses. In addition, temperatures achieved during laser heating are less homogeneous than temperatures during furnace heating. Therefore, the conclusions drawn from the furnace analyses in Section 3 pertaining to the $^{37}\text{Ar}_\text{Ca}$, $^{38}\text{Ar}_\text{Cl}$ and $^{39}\text{Ar}_\text{K}$ release spectra can not be directly applied to the laser analyses. It is worth emphasizing the fact that except for OCA-030 and OCA-079, no significant differences in apparent ages are noted between the two step-heating techniques for the mid-temperature/-power steps (i.e. excluding OCA-030 and OCA-079, each sample's laser and furnace eruption ages are within error of each other at the 95% confidence level; for samples OCA-030 and OCA-079 the age differences between furnace and laser are only marginally significant ($2.3\text{-}2.4\sigma$). Therefore, even though differences are noted between the $^{38}\text{Ar}_\text{Cl}$ and $^{39}\text{Ar}_\text{K}$ release patterns in the low-power/-temperature steps of the two techniques, applying the age assignment criteria outlined in Section 3 to the laser analyses yields consistent results with the furnace analyses.

Although the $^{37}\text{Ar}_\text{Ca}$, $^{38}\text{Ar}_\text{Cl}$ and $^{39}\text{Ar}_\text{K}$ release spectra are dependent on the heating schedule, resulting in the inability of the conclusions generated in Section 3 to be strictly applied to the laser analyses, the conclusion that the interstitial phases degas first can still be validated by use of the K/Ca and Cl/K values seen in the first several steps. Because the K/Ca and Cl/K spectra are not dependent on the heating schedule used and because the interstitial phases contain the highest K/Ca and Cl/K values of any of the phases seen in the representative samples (Table 1), the high K/Ca and Cl/K values seen in samples OCA-073 and -079 for the first several steps in both the furnace and laser step-heating analyses are interpreted to reflect that the interstitial phases are the first to degas.

For sample OCA-036, the unusual pattern of % $^{38}\text{Ar}_{\text{Cl}}$ released is not completely understood. This may be due to degassing of melt inclusions within a high-temperature phenocryst or groundmass phase.

In a similar study comparing the laser and furnace step-heating techniques for single muscovite crystals, Heizler and Ralser (1996) found that the laser step-heating technique appeared to homogenize apparent age gradients to a much greater extent than furnace step-heating. In contrast, for the basalt samples studied here, the laser step-heating technique was able to reproduce the age gradients seen in the furnace step-heating analyses. Therefore, the different behaviors seen between the laser and furnace step-heating techniques for muscovite and basalt samples are interpreted to be due to differences in how the two sample types couple with the CO₂ laser.

In conclusion, the laser technique reproduces the radiogenic yields, K/Ca, Cl/K and age gradients seen in the furnace analyses remarkably well for the basalt samples studied. Therefore, the CO₂ laser step-heating is concluded to be an effective alternative approach to dating basalt samples.

6. Geologic Interpretations

6.1. Results

All data are reported in Appendix A and B. Table 6 summarizes the argon results for each sample as well as listing their locations and the sample type (i.e. samples collected from the surface of a flow, interior of a flow, or proximal to the eruptive vent).

All age spectra were interpreted on the basis of criteria outlined in Section 3. Figure 11 displays the results of the replicate analyses. For these results, five out of the seven replicate analyses display MSWD values within what can be attributed to analytical error (Mahon, 1996) whereas two do not. Figure 12 displays the results of analyses of multiple samples from a given flow unit. These results show that six out of the eight analyses of multiple samples from a given flow unit display MSWD values within what can be attributed to analytical error (Mahon, 1996) whereas two do not.

Figure 13 displays the results from samples collected in stratigraphic order of flows originating from Maxson Crater. All four samples are within analytical error of each other but show progressively younger ages with stratigraphic order. Figure 14 is a histogram of the absolute and percent error (at $\pm 2\sigma$) associated with all of the eruptive ages determined in this study. Overall the results show a high level of precision where 49% of the analyses have errors less than or equal to 1% and 88% have errors less than or equal to 3%. In addition, 76% of the analyses have an absolute error less than or equal to 0.05 Ma.

Figure 15 is a graph of previously published K-Ar ages versus the new $^{40}\text{Ar}/^{39}\text{Ar}$ ages for pairs of samples from the same flow unit. The results show that the new

Table 6: Summary of Results

Sample	Geographic Location	Sample Type	Longitude	Latitude	n ¹	³⁹ Ar (%) ²	Age (Ma)	Error (2σ)
OCA-001	Maxson Crater	Flow Surface	104.8575	35.8783	3	36.7	1.58	0.16
OCA-002	Guadalupita Canyon	Flow Interior	105.2364	36.2419	3	65.3	4.45	0.02
OCA-003	La Mesa	Flow Interior	105.1557	36.0417	3	65.8	4.45	0.05
OCA-004-01	Maxson Crater	Flow Interior	104.3864	35.7284	1	17.7	1.56	0.06
OCA-004-02	Maxson Crater	Flow Interior	104.3864	35.7284	7	61.8	1.64	0.05
OCA-005	Maxson Crater	Flow Surface	104.3864	35.7294	3	36.2	1.59	0.15
OCA-006	Maxson Crater	Flow Interior	104.3869	35.7390	5	56.1	1.57	0.06
OCA-007	Maxson Crater	Flow Interior	104.3867	35.7385	5	66.4	1.54	0.07
PW-OCA-007	Maxson Crater	-	104.8936	35.8615	4	67.9	1.56	0.02
OCA-008-01	Charette Mesa	Flow Interior	104.7138	36.0044	2	48.1	2.98	0.05
OCA-008-02	Charette Mesa	Flow Interior	104.7138	36.0044	5	69.6	3.01	0.04
OCA-009	Charette Mesa	Flow Interior	104.7126	36.0142	3	47.9	2.90	0.04
OCA-010	Ocate Creek area	Flow Interior	105.1147	36.2376	2	55.1	2.51	0.09
OCA-011	Laguna Salada Mesa	Flow Interior	105.1831	36.2921	3	62.9	5.67	0.03
OCA-012	Cerro Pelon	Flow Interior	105.0538	36.1617	4	75.7	2.98	0.03
OCA-013	Cerro Vista Mesa	Flow Interior	105.4483	36.1349	7	81.3	5.65	0.03
OCA-014	Las Mesas Del Conjonlon	Flow Interior	104.6466	35.9886	3	55.0	6.03	0.03
OCA-016	Charette Mesa	Flow Interior	104.8155	36.2085	7	80.5	3.20	0.04
OCA-019	Apache Mesa	Flow Interior	104.9056	36.1846	4	69.2	4.59	0.02
OCA-020	Cerrito Pelon	Flow Interior	104.9100	36.1875	10	87.4	2.28	0.03
OCA-022	Cerro Negro area	Vent	104.8855	36.1189	6	69.3	2.36	0.14
OCA-023	Cerro Negro area	Vent	104.8707	36.1148	5	58.9	1.80	0.02
OCA-024	Cooks Peak	Flow Interior	105.0438	36.2414	6	79.7	4.40	0.03
OCA-025	Gallinas Mesa	Flow Interior	105.0544	36.2244	5	60.9	7.04	0.04
OCA-026	Apache Mesa (West)	Flow Interior	104.9989	36.2260	2	38.0	5.71	0.04
OCA-027	Apache Mesa (West)	Flow Interior	105.0018	36.2355	4	57.2	5.73	0.02
OCA-028	Rivera Mesas	Flow Interior	105.0018	36.2573	7	81.0	4.37	0.02
OCA-029	El Cerro Colorado	Vent	105.2763	36.0646	5	62.3	4.44	0.03
OCA-030	Palo Flechado Mesa	Flow Interior	105.3736	36.4071	4	55.2	20.89	0.08
OCA-030L1	Palo Flechado Mesa	Flow Interior	105.3736	36.4071	4	79.0	21.14	0.14
OCA-030L2	Palo Flechado Mesa	Flow Interior	105.3736	36.4071	2	64.2	21.11	0.10
OCA-031	Maxson Crater	Vent	104.8914	35.9016	3	26.7	1.57	0.04
OCA-032	Black Mesa	Flow Interior	105.0849	35.9734	5	79.7	4.59	0.03
OCA-033	Black Mesa area	Flow Interior	105.0800	35.9746	5	55.7	2.31	0.05
OCA-034	Cerro Pelon	Flow Interior	105.0388	35.9606	6	62.1	2.27	0.03
OCA-035	El Cerro Colorado	Flow Interior	105.2356	36.0451	4	52.5	4.43	0.03
OCA-036	Urraca Mesa	Flow Interior	104.9941	36.4127	5	36.1	4.51	0.06
OCA-036L	Urraca Mesa	Flow Interior	104.9941	36.4127	6	89.8	4.50	0.08
OCA-037	Rayado Mesa	Flow Interior	104.9038	36.2936	7	81.8	4.46	0.04
OCA-038	Rivera Mesas area	Flow Interior	104.9254	36.2646	7	90.4	4.42	0.02

Table 6 continued.

Sample	Geographic Location	Sample Type	Longitude	Latitude	n ¹	³⁹ Ar (%) ²	Age (Ma)	Error (2σ)
OCA-039	Rivera Mesas area	Flow Interior	104.9184	36.2499	4	44.8	3.47	0.05
OCA-040	Rivera Mesas area	Flow Interior	104.9221	36.2681	4	44.4	3.53	0.04
OCA-041	Rivera Mesas area	Flow Interior	104.9239	36.2748	5	54.4	3.51	0.02
OCA-042	Ortega Mesa	Flow Interior	104.9282	36.2765	5	47.6	4.42	0.09
OCA-043	Le Febres Mesa	Flow Interior	105.1039	36.1724	4	54.1	3.01	0.04
OCA-044	Le Febres Mesa	Flow Interior	105.0781	36.2075	5	66.4	3.01	0.03
OCA-045	Le Febres Mesa	Flow Interior	105.1355	36.1888	5	64.7	3.05	0.04
OCA-046	La Mesa	Vent	105.2123	36.2393	4	65.7	4.64	0.07
OCA-047	Ocate Mesa	Flow Interior	105.2035	36.2672	3	51.9	8.16	0.03
OCA-048	Guadalupita Canyon	Flow Interior	105.2298	36.1867	6	85.5	4.48	0.02
OCA-051	Agua Fria Peak	Vent	105.2066	36.3587	6	71.3	4.98	0.04
OCA-052	Agua Fria	Flow Interior	105.2443	36.3725	5	51.3	4.99	0.03
OCA-053	Moreno Valley	Flow Interior	105.2617	36.4159	4	48.4	6.57	0.04
OCA-054	La Grulla Ridge	Flow Interior	105.1406	36.3335	4	62.8	8.17	0.04
OCA-055	Le Febres Mesa	Flow Interior	105.1591	36.1511	8	81.8	3.00	0.03
OCA-057	Charette Mesa area	Flow Interior	104.7035	36.0450	7	76.6	2.20	0.02
OCA-059	Las Mesas Del Conjelon	Flow Interior	104.7474	36.0092	7	79.6	6.03	0.02
OCA-061	Maxson Crater area	Flow Interior	104.7216	35.9331	6	64.0	2.28	0.03
OCA-062	Laguna Salada Mesa	Flow Interior	105.1395	36.2733	8	86.1	6.43	0.03
OCA-063	Cerro Negro	Vent	104.9331	36.1113	4	73.1	1.97	0.03
OCA-064	Encinosa Mesa	Flow Interior	104.9413	36.1169	6	73.0	6.40	0.08
OCA-066	Fowler Mesa	Flow Surface	105.0564	36.3958	4	32.5	4.47	0.06
OCA-067	Fowler Mesa	Flow Surface	105.0564	36.3958	5	43.4	4.48	0.03
OCA-068	Las Mesas Del Conjelon	Flow Interior	104.6959	36.0005	5	81.7	6.07	0.02
OCA-069	Cerrito Pelon	Flow Interior	105.0114	36.1943	6	75.1	2.35	0.02
OCA-070	Ortega Mesa	Flow Interior	105.0564	36.3079	6	57.3	4.68	0.03
OCA-071	White Peak	Vent	105.0197	36.2980	4	45.9	3.53	0.08
OCA-073-01	Rivera Mesa	Flow Surface	105.0226	36.2443	3	20.5	3.50	0.06
OCA-073-02	Rivera Mesa	Flow Surface	105.0226	36.2443	5	26.0	3.52	0.07
OCA-073L	Rivera Mesa	Flow Surface	105.0226	36.2443	5	73.6	3.54	0.12
OCA-075	Encinosa Mesa	Flow Interior	104.9714	36.1209	6	76.4	6.39	0.06
OCA-077	Cerro Negro area	Flow Interior	104.9526	36.1159	4	57.7	1.96	0.03
OCA-077L	Cerro Negro area	Flow Interior	104.9526	36.1159	5	91.9	1.97	0.04
OCA-078	Las Mesas Del Conjelon	Flow Interior	104.7316	36.0082	4	69.5	6.02	0.04
OCA-079	Cerro Pelon	Flow Surface	105.1037	36.0408	3	48.0	2.18	0.04
OCA-079L1	Cerro Pelon	Flow Surface	105.1037	36.0408	3	90.0	2.13	0.05
OCA-079L2	Cerro Pelon	Flow Surface	105.1037	36.0408	5	88.7	2.11	0.02
OCA-080	Cerro Montoso area	Flow Interior	105.1435	36.0754	3	36.4	3.31	0.05
OCA-081	Laguna Salada Mesa	Flow Interior	105.1462	36.2819	4	48.6	5.09	0.04
OCA-082	Agua Fria area	Flow Interior	105.2038	36.2851	7	84.4	4.48	0.03
Cerro Mont.	Cerro Montoso	Vent	-	-	5	86.5	3.07	0.10

¹ represents the number of heating steps used in the eruption age calculation.² represents the total percent ³⁹Ar released of heating steps used in the eruption age calculation.

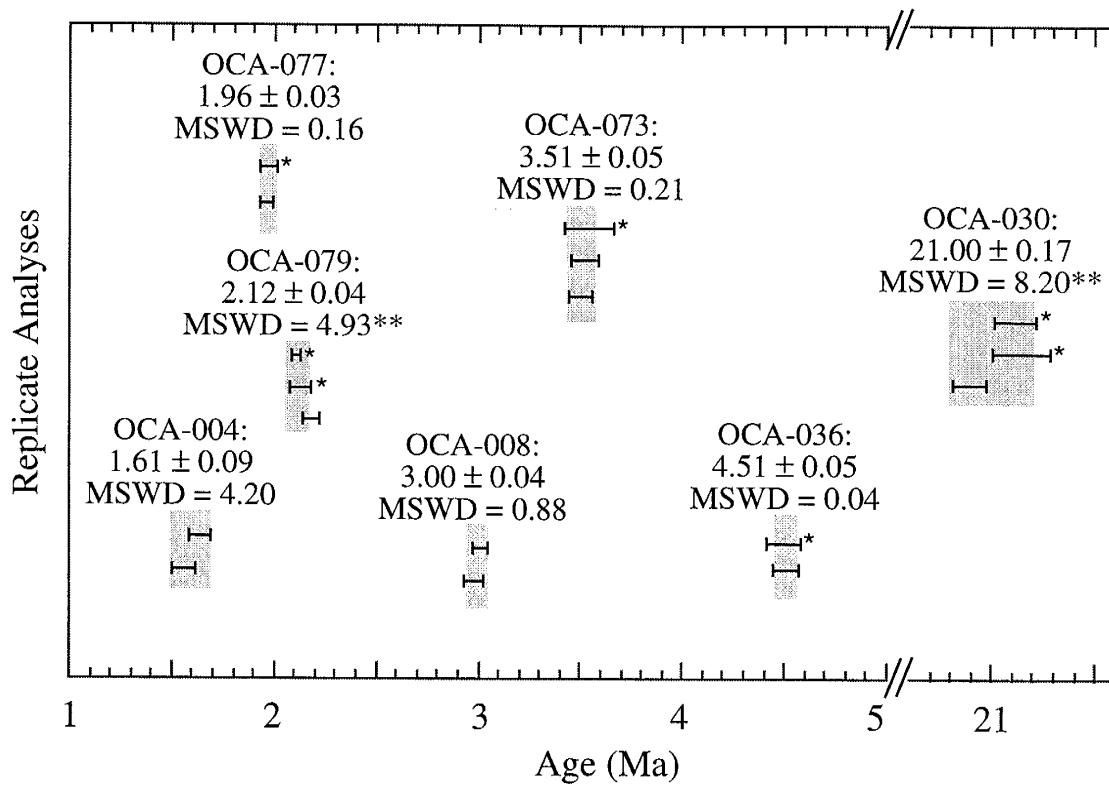


Figure 11. Comparison of replicate analyses. Weighted mean of analyses is given along with the MSWD for the calculation. Laser analysis. **MSWD greater than what can be attributed to analytical error.

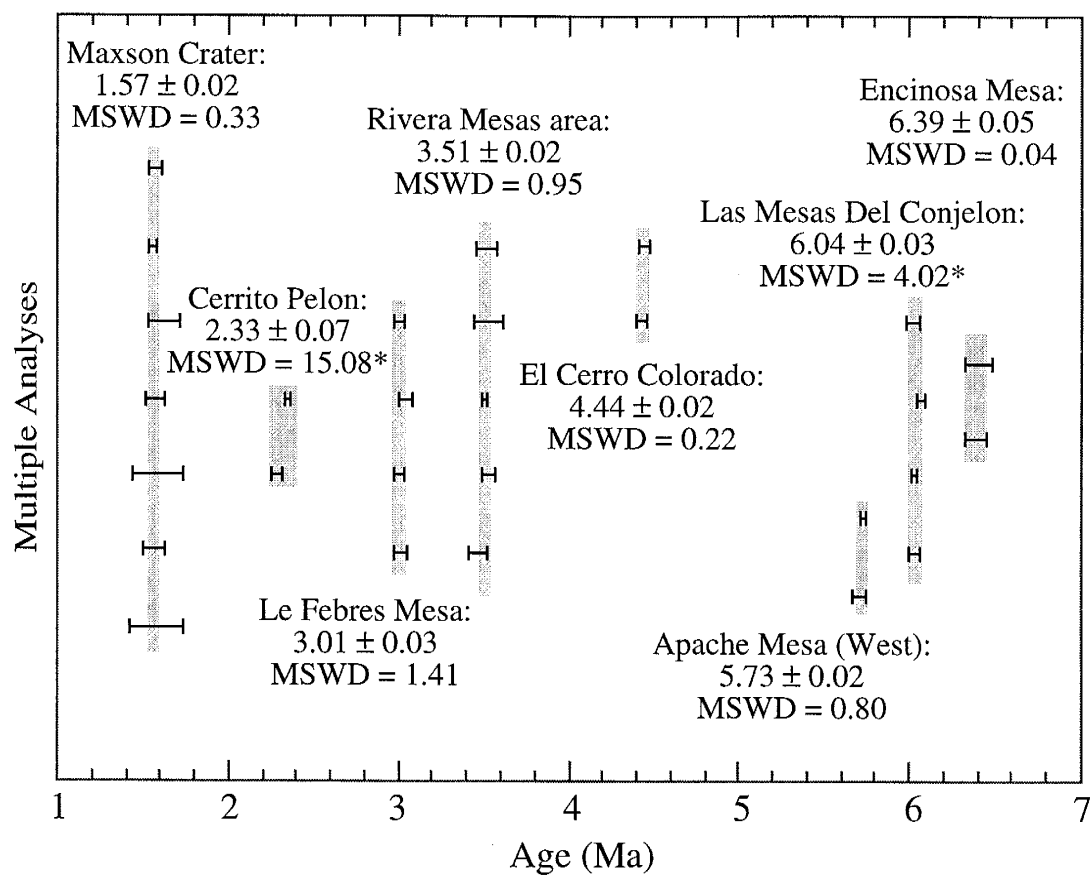


Figure 12. Comparison of analyses of multiple samples from the same flow unit. Weighted mean of analyses is given along with the calculated MSWD. *MSWD greater than what can be attributed to analytical error

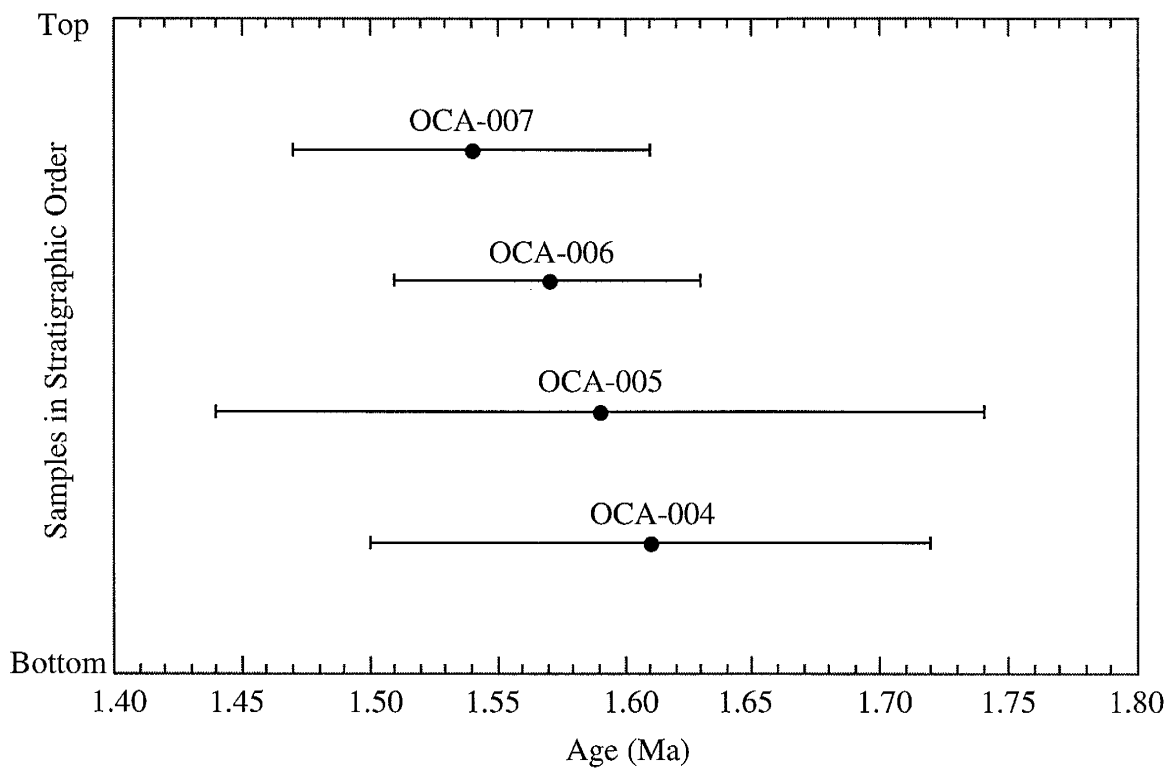


Figure 13. Samples collected in stratigraphic order from Maxson Crater flows. Sample OCA-004 represents weighted mean of two replicate analyses.

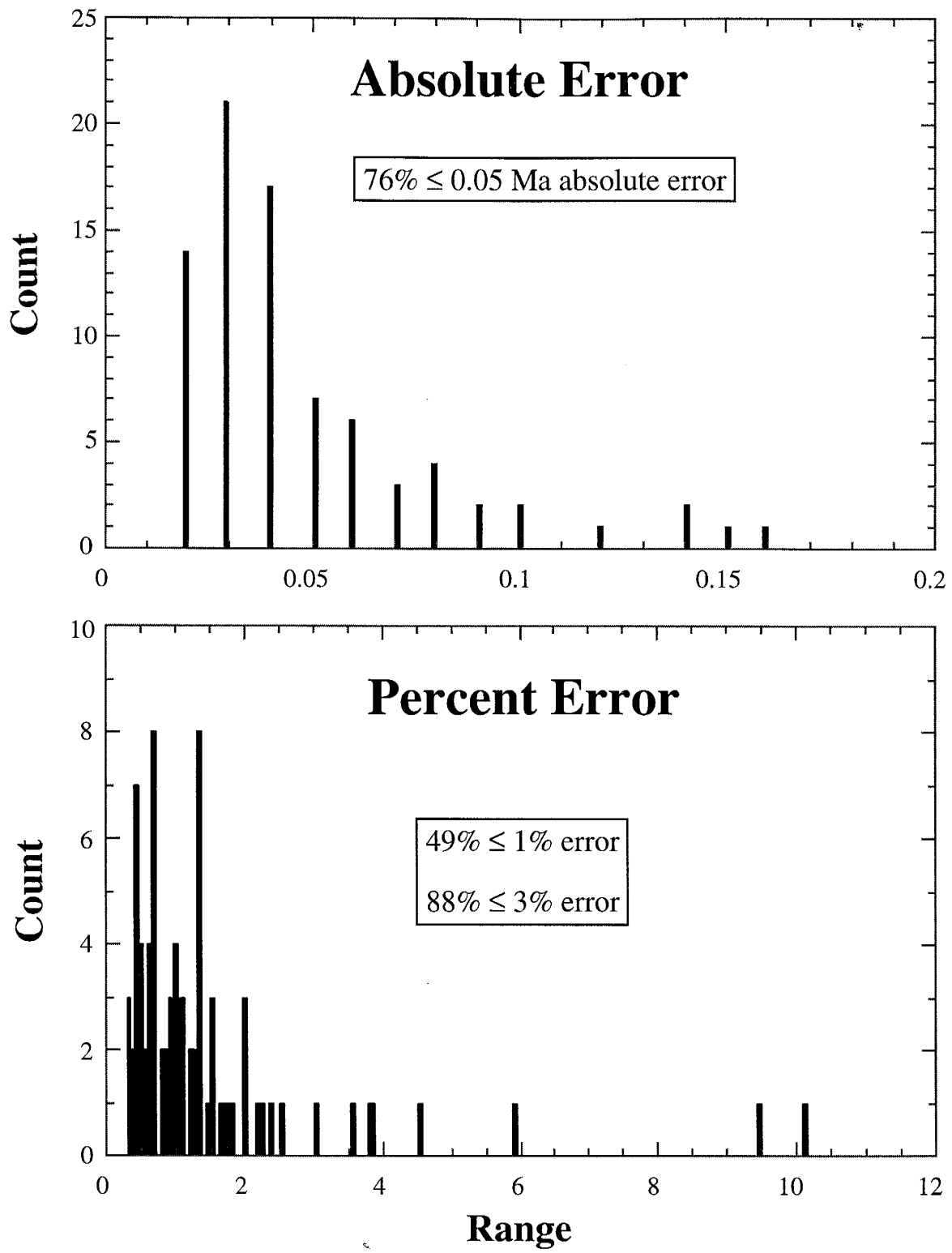


Figure 14. Histogram of absolute error and percent error for all analyses.

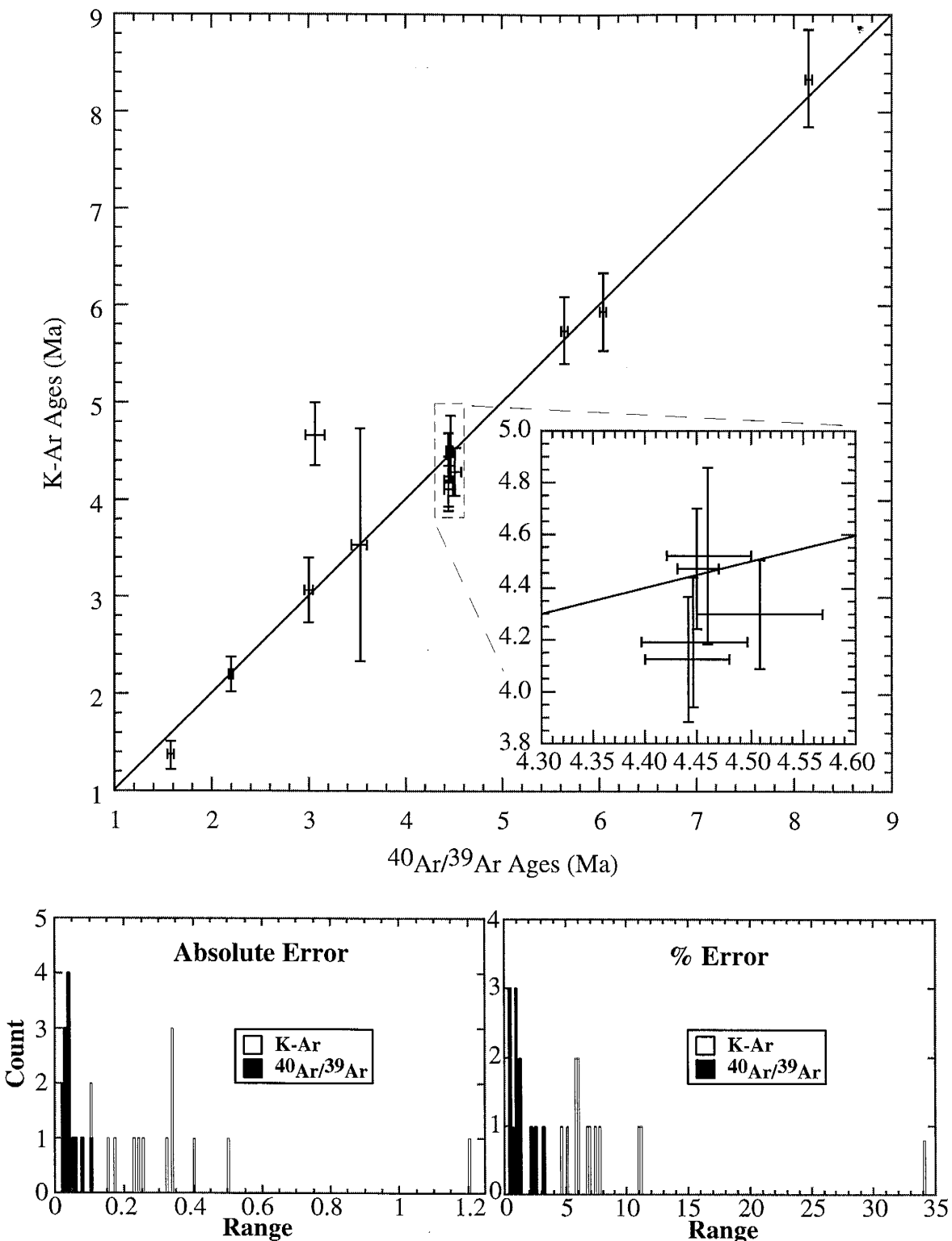


Figure 15. Comparison between previously published K-Ar ages and the new $^{40}\text{Ar}/^{39}\text{Ar}$ ages for pairs of samples from the same flow unit. Error bars are shown along with a one-to-one line for reference. Box diagram is an enlarged portion of the graph to clarify the group of ages around 4.5 Ma.

$^{40}\text{Ar}/^{39}\text{Ar}$ eruption ages are more precise than the ages determined using the K-Ar method with absolute errors less than half of those obtained with the K-Ar method. Eleven of the thirteen flow units dated by both the K-Ar and $^{40}\text{Ar}/^{39}\text{Ar}$ method are within analytical error of each other, whereas two of the thirteen analyses not.

6.2. Discussion

The results of the replicate analyses (Figure 11) show that the eruption ages for five out of the seven samples studied are reproducible and yield individual eruption ages for each sample that are within error of each other. One out of the three analyses for both OCA-030 and OCA-079 are not within error of the two other analyses at the 95% confidence level. Because of this, for both of these samples the MSWD value is greater than what can be attributed to analytical error (Mahon, 1996). This may be due to overestimate of the analytical uncertainty for one or more of the analyses or one out of the three analyses for both OCA-030 and OCA-079 is the statistical outlier at the 95% confidence level.

The results of analyses of multiple samples from a given flow unit (Figure 12) show that two out of the eight flow units (Cerrito Pelon and Las Mesas Del Conjelon) display MSWD values that are greater than what can be attributed to only analytical uncertainty, whereas six of the eight flow units display single statistical populations with analytically acceptable MSWD values. The high MSWD values seen for the Cerrito Pelon and Las Mesas Del Conjelon analyses may be due to an overestimate of the analytical uncertainty for one or more of the analyses, the presence of a statistical outlier

at the 95% confidence level or the occurrence of two or more eruptive events closely spaced in time.

Comparison of K-Ar ages and $^{40}\text{Ar}/^{39}\text{Ar}$ ages (Figure 15) along with the agreement of total gas and eruption ages for individual $^{40}\text{Ar}/^{39}\text{Ar}$ analyses (Appendix A and B) suggests excess ^{40}Ar and $^{40}\text{Ar}^*$ loss are not significant factors affecting the results. In addition, comparison between the two techniques illustrates the use of the $^{40}\text{Ar}/^{39}\text{Ar}$ technique in obtaining high-precision ages, resulting in the ability of the technique at resolving volcanic events that differ in age by approximately >100,000 years (Figure 15).

The neighboring Raton-Clayton and Taos volcanic fields were also recently dated at the NMGRL (Stroud, 1997; Appelt, 1998). Comparing this study to the Raton-Clayton and Taos studies shows a higher level of precision associated with this study (Figure 16). The reason for this may be due to the differences between the age assignment criteria used and/or differences in the type of sample (well crystallized or poorly crystallized) able to be collected. In the Raton-Clayton study, several volcanic bombs were sampled (presumably poorly crystallized relative to flow interior samples) from young eruptive centers. In addition, for the Ocate study the “plateau” approach to age assignment was not used, whereas it was used in the Raton-Clayton and Taos studies. In viewing the age spectra data for both the Raton-Clayton and Taos studies, several “plateaus” consisted of low-temperature steps, contributing to a large error in the eruption age of the sample. All other things being equal, the comparison of analytical uncertainty associated with this study with that of the Raton-Clayton and Taos studies suggests that a high level of precision can be achieved when dating basalt samples if well-crystallized

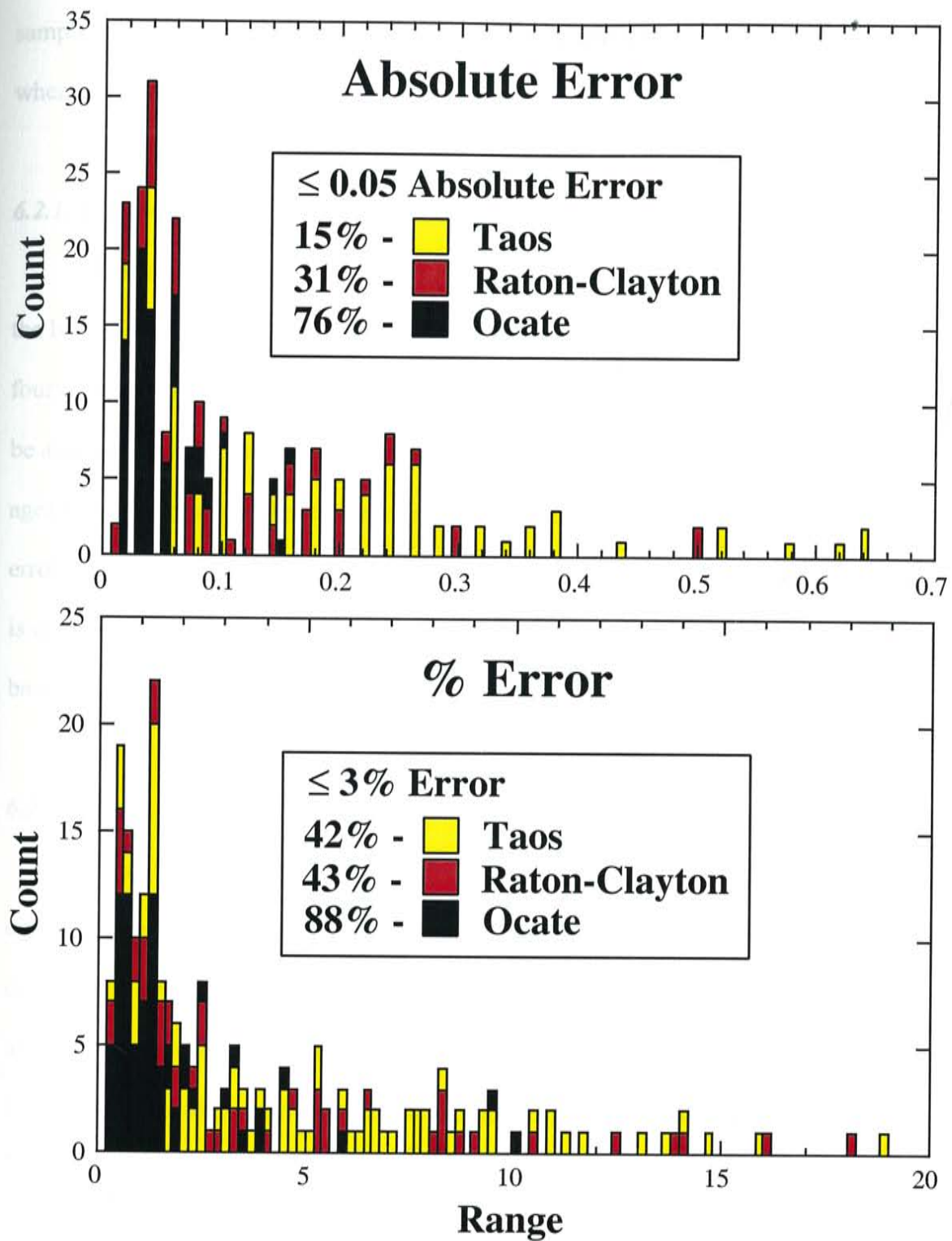


Figure 16. Absolute and Percent Error histograms of the Taos, Raton-Clayton and Ocate Volcanic fields.

samples are analyzed, and if the incorporation of low-temperature steps can be avoided when calculating the eruption age.

6.2.1. Maxson Crater

Numerous remnants of flows originating from Maxson Crater are exposed along the base of the Mora River valley. At the confluence of the Mora and Canadian Rivers four of these flows were sampled in stratigraphic order so that the eruptive history could be assessed. All four samples agree within analytical error (Figure 13). Furthermore, the ages obtained from samples collected proximal to the vent also agree within analytical error of the samples collected in stratigraphic order (Table 6 and Figure 12). Therefore, it is concluded that the eruption of Maxson Crater occurred during a single pulse of activity based on the precision of the eruption ages.

6.2.2. Spatial Distribution of Ages

Figure 17 displays the spatial distribution of ages along with the estimated eruption volumes for each flow unit (See appendix C for how the volume estimates were calculated). Except for Las Mesas Del Conjelón, all eruptive centers greater than 3.5 Ma are within the northern and central portions of the field. A large percentage of these are focused in the northern portion of the field around Agua Fria. Eruptive centers less than 3.4 Ma occur within the central and southern portion of the field. A basalt flow initially mapped as part of the Ocate Volcanic field (O'Neill and Mehnert, 1988) in the northwestern portion of the field is dated at 20.89 ± 0.08 Ma (OCA-030). Based on the

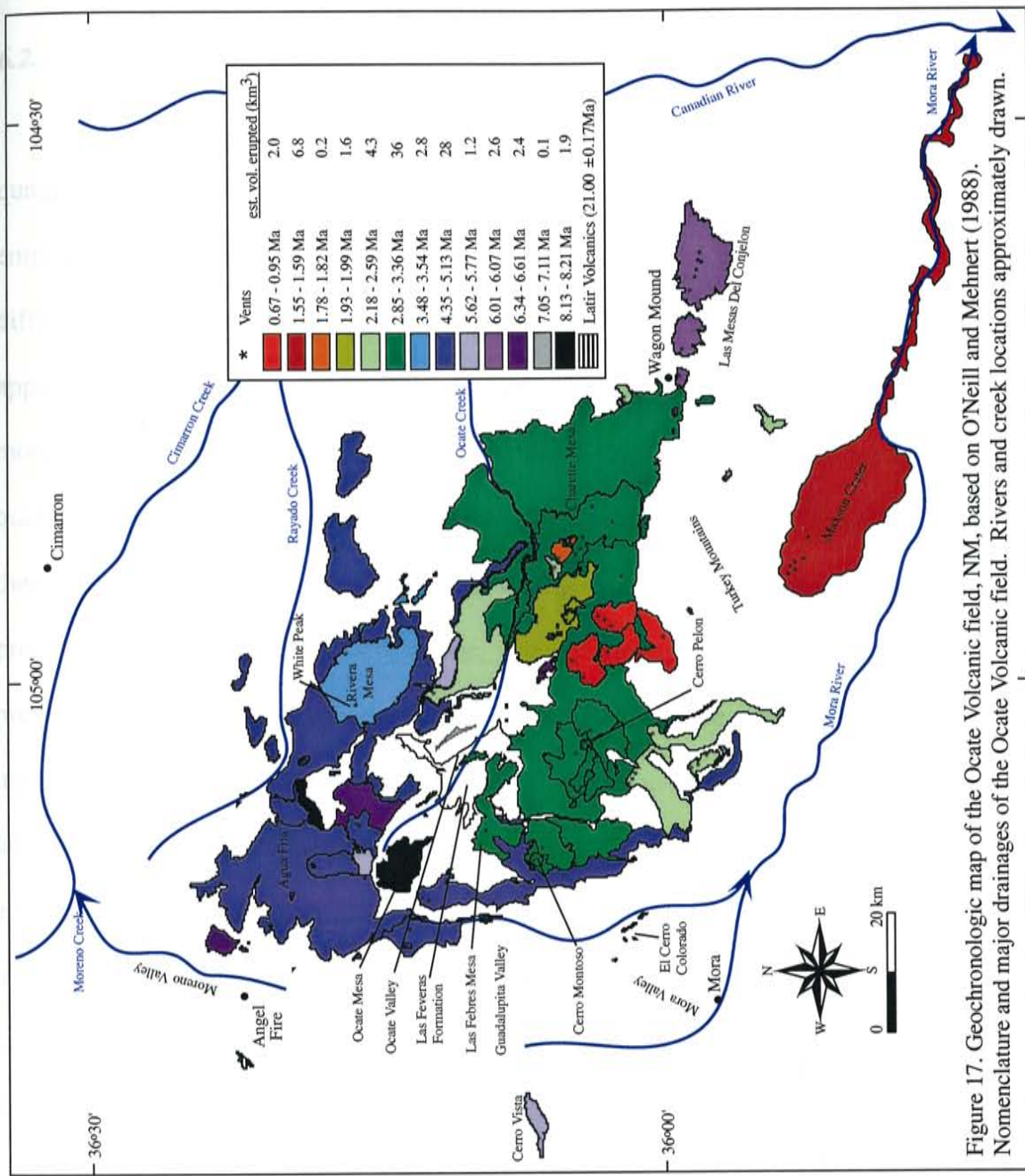


Figure 17. Geochronologic map of the Ocate Volcanic field, NM, based on O'Neill and Mehrt (1988). Nomenclature and major drainages of the Ocate Volcanic field. Rivers and creek locations approximately drawn.

eruptive age, this flow is interpreted to be part of the Latir Volcanic field (cf. Lipman et al., 1986).

6.2.3. Minimum Erosion Rates

Utilizing the inverted topography within the field, minimum erosion rates can be quantified within portions of the field that have not experienced faulting since flow emplacement (Figure 18). Erosion rates are calculated by dividing the elevation difference between the mesa and the underlying valley floor by the age of the mesa (See appendix D for the values used in the calculations). In addition, in areas where two or more mesas exist next to each other, erosion rates during intervals of time can be quantified by dividing the elevation difference between the two flow-capped mesas by their age difference. Errors associated with the $^{40}\text{Ar}/^{39}\text{Ar}$ eruption ages were not propagated in the erosion rate calculations. The uncertainty associated with choosing the present day surface elevation is the largest source of error in the calculations. The uncertainties associated with the minimum erosion rates averaged between two dated lavas are inferred to be much less than those averaged to present day due to the greater accuracy with which the elevations of the flow bottoms can be determined. However, all minimum erosion rates are location specific. Therefore, for these calculations, comparisons to determine increases or decreases in erosion rates with time can only be determined in localized areas.

Within three areas of the field, it appears that erosion rates have decreased with time (Figure 18). The erosion rates calculated here are in the range of that found in a similar study done in the Raton-Clayton field (Stroud, 1997). However, the increase in

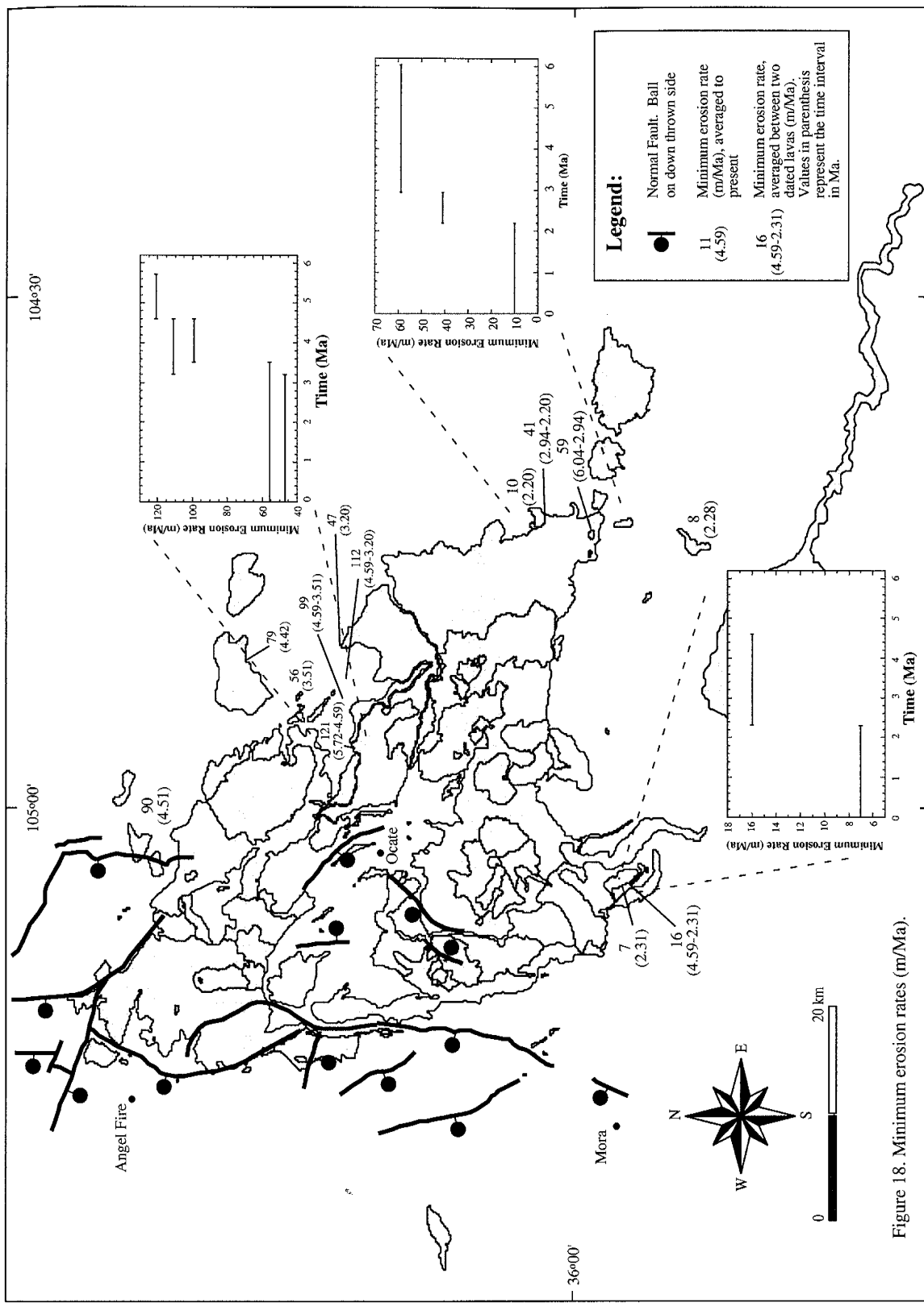


Figure 18. Minimum erosion rates (m/Ma).

erosion rates from 8 Ma to present that Stroud (1997) found in the northeastern portion of the Raton-Clayton field is not seen in the Ocate field. The seemingly contradictory data between the two studies may in part be due to the locations within the respective volcanic fields that the erosion rates were calculated. In the Raton-Clayton field the increase in erosion rates from 8 Ma to present is seen in the northeastern portion of the field near the headwaters of the major drainages. In contrast, in the Ocate field the decrease in erosion rates from 6 Ma to present is seen in the south, southeast and eastern portions of the field closer to the major drainages. Therefore, it is possible that in the Raton-Clayton field the increase in erosion rates from 8 Ma to present may reflect headward erosion. In the Ocate field, the decrease in erosion rates with time may reflect decreased tectonic activity after 2 to 3 Ma or stabilization of base level on the major streams, perhaps by magmatic uplift of the Jemez zone across the course of the Canadian River as suggested by Pazzaglia et al., (1999). The increased volume erupted between 3.36 and 2.85 Ma appears to coincide approximately with the decrease in erosion rates.

6.2.4. Vent Locations and Alignments

Figure 19 shows the spatial distribution of vent locations and the alignment of multiple vents for a given flow unit. There appears to be a major structural control governing the alignment of vents. The Ocate Volcanic field crosses the boundary between the southern Great Plains and Rio Grande rift paleostress provinces (Aldrich et al., 1986). The least principle horizontal stress in the southern Great Plains province has been oriented NNE-SSW to N-S since at least 28 Ma (Aldrich et al., 1986). The WNW vent alignments in the eastern Ocate field (Figure 19) fit the southern Great Plains

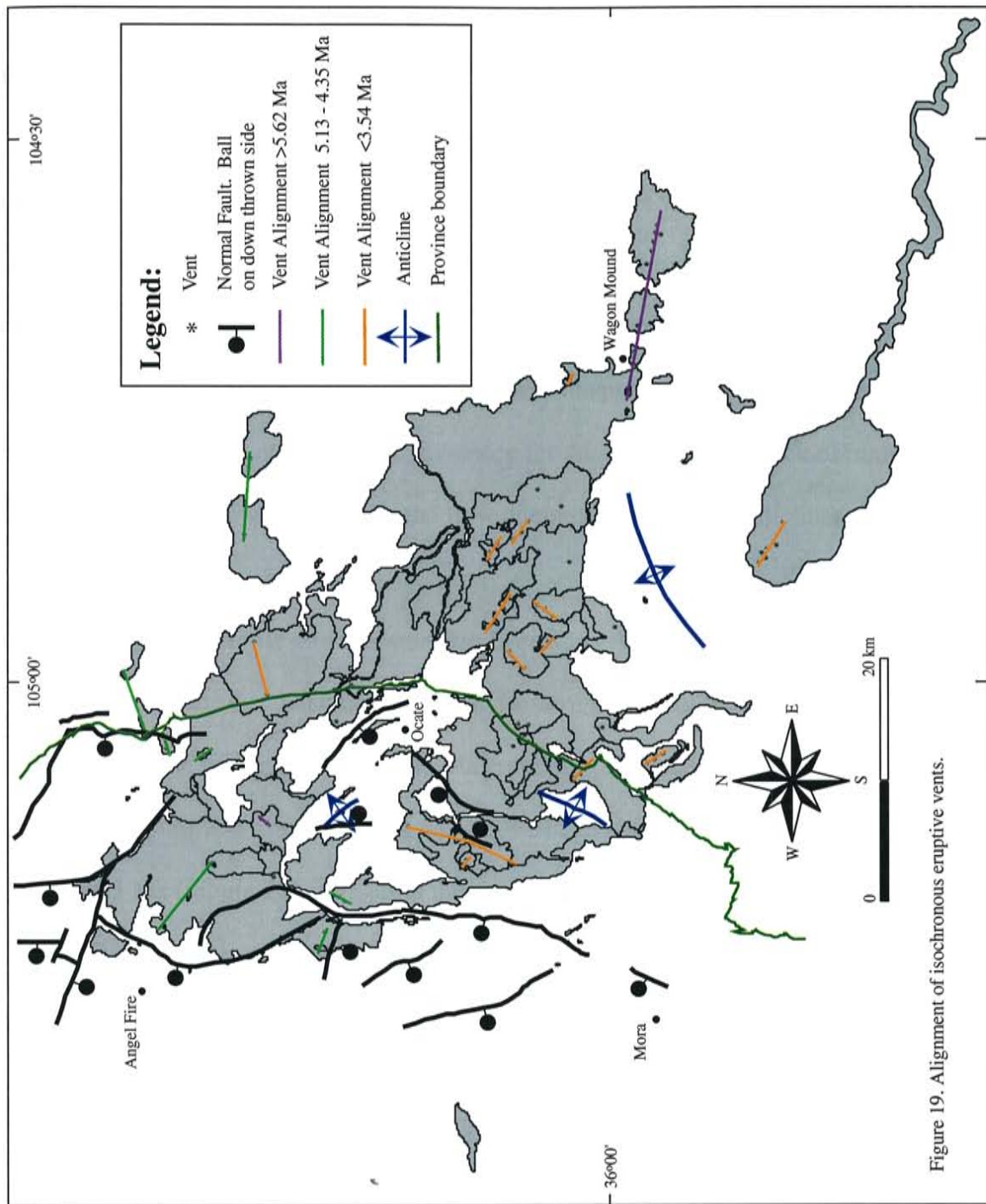


Figure 19. Alignment of isochronous eruptive vents.

province whereas the vent alignments in the central and western Ocate field are more variable, perhaps reflecting the transition between the two paleostress provinces.

6.2.5. Flow Directions

Figure 20 displays the flow directions based on the topography and vent location of the flow units. Except for the Cerro Vista flow, all flows were erupted onto a southeast sloping surface. Localized exceptions are caused by topographic highs associated with the formation of volcanic edifices (e.g. Cerro Pelon and Agua Fria). The two anticlines within the southern portion of the field appear to have been a prominent topographic high since at least 3 Ma. Evidence for this is seen by the lack of remnant flows on top of the anticlines and by the flow directions around the anticlines.

6.2.6. Timing of Tectonic and Geomorphic Events

Onset of late Cenozoic faulting in the western portion of the field appears to have occurred after the widespread 5.13-4.35 Ma eruptions. Evidence for fault offset is seen in the El Cerro Colorado flow dated at 4.44 ± 0.04 Ma and in the Agua Fria flows dated at 4.48 ± 0.03 Ma (Figure 20). Offsets at these two locations are approximately 201 and 183 m. Based on this, minimum fault offset rates along this prominent fault at the El Cerro Colorado and Agua Fria are 45 and 41 m/Ma, respectively.

Between 4.3 and 2.5 Ma, the tectonically developed boundary between the Southern Rocky Mountain and Great Plains provinces is interpreted to have disturbed local drainage patterns for

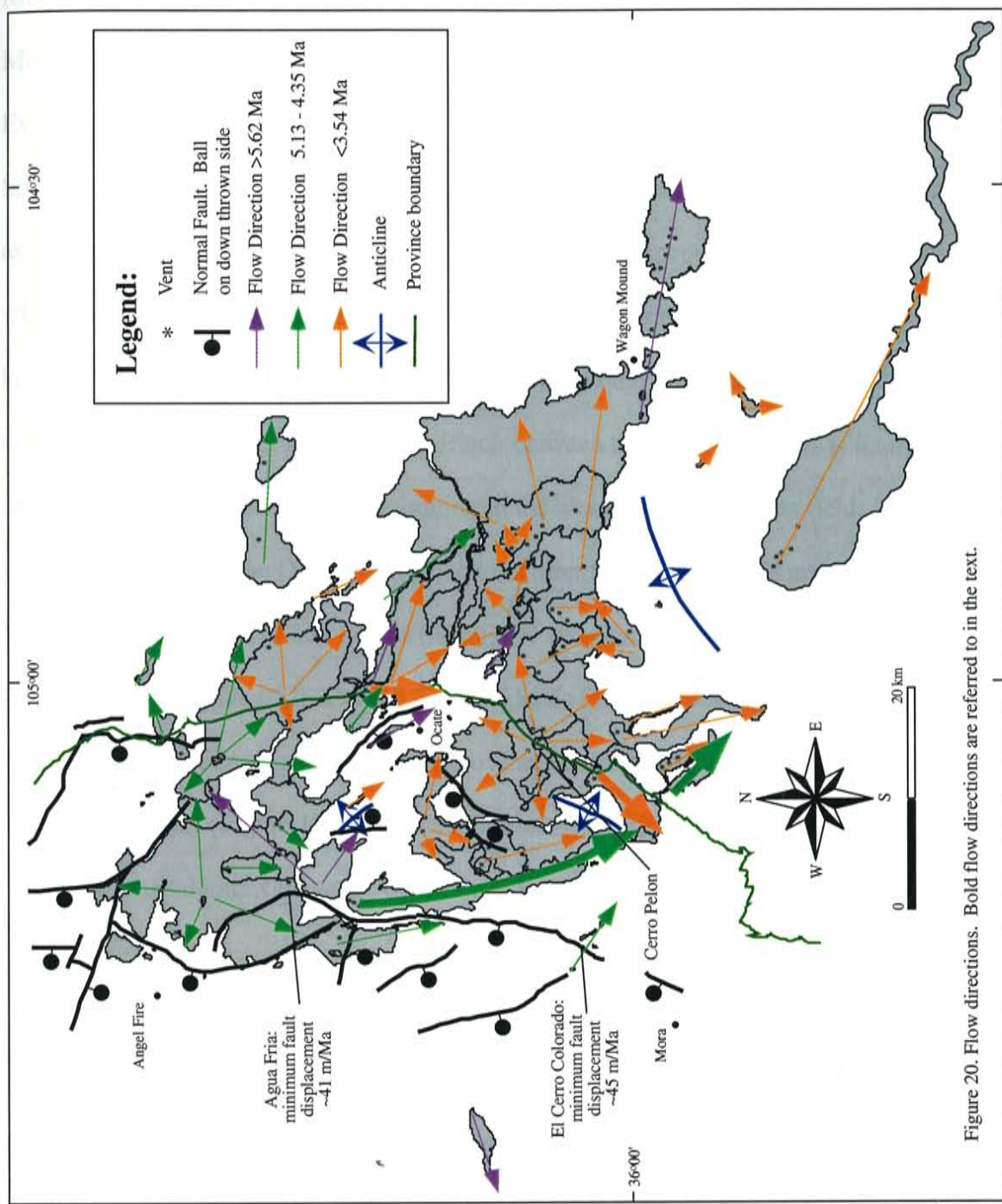


Figure 20. Flow directions. Bold flow directions are referred to in the text.

flows erupted along the boundary due to differential movement of the Cimarron Block relative to the provinces (Figure 20; The Cimarron Block is part of the southern Rocky Mountain province bounded to the west by the frontal faults of the Sangre de Cristo Mountains and to the east by the province boundary (O'Neill and Mehnert, 1988)). Evidence for this is seen in the flow direction just south of Cerro Pelon along the boundary (Figure 20). In this area, the general northwest to southwest flow directions associated with the 5.13-4.35 Ma eruptions are roughly perpendicular to the boundary, while the north-south flow directions of the 2.18-2.59 Ma eruptions are parallel to the boundary (the flow directions discussed are shown in bold on Figure 20). The differential movement of the Cimarron Block between the two boundaries is interpreted to be coeval with the post-4.35 Ma faulting in the western portion of the field.

Formation of the Ocate Valley occurred after the 5.13-4.35 Ma eruptive episode, but before the eruption of Las Febres (mean of 4 samples: 3.01 ± 0.04) and the Cerro Pelon eruptions (OCA-012: 2.98 ± 0.03). Evidence for this is seen by the absence of 5.13-4.35 Ma lava flows and the presence of Las Febres and Cerro Pelon flows within the present day valley (Figure 17; O'Neill and Mehnert, 1988). Formation of the Moreno, Mora and Guadalupita valleys are constrained to after the onset of faulting (post-4.35 Ma).

The Las Feveras Formation, a fluvial valley-fill deposit within the Ocate Valley, is interpreted to have been deposited after the formation of the Ocate Valley and either before, after or during the eruptions of Cerro Pelon. The formation was deposited due to a base level rise associated with either damming of the drainage by the Cerro Pelon flows

or differential movement of the two physiographic provinces along the province boundary (O'Neill and Mehnert, 1988).

6.2.8. Evolution of the Ocate Volcanic Field

Figure 21 is a timeline of events constrained by the $^{40}\text{Ar}/^{39}\text{Ar}$ data that documents the volcanic and geomorphic history of the Ocate Volcanic field. The history of the field began at ~8.2 Ma with the eruption of flows presently occupying the Ocate Mesa and La Grulla Ridge. Up until the widespread eruptions at 5.13-4.35 Ma, the field was marked by a period of small episodic eruptions within the central and northern portions of the field. This period of activity was also a period of crustal stability marked by erosion and pediplanation which supplied sediment for the Miocene Ogallala Formation (Frye and Leonard, 1957, 1959; Scott, 1975).

From 5.13-4.35 Ma a period of increased volcanism within the northern portion of the field ensued with approximately 32 vol. % of the field being erupted during this time (28 km^3). Following this major eruptive event was a period of tectonic activity. Down-to-the-west faulting was occurring within the western portion of the field and lead to the formation of the Moreno, Mora and Guadalupita Valleys. From 4.35-3 Ma the Ocate Valley was also forming by erosion.

After the 5.13-4.35 Ma eruptions a hiatus in activity ensued until the eruption of White Peak in the Rivera Mesas area at 3.51 ± 0.03 Ma. Following this was the largest eruptive episode within the field between 3.36-2.85 Ma where approximately 40 vol. % (36 km^3) of the field was erupted within the central portion of the field. During this time deposition of the Las Feveras Formation within the Ocate Valley began.

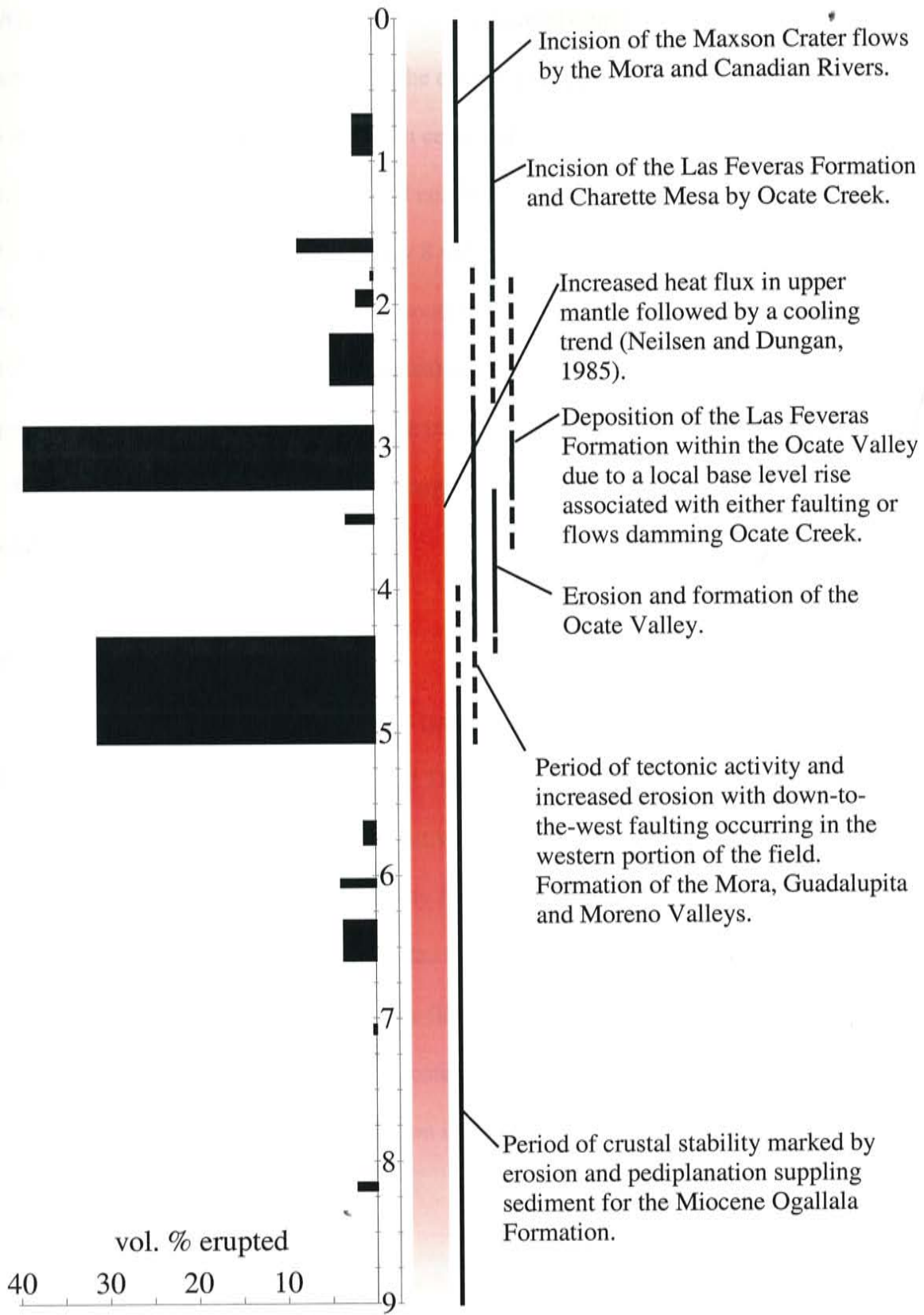


Figure 21. History of the Ocate Volcanic field.

After the 3.36-2.85 Ma eruptions, a period of decreased eruptive activity ensued with small localized centers erupting within the central and southern portions of the field. Deposition of the Las Feveras Formation ceased and incision through it and Charette Mesa by the Ocate Creek began and still continues today. At 1.57 ± 0.04 Ma Maxson Crater erupted, producing approximately 8 vol. % (6.8 km^3) of the field. Flows emanating from Maxson Crater flowed southeasterly into the canyon carved by the Mora River and continued for $\sim 96 \text{ km}$ (60 miles) before coming to a stop $\sim 29 \text{ km}$ (15 miles) past the Mora/Canadian confluence. The incision of the Maxson Crater flows by the Mora River began soon after and, at present, has eroded through the basalt and into the underlying sedimentary rocks.

6.2.9. Regional Relationships

Figure 22 displays the ideograms (an error weighted histogram) for the Ocate field and neighboring Raton-Clayton and Taos volcanic fields (Stroud, 1997; Appelt, 1998). All fields experienced eruptive activity near 5.7, 5.1, 4.7, 3.5, 3.0 and 2.3 Ma as well as an overall peak in eruptive activity from 5.1-2.3 Ma. The Ocate and Raton-Clayton field share more eruptive episodes in common with each other and both show an overall episodic behavior, while the Taos field displays a more or less continuous eruptive behavior. Both the Taos and Ocate field's youngest eruptive products occurred ~ 1 Ma ago, whereas the youngest eruption in the Raton-Clayton field occurred $\sim 50,000$ years ago.

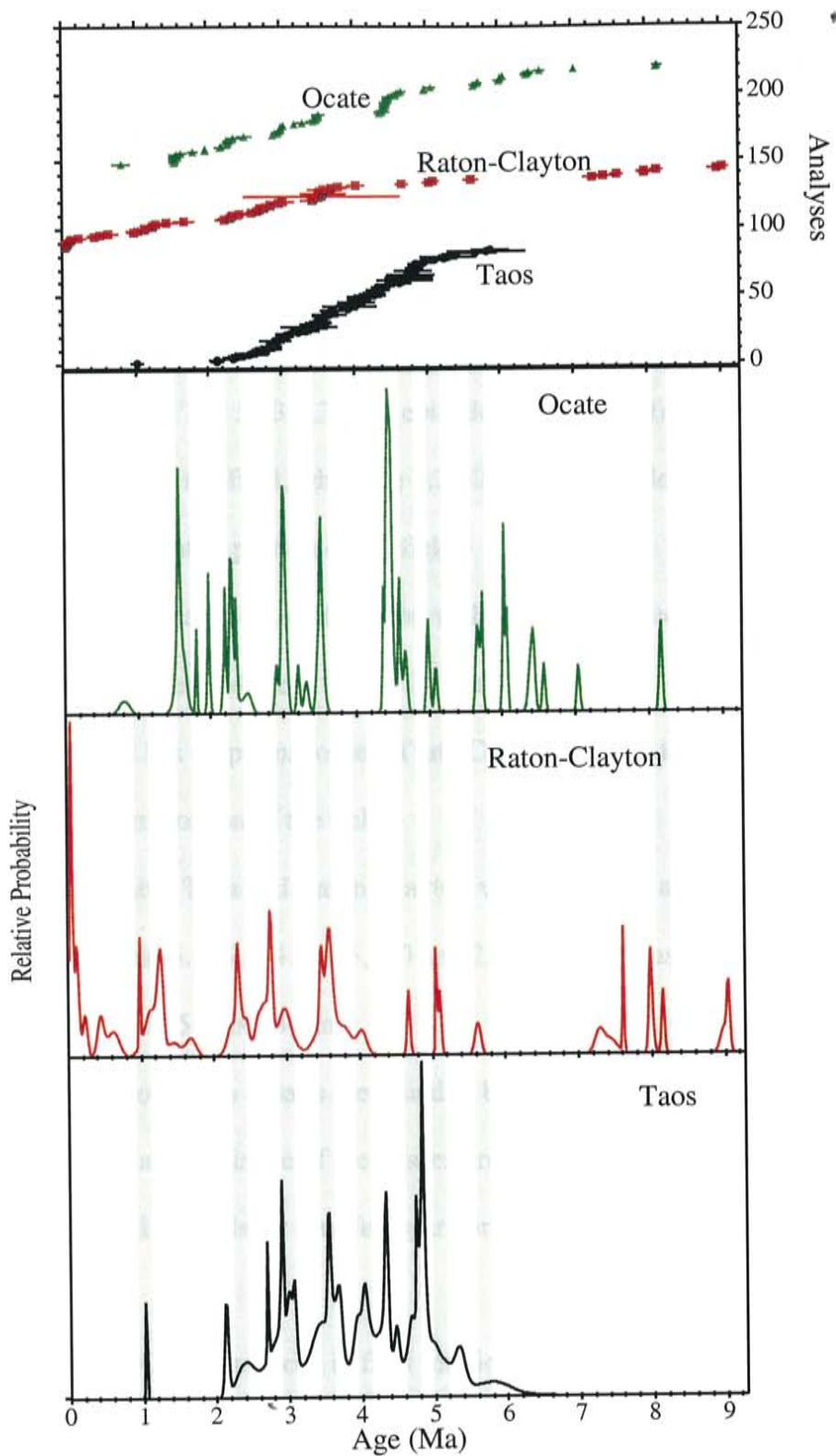


Figure 22. Ideogram of the Ocate, Rayton-Clayton and Taos Volcanic fields.
Shaded bars represent isochronous eruptive events shared by two or more fields.

7. Conclusions

- (1) The Ocate Volcanic field was episodically erupted in approximately sixteen pulses between 8.2 and 0.8 Ma and, in general, a north-to-south time progression of volcanism occurred.
- (2) 5.13-4.35 and 3.36-2.85 Ma mark two volumetrically major eruptive episodes within the Ocate field which produced approximately 32 and 40 vol. % of the field (28 and 36 km³), respectively. The 5.13-4.35 Ma episode was erupted from vents located in the northern portion of the field, while the 3.36-2.85 Ma episode was erupted from vents located in the central portion of the field.
- (3) Between 8.2 and 4.4 Ma a period of erosion without recorded tectonic activity occurred which supplied sediment for the Ogallala Formation.
- (4) After the 5.13-4.35 Ma eruptions, onset of late Cenozoic down-to-the-west faulting began in the western portion of the field.
- (5) Regionally, the Ocate, Taos and Raton-Clayton volcanic fields all experienced eruptive activity near 5.7, 5.1, 4.7, 3.5, 3.0 and 2.3 Ma as well as an overall peak in eruptive activity from 5.1 to 2.3 Ma.
- (6) ⁴⁰Ar/³⁹Ar analyses of Ocate basalts are found to be dependent on the crystallinity, chemistry and modal abundance of the phases present. Interstitial phases are found to degas first followed by feldspar rim, feldspar core, olivine/oxide and lastly by pyroxene.
- (7) Convex upward K/Ca spectra seen in flow interior samples reflect high degrees of recoil redistribution whereas, descending K/Ca spectra seen in flow surface samples reflect samples in which recoil redistribution is minimal.

- (8) The interstitial phases contain the majority of potassium for samples collected from the flow surface and display descending $^{39}\text{Ar}_\text{K}$ release patterns, whereas the feldspar rim contains the majority of potassium for samples collected from the flow interior and display convex upward $^{39}\text{Ar}_\text{K}$ release patterns. Flow interior samples are concluded to yield more precise ages with heating steps comprising a greater percentage of the total $^{39}\text{Ar}_\text{K}$ released than flow surface samples.
- (9) Analysis of plagioclase, pyroxene and olivine phenocryst concentrates confirms previous findings that phenocryst phases degas at temperatures higher than $\sim 1025^\circ\text{C}$. In addition, for the samples studied here, apparent ages associated with the degassing of the olivine and pyroxene phenocryst phases are found to yield geologically inaccurate ages whereas the plagioclase separate yielded apparent ages in agreement with the corresponding groundmass analysis. Excess ^{40}Ar found within the olivine and plagioclase phenocryst concentrates are calculated to be at most 9.58×10^{-14} and 1.64×10^{-13} moles/g, respectively, suggesting that excess ^{40}Ar is minor effect within these samples.
- (10) Comparison of basalt samples step-heated with both the furnace and CO_2 laser show that the laser technique reproduces the radiogenic yields, K/Ca , Cl/K and age gradients seen in the furnace analyses. Based on this, the CO_2 laser step-heating is concluded to be an effective alternative approach to dating basalt samples.

8. References

- Aldrich, M.J.Jr, Chapin, C.E., Laughlin, A.W., 1986. Stress history and tectonic development of the Rio Grande rift, New Mexico. *Journal of Geophysical Research*, 91, 6199-6211.
- Appelt, R.M., 1997. $^{40}\text{Ar}/^{39}\text{Ar}$ geochronology and volcanic evolution of the Taos volcanic field, northern New Mexico and southern Colorado. Masters Thesis, New Mexico Institute of Mining and Technology.
- Baski, A.K., Archibald, D.A., 1997. Mesozoic igneous activity in the Maranhao province, northern Brazil: $^{40}\text{Ar}/^{39}\text{Ar}$ evidence for separate episodes of basaltic magmatism. *Earth & Planetary Science Letters*, 151, 139-153.
- Burke, W.H., Otto, J.B. and Denison, R.E., 1969. Potassium-argon dating of basaltic rocks. *Journal of Geophysical Research*, v. 74, 1082-1086.
- Dalyrmple, G.B. and Moore, J.G., 1968. Argon-40: Excess in submarine pillow basalts from Kilauea volcano, Hawaii. *Science*, 161, 1132-1135.
- Damon, P.E., Laughlin, A.W. and Percious, J.K., 1967. Problem of excess argon-40 in volcanic rocks. In *Radioactive Dating and Methods of Low-level Counting*, International Atomic Energy Agency, Vienna, 463-479.
- Deino, A. and Potts, R., 1990. Single-crystal $^{40}\text{Ar}/^{39}\text{Ar}$ dating of the Olorgesailie Formation, Southern Kenya Rift. *Journal of Geophysical Research*, 95, 8453-8470.
- Feraud, G., York, D., Mevel, C., Cornen, G., Hall, C.M., and Auzende, J-M., 1986. Additional $^{40}\text{Ar}-^{39}\text{Ar}$ dating of the basement and the alkaline volcanism of Gorringe Bank (Atlantic Ocean). *Earth & Planetary Science Letters*, 79, 255-269.
- Fleck, R.J., Sutter, J.F., Elliot, D.H., 1977. Interpretation of discordant $^{40}\text{Ar}/^{39}\text{Ar}$ age-

- spectra of Mesozoic tholeiites from Antarctica. *Geochimica Cosmochimica Acta* 41, 15-32.
- Foland, K.A., Fleming, T.H., Heimann, A., Elliot, D.H., 1993. Potassium-argon dating of fine-grained basalts with massive Ar loss, Application of the $^{40}\text{Ar}/^{39}\text{Ar}$ technique to plagioclase and glass from the Kirkpatrick Basalt Antarctica. *Chemical Geology*, 107, 173-190.
- Frye, J.C. and Leonard, A.B., 1957. Ecological interpretations of Pliocene and Pleistocene stratigraphy in the Great Plains region. *American Journal of Science*, v. 255, no. 1, 1-11.
- 1959. Correlation of the Ogallala Formation (Neogene) in western Texas with the type localities in Nebraska. Bureau of Economic Geology, Texas University, Report of investigations no. 39, 116.
- Funkhouser, J.G., Fisher, D.E. and Bonatti, E., 1968. Excess argon in deep-sea rocks. *Earth and Planetary Science Letters*, 5, 95-100.
- Hart, S.R. and Dodd, R.T.Jr., 1962. Excess radiogenic argon in pyroxenes. *Journal of Geophysical Research*, v. 67, 2998-2999.
- Heizler, M.T. and Ralser, S., 1996. Muscovite age gradients. *American Geophysical Union, Spring Meeting*, GS21A-6.
- Heizler, M.T., Perry, F.V., Crowe, B.M., Peters, L., Appelt, R., 1999. The age of Lathrop Wells volcanic center: An $^{40}\text{Ar}/^{39}\text{Ar}$ dating investigation. *Journal of Geophysical Research*, 104, 767-804.
- Huenke, J.C., and Smith, S.P., 1976. The realities of recoil: ^{39}Ar recoil out of small grains and anomalous age patterns in $^{39}\text{Ar}-^{40}\text{Ar}$ dating. *Proceedings of the Lunar*

- Science Conference 7th, 1987-2008.
- Laughlin, A.W., 1969. Excess radiogenic argon in pegmatite minerals. *Journal of Geophysical Research*, v. 74, 6684-6690.
- Lipman, P.W., Mehnert, H.H., and Naeser, C.W., 1986. Evolution of the Latir volcanic field, northern New Mexico, and its relation to the Rio Grande rift, as indicated by K-Ar and fission-track dating. *Journal of Geophysical Research*, v. 91, 7383-7402.
- Lo, C.-H., Onstott, T.C., Chen, C.-H., Lee, T., 1994. An assessment of $^{40}\text{Ar}/^{39}\text{Ar}$ dating for the whole rock volcanic samples from the Luzon Arc near Taiwan. *Chemical Geology*, 114, 157-178.
- Koppers, A.A.P., Staudigel, H., Wijbrans, J.R., 2000. Dating crystalline groundmass separates of altered Cretaceous seamount basalts by the $^{40}\text{Ar}/^{39}\text{Ar}$ incremental heating technique. *Chemical Geology*, 166, 139-158.
- Mahon, K.I., 1996. The New "York" regression: application of an improved statistical method to geochemistry. *International Geology Review*, 38, 293-303.
- McDougall, I., and Harrison, T.M., 1999. *Geochronology and thermochronology by the $^{40}\text{Ar}/^{39}\text{Ar}$ Method*, 2nd ed. Oxford University Press, New York.
- McDougall, I., Polach, H.A. and Stipp, J.J., 1969. Excess radiogenic argon in young subaerial basalts from the Aukland volcanic field, New Zealand. *Geochimica Cosmochimica Acta*, 33, 1485-1520.
- Nielson, R.L., and Dungan, M.A., 1985. The Petrology and Geochemistry of the Ocate Volcanic Field, North-Central New Mexico. *Geological Society of America Bulletin*, 96: 296-312.
- O'Neill, J.M., and Mehnert, H.H., 1988. Petrology and Physiographic Evolution of the Ocate Volcanic Field, North-Central New Mexico. U.S. Geological Survey,

- Professional Paper 1478.
- Onstott, T.C., Miller, M.L., Ewing, R.C., Arnold, G.W., and Walsh, D.S., 1995. Recoil refinements: Implications for the $^{40}\text{Ar}/^{39}\text{Ar}$ dating technique. *Geochimica Cosmochimica Acta* 59, 1821-1834.
- Pazzaglia, F.J., Duerker, K., Wisniewski, P.A., 1999. Post-Laramide rock-uplift and exhumation of the southern Rocky Mountains: Evidence for the impact of 'Hot-Mantle-Blobs'. *Geological Society of America Abstracts with Programs*, vol. 31, no. 7, session 107.
- Samson, S.D., and Alexander, E.C., Jr., 1987. Calibration of the interlaboratory $^{40}\text{Ar}/^{39}\text{Ar}$ dating standard, Mmhb-1. *Chemical Geology*, 66, 27-34.
- Scott, G.R., 1975. Cenozoic surfaces and deposits in the southern Rocky Mountains. *Geologic Society of America Memoir* 144, 227-248.
- Singer, B.S., Pringle, M.S., 1996. Age and duration of the Matuyama-Brunhes geomagnetic polarity reversal from $^{40}\text{Ar}/^{39}\text{Ar}$ incremental heating analyses of lavas. *Earth & Planetary Science Letters*, 139, 47-61.
- Steiger, R.H., and Jager, E., 1977. Subcommission on geochronology: Convention on the use of decay constants in geo- and cosmochronology. *Earth & Planetary Science Letters*, v. 36, 359-362.
- Stroud, J.R., 1997. The geochronology of the Raton-Clayton volcanic field, with implications for the volcanic history and landscape evolution. Masters Thesis, New Mexico Institute of Mining and Technology.
- Turner, G., and Cadogan, P.H., 1974. Possible effects of ^{39}Ar recoil in $^{40}\text{Ar}-^{39}\text{Ar}$ dating. *Proceedings of the Fifth Lunar Conference*, v. 2, 1601-1615.

Appendix A: $^{40}\text{Ar}/^{39}\text{Ar}$ Data Tables

Appendix A contains all of the $^{40}\text{Ar}/^{39}\text{Ar}$ analytical data from this study. The information given with each sample includes the sample number (i.e. OCA-001), sample type (i.e. groundmass concentrate), sample weight, J-value, discrimination factor, irradiation shipment number (i.e. NM-94), and lab ID number. Samples are listed according to their sample number. The isotopic ratios are corrected for system blank, nuclear interference reactions and radioactive decay of $^{37}\text{Ar}_{\text{Ca}}$. All ages are reported at the 2σ confidence level and propagate uncertainties in J-value, system blank, isotopic peak height regression and mass discrimination. Eruption ages are weighted by the inverse of the variance and uncertainties are calculated using the method of Sampson and Alexander (1987). All ages are calculated using the decay constants recommended by Steiger and Jagar (1977). The % $^{38}\text{Ar}_{\text{Cl}}$ released per step can not be calculated for samples irradiated at Texas due to the shielding of thermal neutrons.

Nuclear interference correction factors:

Irradiation Shipment	Irradiation Facility	$(^{39}\text{Ar}/^{37}\text{Ar})_{\text{Ca}}$	$(^{36}\text{Ar}/^{37}\text{Ar})_{\text{Ca}}$	$(^{38}\text{Ar}/^{39}\text{Ar})_{\text{K}}$	$(^{40}\text{Ar}/^{39}\text{Ar})_{\text{K}}$
NM-94	Michigan	0.00070 ± 0.00005	0.00026 ± 0.00002	0.0119	0.0250 ± 0.005
NM-98	Texas	0.00089 ± 0.00003	0.00028 ± 0.000011	0.0119	0.0002 ± 0.0003
NM-117	Michigan	0.00078 ± 0.00003	0.00028 ± 0.00001	0.0119	0.0236 ± 0.0005
NM-118	Michigan	0.00070 ± 0.00005	0.00026 ± 0.00002	0.0119	0.0250 ± 0.005
NM-120	Michigan	0.00070 ± 0.00005	0.00026 ± 0.00002	0.0119	0.0250 ± 0.005
NM-121	Michigan	0.00070 ± 0.00005	0.00026 ± 0.00002	0.0119	0.0250 ± 0.005

A-3

D	Temp/P (^°C/W)	$^{40}\text{Ar}/^{39}\text{Ar}$	$^{37}\text{Ar}/^{39}\text{Ar}$	$^{38}\text{Ar}/^{39}\text{Ar}$	$^{39}\text{Ar}_\text{K}$ (mol)	K/Ca	Ci/K	$^{37}\text{Ar}_\text{Ca}$ (%)	$^{39}\text{Ar}_\text{Ca}$ (%)	$^{39}\text{Ar}_\text{K}$ (%)	$^{40}\text{Ar}^*$ (%)	^{39}Ar (%)	Age (Ma)	$\pm 2\sigma$ (Ma)
OCA-005; A:3:94, groundmass concentrate, 53.26 mg, J=0.000162326±0.10%, D=1.00362±0.00105, NM-94, Lab#=9522-01														
A	550	1.11E+02	1.05E+00	3.58E-01	1.9E-15	4.8E-01	4.3E-02	3.2	33.3	13.7	4.9	13.7	1.60	0.39
B	625	3.66E+01	1.62E+00	1.08E-01	1.8E-15	3.1E-01	3.4E-02	4.6	24.2	12.9	12.7	26.6	1.37	0.15
C	700	3.04E+01	2.46E+00	8.67E-02	1.7E-15	2.1E-01	2.5E-02	6.8	17.3	12.6	16.3	39.2	1.45	0.16
D	775	2.85E+01	2.76E+00	7.76E-02	1.5E-15	1.8E-01	1.4E-02	6.8	8.7	11.2	20.3	50.4	1.70	0.14
E	850	2.38E+01	2.37E+00	6.27E-02	1.7E-15	2.2E-01	6.3E-03	6.4	4.4	12.4	22.9	62.8	1.60	0.12
F	925	2.07E+01	2.04E+00	5.49E-02	1.3E-15	2.5E-01	2.8E-03	4.3	1.5	9.5	22.4	72.4	1.36	0.13
G	1000	2.48E+01	2.48E+00	6.61E-02	8.0E-16	2.1E-01	4.4E-03	3.1	1.4	5.8	22.0	78.2	1.60	0.20
H	1075	3.73E+01	2.89E+00	1.09E-01	5.4E-16	1.8E-01	7.3E-03	2.5	1.6	3.9	14.1	82.1	1.55	0.28
I	1150	5.04E+01	6.25E+00	1.53E-01	2.5E-16	8.2E-02	5.3E-03	2.5	0.5	1.8	11.3	83.9	1.67	0.53
J	1300	1.68E+02	2.20E+01	5.51E-01	8.4E-16	2.3E-02	1.2E-02	29.4	4.0	6.1	4.0	89.9	2.02	0.71
K	1650	1.76E+02	1.39E+01	5.83E-01	1.4E-15	3.7E-02	5.3E-03	30.5	3.0	10.1	2.6	100.0	1.36	0.74
total gas age		n=11			1.4E-14	2.3E-01							1.54	0.29
Eruption Age		n=3	steps C-E		5.0E-15	2.0E-01						36.2	1.59	0.15
OCA-006; A:5:94, groundmass concentrate, 52.15 mg, J=0.000161039±0.10%, D=1.00362±0.00105, NM-94, Lab#=9523-01														
A	550	3.30E+02	5.32E-01	1.09E+00	1.2E-15	9.6E-01	2.9E-02	1.3	27.3	9.1	2.3	9.1	2.23	1.22
B	625	6.64E+01	1.15E+00	2.09E-01	1.3E-15	4.4E-01	2.2E-02	2.9	21.6	9.7	7.1	18.8	1.38	0.32
C	700	2.95E+01	1.71E+00	8.04E-02	1.5E-15	3.0E-01	1.9E-02	5.1	22.1	11.5	19.7	30.3	1.68	0.14
D	775	2.19E+01	2.39E+00	5.79E-02	1.6E-15	2.1E-01	1.3E-02	7.5	16.1	12.1	22.6	42.4	1.44	0.11
E	850	1.55E+01	2.73E+00	3.46E-02	1.8E-15	1.9E-01	4.0E-03	10.0	5.7	14.0	35.4	56.5	1.60	0.10
F	925	1.12E+01	2.67E+00	2.01E-02	1.8E-15	1.9E-01	1.2E-03	9.8	1.7	14.1	48.6	70.6	1.58	0.06
G	1000	1.05E+01	2.62E+00	1.74E-02	1.4E-15	1.9E-01	1.1E-03	7.2	1.1	10.5	52.6	81.1	1.60	0.07
H	1075	1.38E+01	2.77E+00	2.94E-02	7.0E-16	1.8E-01	1.8E-03	3.9	1.0	5.4	38.6	86.4	1.55	0.12
I	1150	2.22E+01	3.89E+00	5.03E-02	3.6E-16	1.8E-01	2.9E-03	2.8	0.8	2.7	34.2	89.2	2.21	0.25
J	1300	6.02E+01	2.63E+01	1.84E-01	1.7E-16	1.9E-02	2.0E-03	9.2	0.3	1.3	13.1	90.5	2.33	0.75
K	1650	4.12E+01	1.64E+01	1.27E-01	1.2E-15	3.1E-02	2.4E-03	40.4	2.3	9.5	12.1	100.0	1.47	0.26
total gas age		n=11			1.3E-14	2.8E-01							1.64	0.25
Eruption Age		n=5	steps D-H		7.3E-14	1.9E-01						56.1	1.57	0.06
OCA-007; B:3:94, groundmass concentrate, 49.95 mg, J=0.000162534±0.10%, D=1.00362±0.00105, NM-94, Lab#=9525-01														
A	550	1.45E+03	3.90E+00	4.89E+00	3.1E-16	1.3E-01	8.2E-02	2.5	31.8	2.2	0.4	2.2	1.71	9.52
B	625	1.82E+02	5.96E+00	5.92E-01	4.3E-16	8.6E-02	1.6E-02	5.2	8.3	3.1	4.3	5.3	2.29	0.92
C	700	5.55E+01	4.76E+00	1.68E-01	9.0E-16	1.1E-01	5.1E-03	8.7	5.7	6.4	11.2	11.8	1.83	0.31
D	775	2.47E+01	3.34E+00	6.51E-02	1.4E-15	1.5E-01	3.2E-03	9.6	5.7	10.1	22.9	21.9	1.66	0.13
E	850	1.65E+01	1.98E+00	3.84E-02	2.2E-15	2.6E-01	1.1E-03	8.9	3.0	15.9	32.1	37.8	1.55	0.09
F	925	1.70E+01	1.44E+00	4.03E-02	2.4E-15	3.5E-01	1.7E-03	6.9	5.1	16.9	30.5	54.7	1.52	0.08
G	1000	2.97E+01	1.21E+00	8.37E-02	1.8E-15	4.2E-01	2.9E-03	4.4	6.6	13.0	16.8	67.7	1.46	0.12
H	1075	7.09E-01	9.51E-01	2.23E-01	1.5E-15	5.4E-01	4.4E-03	2.8	8.0	10.4	7.9	78.1	1.52	0.26
I	1150	7.46E+01	1.03E+00	2.28E-01	1.1E-15	4.9E-01	4.7E-03	2.2	6.1	7.7	9.9	85.8	2.16	0.35
J	1300	9.74E+01	1.23E+01	3.14E-01	5.2E-16	4.2E-02	7.8E-03	13.0	5.0	3.7	5.8	89.5	1.66	0.57
K	1650	1.10E+02	1.20E+01	3.61E-01	1.5E-15	4.3E-02	8.2E-03	35.7	14.8	10.5	4.2	100.0	1.36	0.42
total gas age		n=11			1.4E-14	2.8E-01							1.62	0.44
Eruption Age		n=5	steps D-H		9.3E-14	3.4E-01						66.4	1.54	0.07
PW-OCA-007; B:6:98, groundmass concentrate, 187.24mg, J=0.00078705±0.10%, D=1.00361±0.00157, NM-98, Lab#=9729-01														
A	550	2.95E+04	2.79E-01	9.92E+01	7.0E-17	1.8E+00	-	0.0	-	0.0	0.6	0.0	247.96	5924.24
B	625	4.49E+02	2.52E+00	1.50E+00	1.2E-15	2.0E-01	-	0.3	-	0.5	1.3	0.5	8.44	8.47
C	700	7.34E+01	1.95E+00	2.40E-01	9.8E-16	2.6E-01	-	0.2	-	0.4	3.8	0.9	3.91	1.81
D	775	9.65E+00	1.48E+00	2.88E-02	2.8E-14	3.5E-01	-	5.0	-	11.4	13.2	12.3	1.81	0.15
E	850	4.22E+00	1.73E+00	1.10E-02	5.1E-14	2.9E-01	-	10.7	-	20.7	26.4	33.0	1.59	0.06
F	925	3.62E+00	1.58E+00	8.96E-03	5.2E-14	3.2E-01	-	9.9	-	20.8	30.4	53.8	1.56	0.05
G	1000	4.27E+00	1.36E+00	1.13E-02	2.8E-14	3.8E-01	-	4.6	-	11.2	24.8	65.0	1.51	0.07
H	1100	6.58E+00	1.46E+00	1.90E-02	3.8E-14	3.5E-01	-	6.6	-	15.2	16.5	80.2	1.54	0.11
I	1200	1.29E+01	2.99E+00	4.02E-02	2.4E-14	1.7E-01	-	8.8	-	9.8	9.7	90.1	1.78	0.21
J	1300	2.36E+01	1.87E+01	8.06E-02	2.0E-14	2.7E-02	-	45.9	-	8.2	5.7	98.3	1.94	0.41
K	1650	1.65E+02	1.52E+01	5.44E-01	4.3E-15	3.3E-02	-	8.0	-	1.7	3.3	100.0	7.80	3.03
total gas age		n=11			2.5E-13	2.8E-01							1.86	1.89
Eruption Age		n=4	steps E-H		1.7E-13	3.3E-01						67.9	1.56	0.02
OCA-008-01; F:2:98, groundmass concentrate, 93.9mg, J=0.000780753±0.10%, D=1.00361±0.00157, NM-98, Lab#=9764-01														
A	550	3.26E+02	2.07E+00	1.10E+00	1.9E-16	2.5E-01	-	0.1	-	0.2	0.0	0.2	-0.22	14.17
B	625	1.36E+01	1.90E+00	3.96E-02	1.6E-15	2.7E-01	-	0.8	-	1.5	15.0	1.7	2.88	0.42
C	700	3.59E+00	1.82E+00	5.86E-03	9.3E-15	2.8E-01	-	4.6	-	8.8	55.9	10.5	2.83	0.10
D	775	2.99E+00	2.19E+00	3.74E-03	1.4E-14	2.3E-01	-	8.4	-	13.5	69.1	24.0	2.91	0.06
E	850	2.66E+00	2.76E+00	2.68E-03	2.7E-14	1.8E-01	-	19.9	-	25.4	79.8	49.4	2.98	0.04
F	925	2.84E+00	1.52E+00	2.82E-03	2.4E-14	3.4E-01	-	9.7	-	22.6	75.0	72.1	3.00	0.04
G	1000	2.62E+00	1.21E+00	2.27E-03	9.4E-15	4.2E-01	-	3.0	-	8.9	78.2	80.9	2.89	0.09
H	1100	3.50E+00	1.68E+00	5.54E-03	1.1E-14	3.0E-01	-	4.7	-	10.0	57.2	90.9	2.82	0.09
I	1200	7.69E+00	4.84E+00	2.19E-02	3.6E-15	1.1E-01	-	4.6	-	3.4	21.2	94.3	2.31	0.31
J	1300	1.26E+01	2.65E+01	4.51E-02	2.9E-15	1.9E-02	-	20.5	-	2.7	11.9	97.0	2.18	0.44
K	1650	7.03E+01	2.78E+01	2.42E-01	3.2E-15	1.8E-02	-	23.6	-	3.0	1.8	100.0	1.79	1.40
total gas age		n=11			1.1E-13	2.6E-01							2.84	0.15
Eruption Age		n=2	steps E-F		5.1E-14	2.6E-01						48.1	2.98	0.05

ID	Temp/P (*C/W)	$^{40}\text{Ar}/^{39}\text{Ar}$	$^{37}\text{Ar}/^{39}\text{Ar}$	$^{38}\text{Ar}/^{39}\text{Ar}$	$^{39}\text{Ar}_k$ (mol)	K/Ca	C/K	$^{37}\text{Ar}_{\text{ca}}$ (%)	$^{38}\text{Ar}_{\text{cl}}$ (%)	$^{39}\text{Ar}_k$ (%)	$^{40}\text{Ar}^*$ (%)	^{38}Ar (%)	Age (Ma)	$\pm 2\sigma$ (Ma)	
OCA-012: G:198, groundmass concentrate, 94.53mg, J=0.00077964±0.10%, D=1.00361±0.00157, NM-98, Lab#=9757-01															
A	550	2.74E+03	3.24E+00	9.12E+00	5.1E-17	1.6E-01	-	0.0	-	0.1	1.5	0.1	57.37	388.23	
B	625	2.05E+02	2.37E+00	6.92E-01	2.4E-16	2.2E-01	-	0.2	-	0.3	0.4	0.3	1.19	9.46	
C	700	8.38E+00	1.81E+00	2.32E-02	2.3E-16	2.8E-01	-	0.1	-	0.2	19.8	0.6	2.33	2.17	
D	775	2.90E+00	1.65E+00	3.33E-03	1.2E-14	3.1E-01	-	5.7	-	13.0	70.8	13.6	2.89	0.06	
E	850	2.47E+00	2.00E+00	1.78E-03	2.2E-14	2.5E-01	-	12.7	-	23.7	85.4	37.3	2.97	0.03	
F	925	2.53E+00	2.26E+00	2.05E-03	2.5E-14	2.3E-01	-	15.8	-	26.3	83.4	63.6	2.97	0.04	
G	1000	2.40E+00	1.87E+00	1.41E-03	1.2E-14	3.0E-01	-	5.8	-	12.9	88.4	76.5	2.98	0.05	
H	1100	2.96E+00	2.14E+00	3.31E-03	1.2E-14	2.4E-01	-	7.3	-	12.8	72.9	89.3	3.03	0.06	
I	1200	4.59E+00	4.14E+00	9.93E-03	4.5E-15	1.2E-01	-	5.3	-	4.8	43.5	94.1	2.81	0.17	
J	1300	1.07E+01	2.75E+01	3.73E-02	3.4E-15	1.9E-02	-	26.4	-	3.6	18.0	97.7	2.77	0.34	
K	1650	5.76E+01	3.40E+01	1.95E-01	2.1E-15	1.5E-02	-	20.6	-	2.3	4.7	100.0	3.95	1.15	
total gas age		n=11		9.4E-14	2.4E-01								3.00	0.33	
Eruption Age		n=4		steps E-H	7.1E-14	2.5E-01							75.7	2.98	0.03
OCA-013; A6:117, groundmass concentrate, 108.41mg, J=0.001068213±0.10%, D=1.00644±0.00091, NM-117, Lab#=50830-01															
A	550	1.20E+02	3.58E+00	3.94E-01	4.8E-15	1.4E-01	1.1E-02	1.0	3.1	1.0	3.2	1.0	7.37	2.96	
B	625	5.81E+00	3.47E+00	6.89E-03	1.8E-14	1.5E-01	1.6E-03	3.7	1.8	3.8	54.2	4.8	6.08	0.19	
C	675	3.95E+00	2.90E+00	4.02E-03	3.0E-14	1.8E-01	7.2E-04	5.2	1.3	6.3	75.4	11.1	5.74	0.08	
D	725	3.50E+00	2.39E+00	2.43E-03	5.4E-15	2.1E-01	4.4E-04	7.6	1.5	11.3	84.5	22.5	5.70	0.04	
E	775	3.34E+00	2.10E+00	1.81E-03	5.8E-14	2.4E-01	5.7E-04	7.3	2.0	12.3	88.5	34.8	5.69	0.04	
F	825	3.31E+00	1.71E+00	1.69E-03	7.6E-14	3.0E-01	6.4E-04	7.7	3.0	16.1	88.5	51.0	5.65	0.04	
G	875	3.32E+00	1.48E+00	1.68E-03	6.8E-14	3.5E-01	9.6E-04	6.0	4.0	14.4	88.0	65.4	5.64	0.04	
H	925	3.40E+00	1.51E+00	1.97E-03	6.1E-14	3.4E-01	1.0E-03	5.4	5.6	12.8	85.9	78.2	5.63	0.04	
I	975	3.69E+00	1.64E+00	3.02E-03	4.2E-14	3.1E-01	2.7E-03	4.1	6.9	8.9	78.8	87.1	5.59	0.05	
J	1025	4.22E+00	1.99E+00	4.86E-03	2.6E-14	2.6E-01	5.3E-03	9.0	8.3	5.4	69.3	92.5	5.64	0.10	
K	1075	4.96E+00	2.75E+00	6.62E-03	1.1E-14	1.9E-01	1.0E-02	1.7	6.8	2.3	64.7	94.7	6.18	0.23	
L	1150	8.00E+00	4.21E+00	1.78E-02	9.3E-15	1.2E-01	1.9E-02	2.3	10.8	2.0	38.3	96.7	5.92	0.36	
M	1225	2.53E+01	1.70E+01	7.99E-02	5.0E-15	3.0E-02	3.1E-02	5.0	9.6	1.1	12.3	97.7	6.08	0.75	
N	1300	3.22E+01	7.34E+01	1.19E-01	3.5E-15	7.0E-03	4.5E-02	15.0	9.6	0.7	9.3	98.5	6.11	1.10	
O	1450	3.44E+01	5.86E+01	1.24E-01	3.7E-15	8.7E-03	5.7E-02	12.9	13.1	0.8	7.5	99.2	5.22	1.01	
P	1650	3.30E+01	5.69E+01	1.16E-01	3.6E-15	9.0E-03	5.7E-02	12.0	12.5	0.8	10.4	100.0	6.91	1.21	
total gas age		n=16		4.7E-13	2.6E-01								5.72	0.14	
Eruption Age		n=7		steps D-J	3.8E-13	2.9E-01							81.3	5.65	0.03
OCA-014; E6:117, groundmass concentrate, 69.58mg, J=0.001064224±0.10%, D=1.00644±0.00091, NM-117, Lab#=50854-01															
A	550	1.36E+02	2.58E+00	4.43E-01	4.2E-15	2.0E-01	5.9E-02	0.8	9.6	1.0	3.7	1.0	9.70	2.79	
B	625	5.56E+00	1.97E+00	7.61E-03	1.8E-14	2.6E-01	1.6E-02	2.4	9.8	3.9	62.0	4.9	6.62	0.15	
C	700	3.73E+00	1.25E+00	2.11E-03	4.6E-14	4.1E-01	6.0E-03	4.5	10.7	11.3	85.4	16.3	6.11	0.06	
D	775	3.46E+00	7.80E-01	9.21E-03	9.1E-14	6.5E-01	2.1E-03	5.5	7.6	22.4	90.8	38.7	6.03	0.03	
E	850	3.44E+00	6.92E-01	1.21E-03	8.5E-14	7.4E-01	1.3E-03	4.6	4.4	21.1	91.4	59.8	6.04	0.03	
F	925	3.54E+00	9.54E-01	1.57E-03	4.6E-15	5.3E-01	1.5E-03	3.5	2.7	11.5	88.5	71.2	6.01	0.05	
G	1000	4.13E+00	1.69E+00	4.07E-03	2.7E-14	3.0E-01	3.9E-03	3.6	4.1	6.6	73.7	77.8	5.85	0.09	
H	1075	4.60E+00	2.46E+00	5.58E-03	1.9E-14	2.1E-01	7.2E-03	3.7	5.4	4.8	68.1	82.6	6.01	0.14	
I	1150	4.55E+00	2.79E+00	5.76E-03	1.8E-14	1.8E-01	8.9E-03	4.0	6.3	4.5	67.2	87.1	5.87	0.12	
J	1300	1.18E+01	1.09E+01	3.34E-02	1.7E-14	4.7E-02	1.7E-02	14.0	11.0	4.1	23.7	91.2	5.40	0.23	
K	1650	1.46E+01	1.91E+01	4.35E-02	3.6E-14	2.7E-02	2.0E-02	53.4	28.3	8.8	22.4	100.0	6.35	0.24	
total gas age		n=11		4.0E-13	4.6E-01								6.08	0.12	
Eruption Age		n=3		steps D-F	2.2E-13	6.6E-01							55.0	6.03	0.03
OCA-016; R3:121, groundmass concentrate, 84.50mg, J=0.000478452±0.10%, D=1.00644±0.00091, NM-121, Lab#=51077-01															
A	550	3.21E+02	3.23E+00	1.0E+00	1.9E-16	1.6E-01	1.3E-01	0.2	7.6	0.3	2.5	0.3	6.92	15.94	
B	625	4.39E+01	3.75E+00	1.39E-01	1.0E-15	1.4E-01	1.2E-02	1.2	3.9	1.5	7.3	1.8	2.76	1.13	
C	675	1.96E+00	3.98E+00	-5.98E-02	3.1E-17	1.3E-01	2.2E-02	0.0	0.2	0.0	1.8	17.09	15.10		
D	725	5.33E+00	3.63E+00	6.50E-03	3.8E-15	1.4E-01	5.4E-03	4.1	6.5	5.5	68.8	7.3	3.17	0.16	
E	775	4.24E+00	3.02E+00	2.48E-03	6.2E-15	1.7E-01	2.3E-03	5.5	4.8	8.9	87.6	16.3	3.21	0.10	
F	825	4.04E+00	2.86E+00	1.72E-03	9.6E-15	1.8E-01	2.0E-03	8.1	5.9	13.9	92.3	30.1	3.23	0.06	
G	875	4.04E+00	2.54E+00	1.81E-03	1.1E-14	2.0E-01	1.5E-03	8.4	5.3	16.2	91.0	46.4	3.17	0.05	
H	925	4.26E+00	1.82E+00	2.26E-03	1.2E-14	2.8E-01	1.6E-03	6.4	5.8	17.2	87.0	63.6	3.20	0.06	
I	975	3.89E+00	1.46E+00	1.25E-03	4.4E-15	3.5E-01	1.8E-03	1.9	2.5	6.4	92.8	70.0	3.12	0.12	
J	1025	4.39E+00	1.73E+00	2.65E-03	8.5E-15	2.9E-01	2.7E-03	4.3	7.3	12.3	84.6	82.3	3.21	0.06	
K	1075	5.17E+00	1.99E+00	6.06E-03	3.8E-15	2.5E-01	4.9E-03	2.2	5.9	5.5	67.9	87.8	3.03	0.15	
L	1150	7.77E+00	2.26E+00	1.41E-02	2.9E-15	2.3E-01	1.0E-02	2.0	9.5	4.2	48.4	92.0	3.25	0.24	
M	1300	1.60E+01	1.03E+01	4.60E-02	1.5E-15	4.9E-02	1.5E-02	4.6	7.3	2.2	19.8	94.2	2.74	0.59	
N	1650	2.24E+01	4.34E+01	7.29E-02	4.0E-15	1.2E-02	2.2E-02	51.2	27.8	5.8	18.7	100.0	3.73	0.37	
total gas age		n=14		6.9E-14	2.2E-01								3.22	0.20	
Eruption Age		n=7		steps D-J	5.6E-14	2.3E-01							80.5	3.20	0.04
OCA-019; U6:117, groundmass concentrate, 59.30mg, J=0.00104432±0.11%, D=1.00644±0.00091, NM-117, Lab#=50872-01															
A	550	1.45E+02	1.65E+00	4.78E-01	4.4E-15	3.1E-01	1.2E-02	0.9	5.9	1.0	2.4	1.0	6.48	2.68	
B	625	5.19E+00	2.44E+00	9.64E-03	1.1E-14	2.1E-01	1.8E-03	3.1	2.1	2.4	48.6	3.4	4.75	0.21	
C	700	2.94E+00	1.88E+00	1.91E-03	2.7E-14	2.7E-01	1.2E-03	6.1	3.5	6.0	86.3	9.4	4.72	0.07	
D	775	2.63E+00	1.46E+00	7.82E-04	5.7E-14	3.5E-01	7.5E-04	10.1	4.7	12.8	94.9	22.2	4.71	0.03	
E	850	2.53E+00	9.76E-01	4.96E-04	8.8E-14	5.2E-01	6.9E-04	10.5	6.8	19.9	96.5				

ID	Temp/P (°C/Pa)	$^{40}\text{Ar}/^{39}\text{Ar}$	$^{37}\text{Ar}/^{39}\text{Ar}$	$^{38}\text{Ar}/^{39}\text{Ar}$	$^{39}\text{Ar}_{\text{Ar}}$	K/Ca	C/I/K	$^{37}\text{Ar}_{\text{Ca}}$	$^{38}\text{Ar}_{\text{Ca}}$	$^{39}\text{Ar}_{\text{K}}$	$^{40}\text{Ar}^*$	^{39}Ar	Age (Ma)	$\pm 2\sigma$ (Ma)
OCA-020: O6:118, groundmass concentrate, 96.89mg, J=0.000149586±0.12%, D=1.00644±0.00091, NM-118, Lab#=50942-01														
A	550	1.13E+04	1.19E+00	3.81E+01	8.6E-16	4.3E-01	4.6E-02	0.5	11.2	0.7	0.4	0.7	13.40	235.33
B	625	4.20E+02	1.83E+00	1.38E+00	3.9E-15	2.8E-01	1.4E-03	3.3	1.6	3.4	2.9	4.1	3.31	1.35
C	675	1.37E+02	1.40E+00	4.34E-01	5.5E-15	3.6E-01	1.6E-04	3.6	0.3	4.8	6.2	8.9	2.27	0.38
D	725	6.93E+01	1.21E+00	2.04E-01	8.7E-15	4.2E-01	5.3E-04	5.0	1.3	7.6	12.9	16.5	2.41	0.18
E	775	4.38E+01	1.02E+00	1.19E-01	8.8E-15	5.0E-01	3.1E-04	4.2	0.8	7.6	19.8	24.1	2.34	0.13
F	825	2.93E+01	8.14E-01	7.04E-02	1.7E-14	6.3E-01	4.8E-04	6.5	2.3	14.7	29.1	38.8	2.30	0.08
G	875	2.35E+01	6.86E-01	5.09E-02	1.7E-14	7.4E-01	2.5E-04	5.3	1.2	14.3	36.2	53.2	2.30	0.06
H	925	2.09E+01	6.38E-01	4.25E-02	1.8E-14	8.0E-01	6.0E-04	5.3	3.0	15.4	40.0	68.6	2.26	0.05
I	975	2.23E+01	6.40E-01	4.71E-02	1.3E-14	8.0E-01	1.3E-03	3.9	4.9	11.3	37.6	79.8	2.26	0.06
J	1025	2.73E+01	7.50E-01	6.38E-02	7.5E-15	6.8E-01	2.2E-03	2.6	4.6	6.5	31.0	86.3	2.28	0.09
K	1075	4.65E+01	1.07E+00	1.29E-01	4.9E-15	4.8E-01	5.6E-03	2.5	7.7	4.2	18.3	90.5	2.29	0.17
L	1150	7.49E+01	1.41E+00	2.25E-01	3.1E-15	3.6E-01	1.2E-02	2.1	10.3	2.7	11.4	93.2	2.30	0.30
M	1300	9.77E+01	7.89E+00	3.03E-01	3.5E-15	6.5E-02	2.2E-02	13.1	22.4	3.1	8.8	96.3	2.34	0.30
N	1650	1.34E+02	2.08E+01	4.21E-01	4.3E-15	2.5E-02	2.3E-02	42.0	28.4	3.7	8.1	100.0	2.95	0.44
total gas age n=14														
Eruption Age n=10 steps D-M 1.0E-13 6.4E-01														
												87.4 2.28 0.03		
OCA-022: T6:118, groundmass concentrate, 100.20mg, J=0.000146519±0.12%, D=1.00644±0.00091, NM-118, Lab#=50954-01														
A	550	1.28E+04	1.58E+00	4.28E+01	1.5E-15	3.2E-01	3.7E-02	1.1	9.8	1.7	1.1	1.7	35.23	279.63
B	625	1.23E+03	1.82E+00	4.12E+00	3.6E-15	2.8E-01	5.3E-03	3.0	3.4	4.0	0.8	5.7	2.74	6.32
C	675	4.32E+02	1.45E+01	1.42E+00	6.1E-15	3.5E-01	3.0E-03	4.0	3.2	6.8	2.8	12.5	3.23	1.09
D	725	2.22E+02	1.16E+00	7.22E-01	1.0E-14	4.4E-01	4.4E-04	5.2	0.8	11.1	4.1	23.5	2.41	0.48
E	775	1.50E+02	9.90E-01	4.78E-01	9.6E-15	5.2E-01	9.9E-04	4.3	1.7	10.6	6.2	34.2	2.45	0.36
F	825	1.05E+02	8.39E-01	3.23E-01	1.5E-14	6.1E-01	8.7E-04	5.6	2.3	16.4	8.8	50.6	2.44	0.24
G	875	9.31E+01	7.74E-01	2.87E-01	1.3E-14	6.6E-01	7.4E-04	4.5	1.7	14.4	9.1	65.0	2.23	0.23
H	925	1.06E+02	8.41E-01	3.30E-01	1.1E-14	6.1E-01	2.3E-03	4.0	4.3	11.7	8.5	76.7	2.38	0.25
I	975	1.82E+02	1.19E+00	5.87E-01	4.6E-15	4.3E-01	4.1E-03	2.4	3.3	5.0	4.8	81.7	2.30	0.49
J	1025	3.06E+02	1.94E+00	9.99E-01	1.9E-02	8.9E-01	8.9E-03	1.6	2.9	2.1	3.6	83.8	2.88	1.18
K	1075	4.08E+02	2.10E+00	1.34E+00	1.7E-15	2.4E-01	9.9E-03	1.6	3.0	1.9	2.8	85.7	3.01	1.77
L	1150	4.51E+02	2.68E+00	1.48E+00	1.7E-15	1.9E-01	1.9E-02	2.1	5.6	1.9	3.4	87.6	4.07	1.80
M	1300	1.64E+02	1.01E+01	5.25E-01	7.6E-15	5.0E-02	3.1E-02	34.5	41.6	8.4	6.0	95.9	2.62	0.41
N	1650	4.23E+02	1.57E+01	1.37E+00	3.7E-15	3.3E-02	2.5E-02	25.9	16.2	4.1	4.4	100.0	4.91	1.27
total gas age n=14														
Eruption Age n=6 steps D-I 6.3E-14 5.6E-01														
												69.3 2.36 0.14		
OCA-023: T2:118, groundmass concentrate, 106.75mg, J=0.000147695±0.12%, D=1.00644±0.00091, NM-118, Lab#=50956-01														
A	550	3.10E+02	1.48E+00	1.03E+00	1.3E-15	3.5E-02	1.2E-01	1.2	5.9	1.6	1.8	1.6	1.51	1.39
B	625	1.34E+01	1.63E+00	2.36E-02	2.7E-15	3.1E-01	1.2E-03	2.7	1.2	3.4	48.7	5.0	1.74	0.11
C	675	9.23E+00	1.46E+00	8.24E-03	3.3E-15	3.5E-01	6.3E-04	3.0	0.8	4.1	74.5	9.1	1.83	0.08
D	725	8.32E+00	1.24E+00	4.52E-03	6.5E-15	4.1E-01	4.5E-04	4.9	1.1	8.1	84.8	17.2	1.88	0.05
E	775	8.42E+00	1.03E+00	5.43E-03	6.1E-15	5.0E-01	6.0E-04	3.9	1.4	7.5	81.6	24.7	1.83	0.04
F	825	7.60E+00	7.81E-01	2.75E-03	1.4E-15	6.5E-01	3.2E-04	6.8	1.7	17.5	89.8	42.2	1.82	0.02
G	875	7.42E+00	6.84E-01	2.34E-03	4.9E-15	7.5E-01	7.9E-04	2.1	1.4	6.1	91.1	48.2	1.80	0.04
H	925	7.42E+00	6.91E-01	2.54E-03	1.1E-14	7.4E-01	5.2E-04	4.8	2.2	13.9	90.3	62.1	1.79	0.02
I	975	7.48E+00	7.60E-01	2.95E-03	1.2E-14	6.7E-01	9.5E-04	5.8	4.4	15.3	88.8	77.5	1.77	0.02
J	1025	7.40E+00	8.56E-01	2.09E-03	4.9E-15	6.0E-01	1.1E-03	2.6	2.0	6.1	92.2	83.6	1.82	0.04
K	1075	8.26E+00	1.11E+00	6.10E-03	6.1E-15	4.6E-01	3.0E-03	4.2	6.9	7.6	78.9	91.2	1.74	0.04
L	1150	1.15E+01	2.19E+00	1.95E-02	1.8E-15	2.3E-01	1.3E-02	2.5	9.1	2.3	51.2	93.5	1.57	0.11
M	1300	2.49E+01	1.09E+01	6.90E-02	1.8E-15	4.7E-02	2.7E-02	12.1	18.2	2.2	21.4	95.7	1.43	0.22
N	1650	4.60E+01	2.05E+01	1.38E-01	3.4E-15	5.2E-02	3.4E-02	43.5	43.8	4.3	14.4	100.0	1.79	0.24
total gas age n=14														
Eruption Age n=5 steps F-J 4.7E-14 6.8E-01														
												58.9 1.80 0.02		
OCA-024: Q2:121, groundmass concentrate, 89.20mg, J=0.000476807±0.10%, D=1.00644±0.00091, NM-121, Lab#=51070-01														
A	550	1.99E+02	7.34E-01	6.56E-01	1.9E-16	7.0E-01	4.4E-02	0.0	1.0	0.1	2.6	0.1	4.49	9.02
B	625	6.02E+01	9.86E-01	1.76E-01	1.3E-15	5.2E-01	9.0E-03	0.4	1.4	0.7	13.7	0.8	7.11	1.10
C	675	1.12E+01	1.18E+00	3.55E-02	1.4E-16	4.3E-01	9.4E-04	0.0	0.0	0.1	7.0	0.9	0.68	2.96
D	725	6.92E+00	1.00E+00	7.03E-03	9.2E-15	5.1E-01	1.6E-03	2.5	1.7	5.1	70.7	6.0	4.21	0.08
E	775	5.75E+00	8.36E-01	2.84E-03	1.1E-14	6.1E-01	6.2E-04	2.5	0.8	6.1	86.1	12.1	4.25	0.06
F	825	5.44E+00	6.94E-01	1.16E-03	2.2E-14	7.4E-01	4.9E-04	4.1	1.2	12.3	94.2	24.4	4.41	0.03
G	875	5.31E+00	5.80E-01	7.73E-04	3.5E-14	8.8E-01	5.3E-04	5.4	2.1	19.2	96.1	43.6	4.38	0.02
H	925	5.28E+00	6.47E-01	6.92E-04	4.0E-14	7.9E-01	7.2E-04	6.9	3.3	22.1	96.6	65.7	4.39	0.02
I	975	5.35E+00	6.06E-01	8.56E-04	1.9E-14	8.4E-01	1.9E-03	3.1	2.7	10.4	95.7	76.1	4.40	0.04
J	1025	5.53E+00	6.50E-01	1.23E-03	2.2E-14	7.9E-01	3.2E-03	3.8	3.8	8.0	12.0	93.9	88.1	4.46
K	1075	6.02E+00	7.52E-01	3.24E-03	6.6E-15	6.8E-01	1.0E-02	1.3	7.8	3.7	84.7	91.7	4.38	0.08
L	1150	6.24E+00	9.55E-01	4.49E-03	4.9E-15	5.3E-01	2.2E-02	1.1	10.8	2.4	79.5	94.1	4.26	0.13
M	1300	8.75E+00	1.13E+01	1.89E-02	2.2E-15	4.5E-02	3.6E-02	6.6	9.0	1.2	45.8	95.3	3.47	0.29
N	1650	1.08E+01	2.75E+01	2.87E-02	8.5E-15	1.9E-02	5.2E-02	62.3	50.1					

ID	Temp/P (°C/W)	$^{40}\text{Ar}/^{39}\text{Ar}$	$^{37}\text{Ar}/^{39}\text{Ar}$	$^{36}\text{Ar}/^{39}\text{Ar}$	$^{39}\text{Ar}_\text{K}$ (mol)	K/Ca	Ci/K	$^{37}\text{Ar}_{\text{Cs}}$ (%)	$^{38}\text{Ar}_{\text{Cl}}$ (%)	$^{39}\text{Ar}_\text{K}$ (%)	$^{40}\text{Ar}^*$ (%)	^{39}Ar (%)	Age (Ma)	$\pm 2\sigma$ (Ma)
OCA-026; C6:117, groundmass concentrate, 52.43mg, J=0.001060252±0.10%, D=1.00644±0.00091, NM-117, Lab#=50842-01														
A	550	3.72E+01	5.77E-01	1.17E-01	7.0E-15	8.8E-01	1.9E-02	0.7	4.1	1.4	7.1	1.4	5.08	0.90
B	625	3.87E+00	1.16E+00	2.70E-03	1.4E-14	4.4E-01	1.2E-02	2.7	5.2	2.9	81.3	4.3	6.01	0.12
C	700	3.48E+00	1.04E+00	1.03E-03	3.5E-14	4.9E-01	7.5E-03	6.1	8.2	7.1	93.1	11.4	6.19	0.06
D	775	3.28E+00	9.17E-01	6.75E-04	7.1E-14	5.6E-01	4.5E-03	10.8	10.0	14.3	95.5	25.7	5.98	0.03
E	850	3.15E+00	7.37E-01	4.98E-04	9.8E-14	6.9E-01	3.1E-03	11.9	9.4	19.7	96.5	45.3	5.80	0.02
F	925	3.11E+00	6.54E-01	4.87E-04	1.1E-13	7.8E-01	2.8E-03	11.4	9.3	21.3	96.4	66.6	5.72	0.03
G	1000	3.13E+00	6.61E-01	6.17E-04	8.3E-14	7.7E-01	4.0E-03	9.0	10.5	16.7	95.2	83.3	5.69	0.03
H	1075	3.34E+00	6.98E-01	1.45E-03	3.7E-14	7.3E-01	1.2E-02	4.2	13.6	7.4	88.2	90.7	5.63	0.06
I	1150	3.56E+00	6.31E-01	2.40E-03	2.2E-14	8.1E-01	2.2E-02	2.3	15.2	4.5	80.9	95.2	5.51	0.09
J	1300	5.73E+00	9.40E+00	1.22E-02	7.2E-15	5.4E-02	1.8E-02	11.1	4.1	1.4	50.0	96.7	5.52	0.25
K	1650	7.63E+00	1.09E+01	1.86E-02	1.7E-14	4.7E-02	2.0E-02	29.8	10.4	3.3	39.3	100.0	5.77	0.22
total gas age		n=11			5.0E-13	6.6E-01							5.78	0.06
Eruption Age		n=2	steps F-G		1.9E-13	7.8E-01						38.0	5.71	0.04
OCA-027; C2:117, groundmass concentrate, 52.59mg, J=0.001067695±0.10%, D=1.00644±0.00091, NM-117, Lab#=50844-01														
A	550	9.40E+01	6.14E-01	3.09E-01	5.9E-14	8.3E-01	1.6E-02	0.5	3.5	1.1	3.0	1.1	5.35	1.85
B	625	4.44E+00	1.08E+00	5.29E-03	1.1E-14	4.7E-01	7.0E-03	1.8	2.9	2.1	66.2	3.2	5.65	0.17
C	700	3.57E+00	9.82E-01	1.33E-03	2.6E-14	5.2E-01	5.1E-03	3.8	4.9	4.9	90.6	8.1	6.22	0.07
D	775	3.29E+00	8.43E-01	6.25E-04	5.9E-14	6.1E-01	3.5E-03	7.5	7.7	11.1	95.8	19.2	6.07	0.04
E	850	3.14E+00	6.97E-01	4.59E-04	8.4E-14	7.3E-01	2.9E-03	8.8	9.1	15.9	96.8	35.1	5.85	0.03
F	925	3.10E+00	6.21E-01	4.95E-04	9.7E-14	8.2E-01	2.6E-03	9.0	9.3	18.3	96.2	53.4	5.73	0.03
G	1000	3.11E+00	5.96E-01	5.21E-04	1.1E-13	8.6E-01	2.9E-03	9.5	11.2	20.1	95.9	73.5	5.73	0.03
H	1075	3.24E+00	6.21E-01	1.03E-03	6.2E-14	8.2E-01	5.2E-03	5.7	11.8	11.6	91.5	85.1	5.71	0.04
I	1150	3.81E+00	5.34E-01	2.90E-03	3.8E-14	9.6E-01	1.2E-02	3.0	17.4	7.2	78.1	92.3	5.71	0.07
J	1300	5.02E+00	3.11E+00	7.70E-03	1.7E-14	1.6E-01	1.1E-02	7.9	6.8	3.2	59.4	95.5	5.75	0.15
K	1650	6.22E+00	1.17E-01	1.38E-02	2.4E-14	4.4E-02	1.7E-02	42.4	15.4	4.5	49.6	100.0	5.98	0.11
total gas age		n=11			5.3E-13	7.2E-01							5.81	0.07
Eruption Age		n=4	steps F-I		3.0E-13	8.5E-01						57.2	5.73	0.02
OCA-028; R1:121, groundmass concentrate, 86.70mg, J=0.000477292±0.10%, D=1.00644±0.00091, NM-121, Lab#=51075-01														
A	550	1.54E+02	1.68E+00	5.17E-01	4.2E-16	3.0E-01	7.3E-02	0.2	4.7	0.2	0.5	0.2	0.65	3.95
B	625	2.63E+01	1.28E+00	7.71E-02	3.8E-15	4.0E-01	1.4E-02	1.4	8.2	1.9	13.7	2.1	3.12	0.41
C	675	1.07E+01	1.09E+00	2.10E-02	8.8E-16	4.7E-01	5.6E-03	0.3	0.8	0.4	42.4	2.6	3.90	0.45
D	725	6.52E+00	9.81E-01	5.16E-03	1.6E-14	5.2E-01	1.6E-03	4.3	3.8	8.0	77.4	10.6	4.35	0.05
E	775	5.69E+00	8.08E-01	2.09E-03	1.7E-14	6.3E-01	5.5E-04	3.9	1.5	8.8	89.8	19.4	4.40	0.04
F	825	5.46E+00	6.90E-01	1.35E-03	2.8E-14	7.4E-01	3.4E-04	5.4	1.5	14.3	93.2	33.7	4.38	0.03
G	875	5.34E+00	6.48E-01	9.77E-04	3.6E-14	7.9E-01	3.1E-04	6.3	1.7	17.7	95.1	51.4	4.36	0.02
H	925	5.33E+00	6.03E-01	9.41E-04	3.2E-14	8.5E-01	3.9E-04	5.4	1.9	16.4	95.2	67.8	4.37	0.02
I	975	5.45E+00	7.26E-01	1.31E-03	4.1E-14	7.0E-01	6.6E-04	2.8	1.4	7.0	93.5	74.8	4.38	0.05
J	1025	5.65E+00	7.57E-01	2.17E-03	2.4E-14	6.7E-01	1.7E-03	5.0	6.3	12.0	89.2	86.8	4.34	0.03
K	1075	6.76E+00	8.75E-01	6.91E-03	9.6E-15	5.8E-01	3.9E-03	2.3	5.7	4.8	74.8	91.6	4.35	0.08
L	1150	1.11E+01	1.59E+00	2.18E-02	8.1E-15	3.2E-01	8.8E-03	3.6	10.8	4.1	42.9	95.7	4.10	0.15
M	1300	5.63E+01	7.51E+00	1.77E-01	5.6E-15	6.8E-02	2.4E-02	11.8	20.8	2.8	7.9	98.5	3.87	0.50
N	1650	2.37E+02	5.80E+01	8.07E-01	2.9E-15	8.8E-03	6.9E-02	47.4	31.0	1.5	1.4	100.0	2.99	3.34
total gas age		n=14			2.0E-13	6.6E-01							4.29	0.12
Eruption Age		n=7	steps E-K		1.6E-13	7.4E-01						81.0	4.37	0.02
OCA-029; a5:120, groundmass concentrate, 89.00mg, J=0.00079±0.10%, D=1.00644±0.00091, NM-120, Lab#=51045-01														
A	550	1.82E+02	5.37E-01	6.07E-01	5.5E-15	9.5E-01	1.7E-02	0.0	29.4	0.1	1.4	0.1	3.76	6.13
B	625	3.04E+01	5.84E-01	1.00E-01	9.0E-15	8.7E-01	2.1E-03	0.9	57.9	1.7	2.8	1.8	1.20	0.48
C	675	9.33E+00	6.48E-01	2.56E-01	5.0E-17	7.9E-01	-2.3E-02	0.0	-3.6	0.0	18.8	1.8	24.82	24.83
D	725	9.74E+00	8.02E-01	2.29E-02	2.2E-14	6.4E-01	4.5E-04	3.0	31.0	4.3	30.8	6.1	4.27	0.15
E	775	6.12E+00	7.63E-01	9.73E-03	2.9E-14	6.7E-01	7.0E-06	3.7	0.6	5.5	53.6	11.6	4.67	0.09
F	825	4.85E+00	6.83E-01	5.44E-03	4.5E-14	7.5E-01	-1.1E-04	5.3	-15.7	8.7	67.4	20.3	4.65	0.06
G	875	4.18E+00	5.86E-01	3.39E-03	7.3E-14	8.7E-01	-1.1E-04	7.2	-24.7	13.9	76.6	34.2	4.56	0.03
H	925	3.81E+00	5.46E-01	2.37E-03	1.1E-13	9.3E-01	-1.1E-04	10.4	-38.3	21.5	82.1	55.6	4.46	0.03
I	975	3.78E+00	5.81E-01	2.28E-03	4.7E-14	8.8E-01	-5.3E-05	4.6	-7.7	8.9	82.7	64.6	4.46	0.05
J	1025	3.61E+00	6.79E-01	2.51E-03	1.1E-13	7.5E-01	-3.6E-05	12.7	-12.2	21.1	81.3	85.7	4.41	0.03
K	1075	5.23E+00	1.05E+00	7.39E-03	4.04E-14	4.8E-01	-8.6E-05	7.1	-10.5	7.6	59.6	93.3	4.44	0.05
L	1150	1.06E+01	1.61E+00	2.56E-02	1.7E-14	3.2E-01	-2.5E-04	4.5	12.9	3.2	29.5	96.5	4.47	0.16
M	1300	2.11E+01	5.75E+00	6.57E-02	1.1E-14	8.9E-02	-9.4E-04	10.8	32.1	2.1	10.1	98.6	3.05	0.34
N	1650	3.99E+01	2.44E+01	1.29E-01	7.2E-15	2.1E-02	-2.2E-03	29.8	48.7	1.4	8.7	100.0	5.03	0.64
total gas age		n=14			5.2E-13	7.5E-01						62.3	4.44	0.08
Eruption Age		n=5	steps H-L		3.3E-13	7.8E-01						55.2	20.89	0.08
OCA-030; A2:117, groundmass concentrate, 81.08mg, J=0.001072496±0.10%, D=1.00644±0.00091, NM-117, Lab#=50832-01														
A	550	5.04E+01	2.03E+00	1.16E-01	2.5E-01	3.9E-02	1.6	19.8	1.9	32.1	1.9	31.15	0.75	
B	625	1.24E+01	9.52E-01	2.53E-03	3.7E-14	5.4E-01	9.8E-03	2.6	17.7	6.8	94.4	8.7	22.48	0.09
C	675	1.12E+01	6.60E-01	5.85E-04	6.0E-01	7.7E-01	4.2E-03	2.9	12.2	10.9	98.7	19.6	21.32	0.10
D	725	1.10E+01	5.55E-01	4.79E-04	9.0E-14	9.2E-01	2.3E-03	4.1	10.9	18.0	98.9	37.6	20.94	0.07
E	775	1.09E+01	4.89E-01	3.74E-04	8.4E-14	1.0E-00	1.5E-03	3.1	6.1	15.3	99.1	52.9	20.82	0.09
F	825	1.10E+01	5.48E-01	4.34E-04	7.0E-14	9.3E-01	9.4E-04	3.2	3.5	14.2	99.0	67.1	20.92	0.10
G	875	1.10E+01	7.84E-01	6.69E-04	4.2E-14									

ID	Temp/P (^°C/W)	⁴⁰ Ar/ ³⁹ Ar	³⁷ Ar/ ³⁹ Ar	³⁶ Ar/ ³⁹ Ar	³⁹ Ar _K	K/Ca	Ci/K	³⁷ Ar _{Ca}	³⁸ Ar _{Cl}	³⁹ Ar _K	⁴⁰ Ar*	³⁹ Ar	Age	±2σ
		(mol)			(%)			(%)	(%)	(%)	(%)	(%)	(Ma)	(Ma)
OCA-030L1: A3; 117, groundmass concentrate, 17.22mg, J=0.001072496±0.10%, D=1.00644±0.00091, NM-117, Lab#=50832-04														
A	2	8.92E+01	1.60E+00	2.35E-01	6.2E-16	3.2E-01	3.2E-07	0.9	11.8	0.6	21.8	0.6	37.31	3.45
B	4	1.44E+01	9.87E-01	6.99E-03	9.9E-15	5.2E-01	5.2E-07	8.9	29.6	9.2	86.1	9.7	23.89	0.17
C	7	1.12E+01	5.79E-01	5.24E-04	4.2E-14	8.8E-01	8.8E-07	22.3	23.8	39.2	98.8	48.9	21.25	0.07
D	10	1.11E+01	5.62E-01	5.79E-04	2.6E-14	9.1E-01	9.1E-07	13.1	10.4	23.8	98.7	72.7	21.03	0.10
E	12	1.12E+01	7.61E-01	1.03E-03	1.0E-14	6.7E-01	6.7E-07	7.0	5.2	9.4	97.6	82.1	21.06	0.13
F	15	1.12E+01	1.03E+00	1.27E-03	7.2E-15	5.0E-01	5.0E-07	6.7	5.6	6.6	97.2	88.7	21.03	0.17
G	20	1.13E+01	1.54E+00	2.19E-03	6.6E-15	3.3E-01	3.3E-07	9.3	5.1	6.1	95.2	94.8	20.68	0.17
H	25	1.15E+01	2.53E+00	3.31E-03	2.9E-15	2.0E-01	2.0E-07	6.7	3.0	2.7	93.1	97.5	20.70	0.34
I	30	1.23E+01	4.58E+00	7.74E-03	1.2E-15	1.1E-01	1.1E-07	5.0	1.8	1.1	84.3	98.6	20.02	0.72
J	40	1.34E+01	1.48E+01	1.41E-02	1.5E-15	3.4E-02	3.4E-08	20.1	3.8	1.4	78.0	100.0	20.36	0.70
total gas age		n=10				1.1E-13		7.3E-01					21.42	0.15
Eruption Age		n=4	steps C-F	8.5E-14	8.3E-01						79.0	21.14	0.14	
OCA-030L2: A3; 117, groundmass concentrate, 22.74mg, J=0.001072496±0.10%, D=1.00644±0.00091, NM-117, Lab#=50832-05														
A	2	2.53E+02	1.94E+00	8.07E-01	8.0E-16	2.6E-01	2.6E-07	1.0	10.8	0.5	5.7	0.5	27.95	8.98
B	4	2.82E+02	9.92E-01	5.36E-02	1.5E-14	5.1E-01	5.1E-07	9.6	31.1	9.8	44.1	10.3	23.97	0.33
C	7	1.27E+01	5.61E-01	5.86E-03	6.4E-14	9.1E-01	9.1E-07	23.8	25.5	42.8	86.5	53.1	21.08	0.10
D	10	1.22E+01	5.81E-01	4.29E-03	3.2E-14	8.8E-01	8.8E-07	12.4	8.5	21.4	89.8	74.6	21.14	0.11
E	12	1.27E+01	8.00E-01	1.18E-03	1.3E-14	6.4E-01	6.4E-07	7.0	5.1	8.8	88.3	83.3	21.51	0.16
F	15	1.26E+01	1.12E+00	5.41E-03	9.3E-15	4.5E-01	4.5E-07	7.0	5.0	6.3	87.8	89.6	21.26	0.19
G	20	1.24E+01	1.58E+00	5.64E-03	8.9E-15	3.2E-01	3.2E-07	9.4	6.6	6.0	87.4	95.6	20.91	0.19
H	25	1.38E+01	2.82E+00	1.11E-02	3.5E-15	1.8E-01	1.8E-07	6.6	3.4	2.4	77.8	97.9	20.64	0.40
I	30	1.56E+01	3.83E+00	1.63E-02	1.3E-15	1.3E-01	1.3E-07	3.4	1.6	0.9	71.1	98.8	21.41	0.75
J	40	1.53E+01	1.71E+01	2.18E-02	1.7E-15	3.0E-02	3.0E-08	19.7	2.5	1.2	66.9	100.0	19.91	0.70
total gas age		n=10				1.5E-13		7.4E-01					21.43	0.21
Eruption Age		n=2	steps C-D	9.5E-14	9.0E-01						64.2	21.11	0.10	
OCA-031: L4:118, groundmass concentrate, 123.97mg, J=0.00015356±0.12%, D=1.00644±0.00091, NM-118, Lab#=50928-01														
A	550	1.23E+03	9.57E-01	4.15E+00	2.2E-15	5.3E-01	4.3E-02	0.9	16.6	2.1	0.4	2.1	1.38	4.82
B	625	1.57E+02	1.48E+00	5.12E-01	4.1E-15	3.5E-03	3.5E-02	2.4	13.1	3.9	3.8	6.0	1.66	0.55
C	675	6.71E+01	1.63E+00	2.07E-01	4.3E-15	3.1E-01	9.4E-03	2.9	7.0	4.1	8.8	10.1	1.63	0.22
D	725	3.20E+01	1.65E+00	8.66E-02	6.5E-15	3.1E-01	5.0E-03	4.4	5.7	6.3	20.2	16.4	1.79	0.12
E	775	2.04E+01	1.46E-02	6.97E-02	6.0E-15	3.5E-01	2.3E-03	3.6	2.4	5.8	28.2	22.2	1.59	0.09
F	825	1.37E+01	1.23E+00	2.71E-02	1.1E-14	4.1E-01	1.2E-03	5.3	2.2	10.1	41.9	32.4	1.59	0.05
G	875	1.11E+01	9.73E-01	1.88E-02	1.1E-14	5.2E-01	1.1E-03	4.4	2.2	10.8	50.4	43.2	1.55	0.04
H	925	9.91E+00	8.31E-01	1.61E-02	1.1E-14	6.1E-01	8.9E-04	3.8	1.7	10.7	52.3	53.9	1.44	0.04
I	975	1.01E+01	7.76E-01	1.68E-02	9.9E-15	6.6E-01	1.2E-03	3.1	2.2	9.6	51.6	63.4	1.45	0.04
J	1025	1.18E+01	8.29E-01	2.04E-02	6.6E-15	6.2E-01	1.5E-03	2.2	1.7	6.3	49.4	69.8	1.62	0.07
K	1075	1.82E+01	9.72E-01	4.31E-02	6.9E-15	5.2E-01	2.9E-03	2.7	3.5	6.7	30.2	76.4	1.52	0.08
L	1150	2.93E+01	1.18E+00	8.26E-02	7.6E-15	4.3E-01	5.9E-03	3.7	7.8	7.3	16.8	83.7	1.36	0.10
M	1300	4.26E+01	6.89E+00	1.29E-01	8.8E-15	7.4E-02	9.7E-03	24.7	14.9	8.5	11.9	92.2	1.40	0.15
N	1650	4.91E+01	1.09E+01	1.46E-01	8.1E-15	4.7E-02	1.3E-02	36.0	19.0	7.8	13.7	100.0	1.88	0.15
total gas age		n=14				1.0E-13		4.2E-01					1.56	0.21
Eruption Age		n=3	steps E-G	2.8E-13	4.4E-01						26.7	1.57	0.04	
OCA-032: G8:117, groundmass concentrate, 60.06mg, J=0.00105673±0.10%, D=1.00644±0.00091, NM-117, Lab#=50866-01														
A	550	4.47E+01	2.85E+00	1.39E-01	3.7E-15	1.8E-01	3.4E-02	1.0	12.9	1.0	8.4	1.0	7.14	1.45
B	625	3.48E+00	1.93E+00	3.24E-03	1.2E-14	2.6E-01	9.0E-03	2.3	11.0	3.3	76.4	4.3	5.06	0.14
C	700	2.75E+00	1.24E+00	1.30E-03	3.6E-14	4.1E-01	3.3E-03	4.4	12.1	10.0	88.8	14.3	4.65	0.06
D	775	2.56E+00	9.18E-01	6.83E-04	6.9E-14	5.6E-01	1.1E-03	6.2	7.7	19.0	94.2	33.3	4.60	0.04
E	850	2.53E+00	7.57E-01	5.20E-04	8.6E-14	6.7E-01	4.2E-04	6.3	3.6	23.6	95.5	56.9	4.60	0.03
F	925	2.53E+00	7.80E-01	6.24E-04	6.4E-14	6.5E-01	2.1E-04	4.9	1.3	17.8	94.3	74.6	4.55	0.03
G	1000	2.67E+00	1.28E-00	1.10E-03	3.4E-14	4.0E-01	6.5E-04	4.3	2.2	9.4	90.9	84.0	4.62	0.06
H	1075	2.81E+00	2.00E+00	2.37E-03	1.2E-14	2.6E-01	2.7E-03	2.3	3.3	3.3	80.1	87.3	4.29	0.14
I	1150	2.83E+00	2.04E+00	2.06E-03	9.1E-15	2.5E-01	3.9E-03	1.8	3.6	2.5	83.7	89.8	4.51	0.16
J	1300	4.42E+00	1.58E+01	1.17E-02	1.2E-14	3.2E-02	7.6E-03	17.9	8.9	3.2	51.2	93.0	4.37	0.17
K	1650	5.13E+00	1.94E+01	1.35E-02	2.5E-14	2.6E-02	1.3E-02	48.5	33.3	7.0	53.3	100.0	5.28	0.18
total gas age		n=11				3.6E-13		4.9E-01					4.67	0.09
Eruption Age		n=5	steps C-G	2.9E-13	5.8E-01						79.7	4.59	0.03	
OCA-033: ..6:120, groundmass concentrate, 71.25mg, J=0.000791±0.10%, D=1.00644±0.00091, NM-120, Lab#=51034-01														
A	550	1.75E+01	2.63E+00	5.26E-02	4.1E-15	1.9E-01	2.2E-01	1.4	21.0	3.0	12.3	3.0	3.06	0.60
B	625	2.40E+00	1.67E+00	2.84E-03	1.9E-14	3.0E-01	3.5E-02	4.0	15.3	13.6	69.3	16.5	2.37	0.06
C	675	1.95E+00	1.29E+00	1.42E-03	1.4E-14	4.0E-01	2.3E-02	2.3	7.5	10.1	82.3	26.6	2.29	0.07
D	725	2.01E+00	1.28E+00	1.57E-03	2.4E-14	4.0E-01	1.8E-02	3.9	9.7	17.0	80.5	43.6	2.31	0.05
E	775	2.09E+00	1.42E+00	1.97E-03	1.2E-14	3.6E-01	1.4E-02	2.2	4.0	8.9	76.2	52.5	2.27	0.08
F	825	2.18E+00	1.63E+00	2.38E-03	8.5E-15	3.1E-01	1.0E-02	1.8	2.1	6.2	72.3	58.7	2.25	0.11
G	875	2.44E+00	1.85E+00	4.07E-03	6.1E-15	2.8E-01	1.3E-02	1.4	1.9	4.4	55.5	63.1	1.93	0.15
H	925	3.17E+00	2.86E+00	6.80E-03	5.3E-15	1.8E-01	2.0E-02	1.9	2.4	3.8	42.8	66.9	1.94	0.21
I	975	2.66E+00	3.78E+00	4.22E-03	3.6E-15	1.3E-01	1.4E-02	1.7	1.2	2.6	63.1	69.5	2.40	0.25
J	1025	2.54E+00	3.05E+00	3.39E-03	4.7E-15	1.7E-01	1.4E-02	1.9	1.5	3.4	69.9	72.9	2.50	0.16
K	1075	2.44E+00	3.31E+00	3.54E-03	4.3E-15	1.5E-01	1.3E-02	1.8	1.3	3.1	66.5	76.0	2.32	0.18
L	1150	2.63E+00	4.13E+00	4.91E-03	5.0E-1									

ID	Temp/P (^°C/W)	⁴⁰ Ar/ ³⁹ Ar	³⁷ Ar/ ³⁹ Ar	³⁶ Ar/ ³⁹ Ar	³⁹ Ar _K (mol)	K/Ca	Ci/I	³⁷ Ar _{Ca} (%)	³⁹ Ar _{Ci} (%)	³⁹ Ar _K (%)	⁴⁰ Ar* (%)	³⁹ Ar (%)	Age (Ma)	±2σ (Ma)
OCA-034; H6:118, groundmass concentrate, 114.42mg, J=0.000154769±0.12%, D=1.00644±0.00091, NM-118, Lab#=50900-01														
A	550	1.42E+02	6.00E+00	4.46E-01	2.2E-15	8.5E-02	6.2E-03	6.9	14.3	5.4	7.8	5.4	3.10	0.74
B	625	1.52E+01	2.95E+00	2.25E-02	7.1E-15	1.7E-01	1.9E-04	10.8	1.4	17.2	57.4	22.6	2.43	0.05
C	675	1.11E+01	1.94E+00	1.05E-02	7.3E-15	2.6E-01	1.2E-04	7.3	0.9	17.7	73.2	40.3	2.27	0.05
D	725	1.05E+01	1.71E+00	8.66E-03	7.2E-15	3.0E-01	1.9E-04	6.3	1.4	17.3	76.7	57.7	2.26	0.05
E	775	1.08E+01	1.66E+00	9.65E-03	3.6E-15	3.1E-01	-1.5E-04	3.0	-0.5	8.7	74.6	66.3	2.25	0.06
F	825	1.05E+01	1.79E+00	8.03E-03	3.8E-15	2.8E-01	-7.1E-05	3.5	-0.3	9.2	78.4	75.5	2.29	0.05
G	875	1.06E+01	2.15E+00	9.04E-03	2.9E-15	2.4E-01	8.5E-04	2.5	2.0	5.5	76.5	81.0	2.30	0.09
H	925	1.19E+01	2.79E+00	1.41E-02	1.5E-15	1.8E-01	1.9E-03	2.2	3.0	3.7	66.6	84.7	2.21	0.11
I	975	1.33E+01	3.65E+00	1.53E-02	8.6E-16	1.4E-01	2.0E-03	1.6	1.8	2.1	68.1	86.8	2.54	0.20
J	1025	1.46E+01	5.16E+00	2.03E-02	4.7E-16	9.9E-02	5.4E-03	1.2	2.6	1.1	61.6	87.9	2.52	0.31
K	1075	1.83E+01	6.46E+00	3.71E-02	4.4E-16	7.9E-02	1.0E-02	1.4	4.6	1.1	42.9	89.0	2.21	0.39
L	1150	2.18E+01	9.50E+00	5.11E-02	4.8E-16	6.0E-02	1.2E-02	2.1	5.7	1.2	33.7	90.1	2.06	0.45
M	1300	2.36E+01	2.20E+01	7.14E-02	1.3E-15	2.3E-02	1.0E-02	14.5	13.3	3.1	17.6	93.2	1.17	0.22
N	1650	2.46E+01	2.56E+01	7.12E-02	2.8E-15	2.0E-02	1.7E-02	36.7	49.9	6.8	22.5	100.0	1.58	0.19
total gas age n=14														
Eruption Age n=6 steps C-H 2.8E-14 2.8E-01														
													62.1	2.27
														0.03
OCA-035; /1:121, groundmass concentrate, 92.10mg, J=0.000478033±0.10%, D=1.00644±0.00091, NM-121, Lab#=51057-01														
A	550	1.57E+02	1.12E+00	5.05E-01	3.5E-16	4.6E-01	8.2E-02	0.1	3.8	0.1	4.8	0.1	6.45	5.67
B	625	1.72E+02	6.72E-01	5.71E-01	3.1E-15	7.6E-01	7.9E-03	0.5	3.1	1.1	1.7	1.3	2.58	1.81
C	675	2.96E+01	1.03E+00	1.00E-01	7.5E-17	4.9E-01	6.8E-03	0.0	0.1	0.0	0.3	1.3	0.07	9.44
D	725	2.78E+01	1.47E+00	8.3E-02	3.5E-15	3.5E-01	3.5E-03	3.1	3.8	3.0	18.5	4.3	4.44	0.27
E	775	6.07E+00	1.36E+00	2.09E-03	8.6E-15	3.8E-01	2.4E-03	3.0	2.7	3.2	91.1	7.5	4.77	0.09
F	825	5.70E+00	1.13E+00	9.72E-04	2.5E-14	4.5E-01	1.3E-03	7.2	4.2	9.1	96.0	16.6	4.72	0.04
G	875	5.38E+00	9.91E-01	5.36E-03	3.2E-14	5.1E-01	1.0E-03	8.2	4.3	11.9	98.0	28.5	4.54	0.03
H	925	5.31E+00	7.36E-01	6.47E-04	4.7E-14	6.9E-01	9.8E-04	8.8	5.9	17.1	97.0	45.5	4.44	0.02
I	975	5.21E+00	6.40E-01	2.59E-04	2.2E-14	8.0E-01	1.1E-03	3.7	3.3	8.2	99.0	53.8	4.44	0.03
J	1025	5.31E+00	6.09E-01	7.95E-04	5.0E-04	8.4E-01	1.8E-03	7.8	10.2	18.4	96.0	72.2	4.39	0.02
K	1075	5.45E+00	5.68E-01	9.72E-04	2.4E-14	9.0E-01	2.9E-03	3.5	9.2	8.8	95.1	81.0	4.46	0.03
L	1150	5.75E+00	6.33E-01	2.58E-03	1.7E-14	8.1E-01	5.9E-03	2.8	13.2	6.3	87.1	87.2	4.32	0.05
M	1300	9.33E+00	4.50E+00	1.59E-02	1.2E-14	1.1E-01	6.6E-03	13.7	10.3	4.4	53.0	91.6	4.28	0.11
N	1650	1.07E+01	6.43E+00	2.03E-02	2.3E-14	7.9E-02	8.7E-03	37.7	25.9	8.4	48.3	100.0	4.47	0.07
total gas age n=14														
Eruption Age n=4 steps H-K 1.4E-13 7.9E-01														
													52.5	4.43
														0.03
OCA-036; B6:117, groundmass concentrate, 71.62mg, J=0.001068649±0.10%, D=1.00644±0.00091, NM-117, Lab#=50836-01														
A	550	1.30E+02	1.95E+00	4.35E-01	6.3E-15	2.6E-01	7.6E-03	1.2	0.9	1.0	1.2	1.0	2.94	2.51
B	625	1.68E+01	8.88E-01	4.88E-02	1.5E-14	5.7E-01	9.7E-04	1.3	0.3	2.5	14.3	3.6	4.61	0.42
C	675	5.43E+00	7.75E-01	1.07E-02	2.4E-14	6.6E-01	2.4E-04	1.8	0.1	4.0	42.3	7.5	4.42	0.13
D	725	4.02E+00	6.65E-01	5.84E-03	3.7E-14	7.7E-01	3.1E-04	2.5	0.2	6.2	57.9	13.8	4.48	0.10
E	775	3.82E+00	6.55E-03	3.9E-03	7.8E-16	4.7E-04	2.5	0.3	6.5	60.1	20.3	4.43	0.08	
F	825	3.86E+00	6.59E-01	5.31E-03	5.1E-14	7.7E-01	8.1E-04	3.3	0.8	8.5	60.1	28.8	4.47	0.09
G	875	4.35E+00	7.61E-01	6.94E-03	4.8E-14	6.7E-01	1.6E-03	3.6	1.5	7.9	53.7	36.8	4.50	0.09
H	925	4.91E+00	1.01E-00	8.82E-03	4.7E-14	5.1E-01	3.2E-03	4.7	2.9	7.9	48.1	44.6	4.54	0.08
I	975	5.25E+00	1.20E+00	1.00E-02	4.1E-14	4.2E-01	5.4E-03	4.9	4.2	6.8	45.1	51.4	4.56	0.13
J	1025	5.04E+00	1.30E+00	9.4E-03	3.0E-14	3.9E-01	1.1E-02	3.9	6.4	5.0	46.2	56.4	4.49	0.13
K	1075	4.62E+00	1.11E+00	7.89E-03	2.1E-14	4.6E-01	1.4E-02	2.3	5.7	3.5	51.0	59.9	4.54	0.13
L	1150	4.11E+00	9.30E-01	6.34E-03	4.9E-14	5.5E-01	1.5E-02	4.5	13.7	8.2	55.7	68.1	4.41	0.10
M	1225	3.65E+00	2.94E+00	5.47E-03	2.8E-14	1.7E-01	1.6E-02	8.0	8.7	4.6	61.8	72.7	4.36	0.09
N	1300	6.21E+00	2.97E+00	1.39E-02	3.8E-14	1.7E-01	1.7E-02	11.1	12.2	6.3	37.6	79.0	4.51	0.12
O	1450	5.34E+00	3.19E+00	1.10E-02	1.1E-13	1.6E-01	1.8E-02	33.9	36.8	17.8	43.7	96.8	4.50	0.07
P	1650	6.05E+00	5.52E+00	1.33E-02	1.9E-14	9.2E-02	1.5E-02	10.5	5.3	3.2	42.4	100.0	4.97	0.22
total gas age n=16														
Eruption Age n=5 steps F-J 6.0E-13 4.6E-01														
													36.1	4.51
														0.06
OCA-036L; B6: 117, groundmass concentrate, 22.90mg, J=0.001068649±0.10%, D=1.00644±0.00091, NM-117, Lab#=50836-02														
A	2	1.88E+02	1.15E+00	6.32E-01	1.1E-15	4.4E-01	4.4E-07	0.7	1.6	0.7	0.8	0.7	2.95	6.04
B	4	9.04E+01	1.45E+00	2.93E-01	1.5E-15	3.5E-01	3.5E-07	1.3	1.3	1.0	4.4	1.7	7.65	2.74
C	7	1.16E+01	9.64E-01	3.16E-02	1.5E-14	5.3E-01	5.3E-07	8.4	1.8	10.0	19.8	11.8	4.43	0.23
D	10	4.74E+00	7.42E-01	8.28E-03	3.0E-14	6.9E-01	6.9E-07	13.0	3.4	20.1	49.1	31.9	4.49	0.09
E	12	4.80E+00	8.16E-01	8.57E-03	2.8E-14	6.3E-01	6.3E-07	13.6	7.5	19.2	48.2	51.1	4.46	0.09
F	15	5.12E+00	1.04E+00	9.76E-03	2.4E-14	4.9E-01	4.9E-07	15.0	15.1	16.5	44.9	67.6	4.44	0.12
G	20	4.86E+00	1.01E+00	8.54E-03	2.2E-14	5.0E-01	5.0E-07	13.1	27.1	14.9	49.3	82.5	4.62	0.11
H	25	5.01E+00	1.48E+00	9.24E-03	1.3E-14	3.5E-01	3.5E-07	11.5	18.7	9.1	47.5	91.6	4.59	0.17
I	30	6.02E+00	2.72E+00	1.22E-02	7.05E-15	1.9E-01	1.9E-07	11.2	12.4	4.7	43.5	96.3	5.04	0.24
J	40	6.92E+00	3.76E+00	1.55E-02	5.4E-14	1.4E-01	1.4E-07	12.1	11.0	3.7	37.9	100.0	5.07	0.34
total gas age n=10														
Eruption Age n=6 steps C-H 1.3E-13 5.6E-01														

ID	Temp/P (*C/W)	⁴⁰ Ar/ ³⁶ Ar	³⁷ Ar/ ³⁹ Ar	³⁶ Ar/ ³⁹ Ar	³⁹ Ar _K	K/Ca (mol)	C/I/K	³⁷ Ar _{Cs} (%)	³⁸ Ar _{Cs} (%)	³⁹ Ar _K (%)	⁴⁰ Ar* (%)	³⁹ Ar (%)	Age (Ma)	±2σ (Ma)
OCA-038; b1:120, groundmass concentrate, 61.60mg, J=0.000794±0.10%, D=1.00644±0.00091, NM-120, Lab#=51047-01														
A	550	3.84E+02	1.31E+00	1.27E+00	4.8E-16	3.9E-01	4.0E-01	0.2	23.8	0.1	2.3	0.1	12.53	14.97
B	625	2.41E+01	1.69E+00	6.72E-02	2.6E-15	3.0E-01	2.8E-02	1.2	9.0	0.7	18.2	0.9	6.28	0.74
C	675	-5.36E-01	1.78E+00	9.26E-04	9.8E-17	2.9E-01	-1.4E-03	0.0	0.0	0.0	130.3	0.9	-1.00	8.03
D	725	3.69E+00	1.18E+00	1.87E-03	2.0E-14	4.3E-01	2.2E-03	6.4	5.6	5.7	86.8	6.6	4.58	0.06
E	775	3.25E+00	8.37E-01	6.49E-04	2.5E-14	6.1E-01	8.1E-04	5.5	6.8	6.8	95.3	13.3	4.43	0.04
F	825	3.22E+01	7.46E-01	5.43E-04	5.4E-14	6.8E-01	4.3E-04	10.7	2.9	15.0	96.0	28.3	4.42	0.03
G	875	3.16E+00	6.28E-01	3.48E-04	7.4E-14	8.1E-01	1.3E-04	12.4	1.2	20.5	97.5	48.8	4.41	0.02
H	925	3.15E+00	4.96E-01	2.73E-04	9.1E-14	1.0E+00	2.2E-04	12.0	2.4	25.2	97.9	74.0	4.42	0.02
I	975	3.18E+00	4.72E-01	2.73E-04	3.1E-14	1.1E+00	3.0E-04	3.9	1.1	8.5	97.8	82.5	4.45	0.04
J	1025	3.18E+00	5.85E-01	3.92E-04	4.5E-14	8.7E-01	1.1E-03	7.0	6.1	12.4	97.0	94.9	4.41	0.03
K	1075	3.28E+01	9.74E-01	7.01E-04	7.4E-15	5.2E-01	5.4E-03	1.9	4.9	2.0	95.2	97.0	4.46	0.09
L	1150	3.43E+00	1.44E+00	2.41E-03	4.3E-15	3.6E-01	1.8E-02	1.6	9.3	1.2	81.7	98.1	4.02	0.16
M	1300	4.96E+00	1.68E+01	1.20E-02	2.6E-15	3.0E-02	3.1E-02	11.6	9.9	0.7	54.3	98.9	3.90	0.25
N	1650	7.42E+00	2.39E+01	2.16E-02	4.1E-15	2.2E-02	4.2E-02	25.6	21.3	1.1	37.9	100.0	4.09	0.32
total gas age		n=14											4.44	0.07
Eruption Age		n=7		steps E-K	3.3E-13	8.6E-01							90.4	4.42
														0.02
OCA-038CPX; b2:120, phenocryst concentrate, 216.20mg, J=0.000789±0.10%, D=1.00644±0.00091, NM-120, Lab#=51048-01														
A	550	2.53E+03	1.01E+01	8.43E+00	1.8E-16	5.0E-02	1.6E+00	0.0	5.3	0.2	1.6	0.2	57.43	1317.10
B	675	2.65E+02	3.85E+00	8.91E-01	2.8E-16	1.3E-01	9.0E-02	0.1	4.8	3.2	0.6	3.4	2.25	15.14
C	775	1.58E+01	2.09E+00	4.17E-02	4.4E-16	2.5E-01	7.5E-03	0.1	0.6	5.1	23.0	8.5	5.19	2.45
D	875	5.39E+00	1.40E+00	7.23E-03	2.9E-15	3.7E-01	2.5E-03	0.3	1.4	33.3	61.9	41.8	4.75	0.39
E	975	7.51E+00	8.77E-01	1.34E-02	1.8E-15	5.8E-01	3.3E-03	0.1	1.2	21.1	47.8	62.8	5.11	0.65
F	1075	9.89E+00	1.55E+00	2.50E-02	7.4E-16	3.3E-01	2.0E-02	0.1	2.9	8.5	26.3	71.4	3.70	1.49
G	1175	2.18E+01	6.95E+00	6.63E-02	3.3E-16	7.3E-02	5.0E-02	0.2	3.1	3.8	12.3	75.2	3.81	3.00
H	1275	4.75E+01	1.57E+02	1.93E-01	3.4E-16	3.3E-03	9.0E-02	4.0	5.8	3.9	4.9	79.0	3.74	4.45
I	975	1.12E+02	3.25E+02	3.95E-01	2.2E-16	1.7E-01	7.8E-02	0.5	0.3	0.2	18.0	79.3	36.72	71.01
J	1375	5.56E+01	7.86E+02	4.00E-01	5.9E-16	6.5E-04	3.2E-01	35.3	36.0	6.8	-4.0	86.1	-7.09	9.23
K	1650	3.98E+01	6.49E+02	3.03E-01	1.2E-15	7.9E-04	1.7E-01	59.4	38.7	13.9	-0.8	100.0	-0.80	4.50
total gas age		n=11											3.22	9.48
Eruption Age		n=4		steps E-K	6.9E-14	4.2E-01								
														0.05
OCA-039; ?2:121, groundmass concentrate, 90.30mg, J=0.000479454±0.10%, D=1.00644±0.00091, NM-121, Lab#=51082-01														
A	550	3.10E+02	4.81E-01	1.04E+00	5.2E-16	1.1E+00	7.6E-02	0.1	3.5	0.3	0.6	0.3	1.74	8.33
B	625	5.83E+01	5.67E-01	1.86E-01	4.8E-15	9.0E-01	3.4E-02	0.7	14.5	3.1	5.8	3.4	2.94	0.66
C	675	4.33E+01	6.61E-01	1.41E-01	4.7E-16	7.7E-01	3.3E-02	0.1	1.4	0.3	3.7	3.8	1.37	1.62
D	725	2.83E+01	1.55E+00	8.27E-02	9.7E-15	3.3E-01	2.3E-02	3.6	19.6	6.3	14.2	10.0	3.47	0.24
E	775	1.77E+01	1.95E+00	4.58E-02	9.5E-15	2.6E-01	1.5E-02	4.4	12.2	6.1	24.3	16.2	3.74	0.18
F	825	1.13E+01	2.10E+00	2.43E-02	1.1E-16	2.4E-01	7.9E-03	5.8	8.0	7.4	37.4	23.6	3.65	0.12
G	875	7.78E+00	1.90E+00	1.24E-02	1.6E-16	2.7E-01	3.6E-03	7.4	5.2	10.6	54.5	34.2	3.66	0.08
H	925	6.45E+00	1.58E+00	8.41E-03	1.9E-14	3.2E-01	1.8E-03	7.2	3.0	12.4	62.9	46.6	3.51	0.07
I	975	6.40E+00	1.31E+00	8.40E-03	1.1E-15	3.9E-01	1.5E-03	9.4	1.5	7.0	62.4	53.6	3.45	0.08
J	1025	7.02E+00	1.13E+00	1.05E-02	2.6E-16	4.5E-01	1.6E-03	6.9	3.6	16.5	56.7	70.1	3.44	0.06
K	1075	1.07E+01	9.85E-01	2.28E-02	1.4E-14	5.2E-01	2.4E-03	3.2	3.0	8.9	37.6	78.0	3.47	0.11
L	1150	2.05E+01	9.04E-01	5.67E-02	1.3E-14	5.6E-01	4.3E-03	2.9	5.0	8.5	18.3	87.6	3.25	0.16
M	1300	3.83E+01	3.63E+00	1.16E-01	9.8E-15	1.4E-01	8.1E-03	7.8	6.4	5.8	11.4	93.4	3.79	0.33
N	1650	4.49E+01	1.90E+01	1.39E-01	1.0E-14	2.7E-02	1.4E-02	46.7	13.1	6.6	11.5	100.0	4.51	0.40
total gas age		n=14											3.56	0.19
Eruption Age		n=4		steps E-K	6.9E-14	4.2E-01							44.8	3.47
														0.05
OCA-039plag; ?6:121, phenocryst concentrate, 159.05mg, J=0.000479502±0.10%, D=1.00644±0.00091, NM-121, Lab#=51080-01														
A	550	5.96E+02	6.61E-01	2.04E+00	5.7E-16	7.7E-01	1.6E-01	0.1	4.3	0.3	-0.9	0.3	-4.50	18.39
B	625	8.24E+01	9.25E-01	2.68E-01	3.3E-16	5.5E-01	3.7E-02	0.5	5.7	1.8	3.8	2.1	2.73	0.89
C	675	2.32E+01	8.00E-01	3.22E-02	1.4E-16	6.4E-01	4.1E-02	0.0	0.3	0.1	59.3	2.1	11.88	3.80
D	725	1.67E+01	2.35E+00	4.43E-02	7.3E-16	2.2E-01	1.6E-02	2.8	5.6	3.9	22.7	6.1	3.28	0.24
E	775	8.88E+00	2.63E+00	1.57E-02	5.7E-15	1.9E-01	9.2E-03	2.5	2.5	3.1	49.7	9.1	3.82	0.16
F	825	6.75E+00	2.54E+00	8.31E-03	9.0E-15	2.0E-01	6.1E-03	3.7	2.6	4.8	66.1	14.0	3.86	0.11
G	875	5.95E+00	2.45E+00	6.66E-03	9.5E-15	2.1E-01	4.3E-03	3.8	1.9	5.1	70.1	19.0	3.61	0.08
H	925	5.40E+00	2.42E+00	4.98E-03	1.5E-14	2.1E-01	3.7E-03	6.0	2.6	8.2	75.7	27.2	3.54	0.06
I	975	5.30E+00	2.58E+00	4.94E-03	7.2E-15	2.0E-01	3.3E-03	3.0	1.1	3.9	75.7	31.1	3.47	0.11
J	1025	5.87E+00	2.91E+00	6.89E-03	1.8E-14	1.8E-01	3.1E-03	8.5	2.6	9.5	68.7	40.7	3.49	0.05
K	1075	7.68E+00	3.33E+00	1.36E-02	7.4E-15	1.5E-01	4.6E-03	4.0	1.6	4.0	50.9	44.7	3.38	0.14
L	1150	1.13E+01	2.91E+00	2.57E-02	1.0E-14	1.8E-01	8.7E-03	5.0	4.3	5.6	34.8	50.3	3.42	0.14
M	1300	2.09E+01	2.97E+00	5.81E-02	4.0E-14	1.7E-01	1.6E-02	19.4	30.5	21.4	18.8	71.7	3.41	0.13
N	1650	4.14E+01	4.75E+00	3.24E-02	5.3E-14	1.1E-01	1.4E-02	40.8	34.3	28.3	34.4	100.0	4.20	0.08
total gas age		n=14											3.66	0.18
Eruption Age		n=4		steps E-K	1.5E-13	7.7E-01							44.4	3.53
														0.04
OCA-040; /4:121, groundmass concentrate, 100.90mg, J=0.000481387±0.10%, D=1.00644±0.00091, NM-121, Lab#=51060-01														
A	550	2.65E+02	5.17E-01	8.91E-01	5.6E-16	9.9E-01	8.1E-02	0.1	1.6	0.2	0.5	0.2	1.22	6.16
B	625	2.31E+01	5.26E-01	7.02E-02	5.4E-15	9.7E-01	1.3E-02	0.8	2.4	1.6	10.3	1.8	2.07	0.34
C	675	1.30E+01	7.67E-01	2.73E-02	1.7E-16	6.7E-01	1.8E-02	0.0	0.1	0.1	38.3	1.9	4.33	2.52
D														

ID	Temp/P (°C/W)	$^{40}\text{Ar}/^{39}\text{Ar}$	$^{37}\text{Ar}/^{39}\text{Ar}$	$^{39}\text{Ar}/^{39}\text{Ar}$	$^{39}\text{Ar}_\text{K}$ (mol)	K/Ca	Ci/K	$^{37}\text{Ar}_{\text{Ca}}$ (%)	$^{38}\text{Ar}_{\text{Cl}}$ (%)	$^{39}\text{Ar}_\text{K}$ (%)	$^{40}\text{Ar}^*$ (%)	^{39}Ar (%)	Age (Ma)	$\pm 2\sigma$ (Ma)
OCA-041; 11:121, groundmass concentrate, 79.90mg, J=0.00047968±0.10%, D=1.00644±0.00091, NM-121, Lab#=51087-01														
A	550	3.96E+02	5.58E-01	1.35E+00	6.8E-16	9.1E-01	3.3E-02	0.1	1.4	0.3	-1.0	0.3	-3.33	7.88
B	625	7.93E+01	9.22E-01	2.59E-01	4.5E-15	5.5E-01	1.1E-02	1.3	2.9	2.1	3.5	2.5	2.40	0.81
C	675	1.12E+01	1.26E+00	4.92E-02	1.3E-16	4.1E-01	1.8E-02	0.1	0.1	0.1	-29.0	2.5	-2.82	3.45
D	725	6.76E+00	1.32E+00	9.71E-03	9.0E-15	3.9E-01	8.5E-03	3.7	4.6	4.3	58.7	6.8	3.43	0.09
E	775	5.31E+00	1.19E+00	3.96E-03	9.8E-15	4.3E-01	6.9E-03	3.7	4.0	4.7	79.2	11.5	3.64	0.06
F	825	4.80E+00	1.06E+00	2.24E-03	2.0E-14	4.8E-01	5.5E-03	6.6	6.6	9.5	87.4	21.0	3.63	0.04
G	875	4.60E+00	9.09E-01	1.61E-03	2.1E-14	5.6E-01	4.6E-03	6.0	5.8	10.0	90.6	31.0	3.61	0.03
H	925	4.47E+00	7.46E-01	1.54E-03	3.2E-14	6.8E-01	3.6E-03	7.6	7.0	15.4	90.5	46.4	3.50	0.03
I	975	4.58E+00	6.75E-01	1.73E-03	1.4E-14	7.6E-01	4.0E-03	2.9	3.3	6.5	89.4	52.9	3.54	0.05
J	1025	4.68E+00	6.79E-01	2.18E-03	3.6E-14	7.5E-01	4.1E-03	7.6	8.9	17.0	86.8	69.9	3.51	0.03
K	1075	5.55E+00	6.42E-01	5.08E-03	1.7E-14	8.0E-01	7.2E-03	3.4	7.4	8.2	73.4	78.1	3.52	0.05
L	1150	8.15E+00	4.97E-01	1.40E-02	1.5E-14	1.0E+00	1.5E-02	2.4	13.4	7.3	49.5	85.4	3.49	0.08
M	1300	1.19E+01	3.70E+00	2.73E-02	1.0E-14	1.4E-01	1.9E-02	11.6	11.3	4.8	34.4	90.2	3.55	0.13
N	1650	1.11E+01	6.69E+00	2.45E-02	2.1E-14	7.6E-02	1.9E-02	43.1	23.4	9.8	39.0	100.0	3.75	0.09
total gas age	n=14		2.1E-13	5.9E-01									3.51	0.10
Eruption Age	n=5	steps H-L	1.1E-13	7.8E-01									54.4	3.51
OCA-042; X3:117, groundmass concentrate, 66.13mg, J=0.00100513±0.11%, D=1.00644±0.00091, NM-117, Lab#=50893-01														
A	550	1.07E+02	3.06E-01	3.55E-01	3.2E-14	1.7E+00	3.8E-02	1.2	23.3	7.8	1.5	7.8	2.93	1.44
B	625	1.73E+01	4.92E-01	4.97E-02	5.3E-16	1.1E-01	3.9E-02	3.1	31.6	12.7	15.3	20.5	4.81	0.24
C	675	1.04E+01	7.93E-01	2.67E-02	3.3E-14	6.4E-01	2.5E-02	3.2	15.4	8.0	24.5	28.5	4.63	0.21
D	725	8.00E+00	1.11E+00	1.83E-02	3.3E-14	4.6E-01	1.4E-02	4.4	8.1	7.9	33.3	36.4	4.82	0.13
E	775	6.18E+00	1.15E+00	1.27E-02	2.8E-14	4.4E-01	6.6E-03	3.9	3.4	6.8	40.4	43.2	4.52	0.14
F	825	4.76E+00	1.05E+00	7.84E-03	4.7E-14	4.9E-01	3.0E-03	6.0	2.6	11.3	52.6	54.5	4.54	0.09
G	875	4.17E+00	9.34E-01	6.04E-03	4.6E-14	5.5E-01	2.0E-03	5.2	1.7	11.1	58.5	65.6	4.42	0.08
H	925	4.04E+00	9.72E-01	5.75E-03	4.6E-14	5.2E-01	2.2E-03	5.3	1.8	10.9	59.3	76.5	4.34	0.07
I	975	4.44E+00	1.22E+00	7.11E-03	3.1E-14	4.2E-01	2.8E-03	4.6	1.6	7.5	54.4	84.0	4.38	0.12
J	1025	5.38E+00	1.69E+00	1.08E-02	1.5E-14	3.0E-01	4.8E-03	3.0	1.3	3.6	43.1	87.6	4.21	0.24
K	1075	6.30E+00	2.04E+00	1.36E-02	1.1E-14	2.5E-01	6.3E-03	2.6	1.2	2.6	38.3	90.1	4.38	0.29
L	1150	8.70E+00	2.41E+00	2.23E-02	1.0E-14	2.1E-01	9.8E-03	3.0	1.8	2.5	26.1	92.6	4.12	0.30
M	1300	2.39E+01	9.93E+00	7.46E-02	1.4E-02	5.1E-02	1.1E-02	16.7	2.9	3.3	11.2	96.0	4.89	0.49
N	1650	2.01E+01	1.86E+01	6.38E-02	1.7E-14	2.7E-02	1.1E-02	37.7	3.3	4.0	13.6	100.0	5.01	0.40
total gas age	n=14		4.2E-13	6.1E-01									4.43	0.28
Eruption Age	n=5	steps E-I	2.0E-13	4.9E-01									47.6	4.42
OCA-043; N6:118, groundmass concentrate, 97.60mg, J=0.000151247±0.12%, D=1.00644±0.00091, NM-118, Lab#=50936-01														
A	550	3.59E+02	6.33E-01	1.18E+00	2.3E-15	8.1E-01	6.3E-02	0.9	24.2	3.6	3.2	3.6	3.16	1.24
B	625	7.66E+01	1.58E+00	2.28E-01	3.8E-15	3.2E-01	4.0E-02	3.9	25.5	6.0	12.3	9.6	2.56	0.26
C	675	4.24E+01	1.87E+00	1.05E-01	3.6E-15	2.7E-01	2.0E-02	4.4	12.0	5.7	27.2	15.3	3.15	0.17
D	725	2.51E+01	1.83E+00	4.67E-02	5.1E-15	2.8E-01	8.0E-03	6.1	6.9	8.0	45.4	23.3	3.11	0.10
E	775	1.89E+01	1.61E+00	2.64E-02	4.3E-15	3.2E-01	3.8E-03	4.6	2.8	6.9	59.3	30.2	3.06	0.07
F	825	1.53E+01	1.32E+00	1.41E-02	1.0E-14	3.9E-01	2.2E-03	8.7	3.6	15.9	73.3	46.1	3.06	0.04
G	875	1.36E+01	1.10E+00	9.14E-03	9.0E-15	4.6E-01	1.4E-03	6.5	2.1	14.3	80.6	60.4	3.00	0.04
H	925	1.31E+01	1.11E+00	7.43E-03	9.2E-15	4.6E-01	1.4E-03	6.7	2.2	14.6	83.7	75.0	2.99	0.04
I	975	1.35E+01	1.34E+00	8.66E-03	5.9E-15	3.8E-01	2.1E-03	5.2	2.1	9.4	81.8	84.4	3.01	0.04
J	1025	1.41E+01	1.71E+00	1.12E-02	2.3E-15	3.0E-01	4.0E-03	2.6	1.5	3.6	77.3	88.0	2.98	0.10
K	1075	1.79E+01	1.95E+00	2.45E-02	1.6E-14	2.6E-01	8.9E-03	2.1	2.4	2.6	60.1	90.5	2.93	0.15
L	1150	1.93E+01	2.17E+00	3.19E-02	1.6E-15	3.0E-01	9.3E-03	1.9	2.6	2.6	51.8	93.2	2.73	0.15
M	1300	3.19E+01	1.03E+01	7.37E-02	1.0E-15	5.0E-02	1.2E-02	7.0	2.1	1.6	34.2	94.8	3.00	0.30
N	1650	4.19E+01	1.82E+01	1.06E-01	3.3E-15	2.8E-02	1.8E-02	39.3	10.0	5.2	28.4	100.0	3.29	0.18
total gas age	n=14		6.3E-14	3.7E-01									3.02	0.13
Eruption Age	n=4	steps F-I	3.4E-14	4.3E-01									54.1	3.01
OCA-044; N2:118, groundmass concentrate, 99.65mg, J=0.000152126±0.12%, D=1.00644±0.00091, NM-118, Lab#=50938-01														
A	550	1.89E+03	2.53E+00	6.33E+00	1.1E-15	2.0E-01	2.2E-02	1.6	19.2	1.8	1.3	1.8	6.61	9.40
B	625	2.20E+01	2.31E+00	3.57E-02	2.6E-16	2.2E-01	9.6E-04	3.6	2.0	4.2	52.6	6.0	3.17	0.14
C	675	1.35E+01	1.86E+00	7.54E-03	3.5E-15	2.7E-01	2.4E-04	3.8	0.7	5.6	84.4	11.6	3.13	0.08
D	725	1.26E+01	1.62E+00	4.65E-03	6.2E-15	3.2E-01	3.0E-04	6.0	1.5	10.2	89.9	21.8	3.10	0.05
E	775	1.24E+01	1.37E+00	3.7E-03	5.1E-15	3.7E-01	4.6E-04	4.5	2.0	8.9	88.4	30.7	3.00	0.04
F	825	1.21E+01	1.15E+00	3.72E-03	1.2E-14	4.4E-01	1.2E-04	7.9	1.1	18.8	91.4	49.6	3.03	0.03
G	875	1.20E+01	1.06E+00	3.71E-03	1.0E-14	4.8E-01	1.9E-04	6.6	1.6	17.0	91.9	66.6	3.01	0.03
H	925	1.22E+01	1.28E+00	4.64E-03	9.4E-15	4.0E-01	5.6E-04	7.1	4.3	15.2	89.3	81.8	2.99	0.03
I	975	1.29E+01	1.82E+00	7.79E-03	3.9E-15	2.8E-01	6.6E-04	4.2	2.1	6.4	83.1	88.2	2.95	0.06
J	1025	1.45E+01	2.67E+00	9.81E-03	1.6E-15	1.9E-01	3.4E-03	2.6	4.5	2.7	81.2	90.8	3.23	0.13
K	1075	1.69E+01	3.56E+00	2.14E-02	1.1E-15	1.4E-01	6.0E-03	2.2	5.1	1.7	63.9	92.6	2.96	0.20
L	1150	1.78E+01	3.89E+00	3.01E-02	9.3E-16	1.3E-01	9.5E-03	2.1	7.2	1.5	51.4	94.1	2.51	0.25
M	1300	2.35E+01	2.25E+01	5.63E-02	1.1E-15	2.3E-02	1.8E-02	14.8	16.5	1.8	36.5	95.9	2.39	0.24
N	1650	3.01E+01	2.21E+01	8.33E-02	2.5E-15	2.9E-02	1.6E-02	33.0	32.2	4.1	23.9	100.0	2.01	0.21
total gas age	n=14		6.1E-14	3.5E-01									3.04	0.23
Eruption Age	n=5	steps E-I	4.1E-14	4.2E-01									66.4	3.01
OCA-045; N4:118, groundmass concentrate, 100.26mg, J=0.000152748±0.12%, D=1.00644±0.00091, NM-118, Lab#=50940-01														
A	550	2.84E+02	6.75E+00	8.85E-01	4.8E-16	7.6E-02	7.9E-03	2.4	8.3	1.3	8.0	1.		

ID	Temp/P (°C/W)	$^{40}\text{Ar}/^{39}\text{Ar}$	$^{37}\text{Ar}/^{39}\text{Ar}$	$^{36}\text{Ar}/^{39}\text{Ar}$	$^{39}\text{Ar}_\text{K}$ (mol)	K/Ca	Ci/K	$^{37}\text{Ar}_{\text{Cs}}$ (%)	$^{38}\text{Ar}_{\text{Cl}}$ (%)	$^{39}\text{Ar}_{\text{K}}$ (%)	$^{40}\text{Ar}^*$ (%)	^{39}Ar (%)	Age (Ma)	#20 (Ma)	
OCA-046; a1:120, groundmass concentrate, 54.30mg, J=0.00079±0.10%, D=1.00644±0.00091, NM-120, Lab#=51041-01															
A	550	1.05E+02	5.81E-01	3.41E-01	9.9E-16	8.8E-01	1.7E-02	0.2	2.6	0.4	3.8	0.4	5.63	3.02	
B	625	1.15E+01	8.15E-01	3.22E-02	7.5E-15	6.3E-01	3.3E-03	1.8	3.7	2.8	17.6	3.2	2.89	0.35	
C	675	-3.02E-01	9.72E-01	-9.07E-03	2.2E-16	5.2E-01	2.9E-03	0.1	0.1	0.1	-6.5	3.3	3.38	3.16	
D	725	3.87E+00	1.10E+00	2.35E-03	1.5E-14	4.7E-01	2.4E-03	4.8	5.5	5.6	83.6	8.9	4.61	0.08	
E	775	3.24E+00	9.44E-01	-3.02E-03	1.8E-15	5.4E-01	2.2E-03	0.5	0.6	0.7	129.0	9.5	5.95	0.43	
F	825	3.60E+00	8.27E-01	6.74E-04	2.7E-14	6.2E-01	1.7E-03	6.7	7.0	10.3	95.5	19.9	4.89	0.04	
G	875	3.43E+00	7.24E-01	5.00E-04	4.5E-14	7.1E-01	1.5E-03	9.6	10.6	17.0	96.6	36.9	4.72	0.03	
H	925	3.38E+00	6.31E-01	4.86E-04	5.5E-14	8.1E-01	1.3E-03	10.2	10.7	20.6	96.5	57.5	4.65	0.02	
I	975	3.34E+00	6.12E-01	4.17E-04	2.7E-14	8.3E-01	1.2E-03	4.9	5.0	10.3	97.0	67.7	4.61	0.04	
J	1025	3.37E+00	6.71E-01	6.74E-04	4.8E-14	7.6E-01	1.4E-03	9.4	10.5	17.9	94.9	85.6	4.55	0.03	
K	1075	3.65E+00	7.99E-01	1.76E-03	1.3E-14	6.4E-01	3.1E-03	3.1	6.3	5.0	86.7	90.6	4.51	0.07	
L	1150	3.60E+00	8.08E-01	2.08E-03	6.9E-15	6.3E-01	6.8E-03	1.6	7.2	2.6	83.9	93.2	4.31	0.11	
M	1300	4.43E+00	8.05E+00	8.14E-03	4.4E-15	6.3E-02	8.5E-03	10.3	5.7	1.6	59.1	94.8	3.75	0.22	
N	1650	5.40E+00	9.07E+00	1.05E-02	1.4E-14	5.6E-02	1.2E-02	36.9	24.6	5.2	54.8	100.0	4.24	0.12	
total gas age				n=14				2.7E-13	6.7E-01				4.57	0.08	
Eruption Age				n=4	steps G-J	1.7E-13	7.7E-01						65.7	4.64	
														0.07	
OCA-047; D2:117, groundmass concentrate, 56.53mg, J=0.001062743±0.10%, D=1.00644±0.00091, NM-117, Lab#=50850-01															
A	550	1.10E+02	1.42E+00	3.48E-01	5.5E-15	3.6E-01	3.0E-02	1.2	20.0	1.1	6.4	1.1	13.53	2.06	
B	625	7.64E+00	1.50E+00	1.08E-02	1.1E-14	3.4E-01	2.4E-03	2.5	3.3	2.2	59.7	3.3	8.73	0.23	
C	700	5.12E+00	1.25E+00	2.58E-03	2.8E-14	4.1E-01	7.9E-04	5.3	2.7	5.5	86.7	8.8	8.51	0.08	
D	775	4.67E+00	9.73E-01	1.03E-03	6.3E-14	5.2E-01	3.1E-04	9.1	2.3	12.2	94.7	21.0	8.47	0.04	
E	850	4.47E+00	6.94E-01	5.68E-04	1.0E-13	7.4E-01	2.3E-04	10.6	2.8	19.9	97.0	40.9	8.30	0.04	
F	925	4.37E+00	5.99E-01	4.43E-04	1.2E-13	8.5E-01	2.8E-04	10.5	3.9	22.8	97.6	63.7	8.16	0.03	
G	1000	4.35E+00	6.30E-01	3.98E-04	1.0E-13	8.1E-01	6.5E-04	9.9	8.1	20.4	98.0	84.1	8.16	0.03	
H	1075	4.40E+00	7.58E-01	6.38E-04	4.4E-14	6.7E-01	1.7E-03	5.0	9.1	8.7	96.6	92.8	8.14	0.05	
I	1150	4.59E+00	1.03E+00	1.50E-03	1.4E-14	5.0E-01	5.9E-03	2.2	10.0	2.8	91.7	95.5	8.06	0.11	
J	1300	5.41E+00	8.28E+00	8.64E-03	8.2E-15	6.2E-02	9.0E-03	10.2	8.9	1.6	65.0	97.1	6.77	0.26	
K	1650	8.41E+00	1.51E+01	1.95E-02	1.5E-13	6.8E-01	3.4E-02	1.6E-02	33.4	28.9	2.9	46.0	100.0	7.49	0.19
total gas age				n=11				5.1E-13	6.8E-01				8.27	0.08	
Eruption age				n=3	steps F-H	2.7E-13	8.1E-01						51.9	8.16	
														0.03	
OCA-048; ..3:120, groundmass concentrate, 63.20mg, J=0.000795±0.10%, D=1.00644±0.00091, NM-120, Lab#=51037-01															
A	550	2.02E+02	1.67E+00	6.60E-01	3.5E-16	3.1E-01	5.3E-02	0.1	3.4	0.1	3.7	0.1	10.66	10.64	
B	625	1.19E+02	1.25E+00	3.79E-01	3.0E-15	4.1E-01	6.4E-03	0.8	3.5	0.9	5.5	1.0	9.90	2.11	
C	675	8.66E+00	1.09E+00	4.19E-02	4.6E-16	4.7E-01	9.5E-04	0.1	0.1	0.1	60.2	1.1	7.46	1.84	
D	725	4.17E+00	9.52E-01	3.37E-03	2.5E-14	5.4E-01	3.4E-04	5.2	1.5	7.5	77.3	8.6	4.62	0.06	
E	775	3.32E+00	6.17E-01	7.90E-03	3.4E-14	8.3E-01	1.4E-04	4.6	0.8	10.2	93.6	18.8	4.45	0.04	
F	825	3.22E+00	3.99E-01	3.36E-04	6.6E-14	1.3E+00	4.4E-05	5.8	0.5	20.0	97.1	38.8	4.48	0.02	
G	875	3.20E+00	3.13E-01	2.61E-04	7.4E-14	1.6E+00	2.0E-05	5.0	0.3	22.2	97.6	61.0	4.47	0.02	
H	925	3.22E+00	3.73E-01	2.94E-04	6.8E-14	1.4E+00	1.8E-05	5.6	0.2	20.6	97.4	81.6	4.50	0.02	
I	975	3.30E+00	4.83E-01	5.04E-04	2.3E-14	1.1E+00	4.5E-04	2.5	1.9	7.1	95.8	88.6	4.53	0.04	
J	1025	3.57E+00	7.21E-01	1.58E-03	1.8E-14	7.1E-01	2.0E-03	2.8	6.4	5.4	87.8	94.1	4.50	0.05	
K	1075	4.38E+00	1.34E+00	4.17E-03	3.8E-15	3.8E-01	8.5E-03	1.1	5.9	1.1	73.7	95.2	4.63	0.25	
L	1150	5.39E+00	2.28E+00	8.33E-03	3.7E-15	2.2E-01	1.7E-02	1.8	11.8	1.1	57.1	96.3	4.42	0.28	
M	1300	1.11E+01	1.85E+01	3.33E-02	4.2E-15	2.8E-02	2.4E-02	16.9	18.3	1.3	23.8	97.6	3.84	0.37	
N	1650	1.71E+01	2.72E+01	5.60E-02	8.0E-15	1.9E-02	3.1E-02	47.7	45.4	2.4	15.0	100.0	3.75	0.37	
total gas age				n=14				3.3E-13	1.1E+00				4.52	0.09	
Eruption Age				n=6	steps E-J	2.8E-13	1.3E+00						85.5	4.48	
														0.02	
OCA-051; Y1:120, groundmass concentrate, 81.50mg, J=0.000789±0.10%, D=1.00644±0.00091, NM-120, Lab#=51017-01															
A	550	1.15E+02	1.03E+00	3.79E-01	3.0E-15	4.9E-01	6.6E-03	0.5	1.7	0.8	2.4	0.8	3.92	2.12	
B	625	8.61E+00	1.84E+00	1.79E-02	5.2E-15	2.8E-01	1.7E-03	1.5	0.7	1.3	39.9	2.0	4.89	0.28	
C	675	5.19E+00	1.80E+00	4.72E-03	5.7E-15	2.8E-01	9.2E-04	1.6	0.4	1.4	75.3	3.5	5.57	0.16	
D	725	4.44E+00	1.64E+00	2.90E-03	1.5E-14	3.1E-01	6.0E-04	3.9	0.8	3.8	86.9	7.3	5.50	0.07	
E	775	4.04E+00	1.42E+00	1.19E-03	2.3E-14	3.6E-01	4.3E-04	5.2	0.8	5.7	93.4	13.0	5.37	0.05	
F	825	3.80E+00	1.23E+00	7.80E-04	3.2E-14	4.2E-01	2.3E-04	6.2	0.6	8.0	95.8	21.0	5.19	0.04	
G	875	3.71E+00	1.03E+00	7.66E-04	4.6E-14	5.0E-01	3.6E-04	7.5	1.4	11.5	95.4	32.5	5.04	0.03	
H	925	3.65E+00	8.19E-01	6.19E-04	5.3E-14	6.2E-01	5.9E-04	6.9	2.7	13.4	96.0	45.9	4.99	0.03	
I	975	3.60E+00	6.95E-01	4.79E-04	5.1E-14	7.3E-01	9.9E-04	5.6	4.0	12.8	96.9	58.7	4.97	0.03	
J	1025	3.60E+00	5.82E-01	5.21E-04	6.0E-14	8.8E-01	1.4E-03	5.5	7.2	15.0	96.3	73.7	4.94	0.02	
K	1075	3.71E+00	5.73E-01	7.87E-04	3.8E-14	8.9E-01	2.7E-03	3.5	8.8	9.7	94.2	83.4	4.97	0.03	
L	1150	3.96E+00	7.60E-01	1.59E-03	2.5E-14	6.7E-01	6.6E-03	3.0	13.8	6.2	89.0	89.6	5.01	0.05	
M	1300	8.20E+00	7.84E+00	1.72E-02	2.6E-14	6.5E-02	1.7E-02	32.6	38.6	8.6	45.1	96.2	5.28	0.11	
total gas age				n=13		3.8E-13	0.60						5.06	0.07	
Eruption Age				n=6	steps G-L	2.7E-13	7.2E-01						71.3	4.98	
														0.04	
OCA-052; Y5:120, groundmass concentrate, 82.00mg, J=0.000792±0.10%, D=1.00644±0.00091, NM-120, Lab#=51021-01															
A	550	2.77E+01	4.36E-01	8.87E-02	2.9E-15	1.5E-02	2.6E-02	0.2	2.2	0.7	5.3	0.7	2.10	0.76	
B	625	5.37E+00	1.07E+00	1.04E-02	9.8E-15	4.7E-01</									

ID	Temp/P (°C/W)	⁴⁰ Ar/ ³⁹ Ar	³⁷ Ar/ ³⁹ Ar	³⁶ Ar/ ³⁹ Ar	³⁹ Ar _K (mol)	K/Ca	Cl/K	³⁷ Ar _{Cs} (%)	³⁸ Ar _{Cl} (%)	³⁹ Ar _K (%)	⁴⁰ Ar [*] (%)	³⁹ Ar (%)	Age (Ma)	±2σ (Ma)	
OCA-053; Z1:120, groundmass concentrate, 83.00mg, J=0.000792±0.10%, D=1.00644±0.00091, NM-120, Lab#=51023-01															
A	550	8.78E+01	1.0E+00	2.91E-01	2.5E-15	4.8E-01	2.3E-02	0.4	4.6	0.7	2.2	0.7	2.82	1.93	
B	625	1.36E+01	1.51E+00	3.22E-02	7.6E-15	3.4E-01	7.1E-03	1.7	4.3	2.1	30.6	2.7	5.94	0.36	
C	675	5.24E+00	1.61E+00	2.23E-04	2.2E-15	3.2E-01	5.1E-03	0.5	0.9	0.6	100.6	3.3	7.54	0.32	
D	725	5.26E+00	1.41E+00	1.18E-03	2.4E-14	3.6E-01	3.8E-03	5.1	7.3	6.5	95.0	9.8	7.13	0.05	
E	775	5.06E+00	1.30E+00	6.58E-04	3.1E-14	3.9E-01	2.4E-03	6.1	6.0	8.4	97.6	18.2	7.06	0.04	
F	825	4.87E+00	1.13E+00	4.83E-04	4.4E-14	4.5E-01	1.7E-03	7.5	6.1	11.9	98.3	30.1	6.84	0.03	
G	875	4.75E+00	9.38E-01	4.12E-04	5.7E-14	5.4E-01	1.2E-03	8.1	5.4	15.4	98.4	45.5	6.68	0.03	
H	925	4.73E+00	8.12E-01	5.05E-04	6.3E-14	6.3E-01	1.1E-03	7.8	5.5	17.1	97.6	62.6	6.59	0.03	
I	975	4.70E+00	8.19E-01	4.40E-04	4.8E-14	6.2E-01	1.3E-03	6.0	5.0	13.0	98.0	75.6	6.58	0.03	
J	1025	4.69E+00	8.72E-01	5.30E-04	5.3E-14	5.8E-01	2.3E-03	7.0	9.6	14.2	97.6	89.9	6.53	0.03	
K	1075	4.77E+00	1.11E+00	8.31E-04	1.5E-14	4.6E-01	7.0E-03	2.5	8.3	4.0	96.1	93.8	6.55	0.06	
L	1150	4.75E+00	1.62E+00	1.29E-03	7.3E-15	3.2E-01	1.7E-02	1.8	9.7	2.0	94.1	95.8	6.38	0.12	
M	1300	5.85E+00	2.32E+01	1.21E-02	5.0E-15	2.2E-02	1.6E-02	17.5	6.5	1.3	68.8	97.2	5.83	0.20	
N	1650	7.70E+00	1.74E+01	1.37E-02	1.1E-14	2.9E-02	2.5E-02	27.8	20.7	2.8	64.3	100.0	7.16	0.12	
total gas age		n=14				3.7E-13	5.0E-01						6.66	0.07	
Eruption Age		n=4	steps H-K	1.8E-13	6.0E-01							48.4	6.57	0.04	
OCA-054; A4:117, groundmass concentrate, 94.22mg, J=0.00106749±0.10%, D=1.00644±0.00091, NM-117, Lab#=50834-01															
A	550	1.49E-02	6.68E+00	4.79E-01	4.5E-15	7.7E-02	7.1E-03	2.5	7.8	0.8	5.4	0.8	15.46	3.10	
B	625	6.32E+00	2.59E+00	6.05E-03	1.9E-14	2.0E-01	3.0E-04	4.0	1.4	3.3	74.7	4.1	9.10	0.15	
C	675	4.77E+00	1.98E+00	1.68E-03	3.6E-14	2.6E-01	1.9E-04	5.8	1.6	6.3	92.5	10.4	8.49	0.05	
D	725	4.47E+00	1.39E+00	8.58E-04	6.9E-14	3.7E-01	7.9E-05	8.0	-0.1	12.2	96.4	22.7	8.28	0.04	
E	775	4.37E+00	1.24E+00	6.36E-04	8.0E-14	4.1E-01	4.4E-06	8.2	0.1	14.2	97.5	36.9	8.19	0.03	
F	825	4.34E+00	9.98E-01	4.63E-04	1.1E-13	5.3E-01	<2.3E-05	8.7	-0.6	19.5	98.1	56.5	8.20	0.03	
G	875	4.35E+00	7.62E-01	5.43E-04	9.8E-14	6.7E-01	5.9E-05	6.2	1.4	17.3	97.2	73.8	8.13	0.04	
H	925	4.38E+00	1.02E+00	6.70E-04	6.7E-14	5.0E-01	1.9E-04	5.6	3.1	11.8	96.9	85.5	8.16	0.04	
I	975	4.51E+00	1.89E+00	2.1E-03	3.1E-14	2.7E-01	6.2E-04	4.9	4.8	5.5	95.0	91.0	8.25	0.07	
J	1025	4.82E+00	3.24E+00	2.77E-03	1.4E-14	1.6E-01	1.2E-03	3.7	4.1	2.4	88.1	93.5	8.17	0.14	
K	1075	4.39E+00	3.22E+00	9.22E-03	7.0E-15	1.6E-01	2.7E-03	1.9	4.6	1.2	99.3	94.7	8.40	0.25	
L	1150	4.93E+00	2.81E+00	2.70E-03	1.2E-14	1.8E-01	5.5E-03	2.7	15.8	2.0	88.1	96.8	8.36	0.18	
M	1225	6.13E+00	5.03E+00	6.94E-03	5.9E-15	1.0E-01	9.7E-03	2.5	14.2	1.0	72.9	97.8	8.62	0.37	
N	1300	1.49E+01	3.89E+01	4.49E-02	1.7E-15	1.3E-01	1.3E-02	5.4	5.5	0.3	31.5	98.1	9.23	1.45	
O	1450	3.18E+01	3.51E+01	1.04E-01	5.4E-15	1.5E-02	1.5E-02	15.8	20.3	1.0	12.6	99.1	7.94	0.87	
P	1650	1.91E+01	3.30E+01	5.88E-02	5.3E-15	1.5E-02	1.2E-02	14.3	16.0	0.9	23.1	100.0	8.68	0.71	
total gas age		n=16				5.7E-13	4.3E-01						8.31	0.10	
Eruption Age		n=4	steps E-H	3.6E-13	5.4E-01							62.8	8.17	0.04	
OCA-055; ..2:120, groundmass concentrate, 78.60mg, J=0.000797±0.10%, D=1.00644±0.00091, NM-120, Lab#=51036-01															
A	550	1.85E+02	3.10E+00	6.23E-01	2.9E-15	1.6E-01	3.6E-02	1.3	22.9	1.4	0.6	1.4	1.66	3.11	
B	625	6.47E+00	2.23E+00	1.49E+00	1.2E-14	2.3E-01	2.2E-03	3.6	5.4	5.4	34.7	6.8	3.23	0.19	
C	675	3.26E+00	1.54E+00	4.33E-03	1.4E-14	3.8E-01	4.4E-04	3.1	1.4	6.7	63.6	13.5	2.99	0.10	
D	725	2.70E+00	1.12E+00	2.34E-03	3.5E-14	4.6E-01	3.1E-04	5.5	2.4	16.1	76.6	29.6	2.97	0.04	
E	775	2.50E+00	1.01E+00	1.61E-03	3.5E-14	5.1E-01	2.7E-04	5.0	2.0	16.5	83.1	46.1	2.99	0.04	
F	825	2.48E+00	8.72E-01	1.34E-03	3.6E-14	5.8E-01	1.7E-04	4.4	1.3	16.7	85.7	62.8	3.06	0.04	
G	875	2.57E+00	9.09E-01	1.80E-03	2.4E-14	5.6E-01	3.6E-04	3.1	1.9	11.4	81.1	74.2	3.00	0.05	
H	925	2.80E+00	1.26E+00	2.74E-03	1.6E-14	4.0E-01	9.9E-04	2.9	3.6	7.7	73.7	81.9	2.97	0.07	
I	975	3.11E+00	1.95E+00	3.99E-03	7.6E-15	2.6E-01	1.9E-03	2.1	3.0	3.6	66.2	85.5	2.97	0.13	
J	1025	3.88E+00	2.93E+00	6.76E-03	6.7E-15	1.7E-01	3.2E-03	2.8	4.7	3.1	53.7	88.6	3.00	0.16	
K	1075	4.98E+00	3.71E+00	1.04E-02	4.1E-15	1.4E-01	4.4E-03	2.2	4.0	1.9	43.4	90.5	3.11	0.26	
L	1150	5.77E+00	3.99E+00	1.29E-02	4.5E-15	1.3E-01	7.8E-03	2.5	7.3	2.1	39.2	92.6	3.26	0.29	
M	1300	2.14E+01	3.18E+01	7.38E-02	8.9E-15	1.6E-02	1.5E-02	40.1	29.1	4.2	9.4	96.8	2.96	0.34	
N	1650	1.85E+01	2.19E+01	6.17E-02	6.9E-15	2.3E-02	7.4E-03	21.4	11.1	3.2	10.5	100.0	2.84	0.41	
total gas age		n=14				2.1E-13	4.1E-01						2.99	0.16	
Eruption Age		n=8	steps C-J	1.7E-13	4.7E-01							81.8	3.00	0.03	
OCA-057; M6:118, groundmass concentrate, 78.60mg, J=0.000152454±0.12%, D=1.00644±0.00091, NM-118, Lab#=50930-01															
A	550	1.08E+03	3.89E+00	3.59E+00	1.3E-01	1.5E-15	3.9E-01	7.6E-03	1.3	2.4	1.2	12.4	1.2	8.25	5.14
B	625	1.74E+01	2.42E+00	2.63E-02	3.6E-15	2.1E-01	1.2E-03	4.7	2.8	5.1	56.3	7.0	2.70	0.10	
C	675	1.02E+01	1.64E+00	6.79E-03	4.7E-15	3.1E-01	4.2E-04	4.2	1.3	6.7	81.3	13.7	2.28	0.05	
D	725	9.24E+00	1.35E+00	4.32E-03	8.9E-15	3.8E-01	2.9E-04	6.5	1.7	12.9	87.0	26.6	2.21	0.03	
E	775	9.09E+00	1.15E+00	3.71E-03	7.6E-15	4.4E-01	6.7E-04	4.2	3.0	9.7	88.6	36.2	2.22	0.03	
F	825	8.86E+00	9.38E-01	3.14E-03	1.4E-14	5.4E-01	4.4E-06	7.0	4.0	20.9	90.1	57.1	2.20	0.02	
G	875	9.05E+00	7.16E-01	3.75E-03	1.1E-14	7.1E-01	2.5E-04	4.3	1.8	15.9	86.1	73.0	2.19	0.04	
H	925	9.63E+00	8.01E-01	5.75E-03	6.6E-15	6.4E-01	6.1E-04	2.9	2.7	9.6	82.7	82.5	2.19	0.04	
I	975	1.09E+01	1.00E-02	3.6E-15	4.4E-04	9.2E-04	2.3	2.2	5.2	5.2	73.6	87.7	2.21	0.06	
J	1025	1.23E+01	1.51E-02	1.8E-15	2.8E-01	2.2E-03	1.8	2.6	2.6	64.8	90.3	2.20	0.11		
K	1075	1.50E+01	2.58E+00	2.50E-02	1.4E-15	2.0E-01	4.7E-03	2.0	4.5	2.1	51.8	92.4	2.13	0.16	
L	1150	1.73E+01	3.55E+00	3.34E-02	1.3E-15	1.4E-01	5.4E-03	2.5	4.6	1.9	44.5	94.3	2.12	0.16	
M	1300	4.84E+01	1.94E+01	1.47E-01	1.0E-15	2.6E-02	1.2E-02	10.6	8.3	1.5	13.4	95.7	1.80	0.34	
N	1650	6.55E+01	2.74E+01	3.05E-01	1.9E-15	1.6E-02	44.2	31.0	4.3	10.7	100.0	1.96	0.21		
total gas age		n=14				6.9E-14	4.5E-01						2.26	0.15	
Eruption Age		n=7	steps D-J	5.9E-14	5.3E-01							76.6	2.20	0.02	
OCA-059; F6:117, groundmass concentrate, 59.72mg, J=0.00106038±0.10%, D=1.00644±0															

ID	Temp/P (°C/W)	$^{40}\text{Ar}/^{39}\text{Ar}$	$^{37}\text{Ar}/^{39}\text{Ar}$	$^{36}\text{Ar}/^{39}\text{Ar}$	$^{39}\text{Ar}_{\text{K}}$	K/Ca (mol)	Cl/K	$^{37}\text{Ar}_{\text{Ca}}$ (%)	$^{38}\text{Ar}_{\text{Cl}}$ (%)	$^{39}\text{Ar}_{\text{K}}$ (%)	$^{40}\text{Ar}^*$ (%)	^{39}Ar (%)	Age (Ma)	$\pm 2\sigma$
OCA-061; L6:118, groundmass concentrate, 12.04mg, J=0.000152936±0.12%, D=1.00644±0.00091, NM-118, Lab#=50924-01														
A	550	2.06E+02	3.49E+00	6.60E-01	1.7E-15	1.5E-01	4.9E-02	2.3	10.5	2.8	5.5	2.8	3.16	0.73
B	625	1.23E+01	2.26E+00	1.12E-02	6.1E-15	2.3E-01	1.9E-02	5.2	14.0	9.9	74.3	12.8	2.53	0.06
C	675	9.54E+00	1.55E+00	5.13E-03	7.0E-15	3.3E-01	1.2E-02	4.2	10.5	11.5	85.1	24.2	2.24	0.04
D	725	9.39E+00	1.31E+00	4.34E-03	9.4E-15	3.9E-01	8.1E-03	4.7	9.4	15.3	87.1	39.6	2.26	0.03
E	775	9.51E+00	1.25E+00	4.29E-03	6.0E-15	4.1E-01	6.0E-03	2.9	4.4	9.8	87.4	49.4	2.29	0.04
F	825	9.80E+00	1.20E+00	5.16E-03	8.2E-15	4.2E-01	3.6E-03	3.8	3.6	13.4	85.1	62.8	2.30	0.03
G	875	1.03E+01	1.30E+00	6.49E-03	5.1E-15	3.9E-01	1.9E-03	2.5	1.2	8.4	82.0	71.1	2.32	0.04
H	925	1.10E+01	1.56E+00	9.79E-03	3.5E-15	3.3E-01	2.8E-03	2.1	1.2	5.7	74.6	76.8	2.27	0.06
I	975	1.21E+01	2.06E+00	1.57E-02	1.9E-15	2.5E-01	2.9E-03	1.5	0.7	3.1	62.9	79.9	2.11	0.11
J	1025	1.34E+01	2.68E+00	1.73E-02	1.0E-15	1.9E-01	5.2E-03	1.0	0.7	1.7	63.2	81.6	2.34	0.18
K	1075	1.60E+01	3.37E+00	2.79E-02	1.1E-15	1.5E-01	1.0E-02	1.4	1.3	1.7	49.8	83.3	2.20	0.21
L	1150	2.06E+01	4.66E+00	4.91E-02	1.2E-15	1.1E-01	1.2E-02	2.1	1.8	1.9	31.2	85.2	1.78	0.21
M	1300	3.13E+01	2.06E+01	9.16E-02	3.6E-15	2.5E-02	3.2E-02	28.0	14.3	5.8	18.4	91.0	1.61	0.14
N	1650	2.60E+01	1.82E+01	7.02E-02	5.5E-15	2.8E-02	3.9E-02	38.3	26.4	9.0	25.4	100.0	1.85	0.10
total gas age		n=14		6.1E-14	2.9E-01								2.24	0.09
Eruption Age		n=6	steps C-H	3.9E-14	3.8E-01								64.0	2.28
														0.03
OCA-062; b5:120, groundmass concentrate, 72.55mg, J=0.000789±0.10%, D=1.00644±0.00091, NM-120, Lab#=51051-01														
A	550	1.00E+02	1.75E+00	3.17E-01	2.0E-16	2.9E-01	8.4E-02	0.1	1.8	0.1	6.4	0.1	9.04	9.46
B	625	3.19E+01	2.54E+00	8.26E-02	1.5E-16	2.0E-01	1.6E-02	0.6	2.7	0.7	24.1	0.8	10.94	1.25
C	675	1.67E+01	3.07E+00	5.02E-02	1.1E-16	1.7E-01	2.8E-03	0.1	0.0	0.1	12.6	0.9	3.00	7.37
D	725	5.82E+00	2.37E+00	4.27E-03	9.3E-15	2.2E-01	1.5E-03	3.6	1.4	4.5	81.0	5.4	6.71	0.13
E	775	5.01E+00	1.64E+00	2.11E-03	1.6E-14	3.1E-01	4.7E-04	4.2	0.8	7.7	89.6	13.1	6.38	0.07
F	825	4.82E+00	1.33E+00	1.17E-03	2.0E-14	3.8E-01	1.5E-04	4.3	0.3	9.6	94.4	22.7	6.47	0.06
G	875	4.68E+00	1.19E+00	7.96E-04	3.6E-14	4.3E-01	2.8E-04	7.1	1.1	17.7	96.4	40.4	6.42	0.04
H	925	4.68E+00	1.10E+00	7.21E-04	3.9E-14	4.7E-01	4.0E-04	7.0	1.6	19.1	96.7	59.5	6.43	0.04
I	975	4.60E+00	1.23E+00	4.17E-04	1.9E-14	4.2E-01	6.9E-04	3.7	1.4	9.1	98.8	68.6	6.47	0.07
J	1025	4.69E+00	1.53E+00	9.76E-04	3.3E-14	3.3E-01	1.6E-03	8.2	5.6	16.0	95.8	84.5	6.39	0.04
K	1075	4.90E+00	1.75E+00	1.56E-03	8.1E-15	2.9E-01	6.2E-03	2.3	5.3	3.9	92.8	88.5	6.47	0.12
L	1150	5.42E+00	2.34E+00	3.58E-03	6.3E-15	2.2E-01	1.7E-02	2.4	11.5	3.1	83.4	91.5	6.44	0.18
M	1300	8.68E+00	1.62E+01	2.06E-02	4.9E-15	3.1E-02	3.3E-02	13.1	17.2	2.4	44.0	93.9	5.49	0.34
N	1650	1.21E+01	2.12E+01	3.27E-02	1.2E-14	2.4E-02	3.7E-02	43.2	49.3	6.1	33.6	100.0	5.87	0.19
total gas age		n=14		2.1E-13	3.5E-01								6.42	0.12
Eruption Age		n=8	steps E-L	1.8E-13	3.9E-01								86.1	6.43
														0.03
OCA-063; S6:118, groundmass concentrate, 93.68mg, J=0.000147568±0.12%, D=1.00644±0.00091, NM-118, Lab#=50948-01														
A	550	4.61E+03	2.92E+00	1.53E+01	1.3E-16	2.2E-01	7.7E-02	0.2	2.8	0.3	1.8	0.3	21.93	131.93
B	625	1.17E+03	2.98E+00	3.87E+00	4.7E-16	1.7E-01	7.8E-03	0.9	1.0	1.0	2.1	1.2	6.49	11.04
C	675	7.94E+01	3.08E+00	2.32E+01	1.0E-15	1.7E-01	2.5E-03	2.0	0.7	2.1	14.0	3.4	2.96	0.55
D	725	-2.24E+02	0.00E+00	-9.84E-01	1.4E-17	-	-1.8E-02	-	-0.1	0.0	-30.1	3.4	17.84	33.76
E	775	3.32E+01	2.87E+00	8.92E-02	1.7E-16	1.8E-01	3.3E-03	0.3	0.2	0.4	21.3	3.8	1.88	1.01
F	825	1.55E+01	1.83E+00	2.79E-02	1.3E-14	2.8E-01	5.4E-04	15.8	2.0	28.1	47.6	31.8	1.96	0.04
G	875	9.81E+00	1.16E+00	8.08E-03	6.1E-15	4.4E-01	7.1E-04	4.5	1.2	12.7	76.3	44.5	1.99	0.05
H	925	8.96E+00	1.08E+00	5.44E-03	9.2E-15	4.7E-01	7.6E-04	6.4	2.0	19.2	82.7	63.8	1.97	0.03
I	975	8.82E+00	1.39E+00	5.23E-03	6.3E-15	3.7E-01	1.7E-03	5.6	3.1	13.1	83.4	76.9	1.96	0.04
J	1025	8.41E+00	1.75E+00	5.45E-03	2.3E-15	2.9E-01	3.7E-03	2.6	2.4	4.7	82.1	81.6	1.84	0.08
K	1075	1.04E+01	2.50E+00	1.71E-02	2.7E-15	2.0E-01	1.1E-02	4.4	8.1	5.7	68.2	87.3	1.88	0.07
L	1150	1.87E+01	3.57E+00	3.99E-02	7.2E-16	1.4E-01	3.7E-02	1.7	7.5	1.5	38.2	88.8	1.90	0.26
M	1300	4.56E+01	1.26E+01	1.37E-01	9.5E-16	4.0E-02	3.9E-02	7.6	10.4	2.0	13.0	90.8	1.59	0.39
N	1650	5.13E+01	1.69E+01	1.58E-01	4.4E-15	3.0E-02	4.7E-02	48.0	58.7	9.2	11.4	100.0	1.57	0.21
total gas age		n=14		4.8E-14	3.1E-01								2.04	0.55
Eruption Age		n=4	steps F-J	3.5E-14	3.7E-01								73.1	1.97
														0.02
OCA-064; D4:117, groundmass concentrate, 60.53mg, J=0.001060016±0.10%, D=1.00644±0.00091, NM-117, Lab#=50852-01														
A	550	8.50E+01	2.86E+00	2.73E-01	2.9E-15	1.8E-01	6.3E-02	1.0	11.8	0.9	5.2	0.9	8.40	2.29
B	625	7.76E+00	2.33E+00	1.48E-02	8.6E-15	2.2E-01	2.3E-03	2.3	1.3	2.6	45.9	3.5	6.81	0.26
C	700	4.19E+00	1.66E+00	2.76E-03	2.1E-14	3.1E-01	9.9E-04	4.1	1.4	6.5	83.3	10.0	6.67	0.08
D	775	3.73E+00	1.35E+00	1.31E-03	4.1E-14	3.8E-01	5.3E-04	6.5	1.4	12.7	92.0	22.7	6.56	0.06
E	850	3.62E+00	1.12E+00	1.03E-03	4.8E-14	4.6E-01	5.1E-04	6.2	1.6	14.7	93.5	37.5	6.46	0.04
F	925	3.65E+00	1.07E+00	1.21E-03	3.7E-14	4.8E-01	1.0E-03	4.6	2.5	11.3	91.9	48.8	6.41	0.06
G	1000	3.60E+00	1.36E+00	1.28E-03	4.4E-14	3.7E-01	1.9E-03	6.9	5.4	13.5	92.0	62.3	6.32	0.05
H	1075	3.69E+00	1.48E+00	1.60E-03	3.0E-14	3.4E-01	4.8E-03	5.1	9.2	9.1	89.9	71.4	6.35	0.06
I	1150	3.67E+00	1.08E+00	1.43E-03	3.8E-14	4.7E-01	5.2E-03	4.7	12.9	11.7	90.2	83.1	6.33	0.05
J	1300	5.36E+00	4.34E+00	8.35E-03	1.9E-14	1.2E-01	8.2E-03	9.8	10.4	6.0	60.4	89.1	6.22	0.14
K	1650	8.17E+00	1.18E+01	1.96E-02	3.6E-14	4.3E-02	1.8E-02	48.9	42.2	10.9	40.7	100.0	6.40	0.17
total gas age		n=11		3.2E-13	3.5E-01								6.44	0.11
Eruption Age		n=6	steps D-I	2.4E-13	4.2E-01								73.0	6.40
														0.08
OCA-066; B2:117, groundmass concentrate, 62.60mg, J=0.001066232±0.10%, D=1.00644±0.00091, NM-117, Lab#=50838-01														
A	550	6.46E+01	4.12E-01	2.12E-01	4.6E-15	1.2E-00	2.1E-02	0.3	1.2	0.6	2.9	0.6	3.55	1.78
B	625	2.05E+01	4.48E-01	6.36E-02	2.2E-14	1.1E								

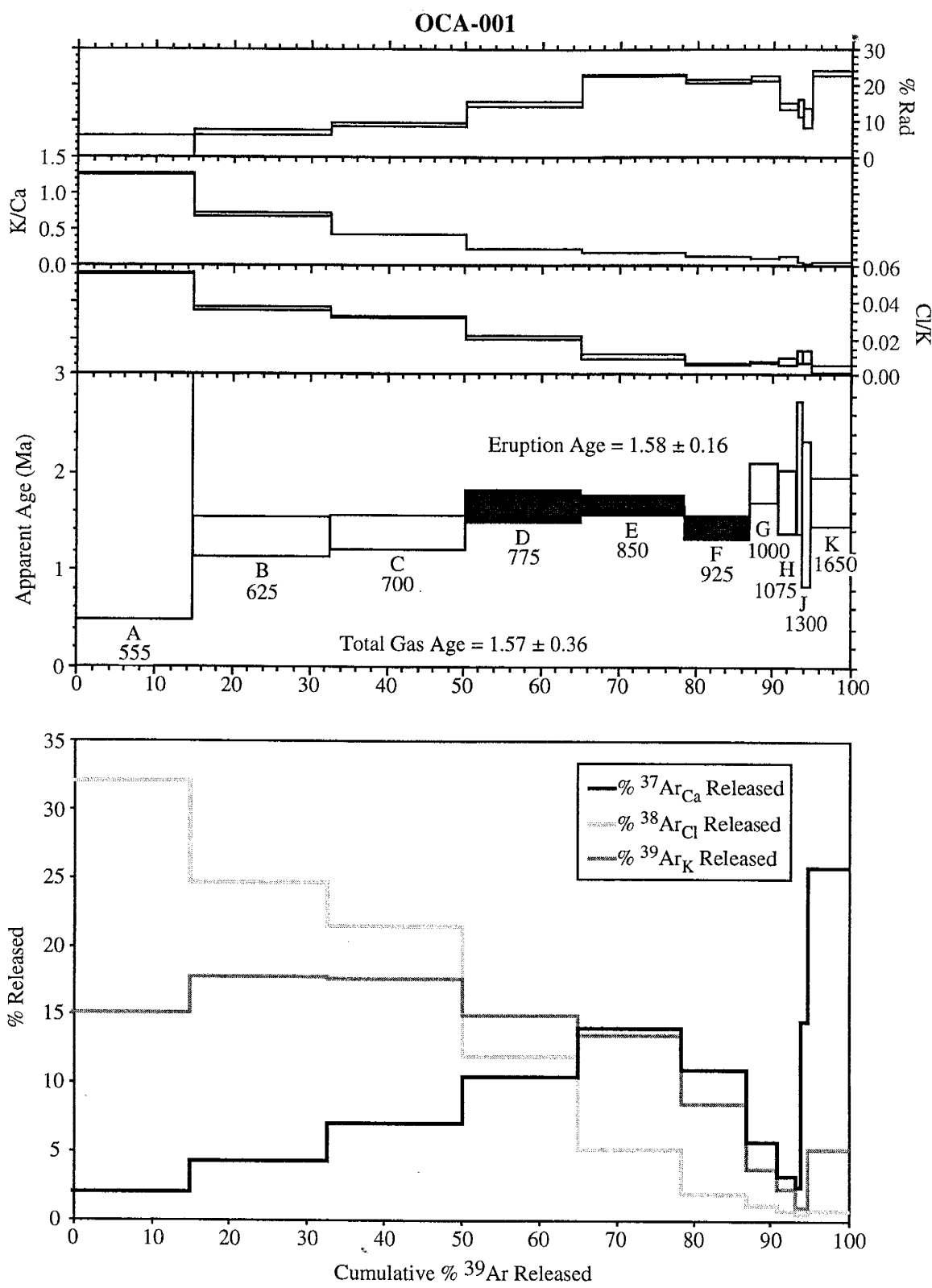
ID	Temp/P (°C/W)	⁴⁰ Ar/ ³⁹ Ar	³⁷ Ar/ ³⁹ Ar	³⁸ Ar/ ³⁹ Ar	³⁹ Ar _K (mol)	K/Ca	Ci/K	³⁷ Ar _{Ca} (%)	³⁸ Ar _{Ca} (%)	³⁹ Ar _K (%)	⁴⁰ Ar* (%)	³⁹ Ar (%)	Age (Ma)	$\pm 2\sigma$ (Ma)	
OCA-067; B4:117, groundmass concentrate, 67.15mg, J=0.001062819±0.10%, D=1.00644±0.00091, NM-117, Lab#=50840-01															
A	550	4.77E+01	3.30E-01	1.55E-01	2.9E-14	1.5E+00	1.3E-02	1.3	4.1	2.5	3.8	2.5	3.43	0.85	
B	625	3.75E+00	5.40E-01	4.72E-03	9.4E-14	9.5E-01	1.1E-02	3.2	5.3	3.7	63.3	6.2	4.55	0.08	
C	700	2.83E+00	5.47E-01	9.55E-04	7.0E-14	9.3E-01	7.9E-03	6.8	7.8	7.7	90.8	14.0	4.93	0.04	
D	775	2.63E+00	4.45E-01	4.97E-04	1.6E-13	1.1E+00	5.6E-03	12.4	12.4	17.4	94.9	31.4	4.79	0.02	
E	850	2.51E+00	3.63E-01	4.02E-04	2.0E-13	1.4E+00	4.3E-03	13.1	12.3	22.4	95.5	53.8	4.60	0.02	
F	925	2.49E+00	3.56E-01	5.17E-04	1.8E-13	1.4E+00	4.1E-03	11.4	10.6	20.0	94.1	73.8	4.49	0.02	
G	1000	2.69E+00	4.29E-01	1.25E-03	1.2E-13	1.2E+00	6.9E-03	8.8	11.2	12.8	86.7	86.5	4.48	0.03	
H	1075	3.64E+00	5.12E-01	4.91E-04	1.0E+00	1.7E-02	4.4	11.9	5.4	63.1	91.9	4.40	0.08		
I	1150	4.52E+00	4.62E-01	7.50E-03	3.5E-14	1.1E+00	2.4E-02	2.8	11.5	3.8	51.3	95.8	4.44	0.09	
J	1300	5.00E+00	4.65E+00	1.02E-02	1.2E-14	1.1E-01	2.0E-02	10.1	3.5	1.4	46.8	97.1	4.50	0.23	
K	1650	5.79E+00	5.56E+00	1.20E-02	9.2E-14	2.6E-02	2.6E-02	25.6	9.4	2.9	46.1	100.0	5.14	0.14	
total gas age			n=11		9.1E-13	1.2E+00							4.59	0.06	
Eruption Age			n=5		steps F-J	3.9E-13	1.2E+00						43.4	4.48	0.03
OCA-068; E4:117, groundmass concentrate, 65.06mg, J=0.00105798±0.10%, D=1.00644±0.00091, NM-117, Lab#=50858-01															
A	550	4.19E+01	8.38E-01	1.23E-01	6.2E-15	6.1E-01	1.0E-02	0.6	1.8	1.3	13.5	1.3	10.73	1.04	
B	625	4.01E+00	1.07E+00	2.07E-03	2.2E-15	4.8E-01	3.6E-04	2.5	0.2	4.5	86.4	5.8	6.60	0.10	
C	700	3.31E+00	9.53E-01	6.06E-04	5.9E-15	5.4E-01	1.0E-04	6.0	0.2	12.1	96.3	17.9	6.08	0.04	
D	775	3.26E+00	7.10E-01	3.64E-04	1.1E-13	7.2E-01	8.5E-05	8.7	0.3	23.7	97.8	41.6	6.08	0.03	
E	850	3.26E+00	6.42E-01	3.67E-04	1.2E-13	7.9E-01	2.7E-04	8.3	0.9	25.0	97.6	66.6	6.06	0.03	
F	925	3.35E+00	9.28E-01	7.70E-04	6.9E-14	5.5E-01	1.4E-03	6.8	2.6	14.2	94.8	80.8	6.05	0.03	
G	1000	3.45E+00	1.21E-00	1.10E-03	3.2E-14	4.2E-01	4.8E-03	4.2	4.3	6.7	92.8	87.5	6.11	0.05	
H	1075	3.67E+00	1.79E-00	2.99E-03	1.0E-14	2.9E-01	1.6E-02	2.0	4.7	2.1	79.3	89.6	5.55	0.15	
I	1150	4.13E+00	2.13E-00	5.68E-03	5.1E-15	2.4E-01	2.5E-02	1.2	3.6	1.1	63.0	90.7	4.97	0.32	
J	1300	5.13E+00	1.38E-01	1.32E-02	7.0E-15	3.7E-02	5.8E-02	10.3	11.3	1.5	45.7	92.1	4.51	0.29	
K	1650	5.32E+00	1.21E-01	1.17E-02	3.8E-14	4.2E-02	6.6E-02	49.5	70.2	7.9	53.5	100.0	5.47	0.13	
total gas age			n=11		4.8E-13	5.8E-01							6.06	0.07	
Eruption Age			n=5		steps C-G	4.0E-13	6.6E-01						81.7	6.07	0.02
OCA-069; M4:118, groundmass concentrate, 96.76mg, J=0.000153092±0.12%, D=1.00644±0.00091, NM-118, Lab#=50934-01															
A	550	5.07E+02	2.45E+00	1.67E+00	1.1E-15	2.1E-01	7.5E-02	1.5	23.6	1.6	2.6	1.6	3.64	2.81	
B	625	3.00E+01	2.04E+00	6.69E-02	3.1E-15	2.5E-01	9.8E-03	3.4	8.6	4.5	34.5	6.1	2.86	0.15	
C	675	1.44E+01	1.43E+00	1.89E-02	3.7E-15	3.6E-01	3.9E-03	2.9	4.2	5.4	61.6	11.5	2.45	0.08	
D	725	1.06E+01	1.09E-00	6.65E-03	7.0E-15	4.7E-01	1.5E-03	4.1	3.0	10.1	82.0	21.6	2.39	0.04	
E	775	1.00E+01	8.92E-01	5.48E-03	5.9E-15	5.7E-01	7.2E-04	2.8	1.2	8.6	84.2	30.2	2.33	0.05	
F	825	9.54E+00	6.99E-01	3.47E-03	1.4E-15	7.3E-01	6.9E-04	5.2	2.7	20.1	89.6	50.3	2.36	0.02	
G	875	9.41E+00	5.52E-01	3.23E-03	1.2E-14	9.2E-01	5.6E-04	3.4	1.8	16.7	90.0	67.0	2.34	0.03	
H	925	9.87E+00	6.98E-01	4.64E-03	9.2E-15	7.3E-01	1.2E-03	3.5	3.0	13.4	86.4	80.4	2.35	0.03	
I	975	1.10E+01	9.67E-01	8.36E-03	4.3E-15	5.3E-01	1.8E-03	2.2	2.2	6.2	78.0	86.6	2.36	0.06	
J	1025	1.23E+01	1.54E+00	1.00E-02	1.7E-15	3.9E-01	3.6E-03	1.4	1.8	2.5	76.7	89.1	2.60	0.12	
K	1075	1.47E+01	1.99E+00	2.17E-02	1.5E-15	2.6E-01	8.0E-03	1.7	3.5	2.2	57.1	91.3	2.31	0.15	
L	1150	1.75E+01	2.59E+00	3.29E-02	1.4E-15	2.0E-01	1.2E-02	2.0	4.6	2.1	45.6	93.4	2.21	0.17	
M	1300	3.89E+01	9.75E+00	1.09E-01	1.2E-15	5.2E-02	1.6E-02	6.2	5.5	1.7	19.5	95.1	2.11	0.30	
N	1650	9.62E+01	3.28E+01	3.10E-01	3.4E-15	1.6E-02	3.6E-02	59.7	34.3	4.9	7.3	100.0	1.99	0.34	
total gas age			n=14		6.9E-14	5.8E-01							2.38	0.11	
Eruption Age			n=6		steps D-I	5.2E-14	7.0E-01						75.1	2.35	0.02
OCA-070; W1:117, groundmass concentrate, 58.70mg, J=0.001023432±0.11%, D=1.00644±0.00091, NM-117, Lab#=50885-01															
A	550	1.51E+02	8.20E-01	5.00E-01	6.3E-15	6.2E-01	1.8E-02	0.8	3.3	1.4	1.9	1.4	5.39	2.70	
B	625	8.28E+00	1.35E+00	2.07E-02	1.2E-14	3.8E-01	7.1E-03	2.4	2.6	2.6	27.1	4.0	4.14	0.27	
C	675	4.14E+01	1.18E+00	4.96E-03	1.3E-14	4.3E-01	5.6E-03	2.3	2.2	2.8	66.4	6.8	5.08	0.17	
D	725	3.31E+01	1.08E+00	2.8E-03	2.8E-15	4.7E-01	4.1E-03	4.6	3.5	6.1	82.5	12.8	5.03	0.08	
E	775	3.05E+01	1.03E+00	1.52E-03	2.7E-14	4.9E-01	3.6E-03	4.2	3.0	5.9	87.3	18.7	4.91	0.07	
F	825	2.86E+00	1.02E+00	1.13E-03	5.7E-14	5.0E-01	3.5E-03	8.7	6.0	12.3	90.5	31.0	4.78	0.04	
G	875	2.79E+00	9.18E-01	9.89E-04	5.7E-14	5.6E-01	3.6E-03	7.6	8.2	12.3	91.4	43.3	4.71	0.04	
H	925	2.78E+00	8.01E-01	9.43E-04	6.1E-14	6.4E-01	3.8E-03	7.2	7.0	13.0	91.5	56.3	4.70	0.03	
I	975	2.85E+00	7.68E-01	1.24E-03	5.6E-14	6.6E-01	5.3E-03	6.4	8.9	11.9	68.5	68.2	4.65	0.04	
J	1025	2.99E+00	7.02E-01	1.69E-03	3.0E-15	7.1E-01	8.3E-03	3.3	7.5	6.5	84.5	74.8	4.66	0.06	
K	1075	3.20E+00	5.77E-01	2.34E-03	2.8E-14	8.8E-01	1.3E-02	2.4	11.0	6.0	79.1	80.8	4.67	0.07	
L	1150	3.38E+00	5.09E-01	2.93E-03	3.5E-14	1.0E+00	1.5E-02	2.7	15.7	7.6	75.0	88.3	4.68	0.07	
M	1300	3.95E+00	3.52E+00	6.06E-03	1.4E-14	1.4E-02	1.2E-02	7.4	4.9	3.0	61.4	91.3	4.48	0.15	
N	1650	4.90E+00	6.63E+00	9.78E-03	4.0E-14	7.7E-02	1.5E-02	39.9	18.3	8.7	51.8	100.0	4.70	0.09	
total gas age			n=14		4.7E-13	5.7E-01							4.73	0.10	
Eruption Age			n=6		steps G-L	2.7E-13	7.1E-01						57.3	4.68	0.08
OCA-071; P1:121, groundmass concentrate, 76.05mg, J=0.000476909±0.10%, D=1.00644±0.00091, NM-121, Lab#=51063-01															
A	550	7.28E+01	2.94E-01	2.37E-01	2.4E-15	1.7E+00	5.2E-02	0.3	6.6	1.7	3.7	1.7	2.34	1.01	
B	625	3.19E+01	2.59E-01	9.56E-02	2.0E-14	2.0E+00	4.1E-02	2.0	44.8	14.8	11.4	16.5	3.11	0.22	
C	675	3.02E+01	2.43E-01	8.76E-02	9.4E-16	2.1E+00	4.1E-02	0.1	2.1	0.7	14.1	17.2	3.67	0.94	
D	725	2.07E+01	7.10E-01	5.62E-02	2.1E-14	7.2E-01	2.5E-02	5.8	29.2	15.6	19.9	32.8	3.55	0.15	
E	775	1.37E+01	1.14E+00	3.14E-02	1.2E-14	4.5E-01	6.8E-03	5.4	4.6	9.1	32.7	41.9	3.85	0.16	
F	825	9.91E+00	1.26E+00	1.96E-02	1.5E-14	4.1E-01	2.1E-03	7.3	1.7	11.1	42.1	53.0			

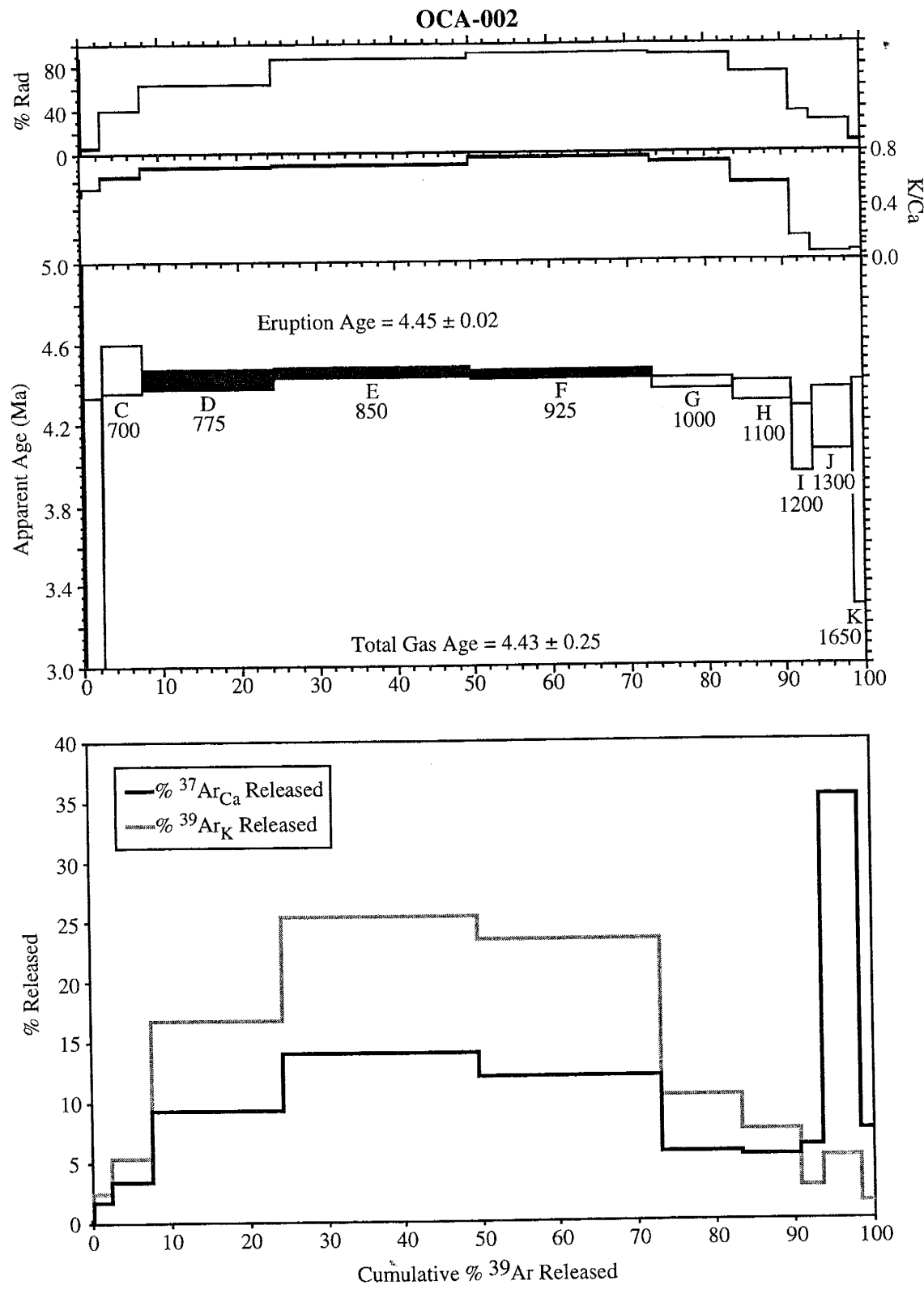
ID	Temp/P (^°C/kN)	⁴⁰ Ar/ ³⁹ Ar	³⁷ Ar/ ³⁹ Ar	³⁸ Ar/ ³⁹ Ar	³⁹ Ar _K	K/Ca (mol)	Ci/K	³⁷ Ar _{Ca}	³⁸ Ar _{Cl}	³⁹ Ar _K	⁴⁰ Ar*	³⁹ Ar	Age (Ma)	$\pm 2\sigma$ (Ma)
OCA-073-01: V1:117, groundmass concentrate, 55.79mg, J=0.001038789±0.11%, D=1.00644±0.00091, NM-117, Lab#=50879-01														
A	550	2.08E+01	3.61E-01	6.49E-02	6.3E-14	1.4E+00	3.5E-02	2.7	34.3	20.4	8.0	20.4	3.14	0.31
B	625	6.07E+00	5.69E-01	1.48E-02	5.7E-14	9.0E-01	2.9E-02	3.8	25.9	18.5	29.6	38.8	3.36	0.12
C	675	4.98E+00	1.02E+00	1.07E-02	3.6E-14	5.0E-01	2.5E-02	4.3	14.1	11.6	37.7	50.5	3.52	0.11
D	725	4.14E+00	1.76E+00	7.93E-03	3.2E-14	2.9E-01	1.8E-02	6.5	9.0	10.2	46.3	60.7	3.59	0.10
E	775	3.47E+00	2.38E+00	5.79E-03	2.4E-14	2.1E-01	1.2E-02	6.6	4.3	7.7	55.7	68.4	3.63	0.14
F	825	2.94E+00	2.74E+00	4.33E-03	2.8E-14	1.9E-01	6.7E-03	9.1	2.9	9.2	63.4	77.6	3.49	0.08
G	875	2.78E+00	3.02E+00	3.84E-03	2.1E-14	1.7E-01	4.9E-03	7.5	1.6	6.9	67.3	84.5	3.51	0.11
H	925	2.87E+00	3.26E+00	4.25E-03	1.4E-14	1.6E-01	5.4E-03	5.3	1.2	4.5	64.8	89.0	3.49	0.12
I	975	3.15E+00	3.79E+00	4.95E-03	7.3E-15	1.3E-01	8.2E-03	3.2	0.9	2.3	62.7	91.3	3.71	0.24
J	1025	3.21E+00	4.34E+00	6.05E-03	3.7E-15	1.2E-01	9.9E-03	1.9	0.6	1.2	54.7	92.5	3.30	0.39
K	1075	3.31E+00	4.71E+00	8.03E-03	3.3E-15	1.1E-01	1.1E-02	1.8	0.6	1.1	39.3	93.5	2.44	0.42
L	1150	3.79E+00	5.09E+00	4.05E-03	4.0E-15	1.0E-01	9.9E-03	2.4	0.6	1.3	43.4	94.8	3.09	0.40
M	1300	5.67E+00	2.41E+01	2.03E-02	8.6E-15	2.1E-02	1.5E-02	24.2	2.0	2.8	28.8	97.6	3.11	0.31
N	1850	8.10E+00	2.41E+01	2.55E-02	7.4E-15	2.1E-02	1.8E-02	20.8	2.0	2.4	31.5	100.0	4.86	0.31
total gas age		n=14			3.1E-13	6.0E-01							3.43	0.18
Eruption Age		n=3	steps F-H	6.4E-14	1.7E-01								20.5	3.50
														0.06
OCA-073-02: V3:117, groundmass concentrate, 55.73mg, J=0.001031232±0.11%, D=1.00644±0.00091, NM-117, Lab#=50881-01														
A	550	1.92E+01	3.86E-01	5.96E-02	4.3E-14	1.3E+00	3.1E-02	2.6	28.8	18.2	8.3	18.2	2.96	0.38
B	625	6.19E+00	6.01E-01	1.48E-02	4.4E-14	8.5E-01	2.9E-02	4.0	26.9	18.3	29.7	36.5	3.42	0.13
C	675	5.18E+00	1.05E+00	1.16E-02	2.7E-14	4.9E-01	2.5E-02	4.3	14.0	11.3	34.8	47.8	3.35	0.14
D	725	4.34E+00	1.75E+00	8.90E-03	2.5E-14	2.9E-01	1.8E-02	6.7	9.5	10.5	42.2	58.3	3.40	0.13
E	775	3.68E+00	2.34E+00	6.19E-03	1.9E-14	2.2E-01	1.2E-02	6.7	4.5	7.8	54.6	66.1	3.72	0.14
F	825	3.16E+00	2.75E+00	4.93E-03	2.2E-14	1.9E-01	7.2E-03	9.4	3.4	9.4	60.3	75.5	3.54	0.10
G	875	3.01E+00	2.90E+00	4.50E-03	1.8E-14	1.8E-01	5.7E-03	7.9	2.1	7.4	63.1	82.9	3.54	0.10
H	925	3.25E+00	3.08E+00	5.41E-03	1.2E-14	1.7E-01	6.6E-03	5.6	1.7	5.0	57.9	87.9	3.50	0.14
I	975	3.84E+00	3.59E+00	7.67E-03	6.5E-15	1.4E-01	9.9E-03	3.6	1.4	2.7	48.1	90.7	3.44	0.23
J	1025	3.87E+00	3.61E+00	7.83E-03	3.5E-15	1.4E-01	1.4E-02	1.9	1.0	1.5	47.4	92.1	3.42	0.40
K	1075	3.65E+00	3.71E+00	6.54E-03	3.4E-15	1.4E-01	1.3E-02	1.9	1.0	1.4	54.9	93.5	3.74	0.43
L	1150	3.75E+00	4.73E+00	8.33E-03	3.5E-15	1.1E-01	1.6E-02	2.5	1.2	1.4	44.2	95.0	3.10	0.42
M	1300	5.27E+00	2.50E+01	1.90E-02	5.2E-15	2.0E-02	1.8E-02	19.8	2.0	2.2	32.1	97.2	3.21	0.47
N	1650	7.43E+00	2.21E+01	2.22E-02	6.8E-15	2.3E-02	1.7E-02	23.1	2.5	2.8	35.9	100.0	5.04	0.33
total gas age		n=14			2.4E-13	5.5E-01							3.42	0.21
Eruption Age		n=5	steps F-J	6.2E-14	1.7E-01								26.0	3.52
														0.07
OCA-073L: V5; 117, groundmass concentrate, 20.4mg, J=0.0010801±0.10%, D=1.0052±0.00121, NM-117, Lab#=50883-03														
A	2	2.87E+01	6.51E-01	9.77E-02	7.4E-16	6.0E-01	3.6E-02	0.4	1.5	0.8	-0.5	0.8	-0.26	2.05
B	4	1.40E+01	4.53E-01	4.18E-02	3.7E-15	1.1E+00	3.1E-02	1.2	6.2	4.1	11.7	5.0	3.18	0.54
C	7	7.19E+00	4.63E-01	1.88E-02	1.5E-14	1.1E+00	3.0E-02	5.0	25.0	17.2	22.9	22.2	3.20	0.21
D	10	4.91E+00	1.05E-00	1.09E-02	2.9E-14	4.8E-01	2.4E-02	21.5	38.7	32.9	35.6	55.1	3.41	0.11
E	12	3.73E+00	1.96E+00	6.76E-03	1.7E-14	2.6E-01	1.6E-02	23.1	15.1	19.0	50.1	74.1	3.64	0.10
F	15	3.18E+00	2.39E+00	5.08E-03	9.2E-15	2.1E-01	1.1E-02	15.5	5.4	10.5	58.3	84.6	3.62	0.13
G	20	2.97E+00	2.65E+00	4.57E-03	6.7E-15	1.9E-01	9.2E-03	12.5	3.4	7.6	61.2	92.2	3.55	0.12
H	25	3.17E+00	3.54E+00	6.01E-03	3.2E-15	1.4E-01	1.1E-02	8.0	2.0	3.7	52.5	95.8	3.25	0.27
I	30	3.65E+00	4.06E+00	8.37E-03	1.8E-15	1.3E-01	1.2E-02	5.2	1.2	2.1	40.8	97.9	2.92	0.34
J	40	3.73E+00	5.78E+00	9.62E-03	1.9E-15	8.8E-02	1.5E-02	7.6	1.5	2.1	36.0	100.0	2.63	0.39
total gas age		n=10			8.8E-14	5.0E-01							3.38	0.18
Eruption Age		n=5	steps D-H	6.5E-14	3.4E-01								73.6	3.54
														0.12
OCA-075: D6:117, groundmass concentrate, 62.42mg, J=0.001064741±0.10%, D=1.00644±0.00091, NM-117, Lab#=50848-01														
A	550	1.98E+02	2.74E+00	6.51E-01	3.1E-15	1.9E-01	4.8E-02	0.9	7.2	0.9	3.0	0.9	11.36	4.77
B	625	1.38E+01	2.16E+00	3.41E-02	9.7E-15	2.4E-01	2.7E-02	3.2	1.3	2.9	28.2	3.8	7.47	0.47
C	700	5.67E+00	1.69E+00	8.00E-03	2.5E-14	3.0E-01	1.2E-03	4.4	1.4	7.4	60.4	11.2	6.57	0.15
D	775	4.18E+00	1.38E+00	3.05E-03	5.4E-14	3.7E-01	4.9E-04	7.7	1.3	15.7	80.6	26.9	6.47	0.06
E	850	3.80E+00	1.19E+00	1.81E-03	7.3E-14	4.3E-01	4.4E-04	9.1	1.6	21.5	87.9	48.4	6.40	0.04
F	925	3.75E+00	1.08E+00	1.57E-03	5.3E-14	4.3E-01	8.5E-04	6.6	2.2	15.7	89.6	64.1	6.44	0.05
G	1000	3.70E+00	1.50E+00	1.74E-03	4.2E-14	3.4E-01	2.0E-03	6.5	4.1	12.3	88.8	76.4	6.30	0.05
H	1075	3.90E+00	1.72E+00	2.49E-03	2.2E-14	3.0E-01	6.4E-03	4.0	6.8	6.5	84.3	82.9	6.31	0.08
I	1150	4.03E+00	1.70E+00	2.90E-03	1.6E-14	3.0E-01	1.3E-02	2.8	9.9	4.7	81.6	87.6	6.32	0.11
J	1300	7.30E+00	7.83E+00	1.60E-02	1.1E-14	6.5E-02	2.2E-02	8.7	11.2	3.1	43.7	90.7	6.15	0.26
K	1650	9.19E+00	1.44E+01	2.45E-02	3.1E-14	3.5E-02	3.5E-02	47.2	53.1	9.3	33.9	100.0	6.05	0.17
total gas age		n=11			3.4E-13	3.3E-01							6.44	0.14
Eruption Age		n=6	steps D-I	2.6E-13	3.8E-01								76.4	6.39
														0.06
OCA-077: I4:118, groundmass concentrate, 122.10mg, J=0.000156553±0.11%, D=1.00644±0.00091, NM-118, Lab#=50910-01														
A	550	2.29E+02	9.36E-01	7.45E-01	2.9E-15	5.5E-01	6.1E-02	1.9	27.3	3.3	3.7	3.3	2.40	0.71
B	625	1.48E+01	1.82E+00	2.61E-02	4.7E-15	2.9E-01	2.5E-02	6.1	17.8	5.4	48.6	8.7	2.03	0.07
C	675	1.09E+01	1.97E+00	1.18E-02	4.7E-15	2.6E-01	8.9E-03	6.6	6.4	5.4	69.0	14.1	2.12	0.07
D	725	9.59E+00	1.83E+00	8.55E-03	7.5E-15	2.8E-01	4.5E-03	9.7	5.1	8.6	74.9	22.7	2.03	0.04
E	775	9.04E+00	1.54E+00	6.75E-03	7.4E-15	3.3E-01	2.2E-03	8.2	2.5	8.5	79.0	31.2	2.02	0.03
F	825	8.47E+00	1.19E+00	5.18E-03	1.5E-14	4.3E-01	1.3E-03	12.6						

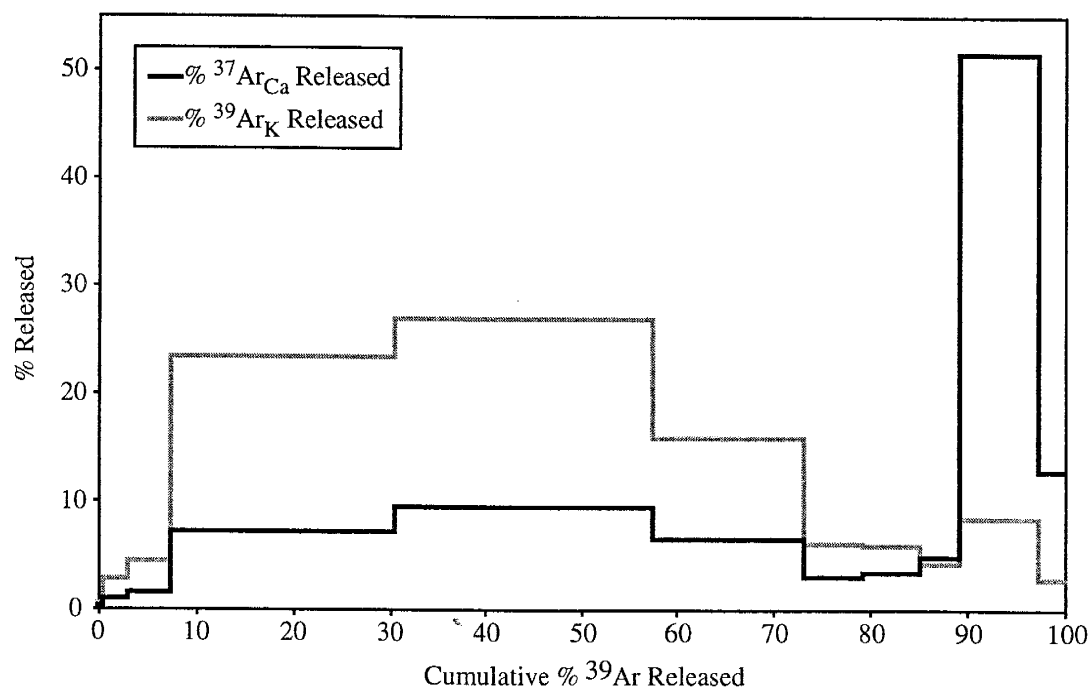
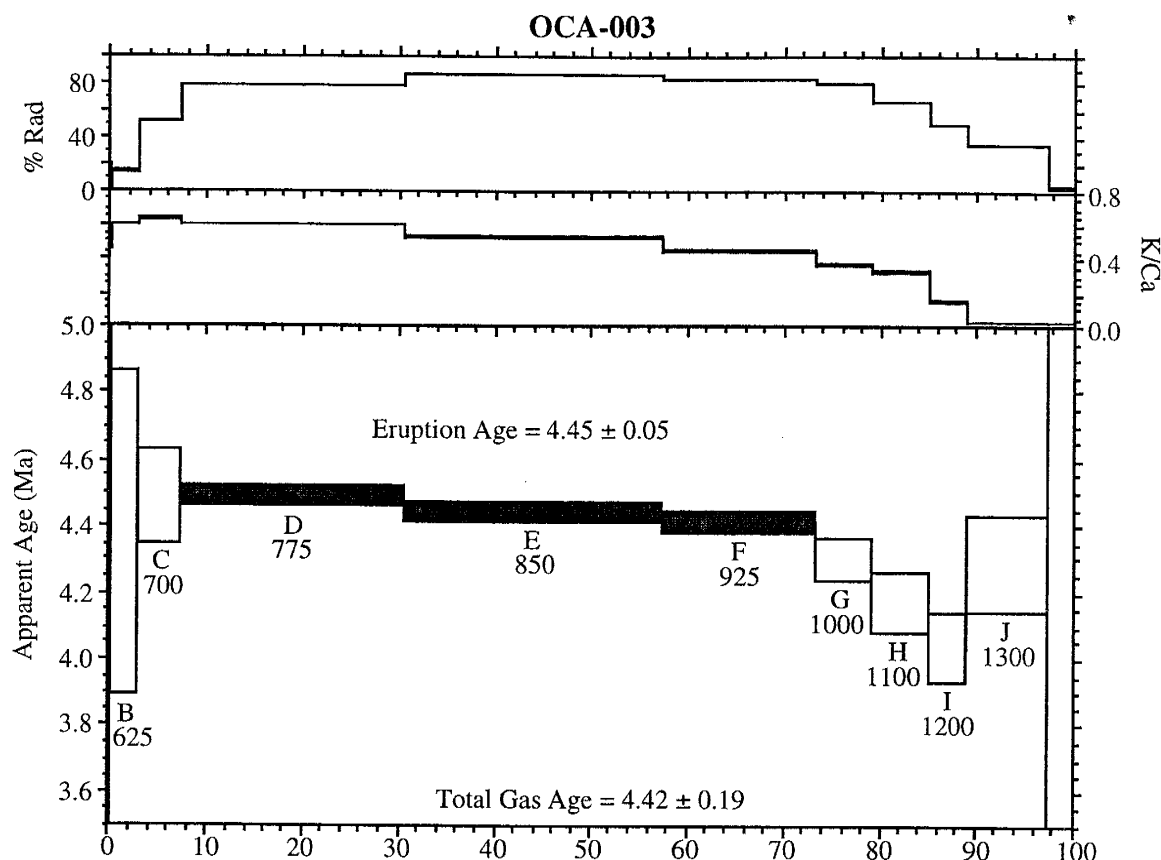
ID	Temp/P (°C/W)	$^{40}\text{Ar}/^{39}\text{Ar}$	$^{37}\text{Ar}/^{39}\text{Ar}$	$^{38}\text{Ar}/^{39}\text{Ar}$	$^{39}\text{Ar}_\text{K}$ (mol)	K/Ca	Ci/K	$^{37}\text{Ar}_{\text{ca}}$ (%)	$^{39}\text{Ar}_{\text{ci}}$ (%)	$^{39}\text{Ar}_\text{K}$ (%)	$^{40}\text{Ar}^*$ (%)	^{39}Ar (%)	Age (Ma)	$\pm 2\sigma$
OCA-077L; IS; 118, groundmass concentrate, 34.53mg, J=0.000156553±0.11%, D=1.00644±0.00091, NM-118, Lab#=50910-02														
A	2	4.48E+02	1.33E+00	1.50E+00	1.4E-16	3.8E-01	3.8E-07	0.4	2.9	0.5	1.1	0.5	1.35	6.51
B	4	3.56E+01	2.23E+00	9.85E-02	1.2E-15	2.3E-01	2.3E-07	6.0	5.5	4.2	18.6	4.7	1.88	0.23
C	7	9.79E+00	1.69E+00	9.54E-03	8.3E-15	3.0E-01	3.0E-07	31.7	20.0	29.2	72.3	33.9	2.00	0.03
D	10	8.75E+00	1.11E+00	6.26E-03	1.0E-14	4.6E-01	4.6E-07	25.2	12.5	35.3	79.5	69.2	1.97	0.03
E	12	9.92E+00	1.09E+00	1.09E-02	4.4E-15	4.7E-01	4.7E-07	10.9	9.3	15.5	68.2	84.7	1.91	0.04
F	15	1.48E+01	1.30E+00	2.63E-02	2.1E-15	3.9E-01	3.9E-07	6.3	8.6	7.5	47.9	92.2	2.00	0.10
G	20	2.45E+01	1.57E+00	6.02E-02	1.2E-15	3.2E-01	3.2E-07	4.4	13.2	4.4	27.8	96.6	1.92	0.20
H	25	3.42E+01	4.20E+00	9.90E-02	5.3E-16	1.2E-01	1.2E-07	5.1	9.9	1.9	15.4	98.5	1.49	0.38
I	30	4.58E+01	9.12E+00	1.40E-01	2.5E-16	5.6E-02	5.6E-08	5.2	9.3	0.9	11.1	99.3	1.45	0.61
J	40	5.05E+01	1.16E+01	1.41E-01	1.9E-16	4.4E-02	4.4E-08	4.8	8.9	0.7	19.1	100.0	2.74	0.95
total gas age		n=10			2.8E-14	3.8E-01							1.95	0.10
Eruption Age		n=5			steps C-G	2.6E-14	4.0E-01						91.9	1.97
														0.04
OCA-078; G3:117, groundmass concentrate, 59.74mg, J=0.00104927±0.10%, D=1.00644±0.00091, NM-117, Lab#=50869-01														
A	550	8.13E+01	5.20E+00	3.45E-15	3.4E-15	8.6E-03	0.7	1.2	1.3	6.6	1.3	10.13	1.77	
B	625	7.46E+00	1.65E+00	1.52E-02	1.3E-14	3.1E-01	1.4E-03	2.0	0.5	3.2	41.2	4.6	5.82	0.26
C	700	3.89E+00	1.57E+00	3.11E-03	3.1E-14	3.3E-01	8.2E-04	4.7	0.7	8.0	79.1	12.6	5.82	0.08
D	775	3.54E+00	1.14E+00	1.49E-03	6.4E-14	4.5E-01	5.4E-04	7.0	0.9	16.6	89.6	29.2	6.00	
E	850	3.49E+00	8.84E-01	1.26E-03	8.1E-14	5.8E-01	8.2E-04	6.9	1.7	20.9	90.8	50.1	5.99	0.03
F	925	3.49E+00	8.68E-01	1.15E-03	7.9E-14	5.9E-01	1.5E-03	6.0	2.9	18.8	91.6	68.8	6.04	
G	1000	3.69E+00	1.07E+00	1.89E-03	5.1E-14	4.8E-01	4.8E-03	5.3	6.5	13.3	86.9	82.1	6.06	0.05
H	1075	4.49E+00	1.65E+00	5.36E-03	2.0E-14	3.1E-01	1.8E-02	3.1	9.5	5.1	67.2	87.2	5.71	0.11
I	1150	5.65E+00	2.56E+00	9.08E-03	1.1E-14	2.0E-01	3.5E-02	2.6	9.9	2.8	55.8	90.0	5.98	0.23
J	1300	1.54E+01	1.32E+01	4.66E-02	8.2E-15	3.9E-02	5.0E-02	10.4	10.9	2.1	17.4	92.1	5.13	0.43
K	1650	1.75E+01	1.74E+01	5.48E-02	3.1E-14	2.9E-02	6.9E-02	51.2	55.4	7.9	15.4	100.0	5.17	0.29
total gas age		n=11			3.9E-13	4.3E-01							5.95	0.12
Eruption Age		n=4			steps D-G	2.7E-13	5.3E-01						69.5	6.02
														0.04
OCA-079; K2:118, groundmass concentrate, 97.00mg, J=0.000154005±0.12%, D=1.00644±0.00091, NM-118, Lab#=50920-01														
A	550	3.70E+01	5.58E-01	9.78E-02	1.8E-14	9.1E-01	9.9E-02	4.2	44.8	23.8	22.0	23.8	2.26	0.09
B	625	1.51E+01	7.13E-01	2.47E-02	1.9E-14	7.2E-01	7.0E-02	5.8	33.8	25.7	51.9	49.4	2.18	0.03
C	675	1.92E+00	1.17E+00	1.86E-02	1.1E-14	4.4E-01	3.8E-02	5.3	10.2	14.1	58.6	63.6	2.14	0.04
D	725	1.33E+01	1.75E+00	1.85E-02	6.1E-15	2.9E-01	1.9E-02	4.5	2.9	8.2	59.8	71.8	2.22	0.05
E	775	1.52E+01	2.28E+00	2.26E-02	2.8E-15	2.2E-01	9.8E-03	2.7	0.7	3.7	57.3	75.5	2.43	0.09
F	825	1.58E+01	2.15E+00	2.22E-02	3.4E-15	2.4E-01	6.3E-03	3.1	0.5	4.5	59.2	79.9	2.59	
G	875	1.59E+01	2.17E+00	2.20E-02	3.0E-15	2.4E-01	4.9E-03	2.7	0.4	3.9	59.9	83.9	2.64	0.09
H	925	1.70E+01	2.46E+00	2.72E-02	2.3E-15	2.1E-01	7.5E-03	2.4	0.4	3.1	53.7	87.0	2.54	0.12
I	975	1.90E+01	2.88E+00	3.35E-02	1.5E-15	1.8E-01	1.1E-02	1.8	0.4	1.9	48.9	89.0	2.58	0.19
J	1025	1.97E+01	3.47E+00	4.01E-02	8.6E-16	1.5E-01	1.7E-02	1.3	0.4	1.1	40.9	90.1	2.24	0.28
K	1075	2.42E+01	4.07E+00	6.51E-02	8.7E-16	1.3E-01	2.5E-02	1.5	0.6	1.2	21.8	91.3	1.47	0.30
L	1150	3.31E+01	5.68E+00	9.58E-02	9.5E-16	9.0E-02	1.9E-02	2.3	0.5	1.3	15.6	92.5	1.44	0.31
M	1300	5.14E+01	3.01E+01	1.62E-01	1.1E-15	1.7E-02	2.5E-02	13.5	0.7	1.4	11.2	93.9	1.63	0.38
N	1650	5.66E+01	2.54E+01	1.76E-01	4.6E-15	2.0E-02	3.3E-02	49.0	3.8	6.1	11.6	100.0	1.86	
total gas age		n=14			7.5E-14	5.3E-01							2.22	0.09
Eruption Age		n=3			steps B-D	3.6E-14	5.6E-01						48.0	2.18
														0.04
OCA-079L1; K3; 118, groundmass concentrate, 25.32mg, J=0.000155028±0.12%, D=1.00644±0.00091, NM-118, Lab#=50921-01														
A	2	4.64E+01	8.68E-01	1.22E-01	2.3E-16	5.9E-01	5.9E-07	0.6	2.1	1.1	22.2	1.1	2.88	0.74
B	4	1.95E+01	5.97E-01	3.70E-02	1.3E-15	8.5E-01	8.5E-07	2.2	10.7	6.3	43.9	7.4	2.39	0.15
C	7	1.27E+01	7.54E-01	1.68E-02	9.0E-15	6.8E-01	6.8E-07	20.2	57.6	44.9	61.1	52.3	2.17	0.04
D	10	1.07E+01	1.54E+00	1.11E-02	8.4E-15	3.3E-01	3.3E-07	38.4	27.6	42.0	70.2	94.3	2.10	0.03
E	12	1.20E+01	4.26E+00	1.55E-02	6.3E-16	1.2E-01	1.2E-07	8.0	1.0	3.1	64.3	97.4	2.16	0.21
F	15	1.16E+01	6.17E+00	2.14E-02	2.8E-16	8.3E-02	8.3E-08	5.2	0.5	1.4	49.3	98.8	1.60	
G	20	1.48E+01	1.44E+01	2.77E-02	1.4E-16	3.6E-02	3.6E-08	5.9	0.2	0.7	51.8	99.5	2.16	0.78
H	25	2.86E+01	4.93E+01	8.47E-02	9.3E-17	1.0E-02	1.0E-08	4.8	0.0	0.2	25.6	99.7	2.12	3.13
I	30	3.00E+01	5.03E+01	6.79E-02	1.4E-17	1.0E-02	1.0E-08	2.1	0.0	0.1	45.9	99.7	3.98	7.50
J	40	3.13E+01	8.38E+01	8.23E-02	5.1E-17	6.1E-03	6.1E-09	12.7	0.3	0.3	42.8	100.0	3.97	2.39
total gas age		n=10			2.0E-14	5.1E-01							2.16	0.08
Eruption Age		n=3			steps C-E	1.8E-14	5.0E-01						90.0	2.13
														0.05
OCA-079L2; K3; 118, groundmass concentrate, 36.42mg, J=0.000155028±0.12%, D=1.00644±0.00091, NM-118, Lab#=50921-03														
A	2	5.38E+01	7.94E-01	1.47E-01	9.7E-16	6.4E-01	6.4E-07	0.6	2.2	1.2	19.2	1.2	2.89	0.51
B	4	1.90E+01	5.60E+00	3.61E-02	2.8E-15	9.1E-01	9.1E-07	3.4	16.1	9.5	44.0	10.7	2.34	0.11
C	7	1.21E+01	8.42E-01	1.55E-02	1.7E-14	6.1E-01	6.1E-07	30.0	63.2	55.6	62.5	66.4	2.12	0.02
D	10	1.08E+01	1.69E+00	1.15E-02	8.4E-15	3.0E-01	3.0E-07	30.3	16.2	28.1	69.6	94.5	2.10	0.03
E	12	1.22E+01	4.05E+00	1.62E-02	7.7E-16	1.3E-01	1.3E-07	6.7	1.0	2.6	63.1	97.1	2.17	0.16
F	15	1.21E+01	5.58E+00	1.78E-02	4.2E-16	9.1E-02	9.1E-08	5.0	0.6	1.4	60.0	98.5	2.04	0.31
G	20	1.34E+01	9.06E+00	2.29E-02	2.8E-16	5.6E-02	5.6E-08	5.4	0.3	0.9	54.7	99.4	2.07	0.40
H	25	1.90E+01	2.49E+01	4.71E-02	8.5E-17	2.1E-02	2.1E-08	4.6	0.1	0.3	36.7	99.7	1.99	1.24
I	30	2.82E+01	3.01E+01	7.28E-02	3.3E-17	1.7E-02	1.7E-08	2.1	0.1	0.1	31.8	99.8	2.56	3.29
J	40	3.55E+01	9.19E+01	1.31E-01	6.0E-17	5.6E-03	5.6E-09	11.9	0.1	0.2	10.5	100.0	1.11	1.93
total gas age		n=10			3.0E-14	5.2E-01	</							

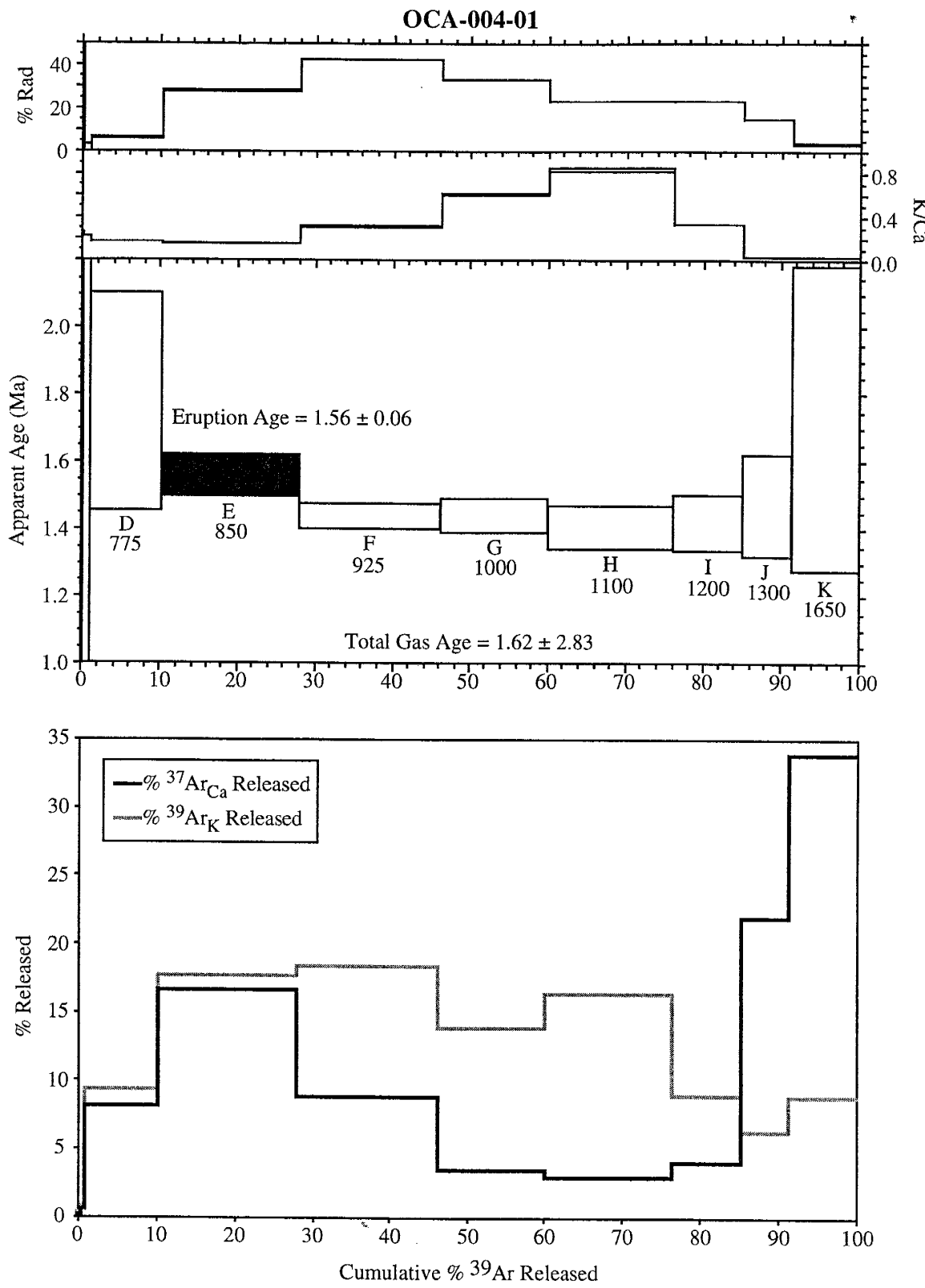
Appendix B: $^{40}\text{Ar}/^{39}\text{Ar}$ Age Spectra

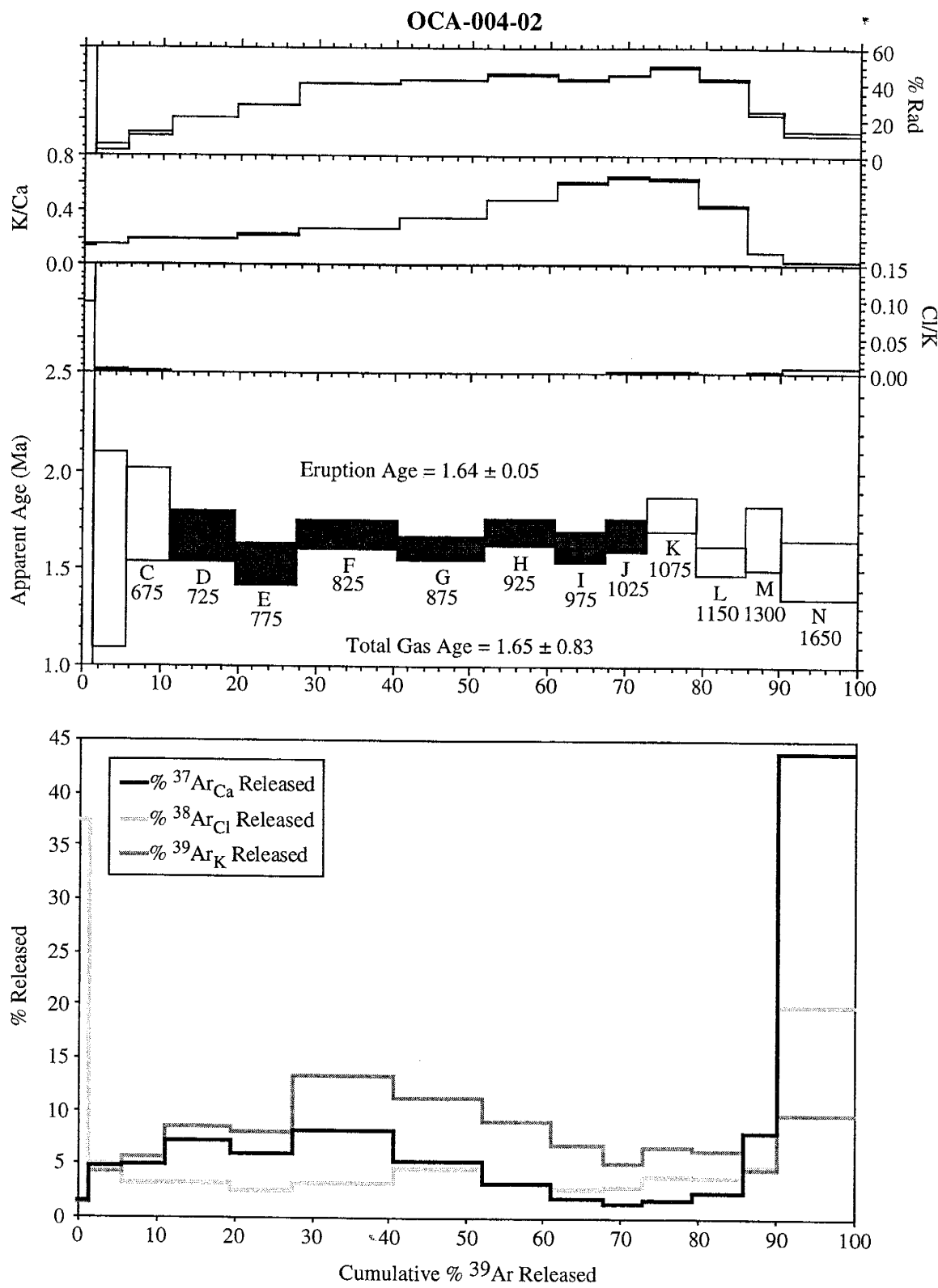
Appendix B contains the radiogenic percent, K/Ca, Cl/K, apparent age and $^{37}\text{Ar}_{\text{Ca}}$, $^{38}\text{Ar}_{\text{Cl}}$ and $^{39}\text{Ar}_{\text{K}}$ release spectra for all samples documented in this study. Two sigma errors are plotted and solid apparent age boxes reflect the steps used in the eruption age calculations. Eruption ages are weighted by the inverse of the variance and uncertainties are calculated using the Samson and Alexander method (Samson and Alexander, 1987). Refer to appendix A for additional analytical values.

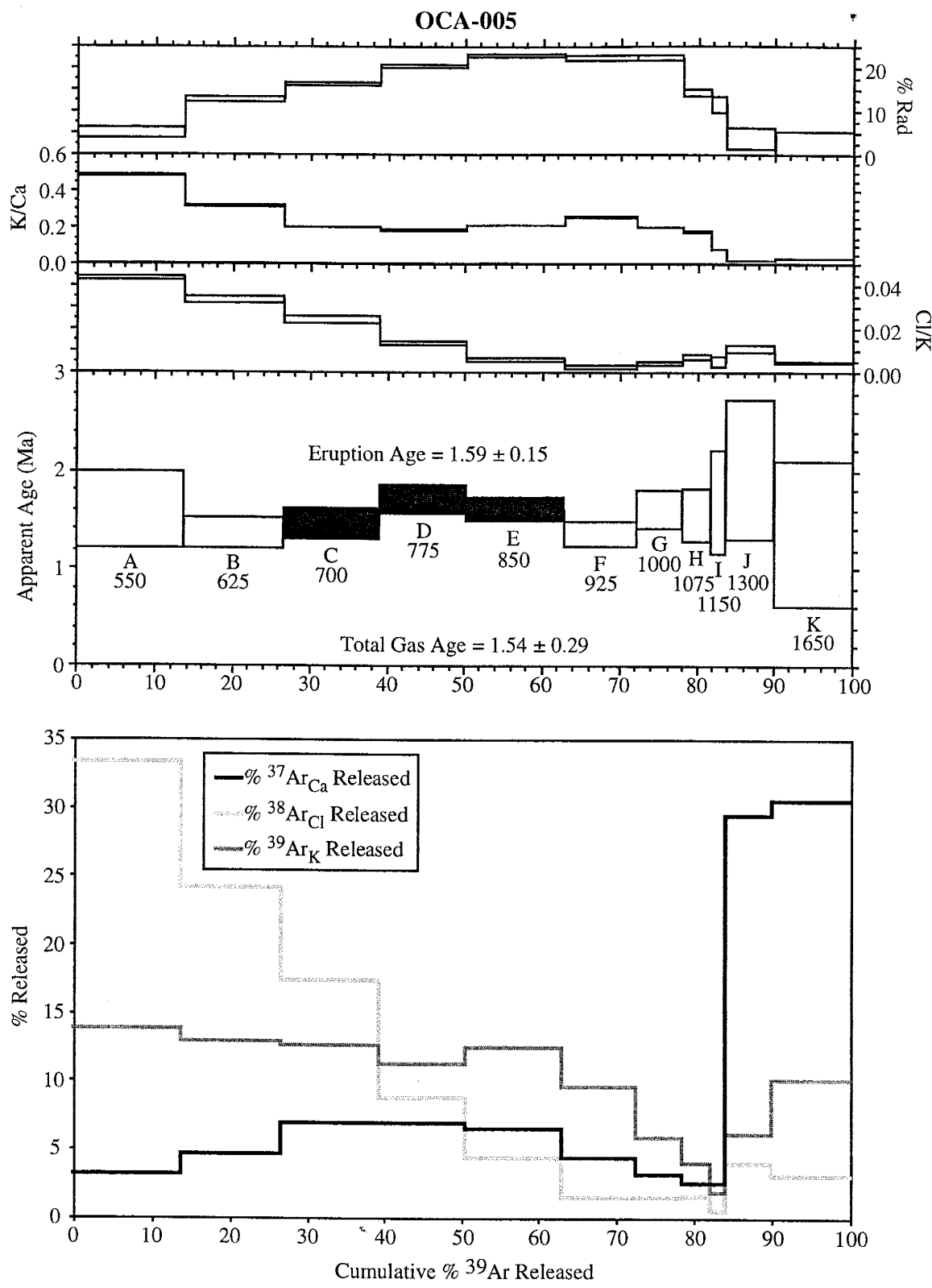


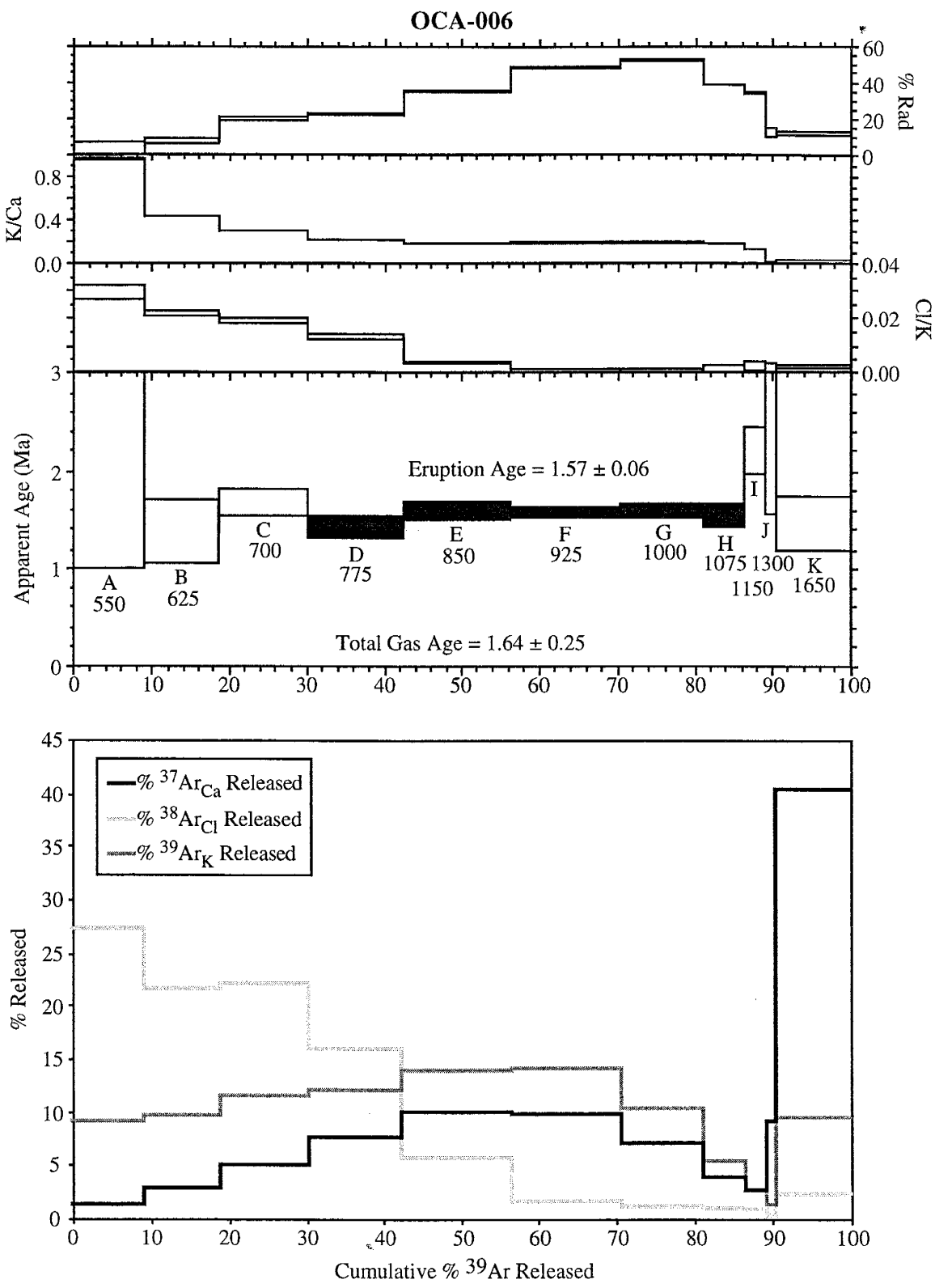




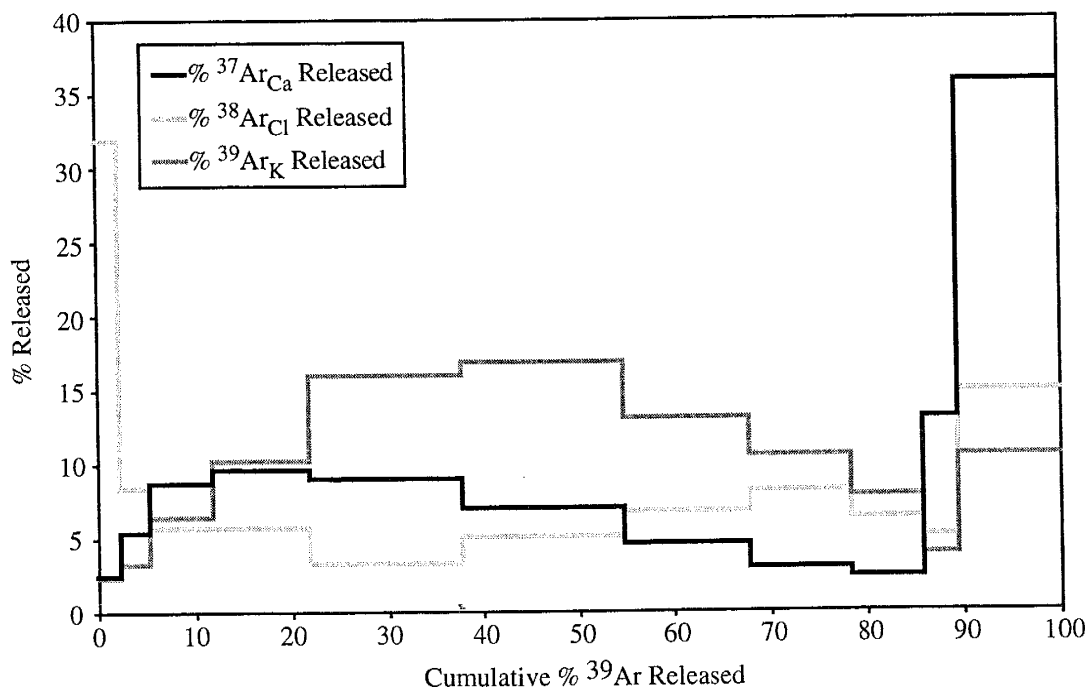
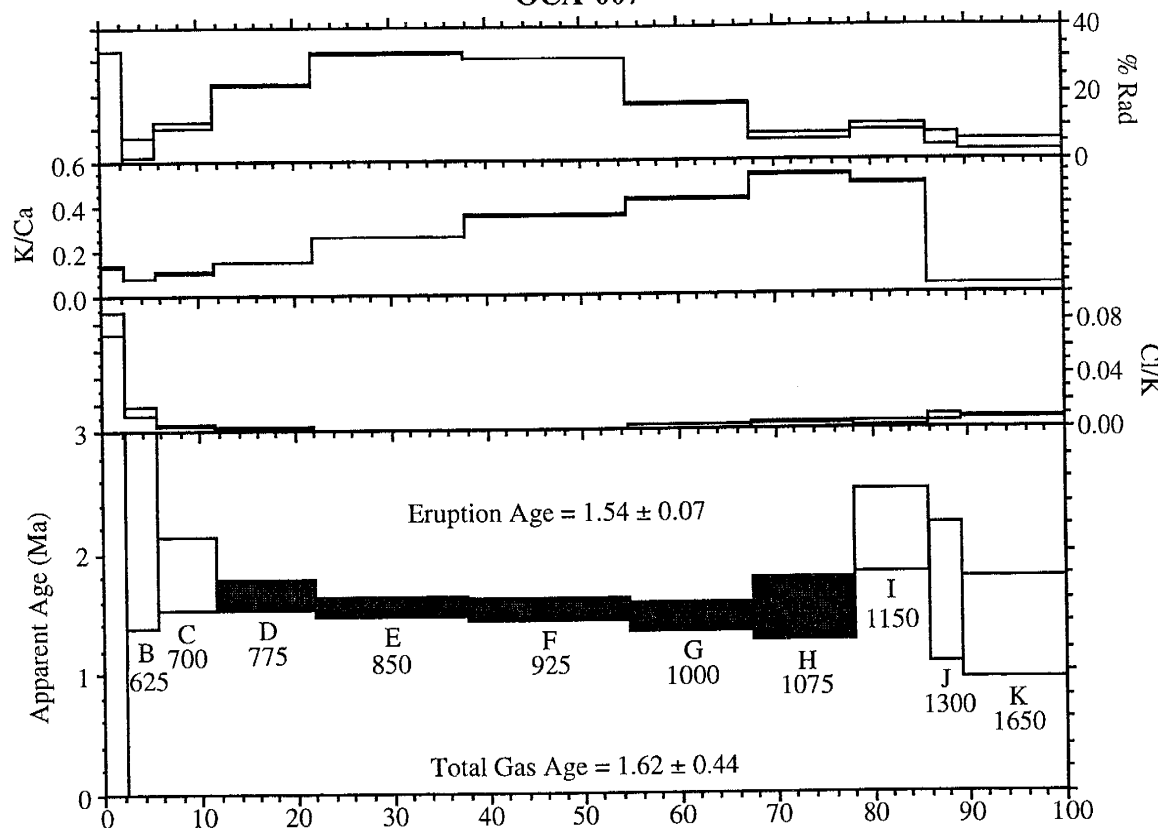


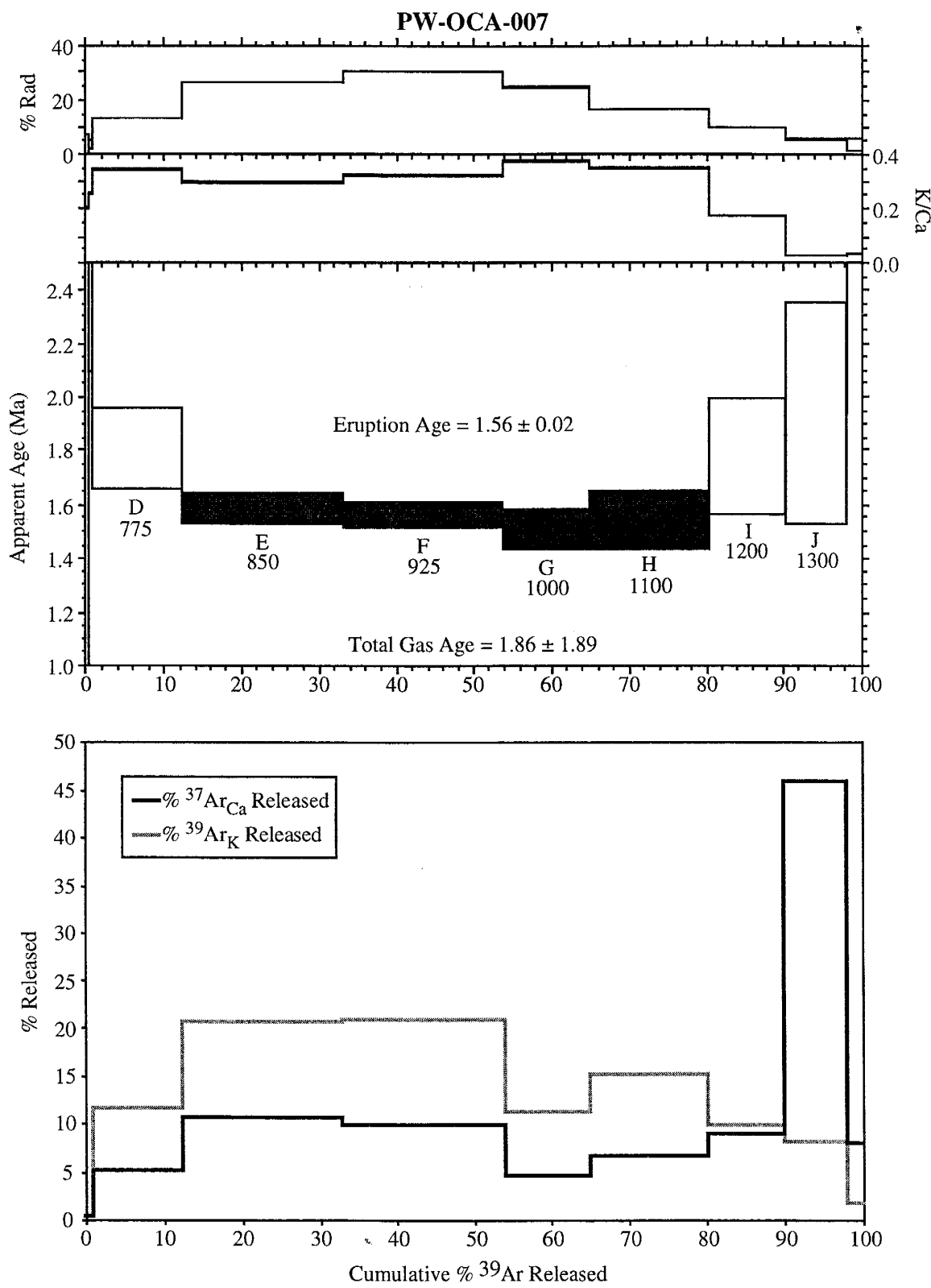


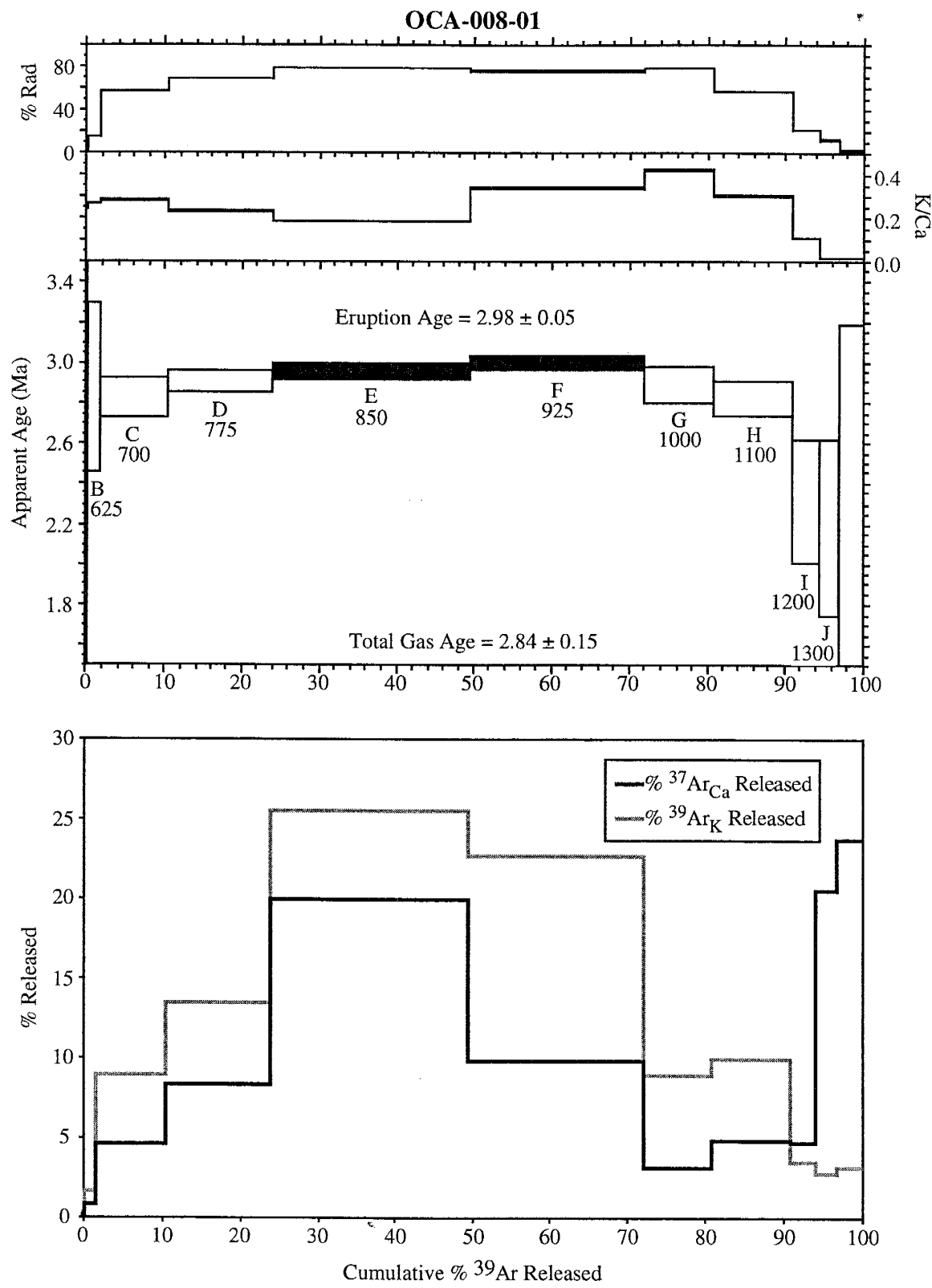


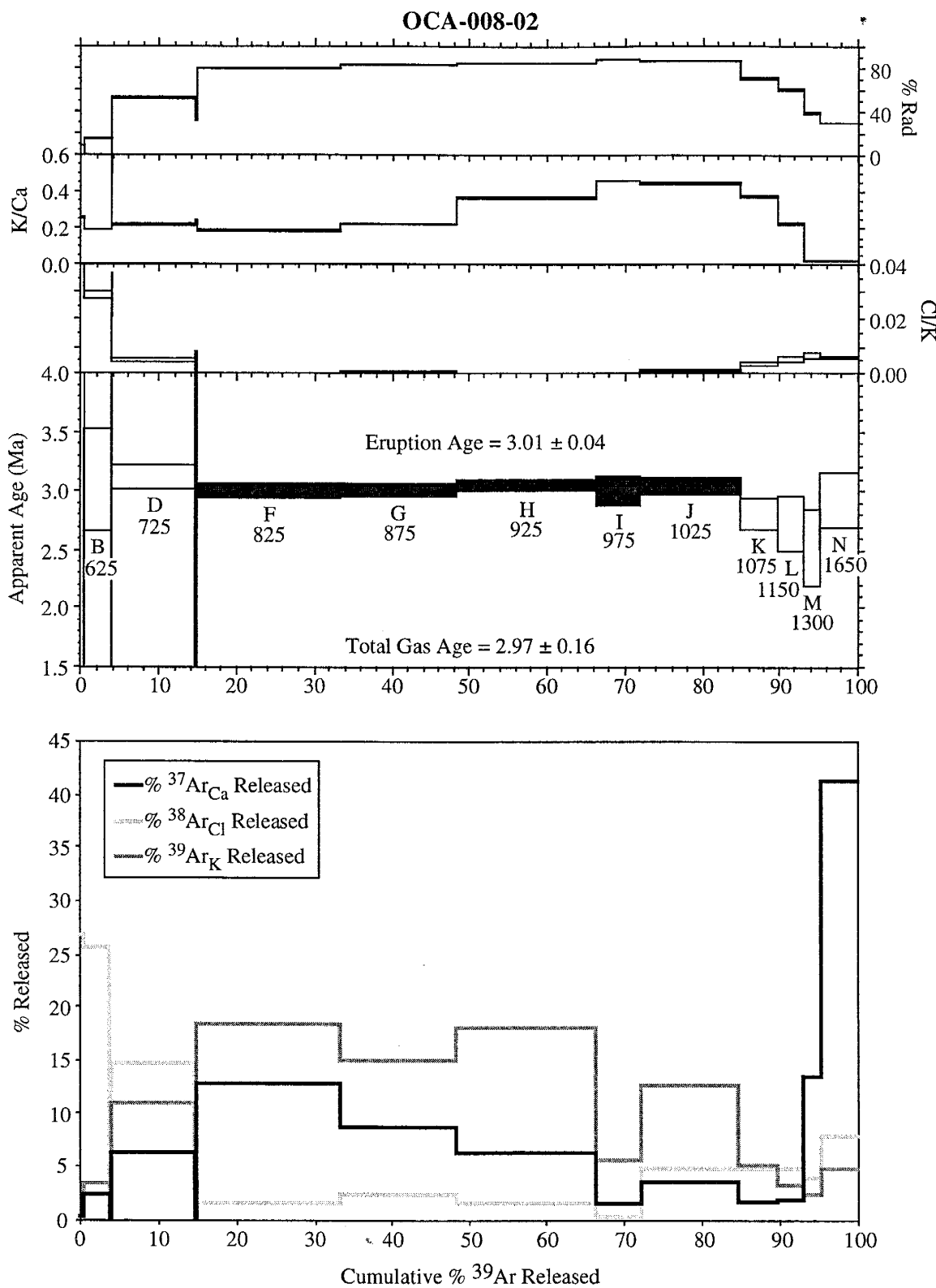


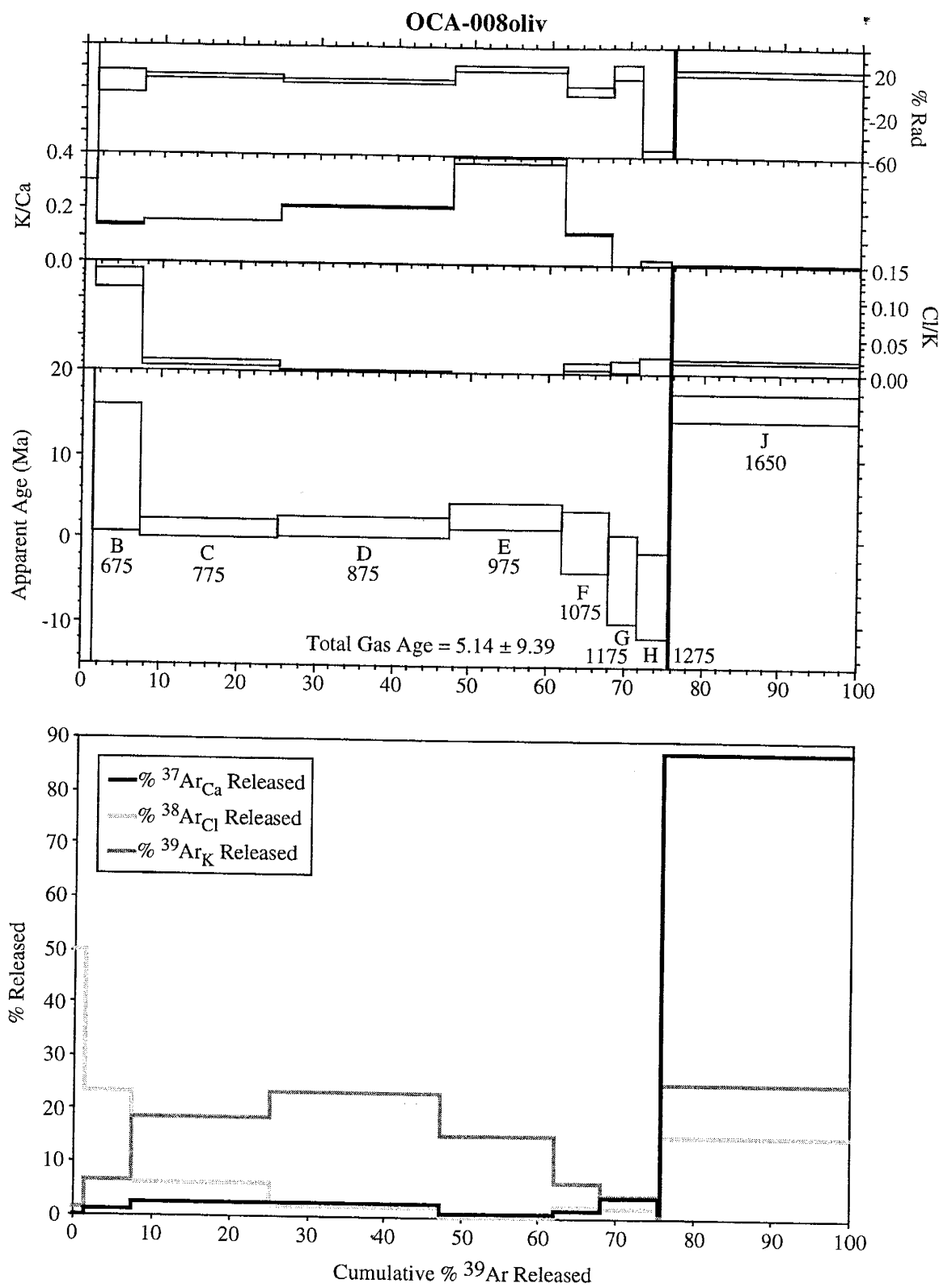
OCA-007

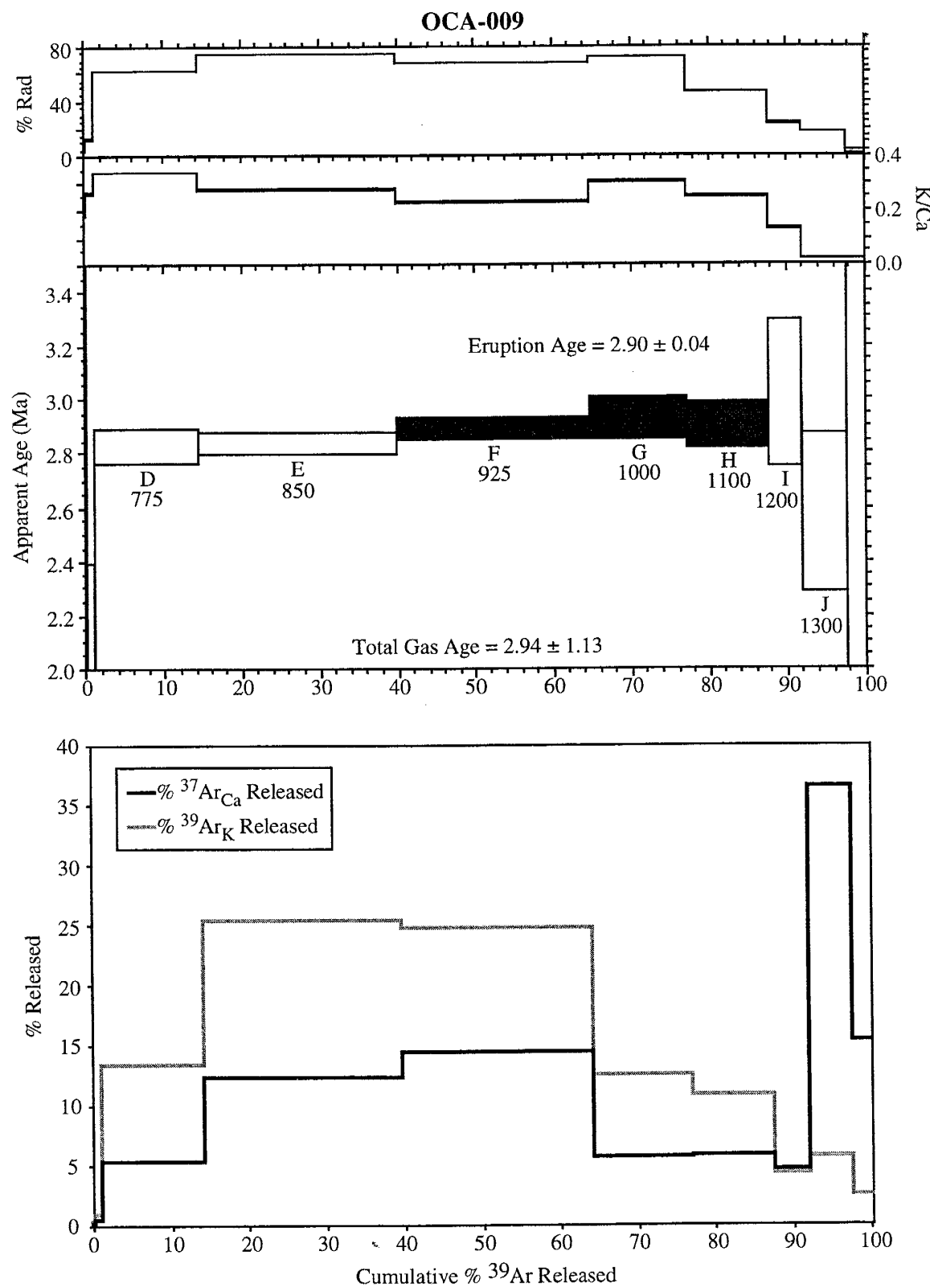


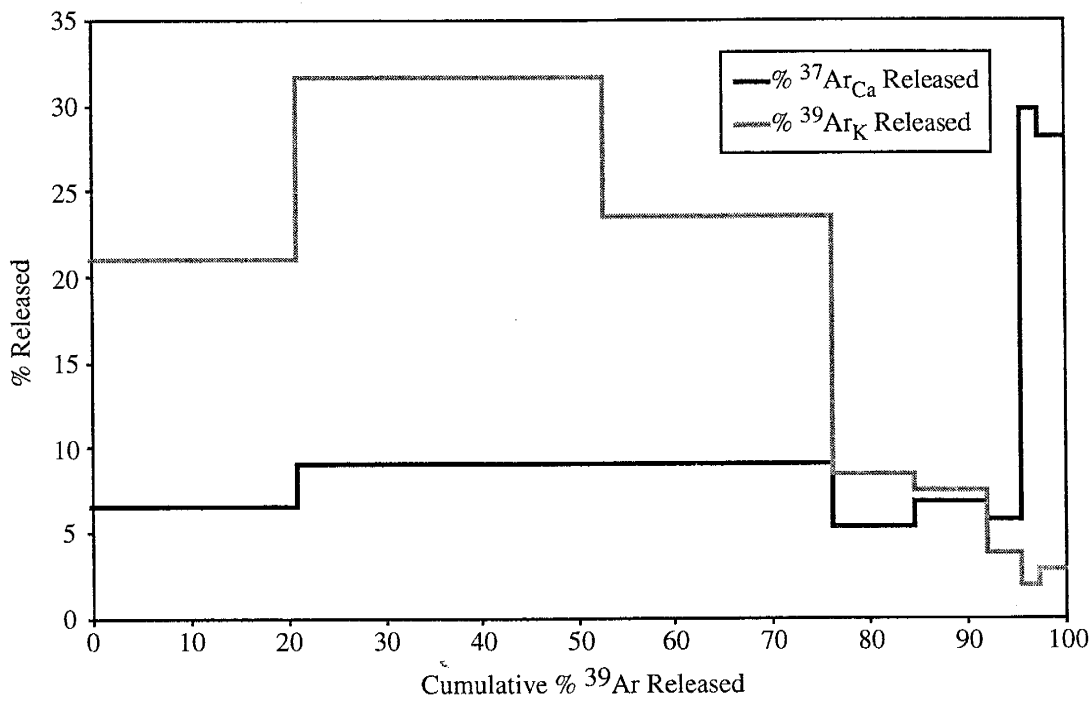
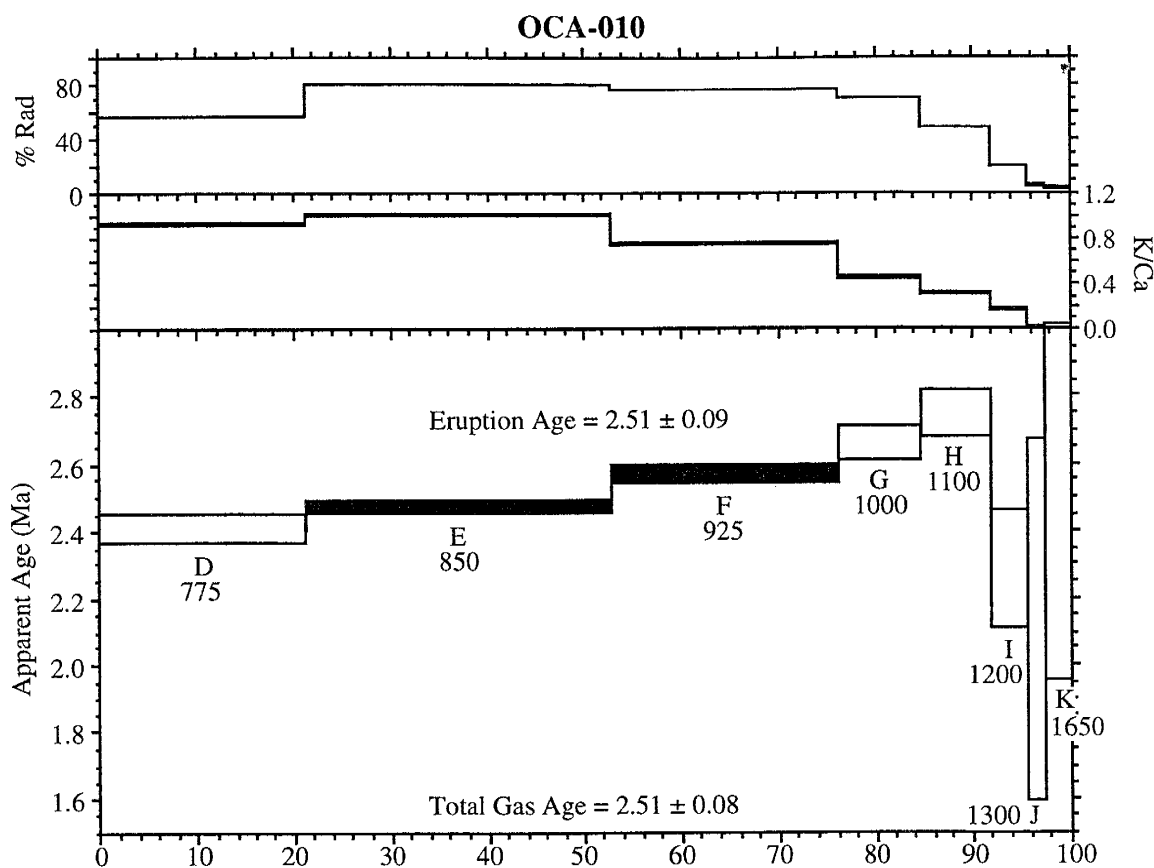


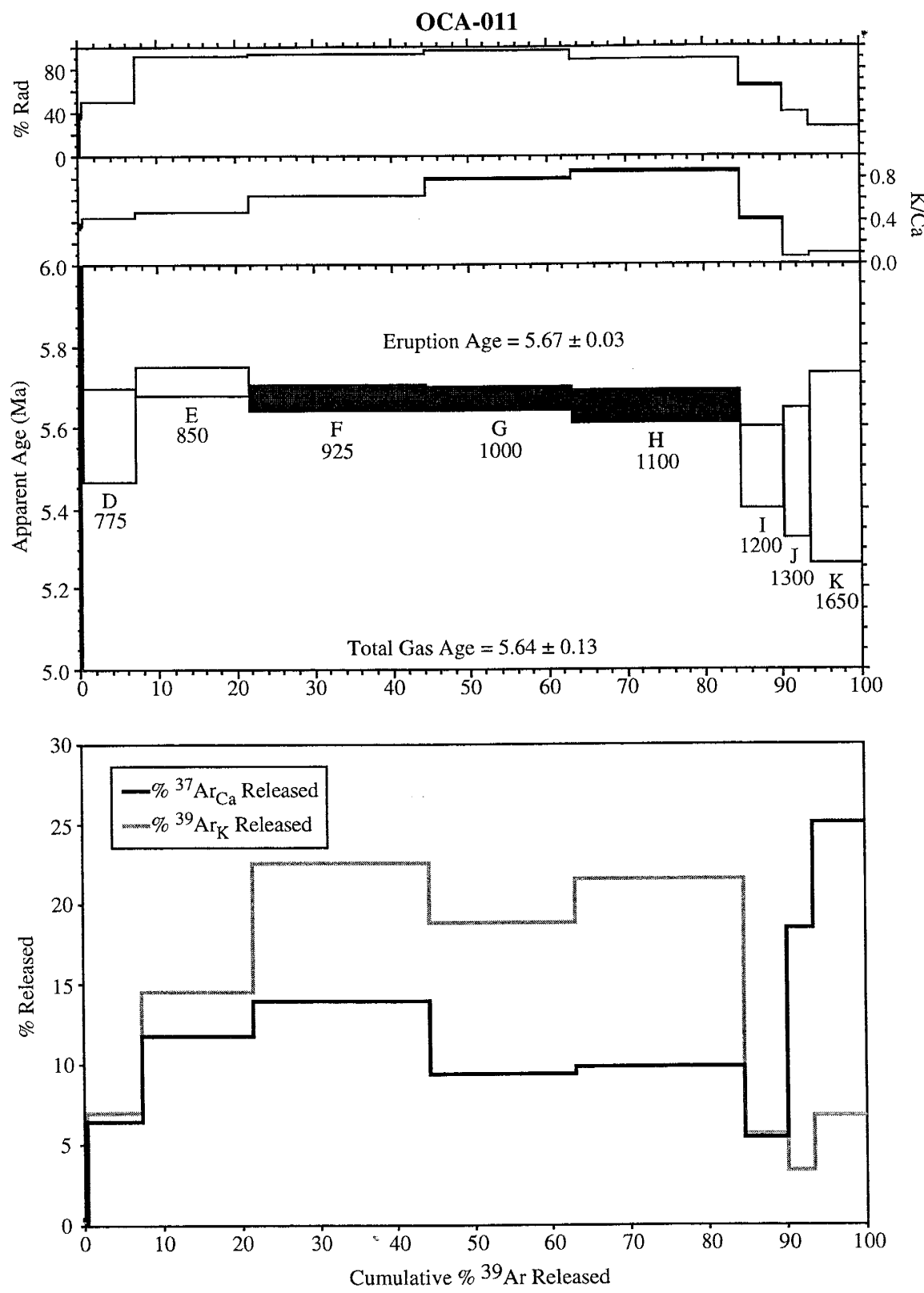


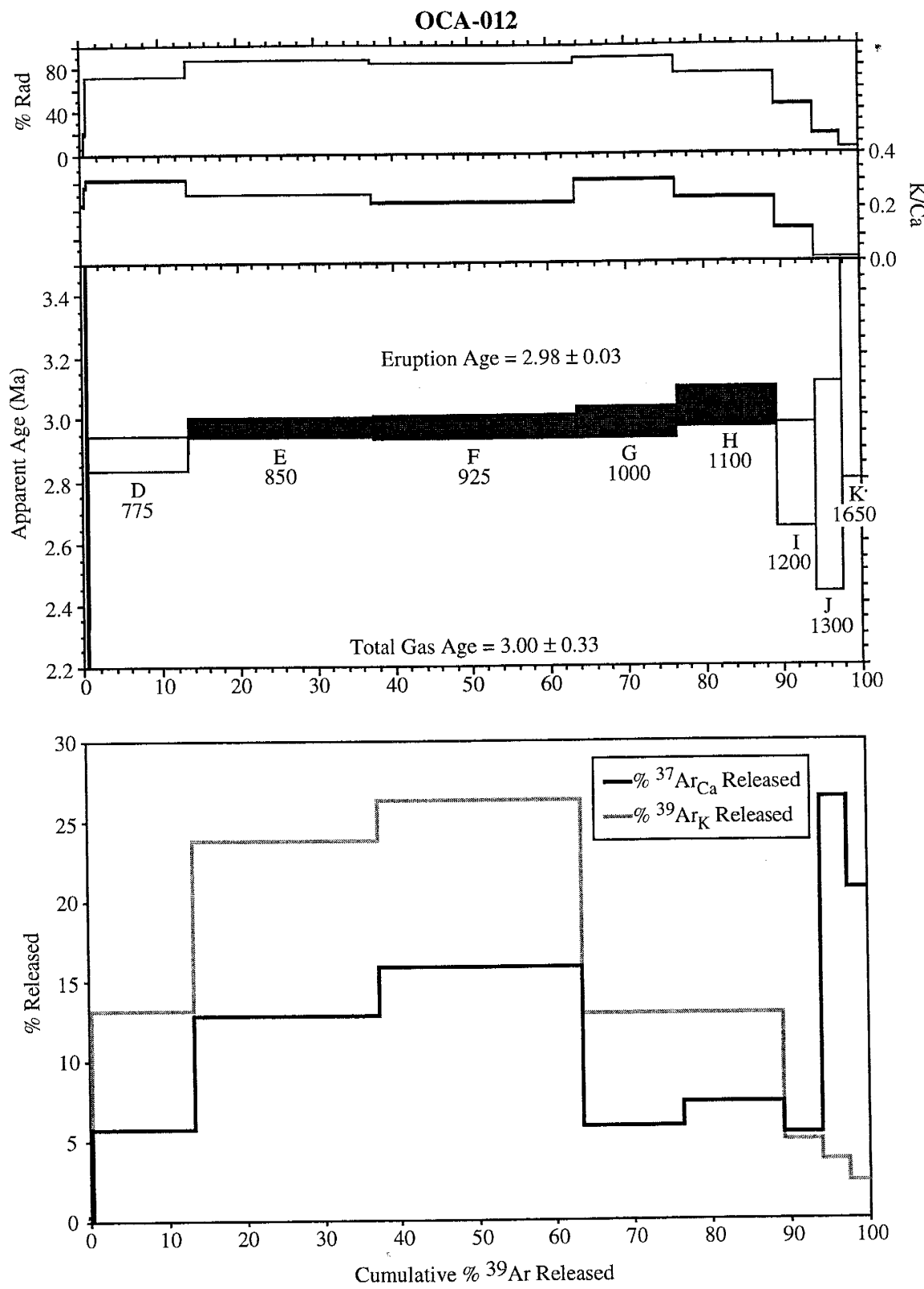




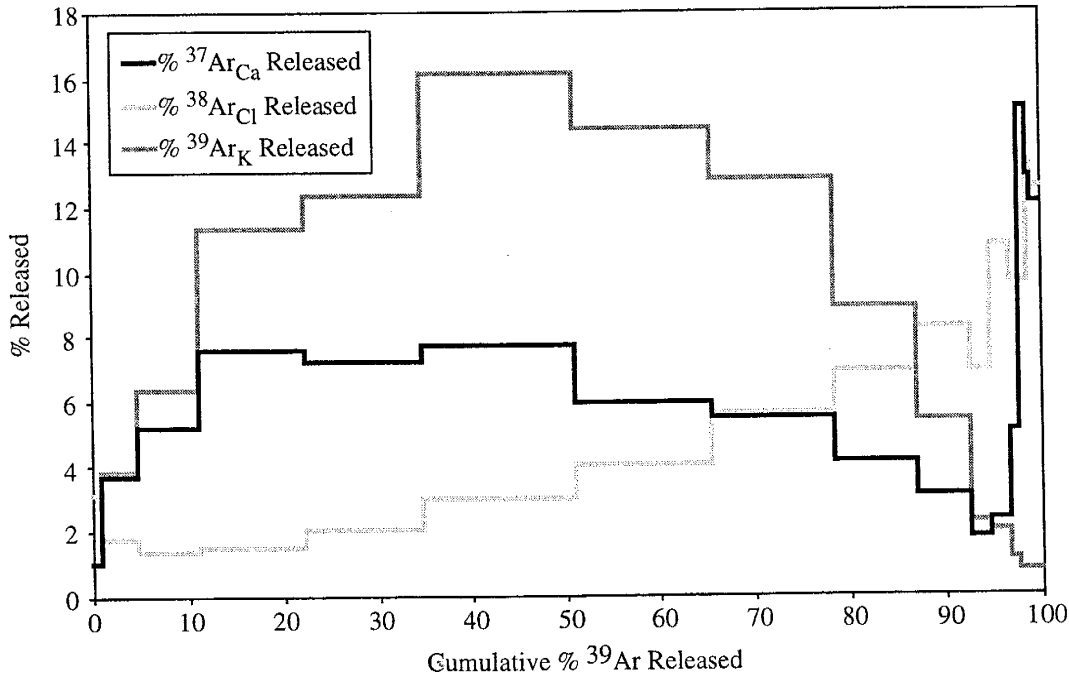
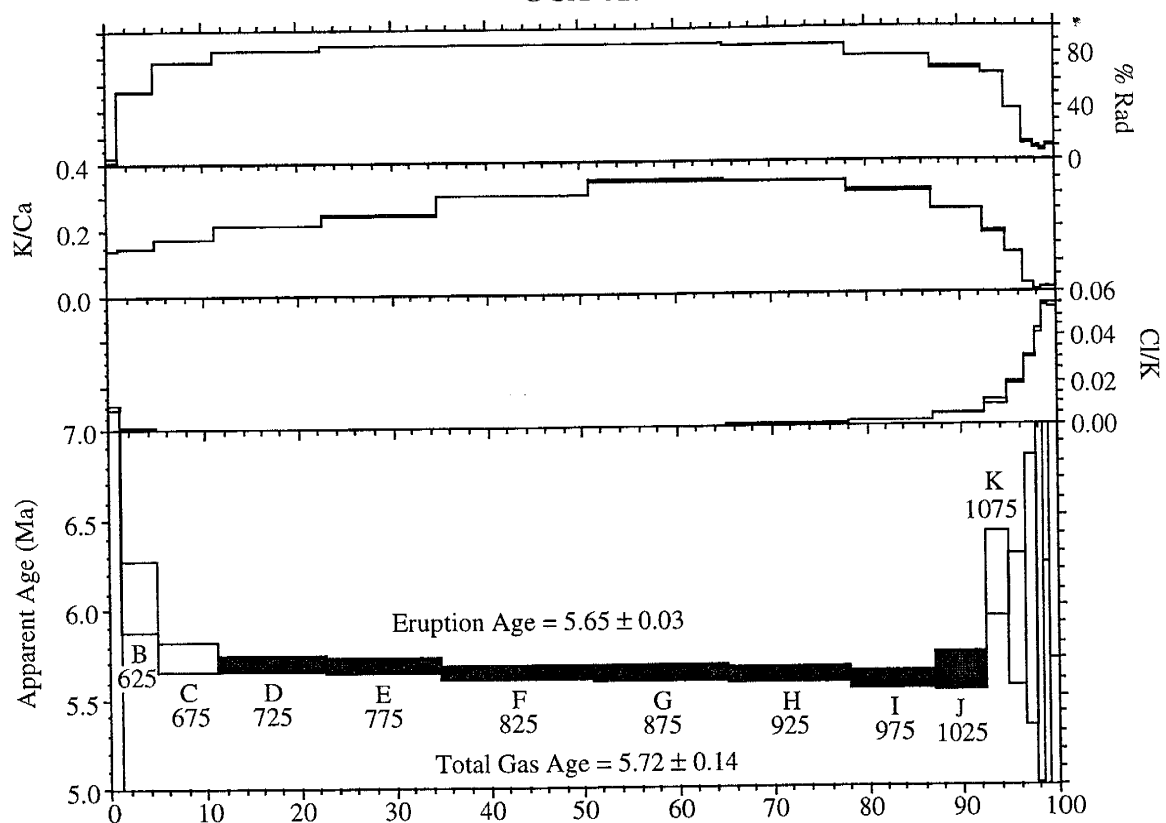


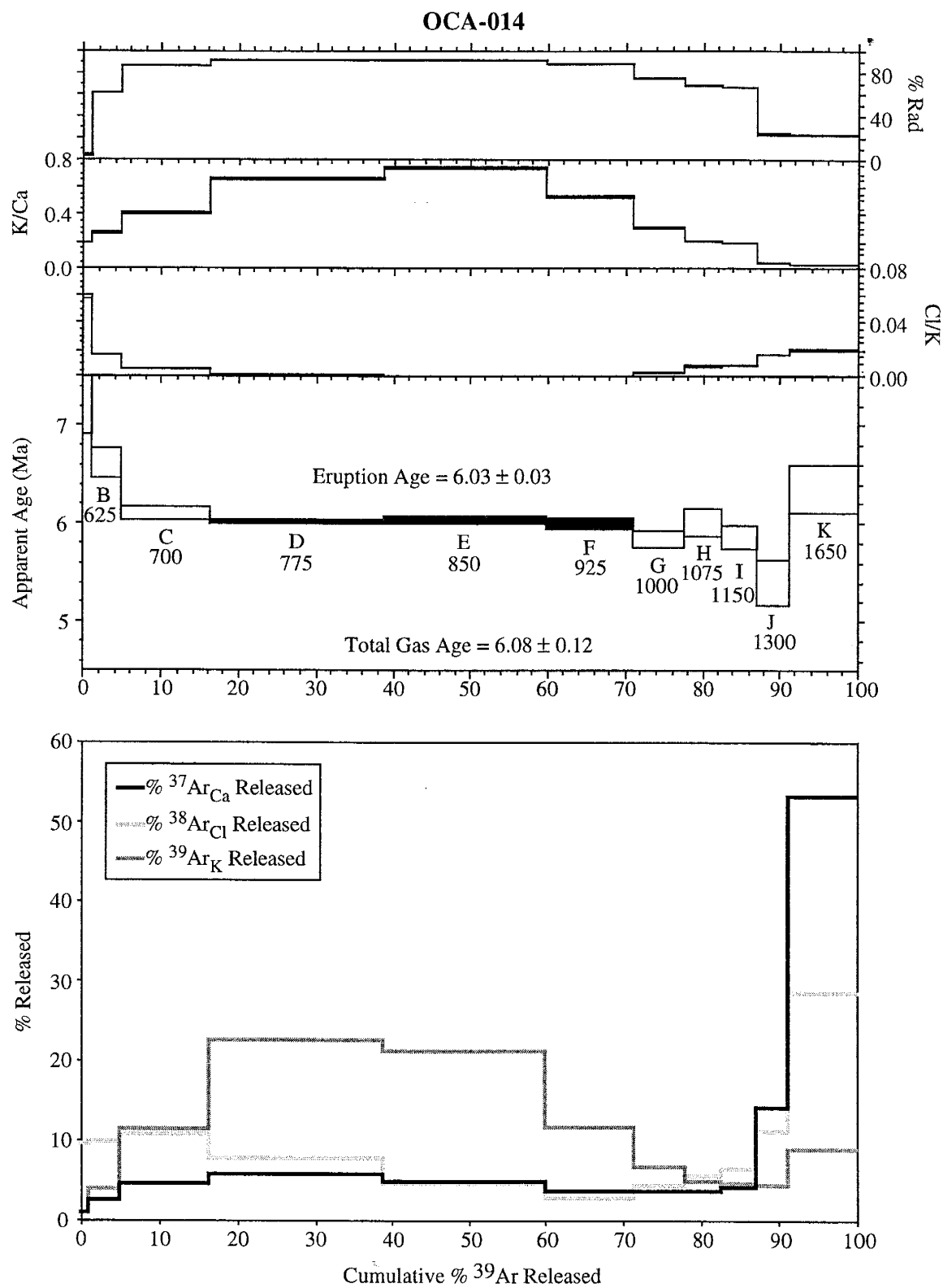


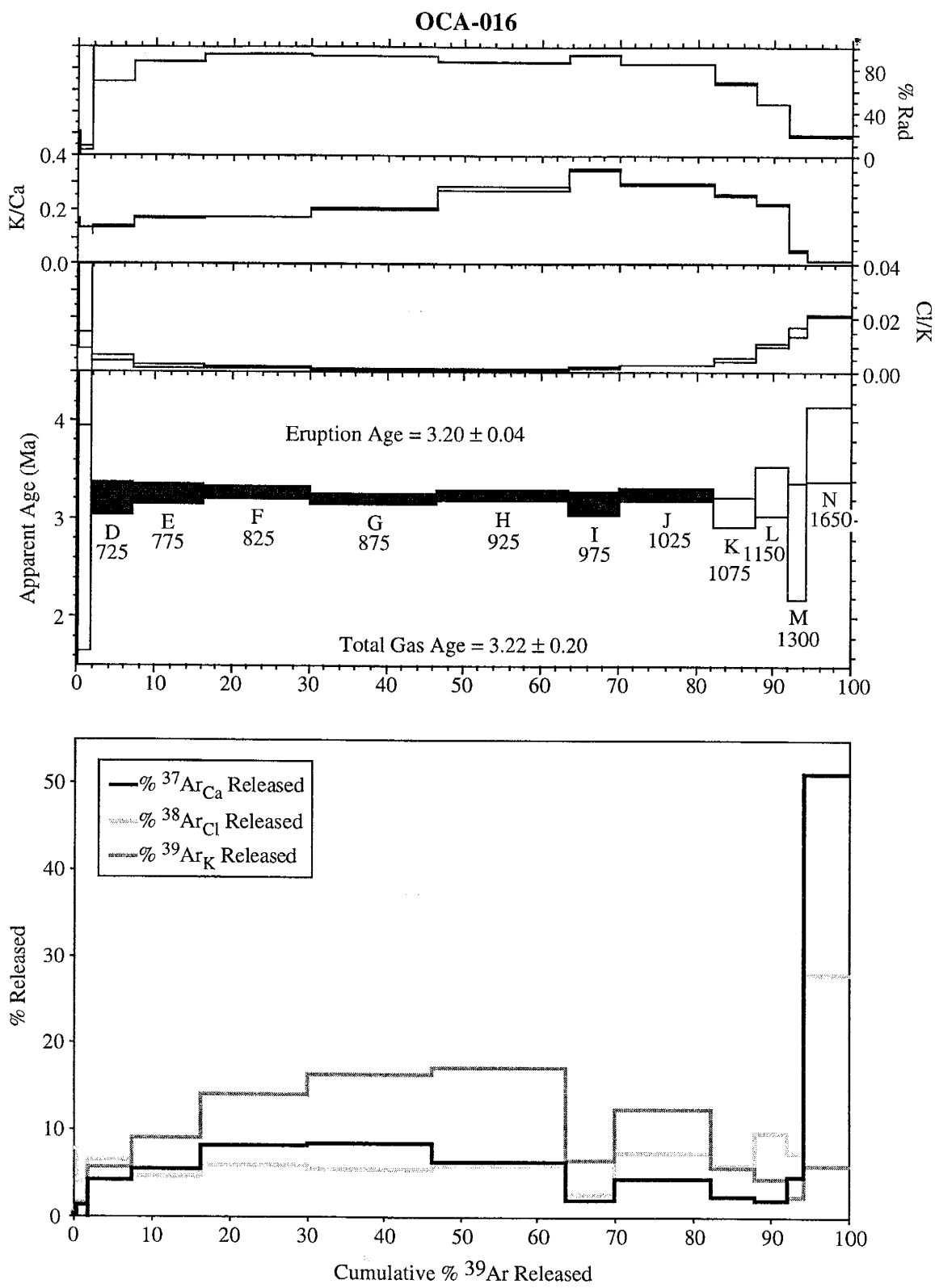


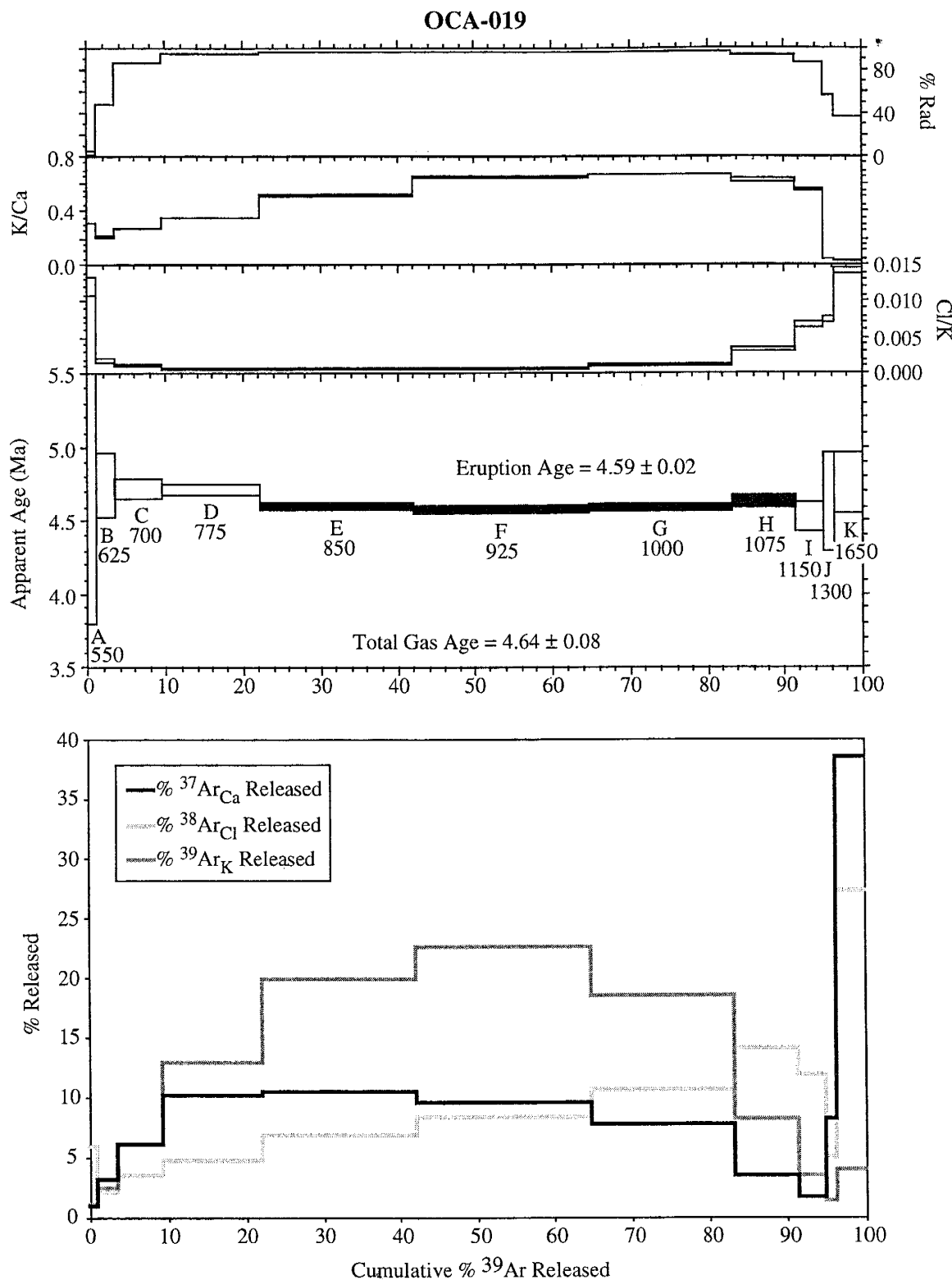


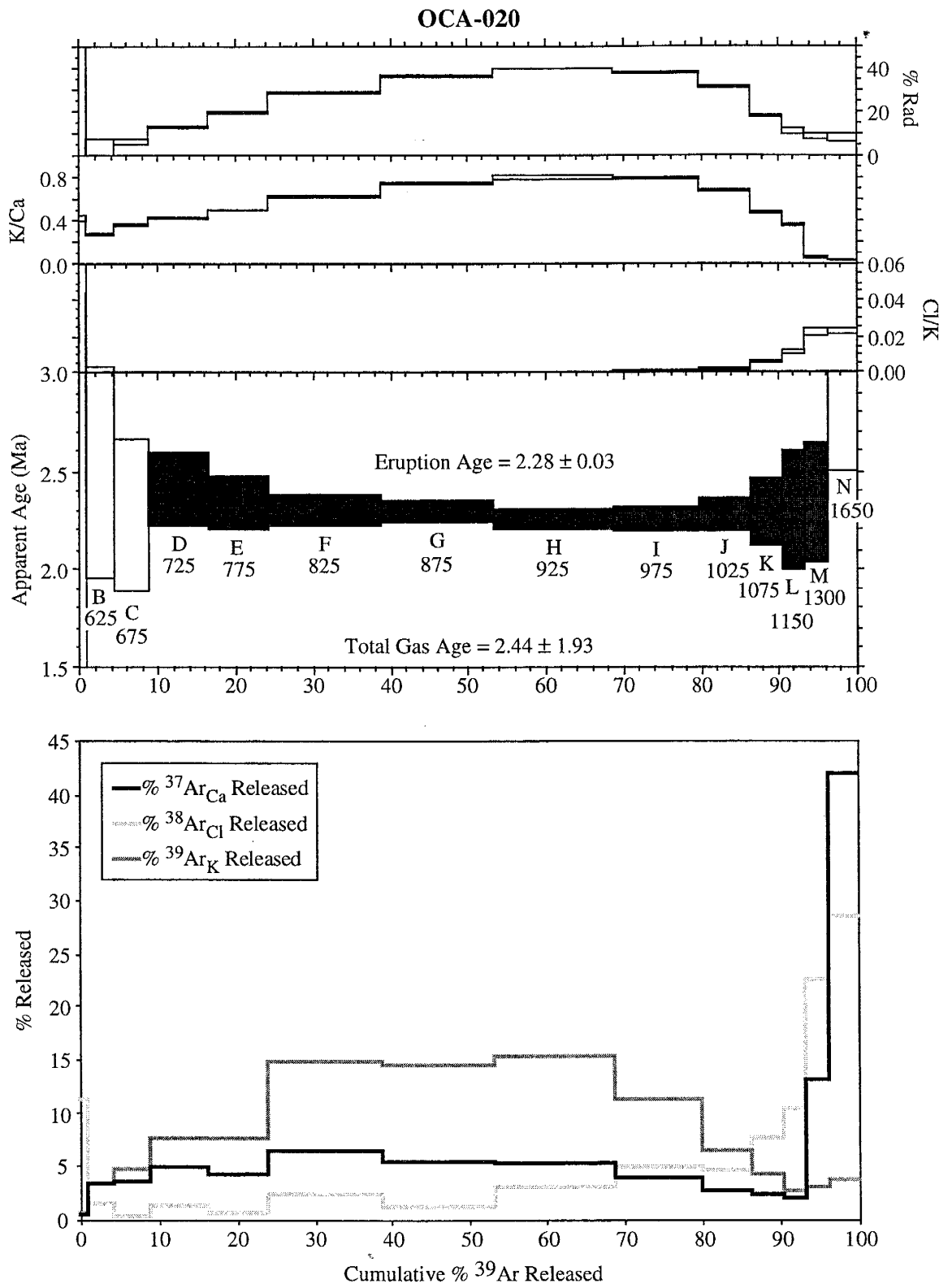
OCA-013

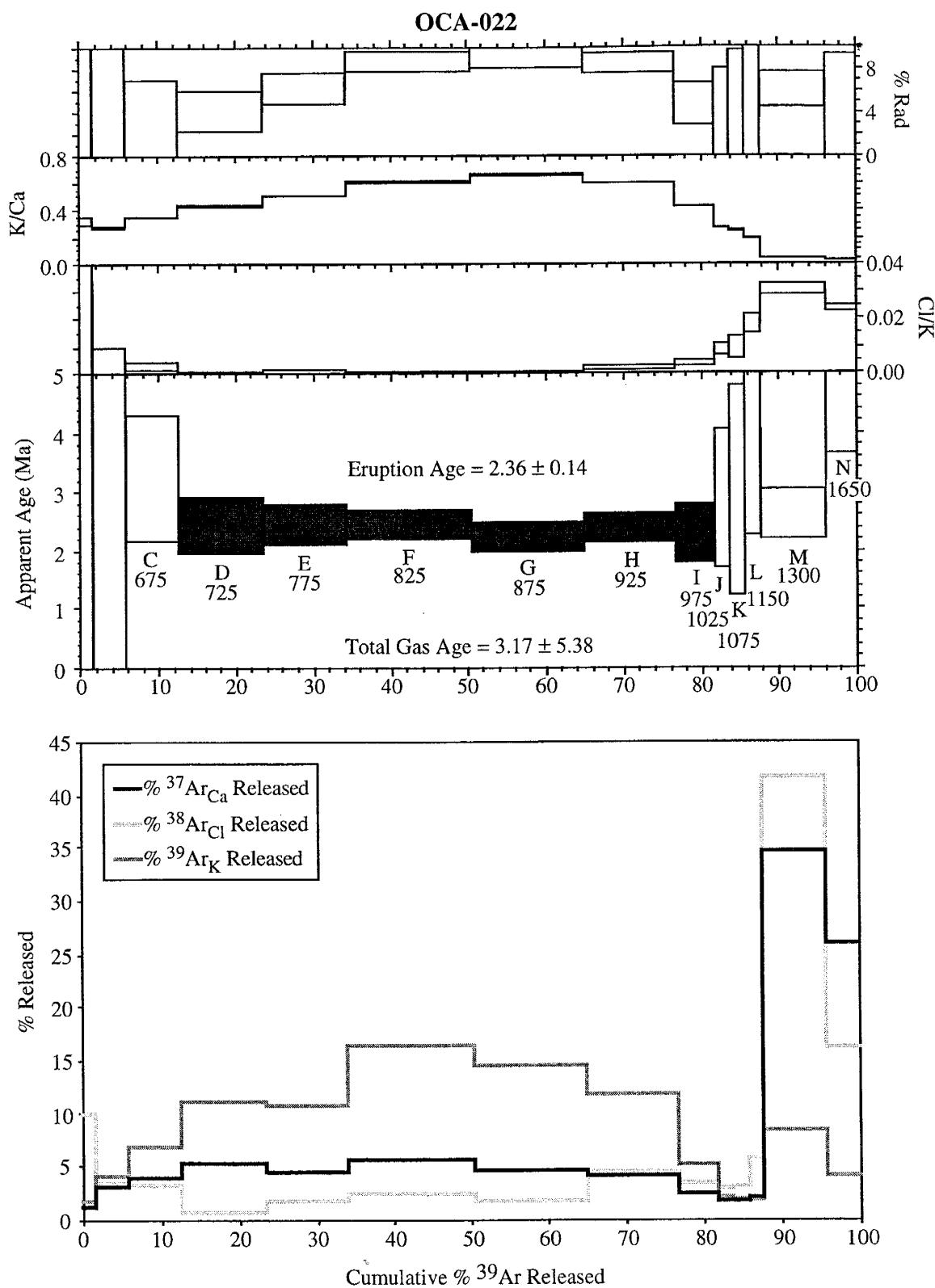


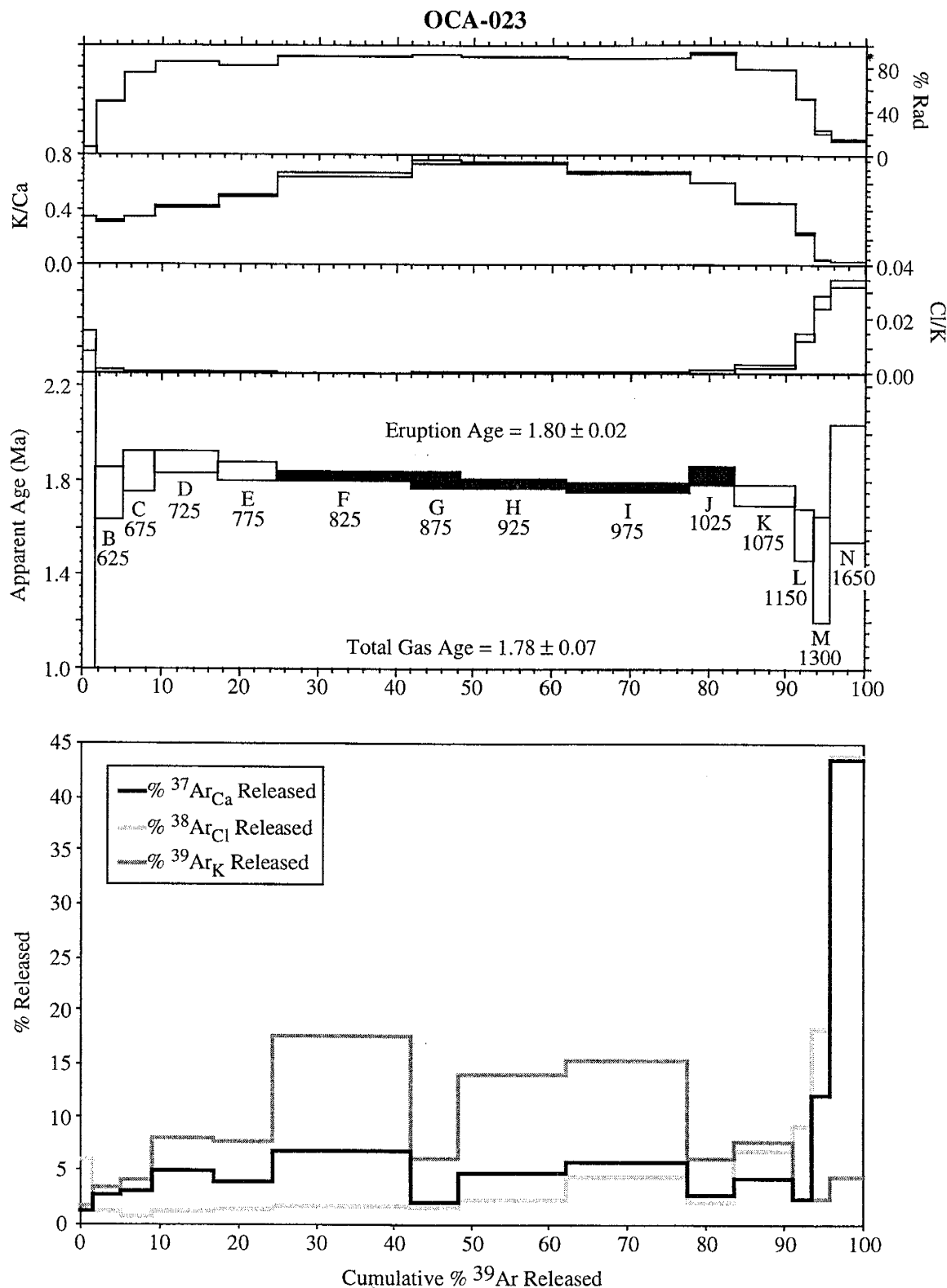


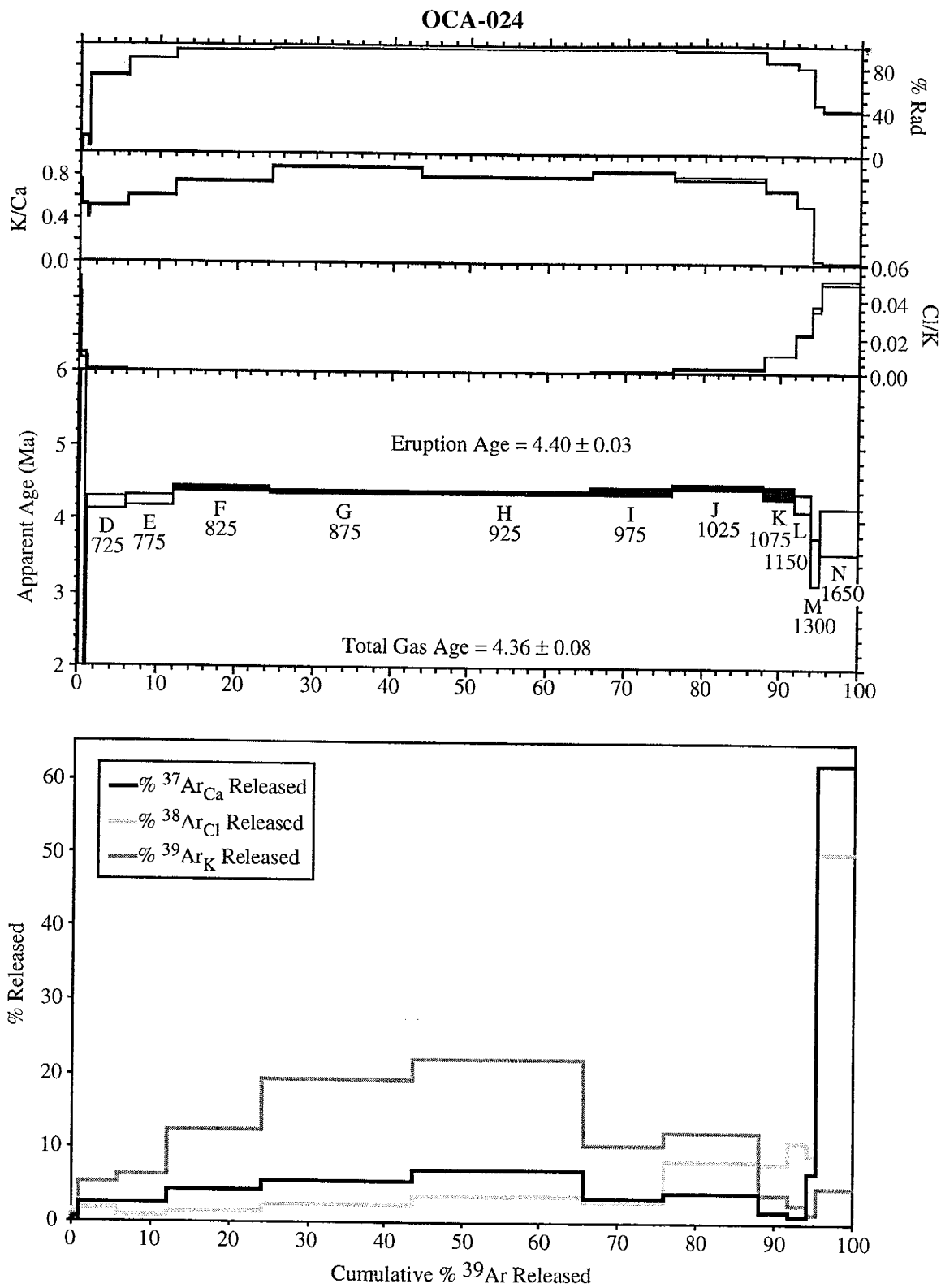


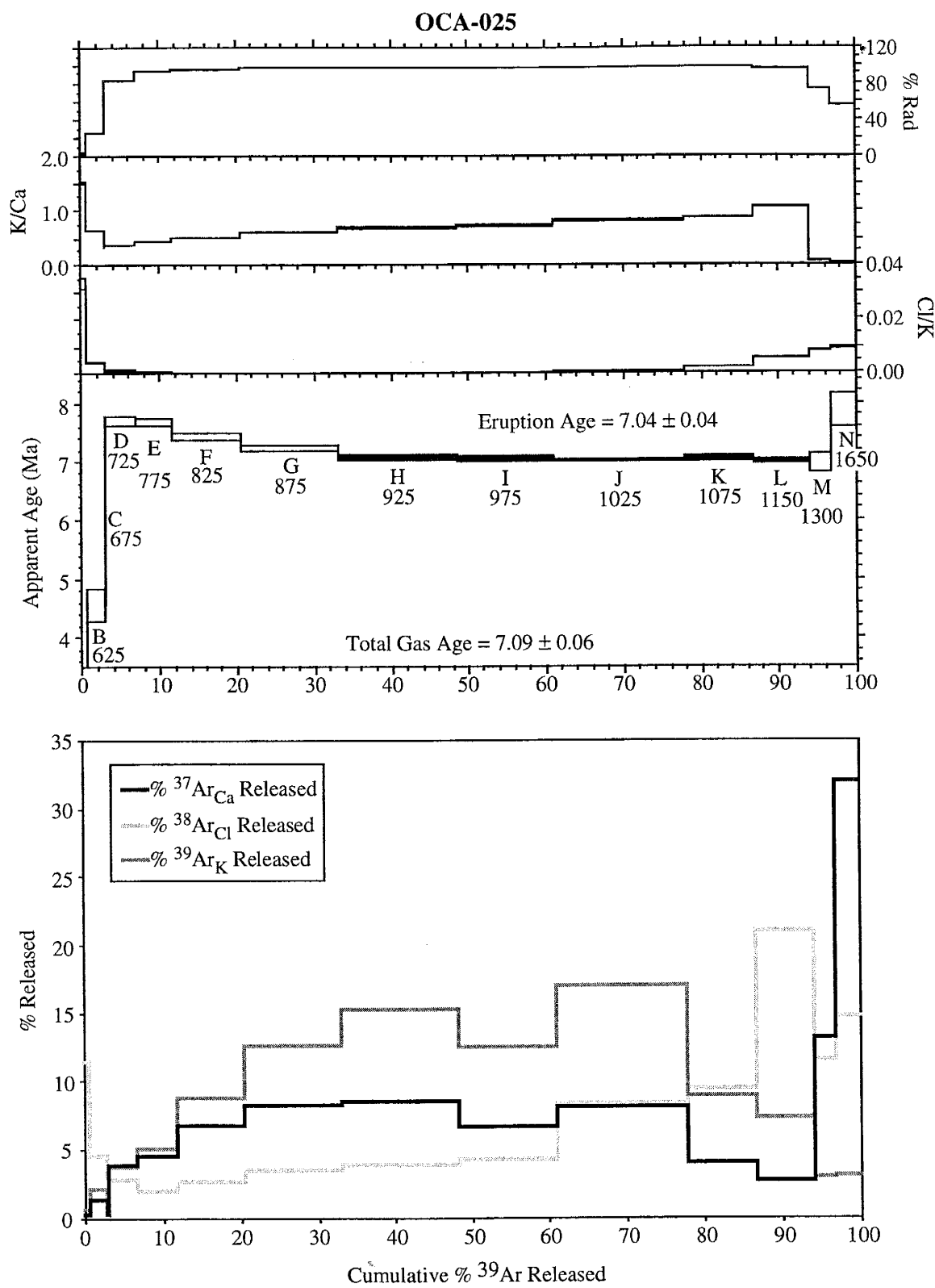


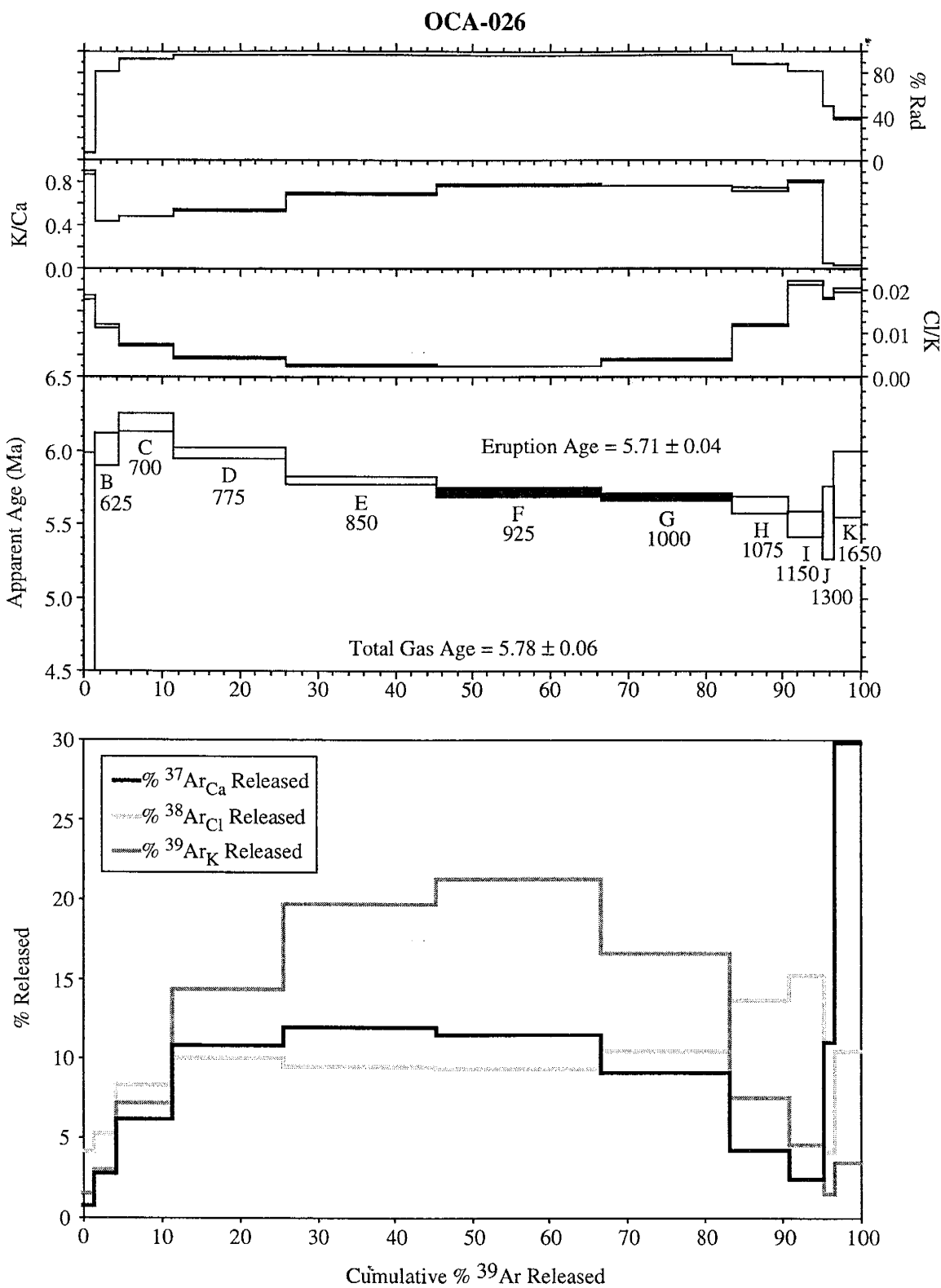


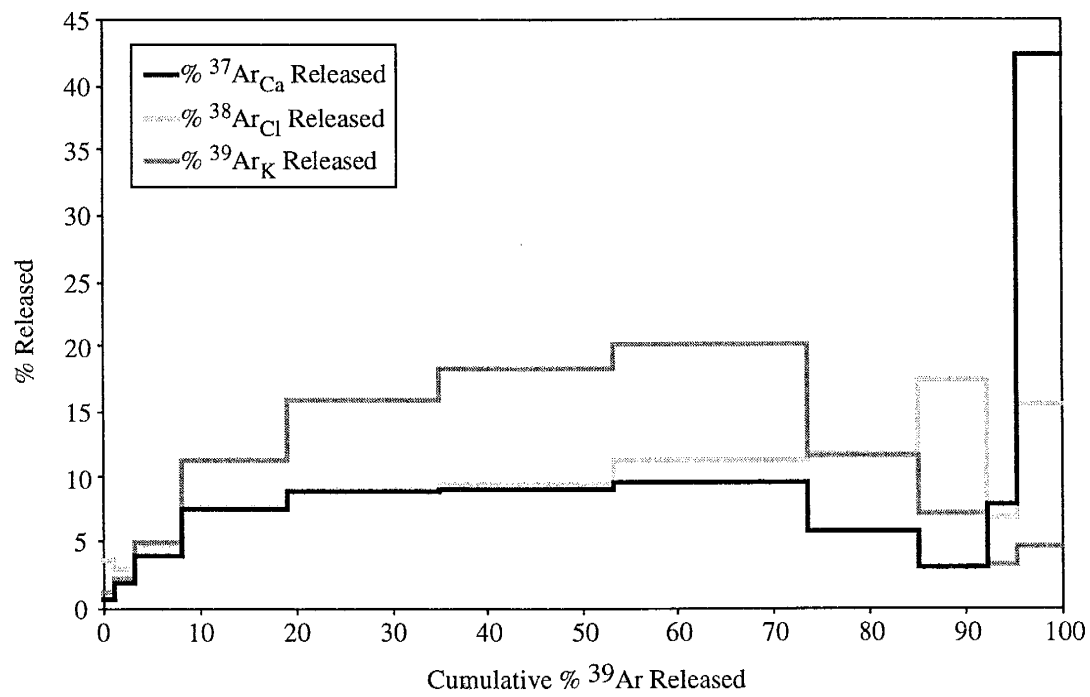
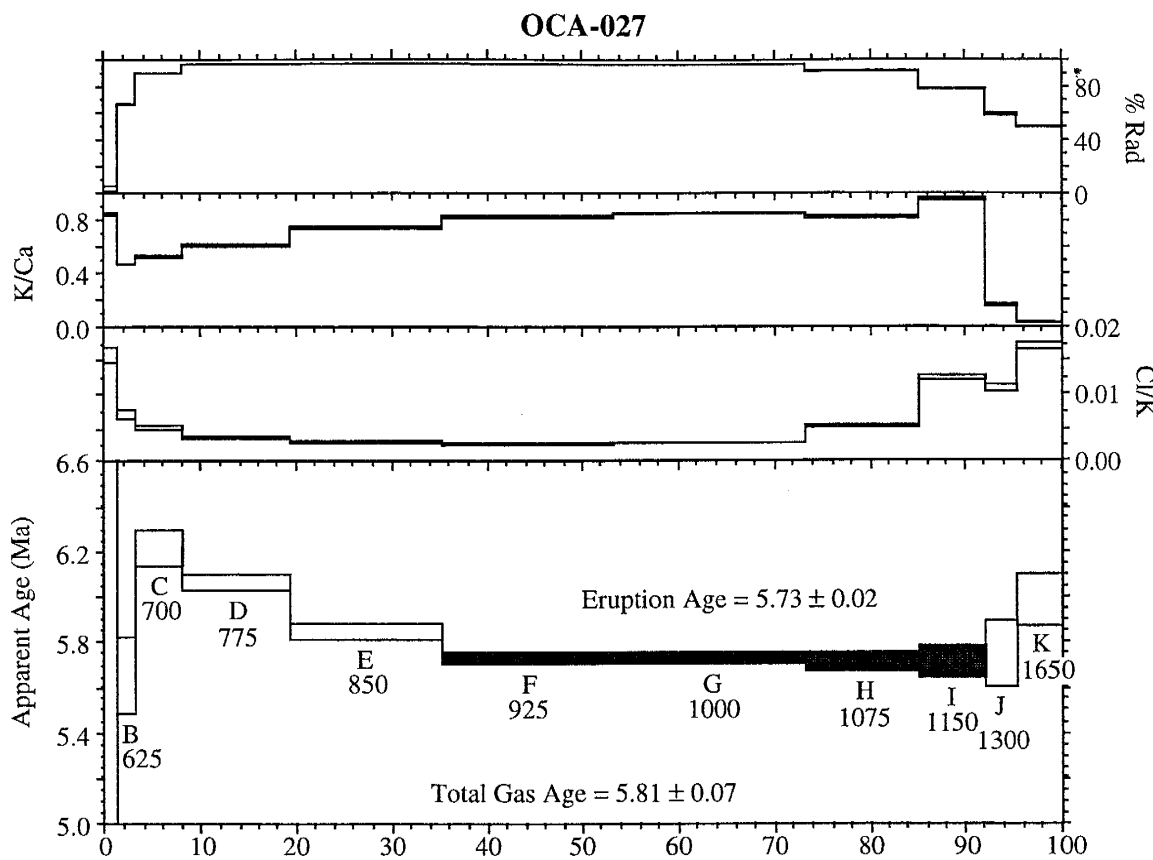


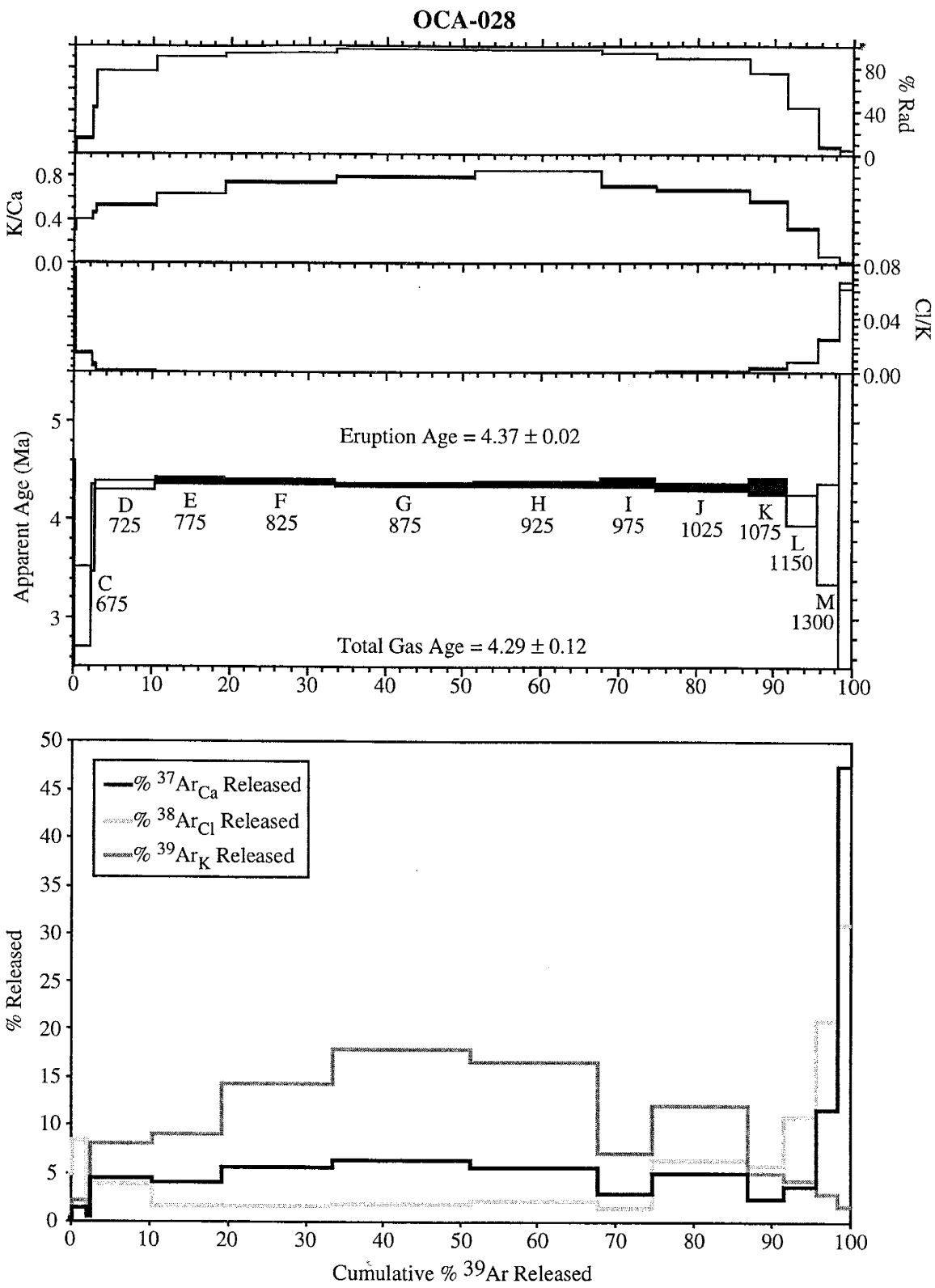


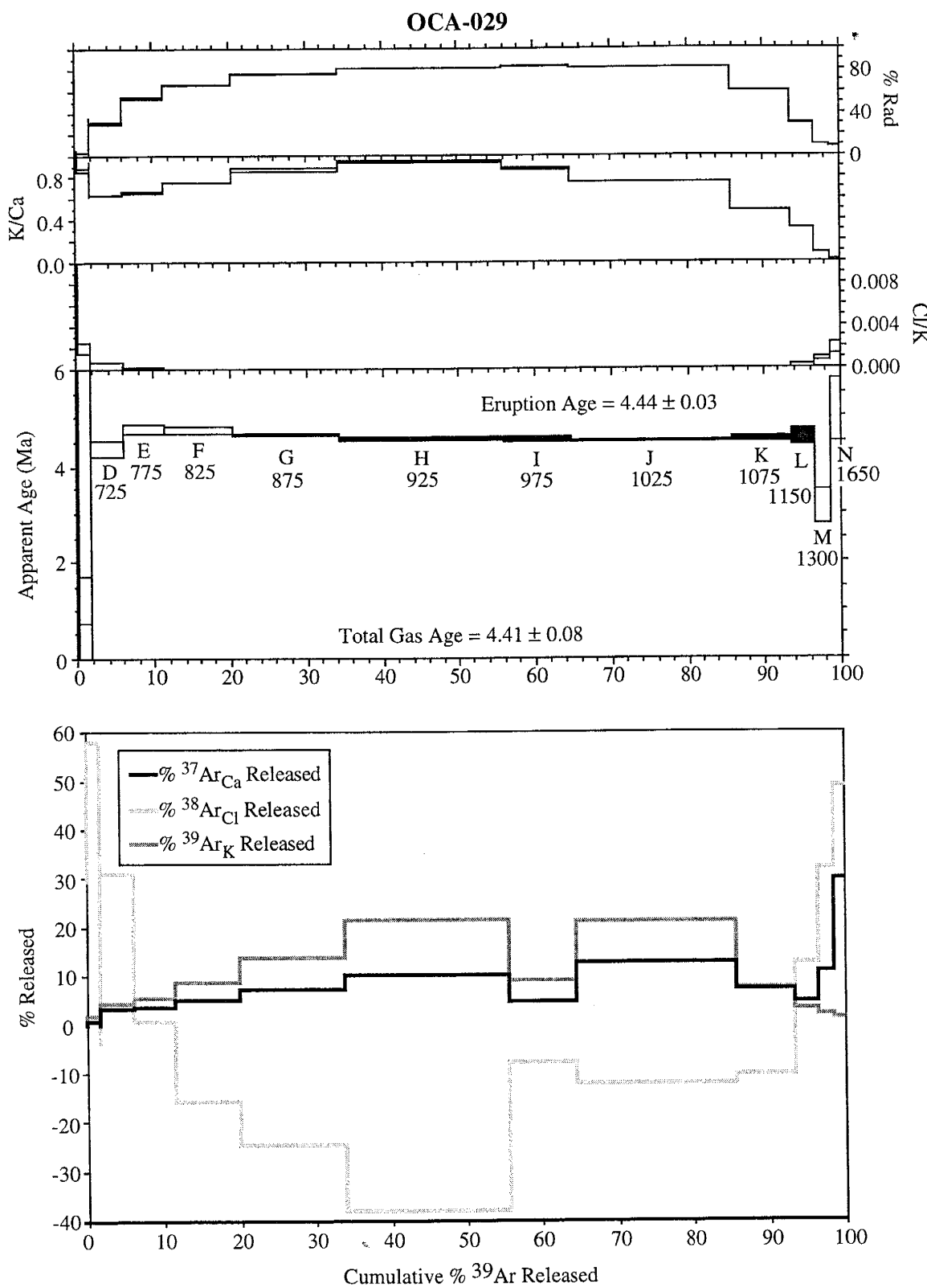


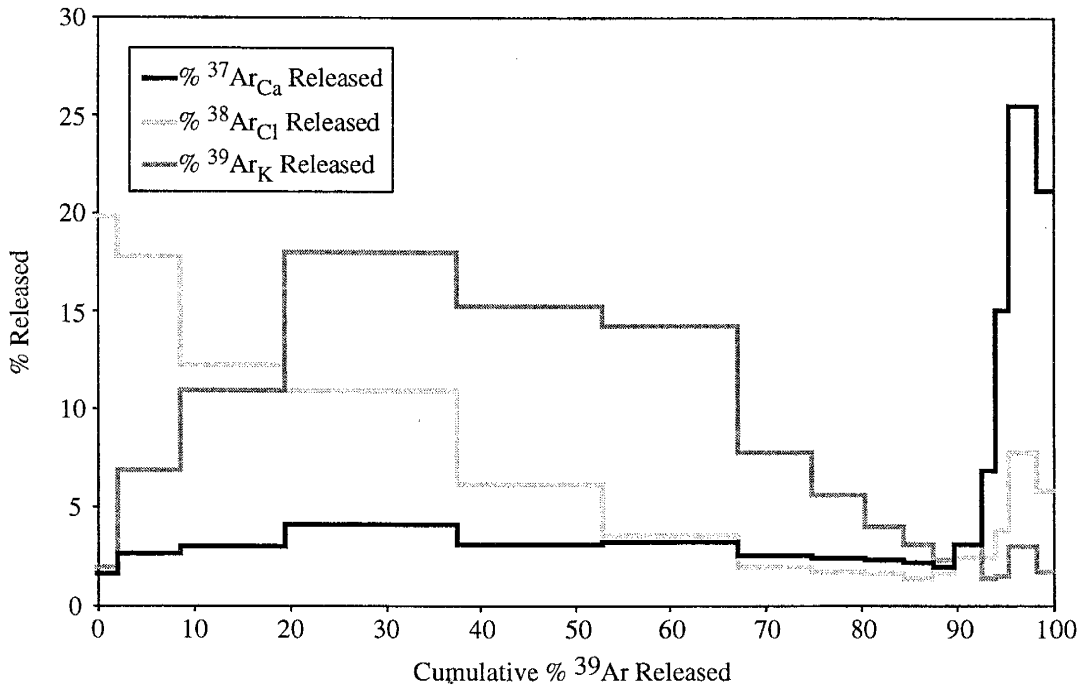
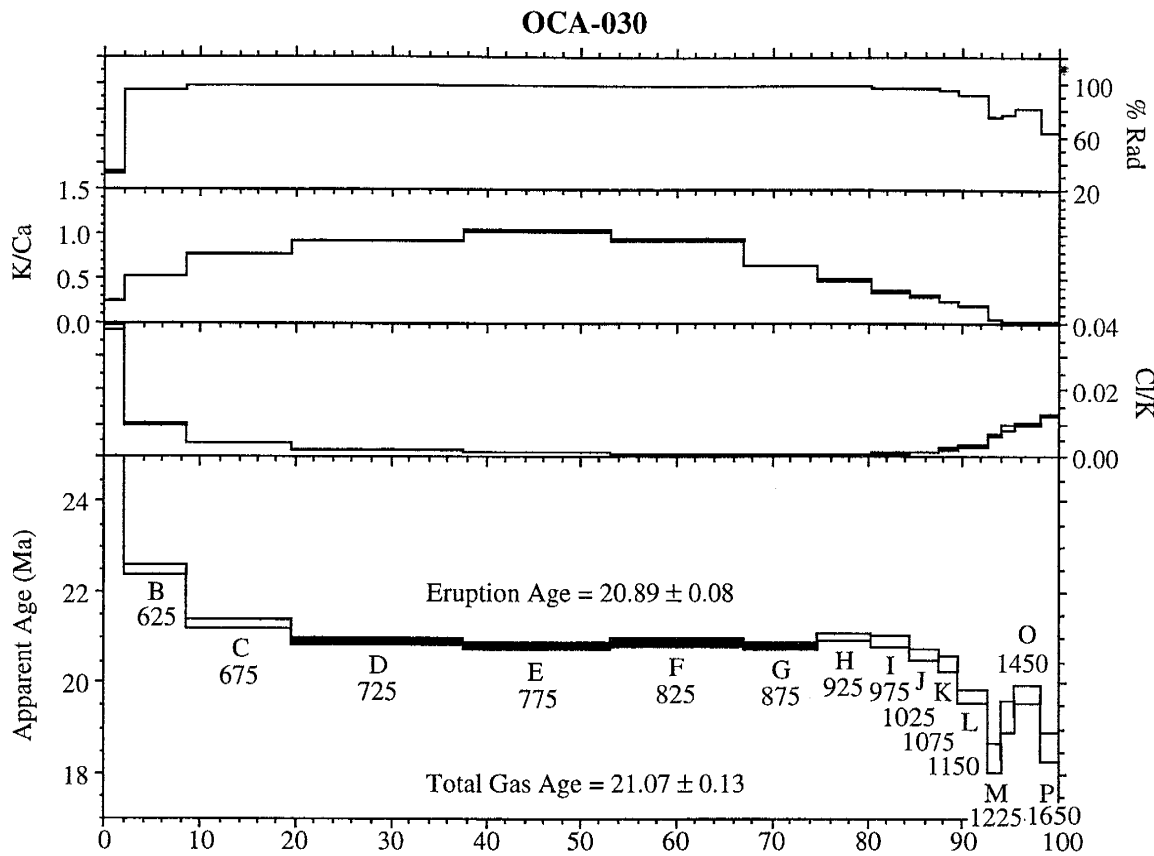


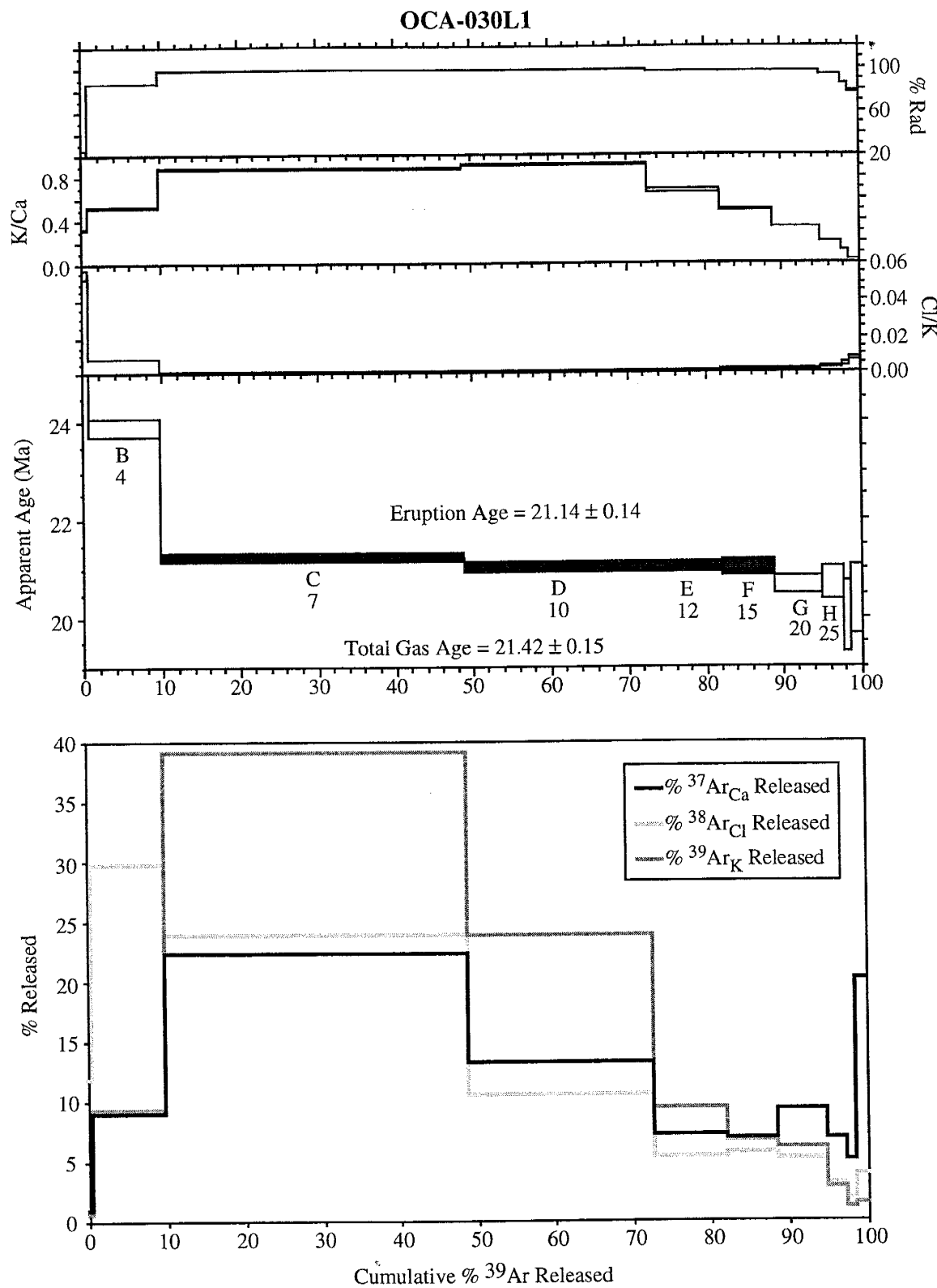


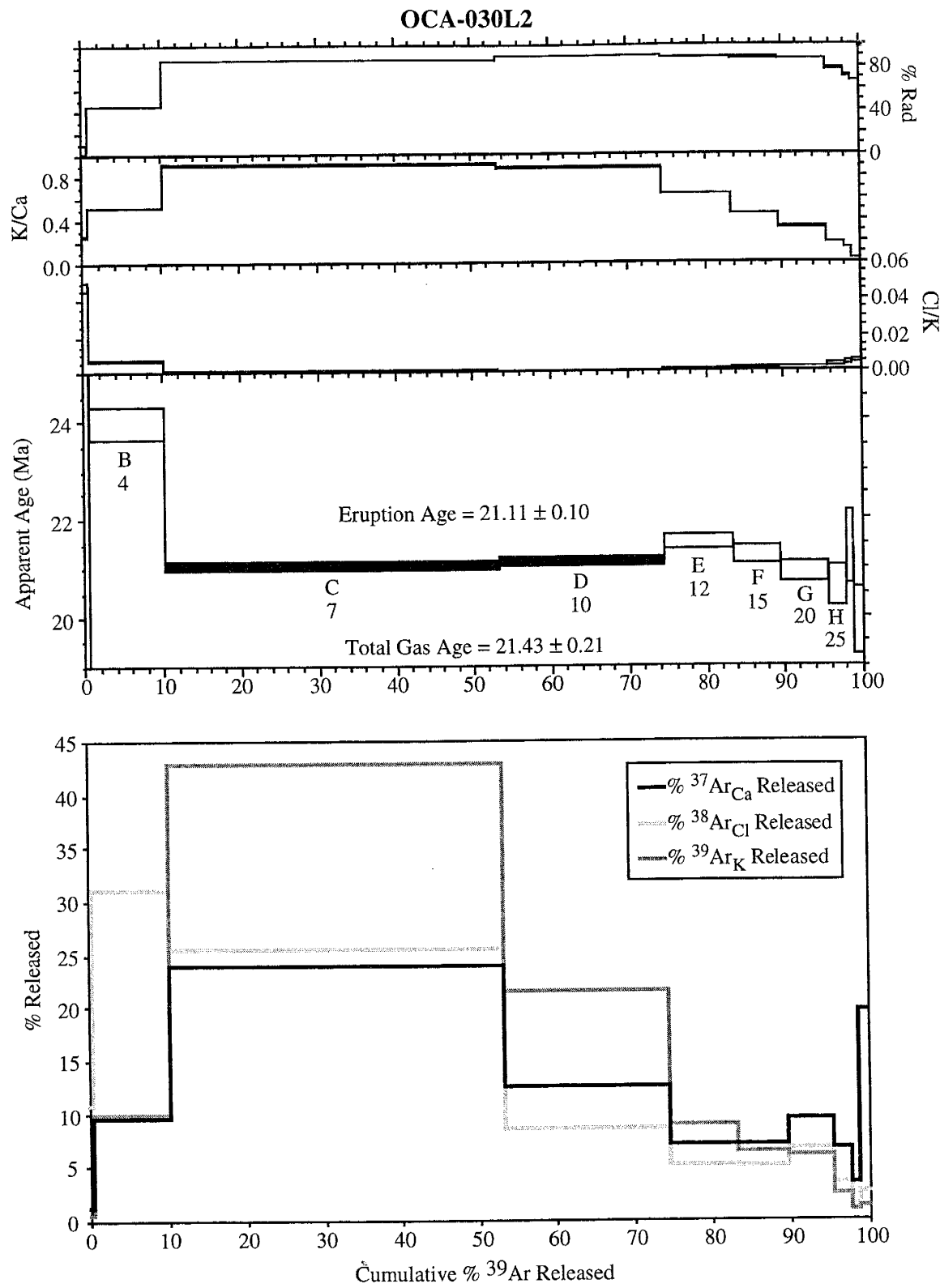


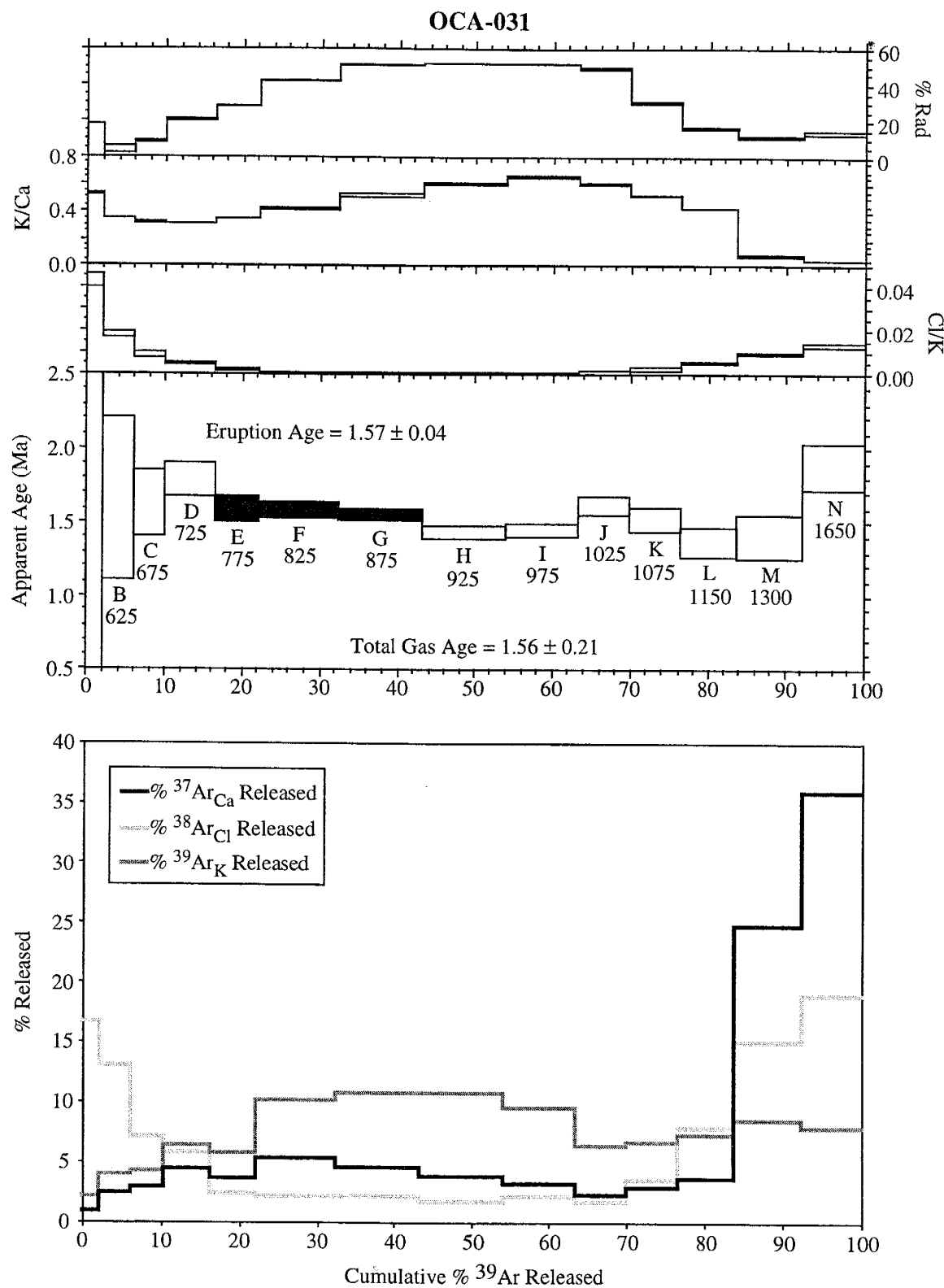




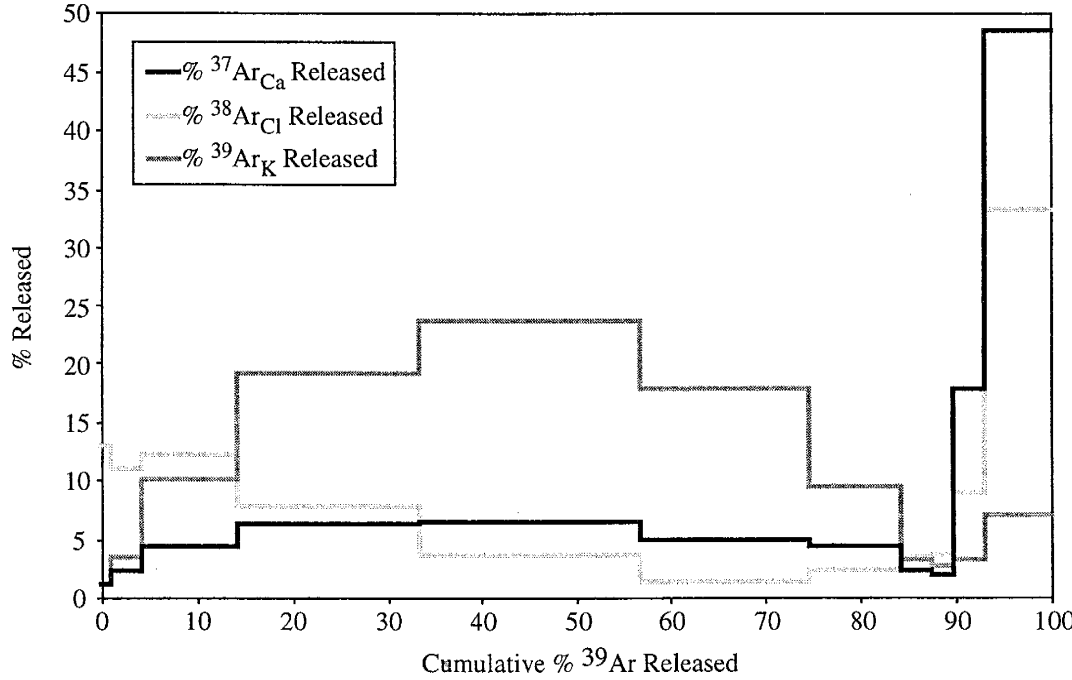
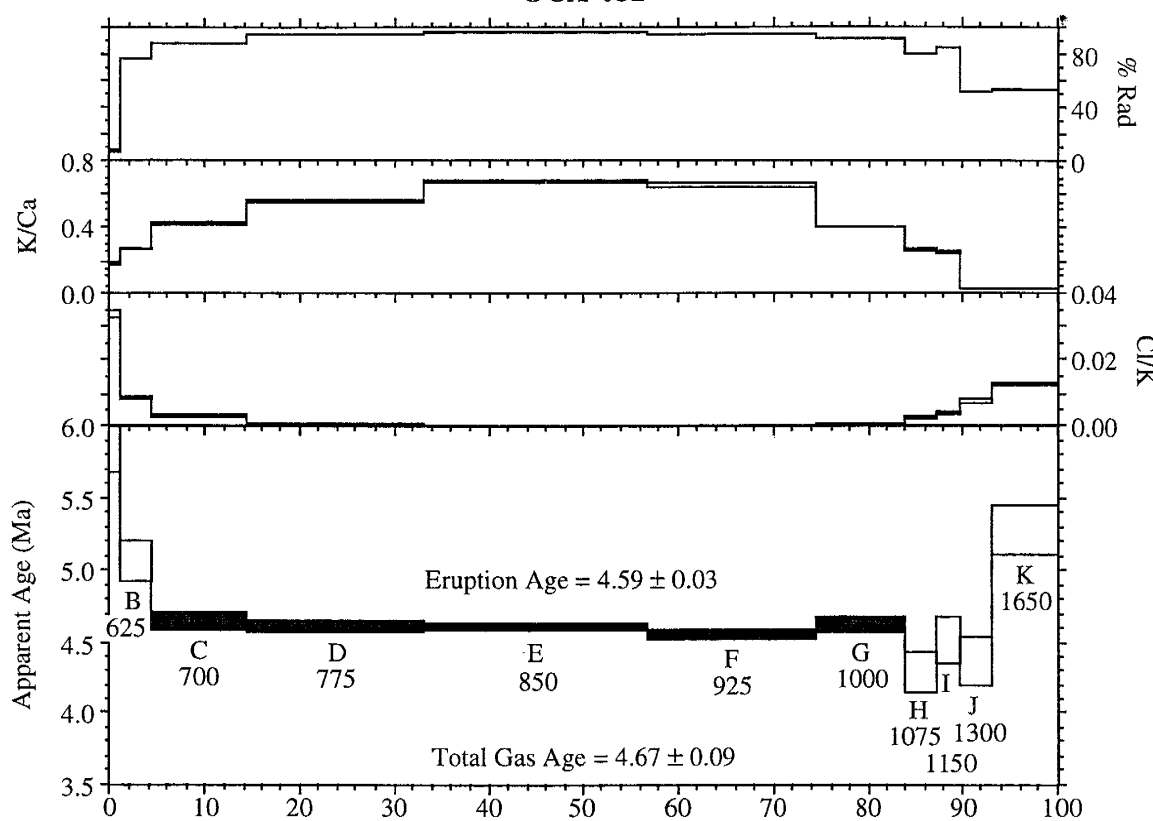


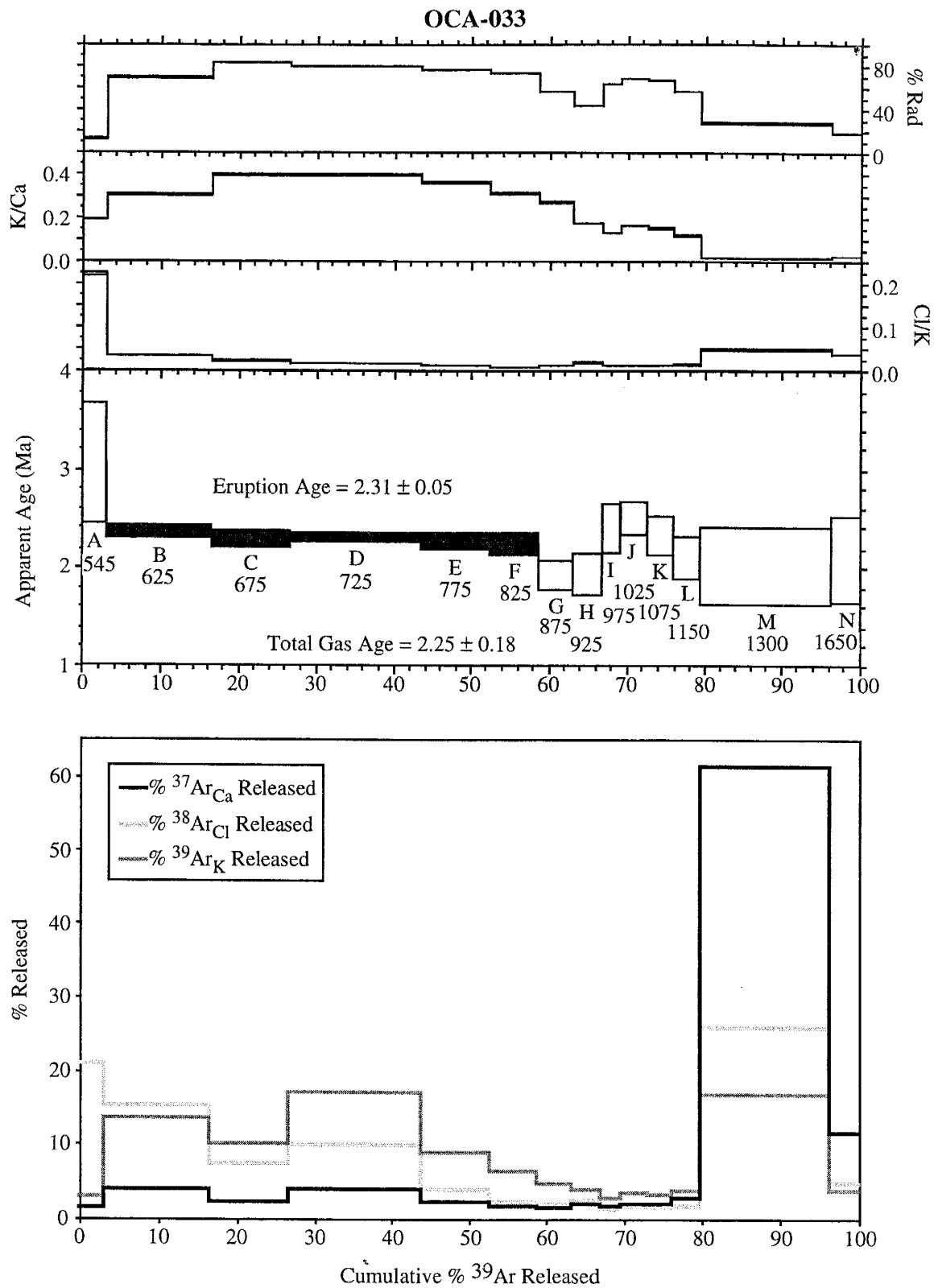


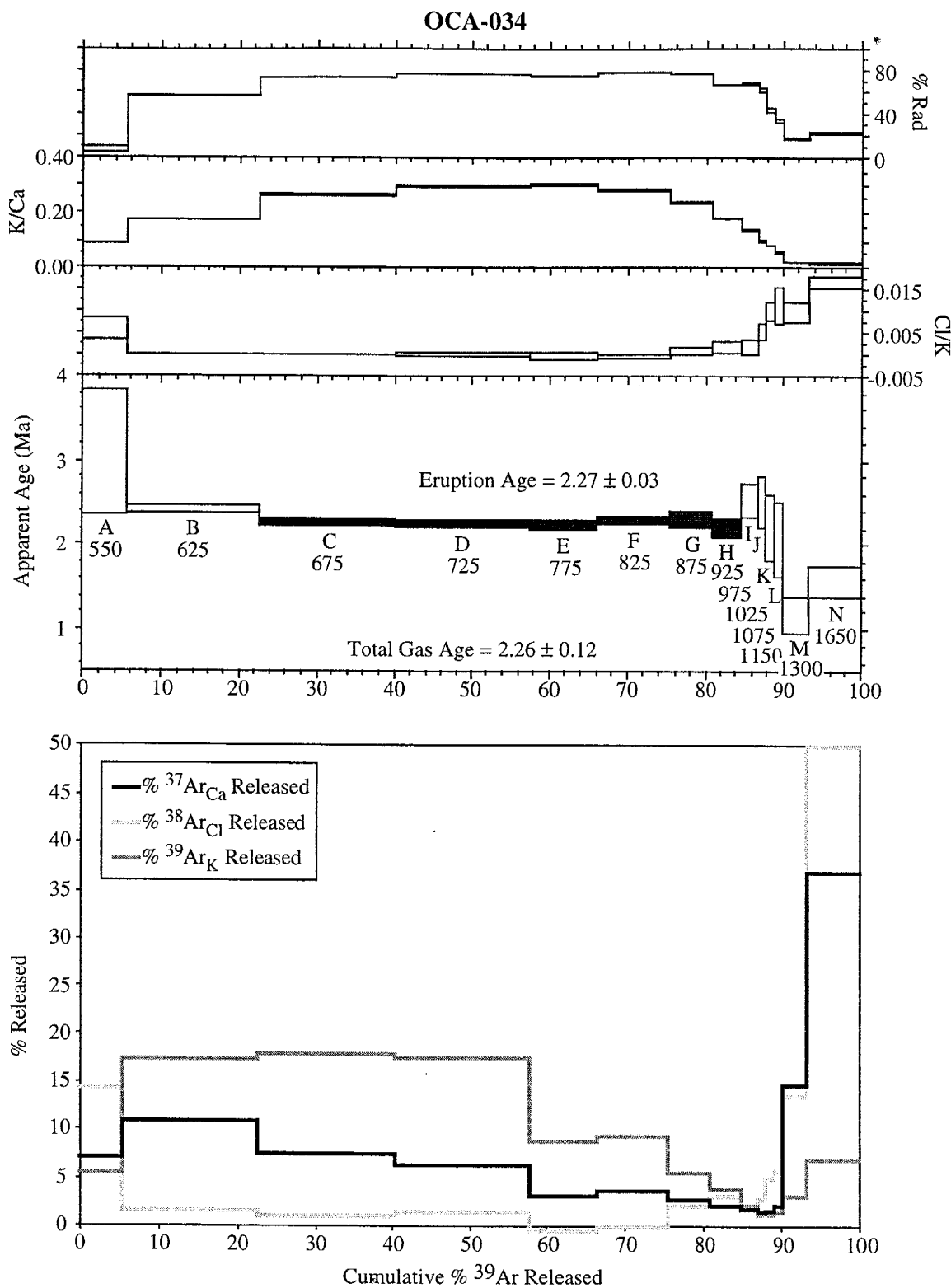


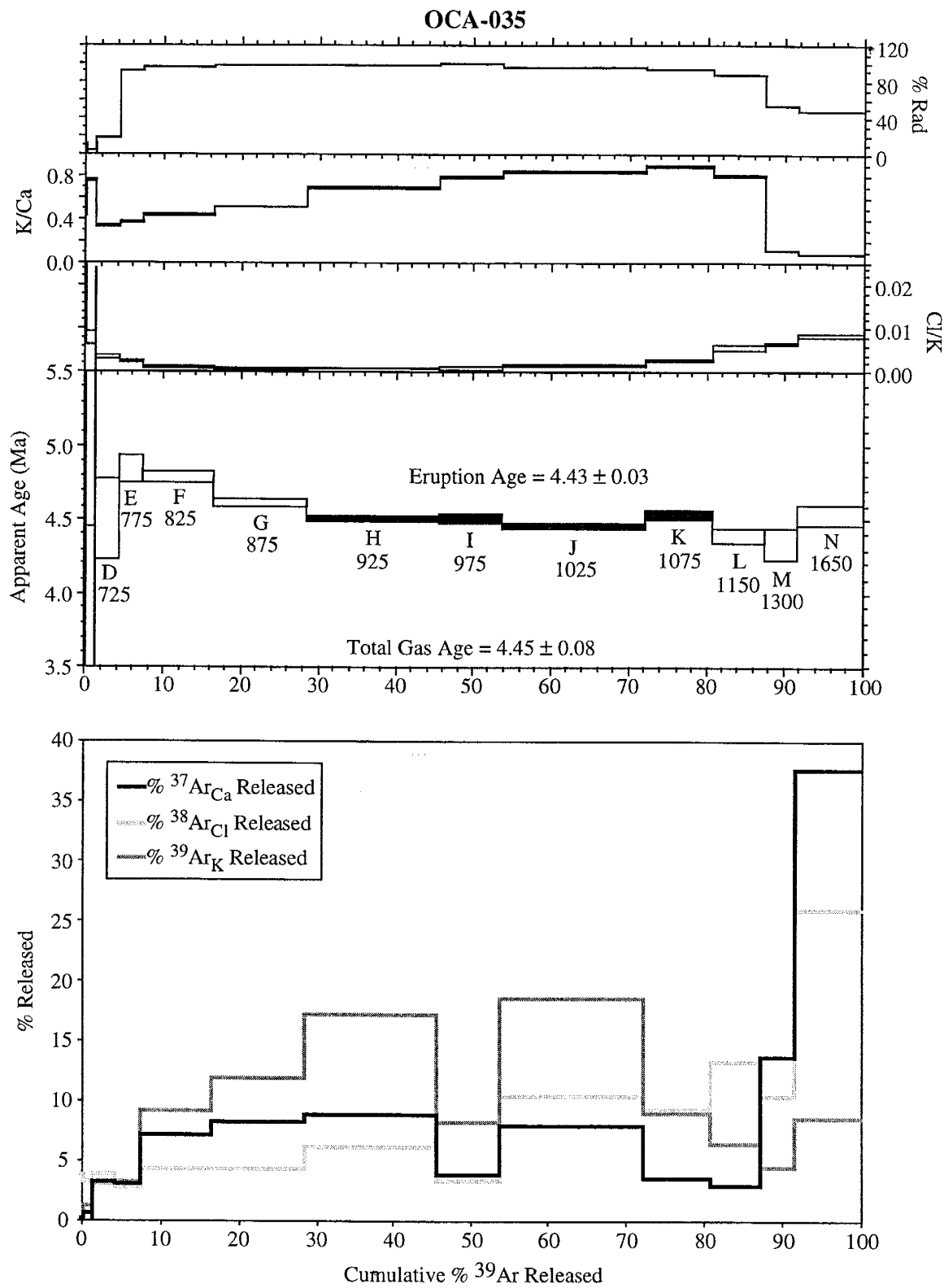


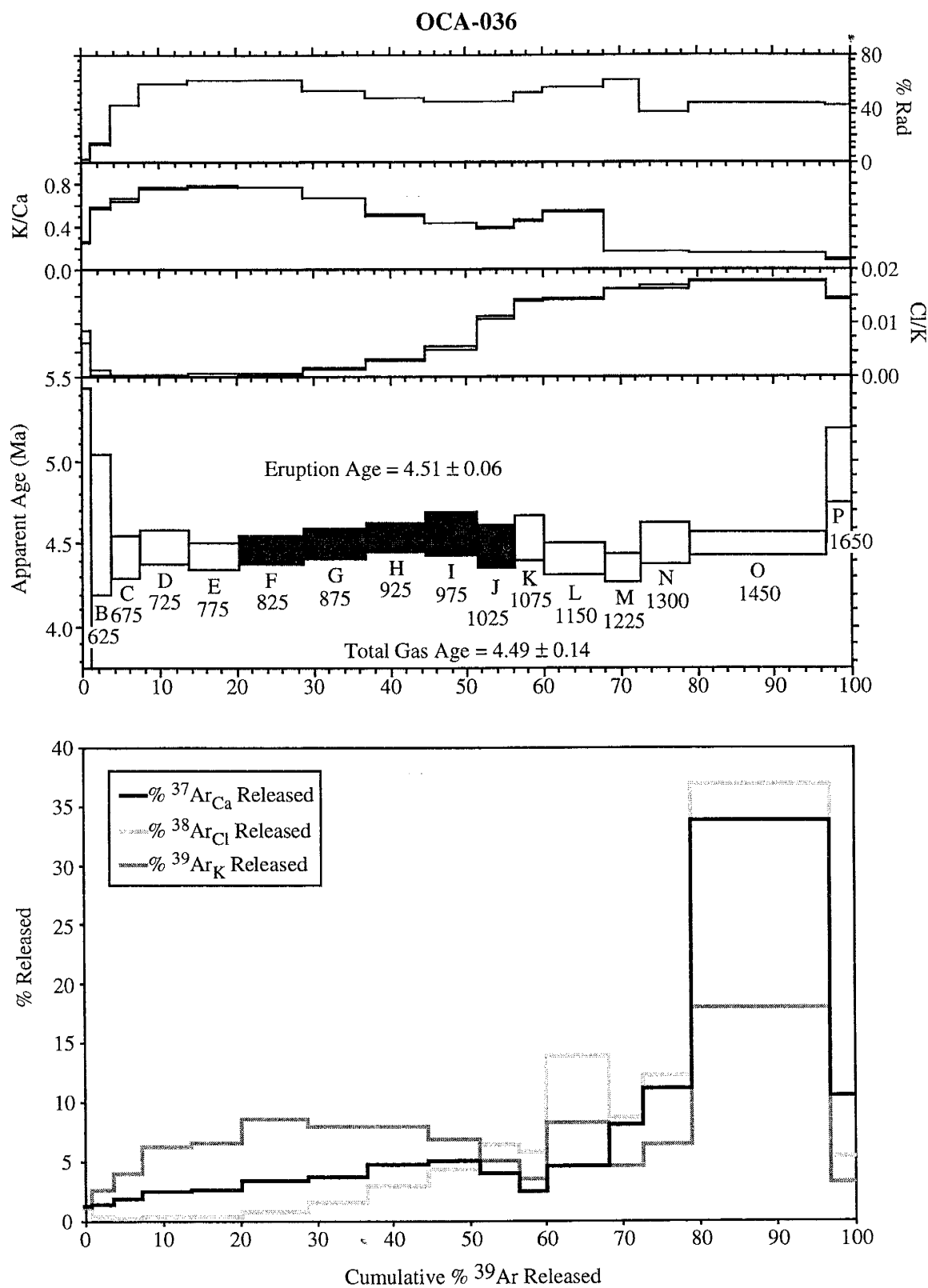
OCA-032

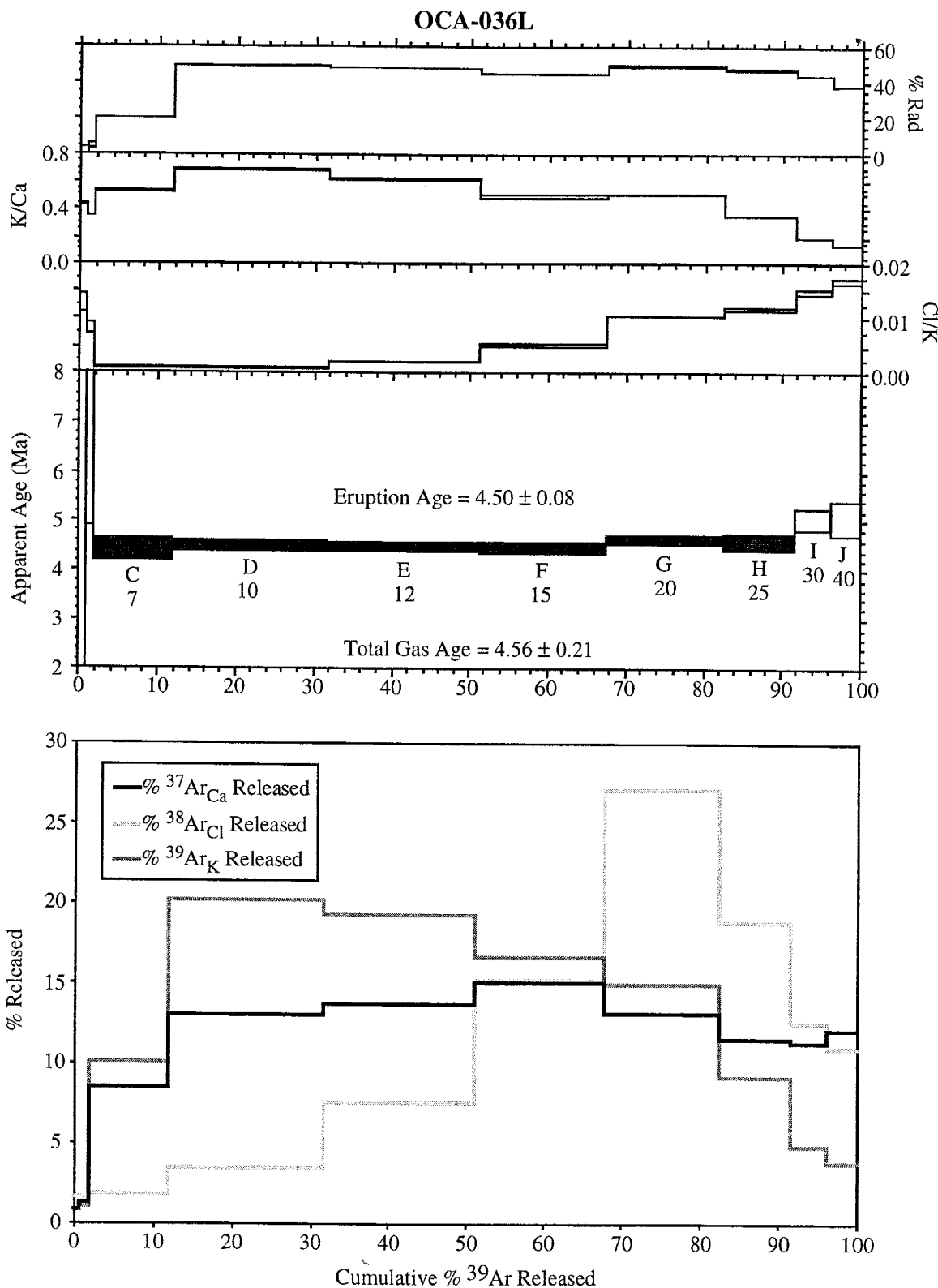


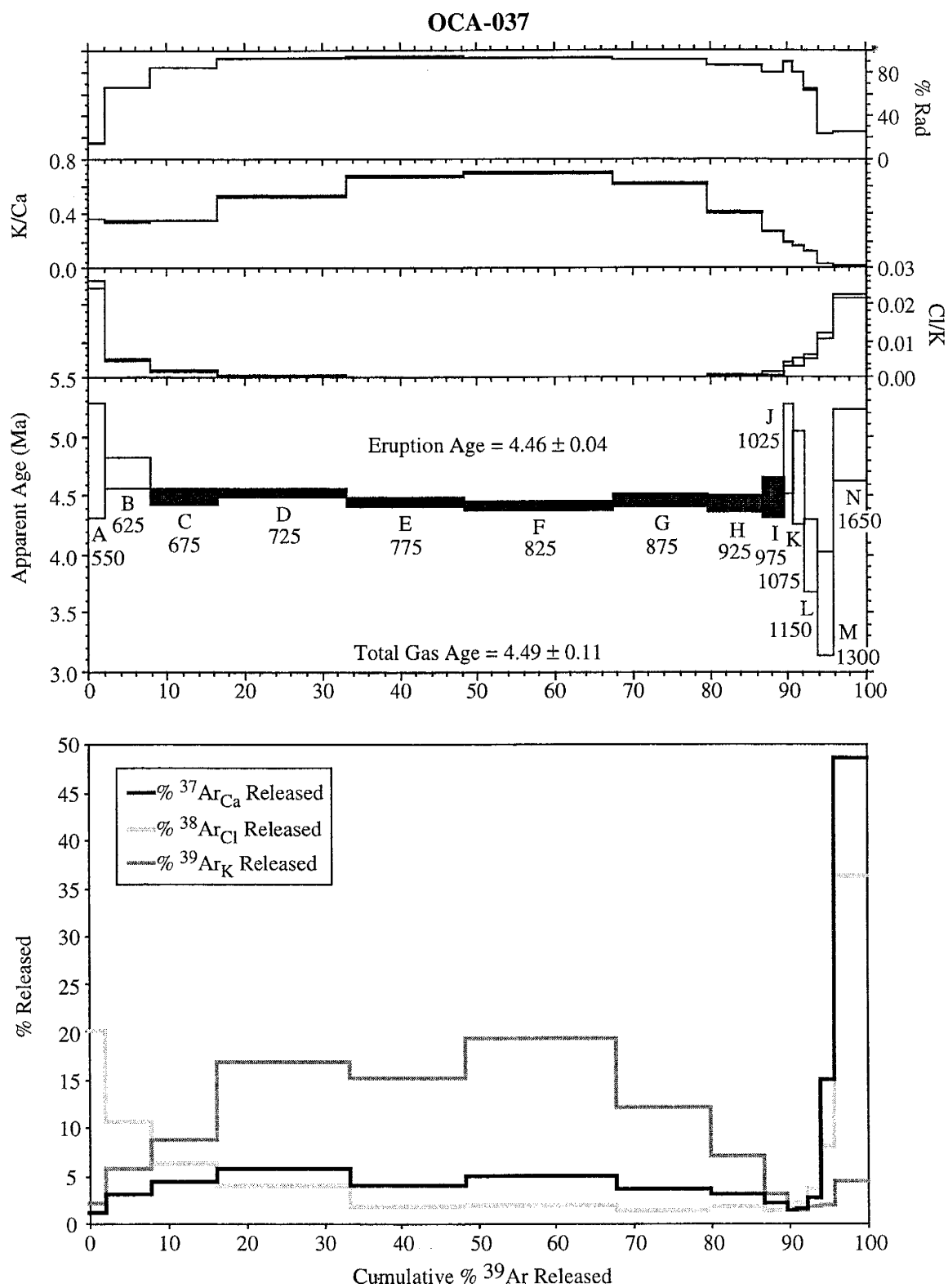


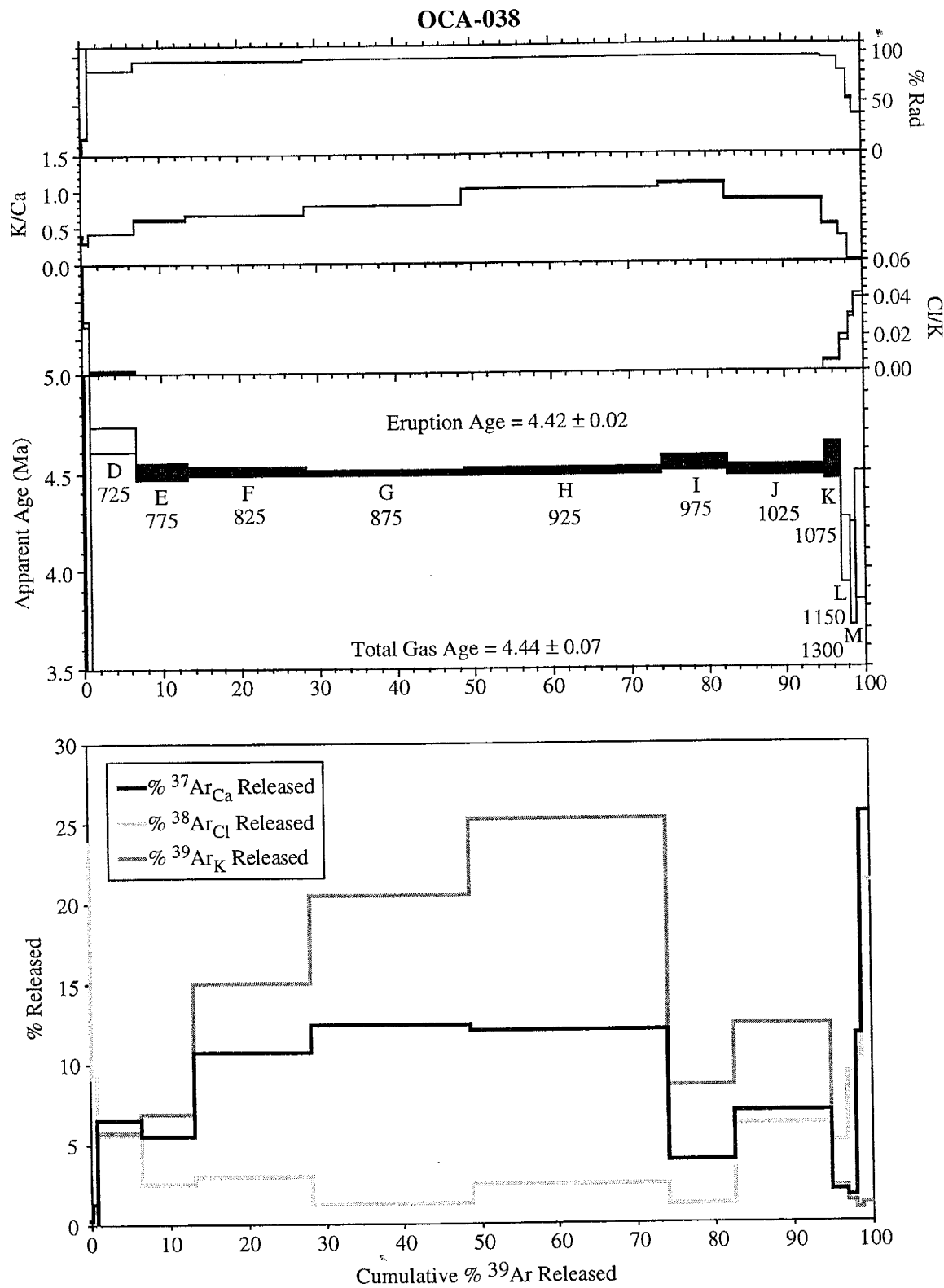


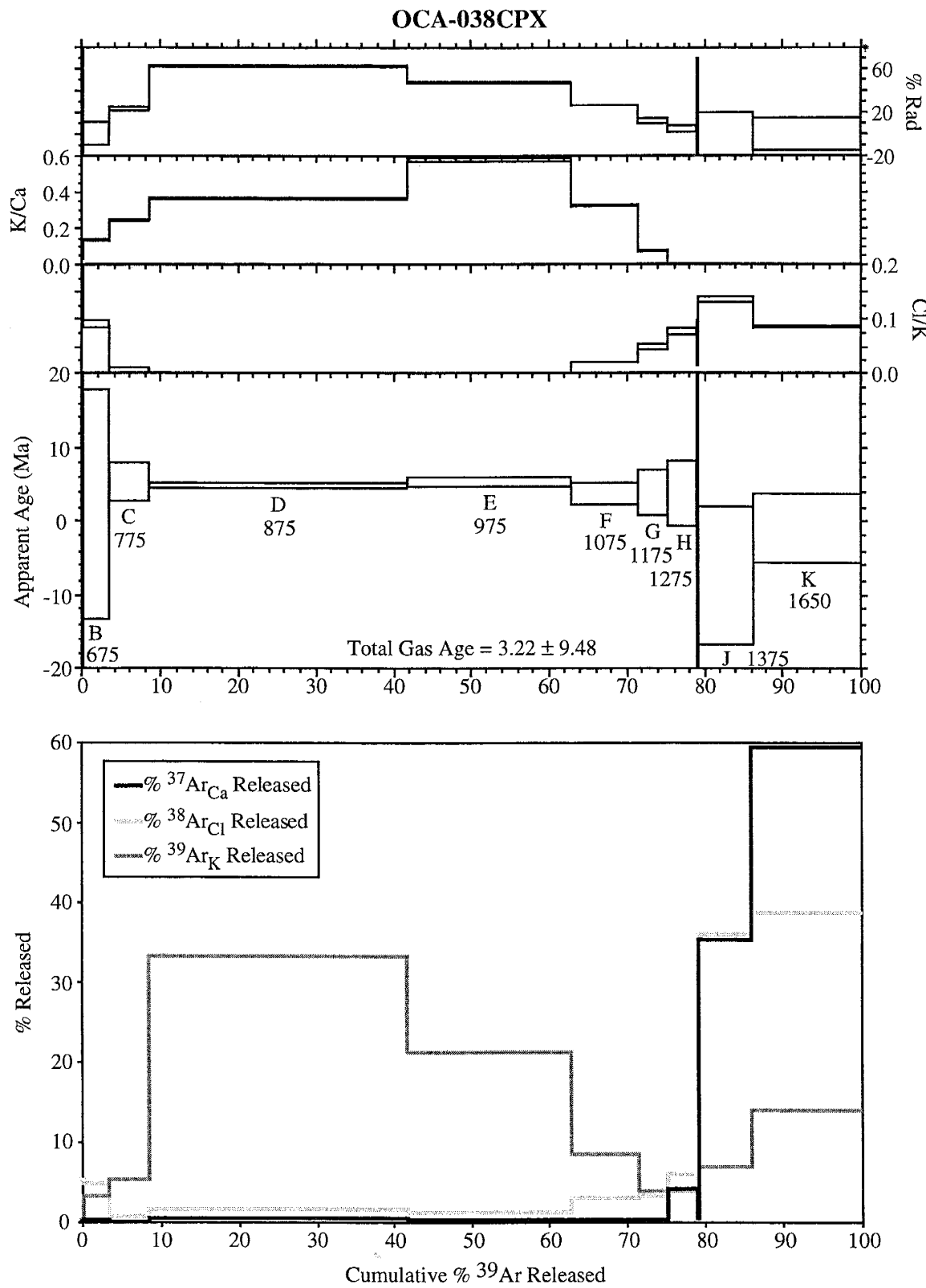


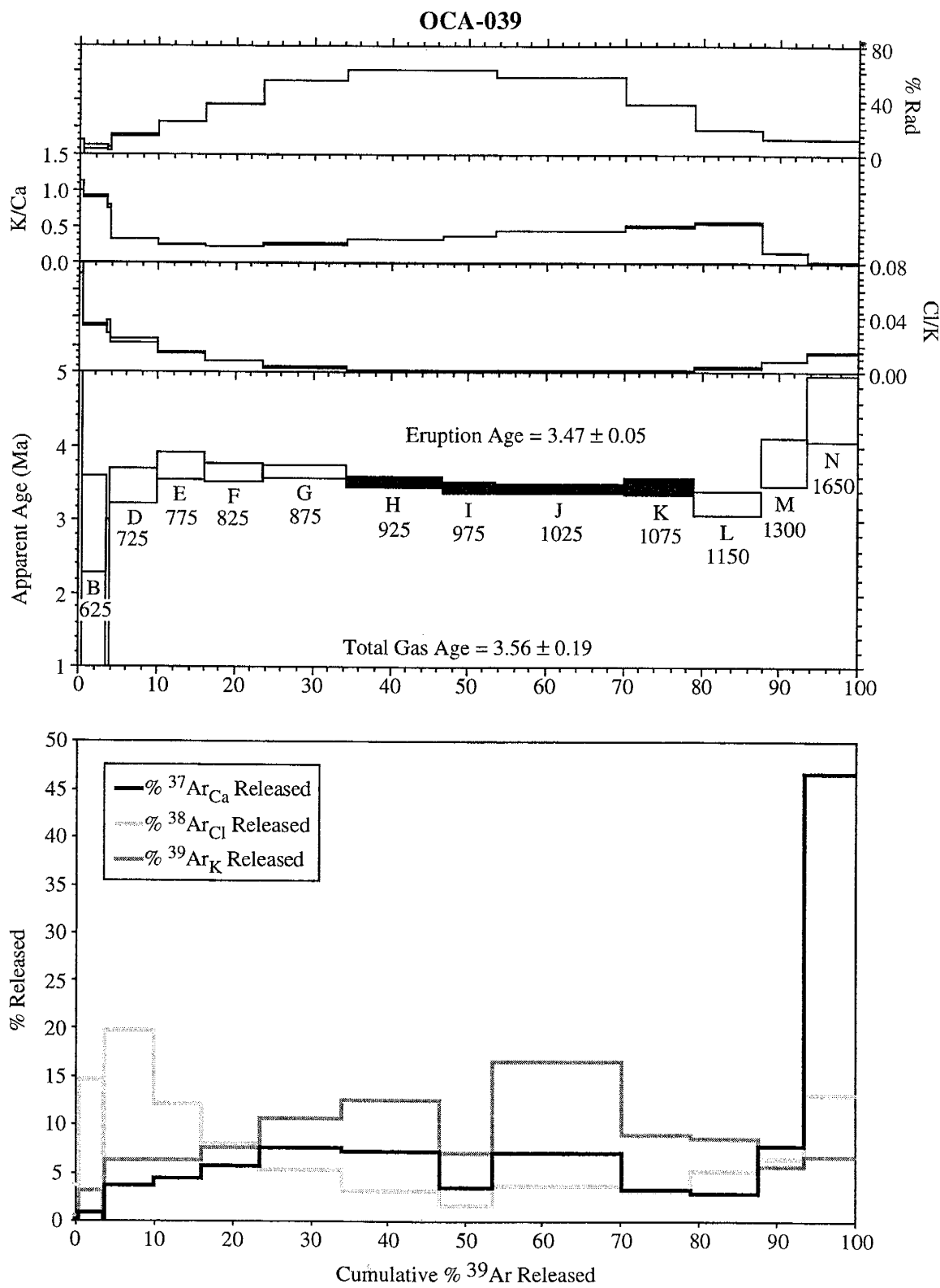


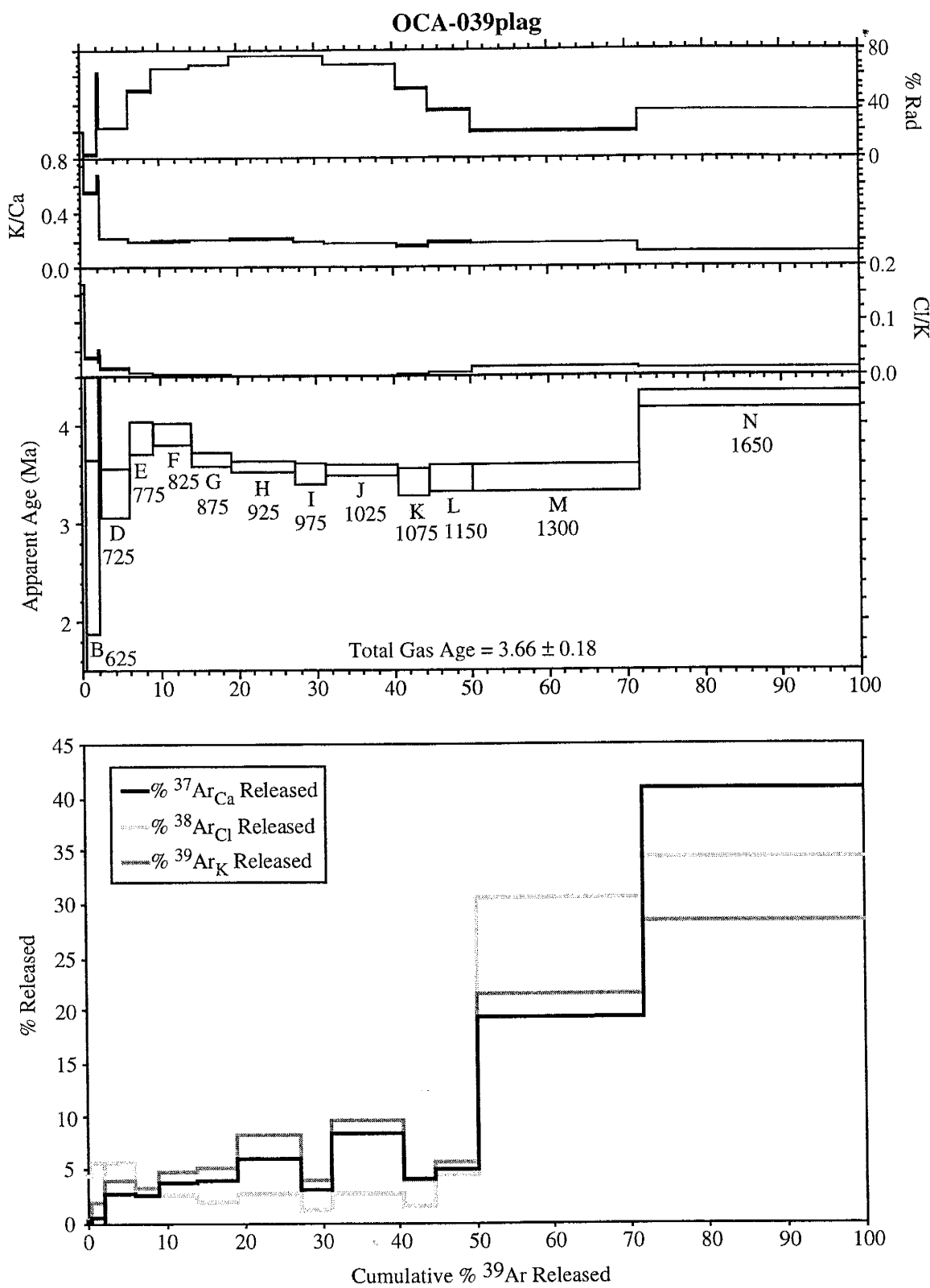


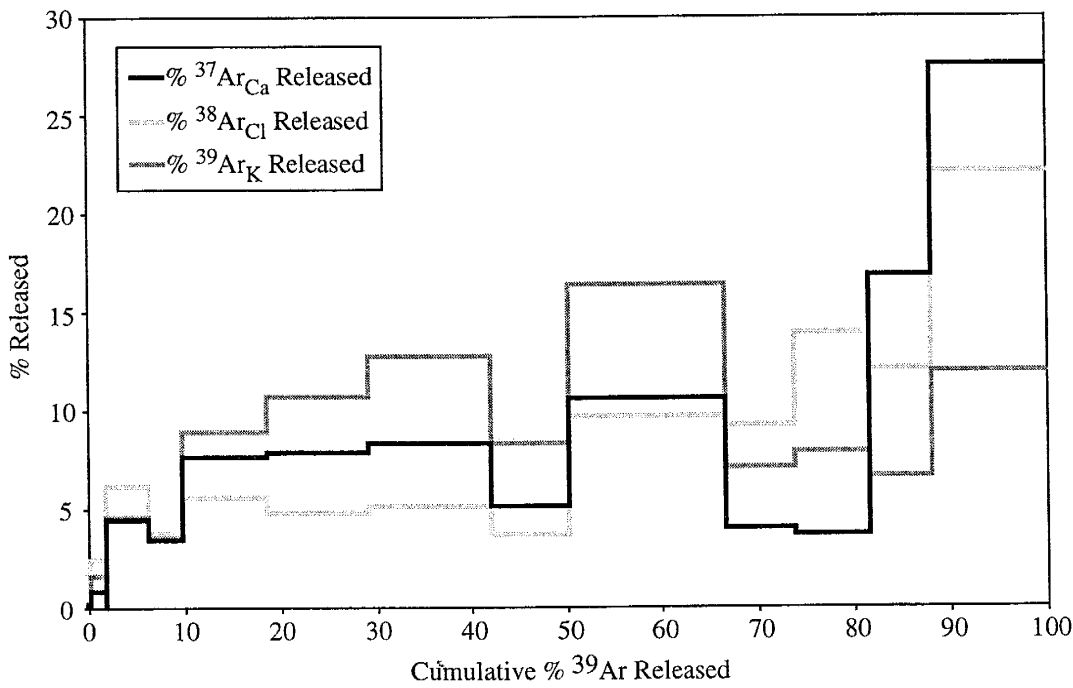
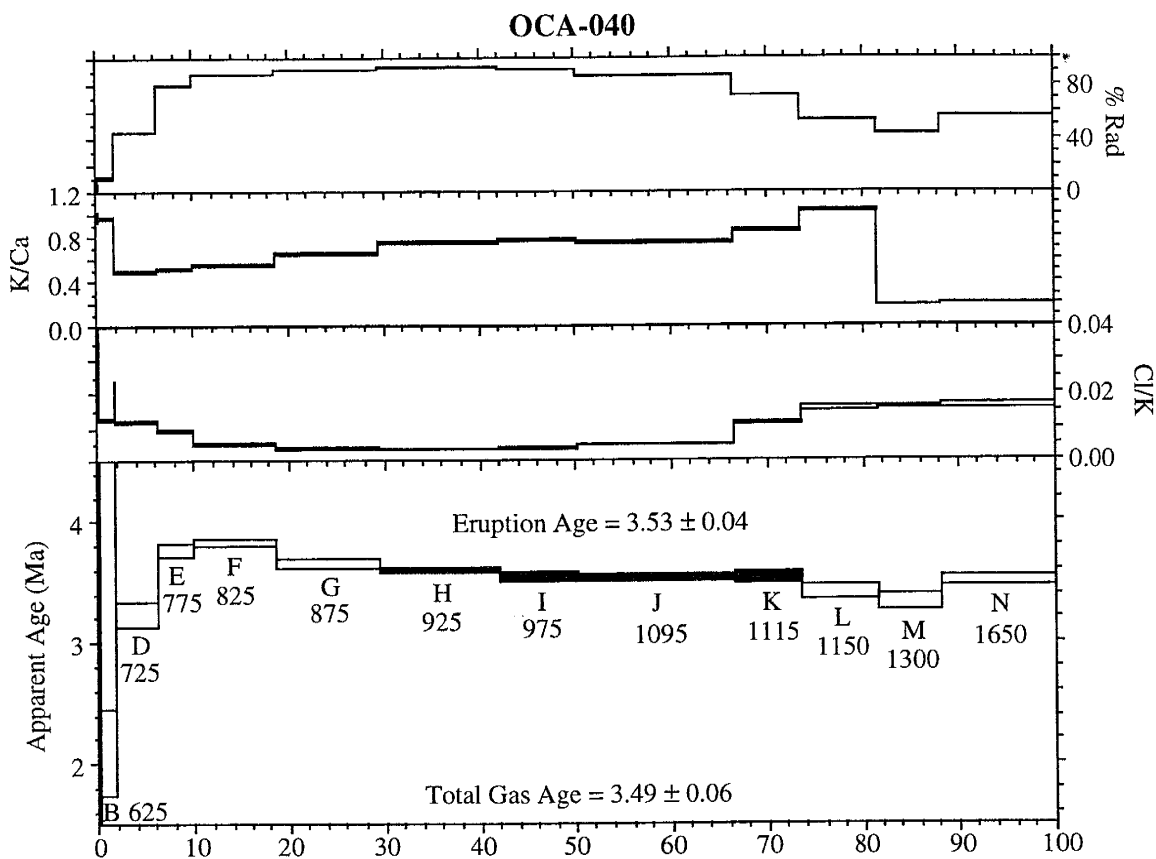


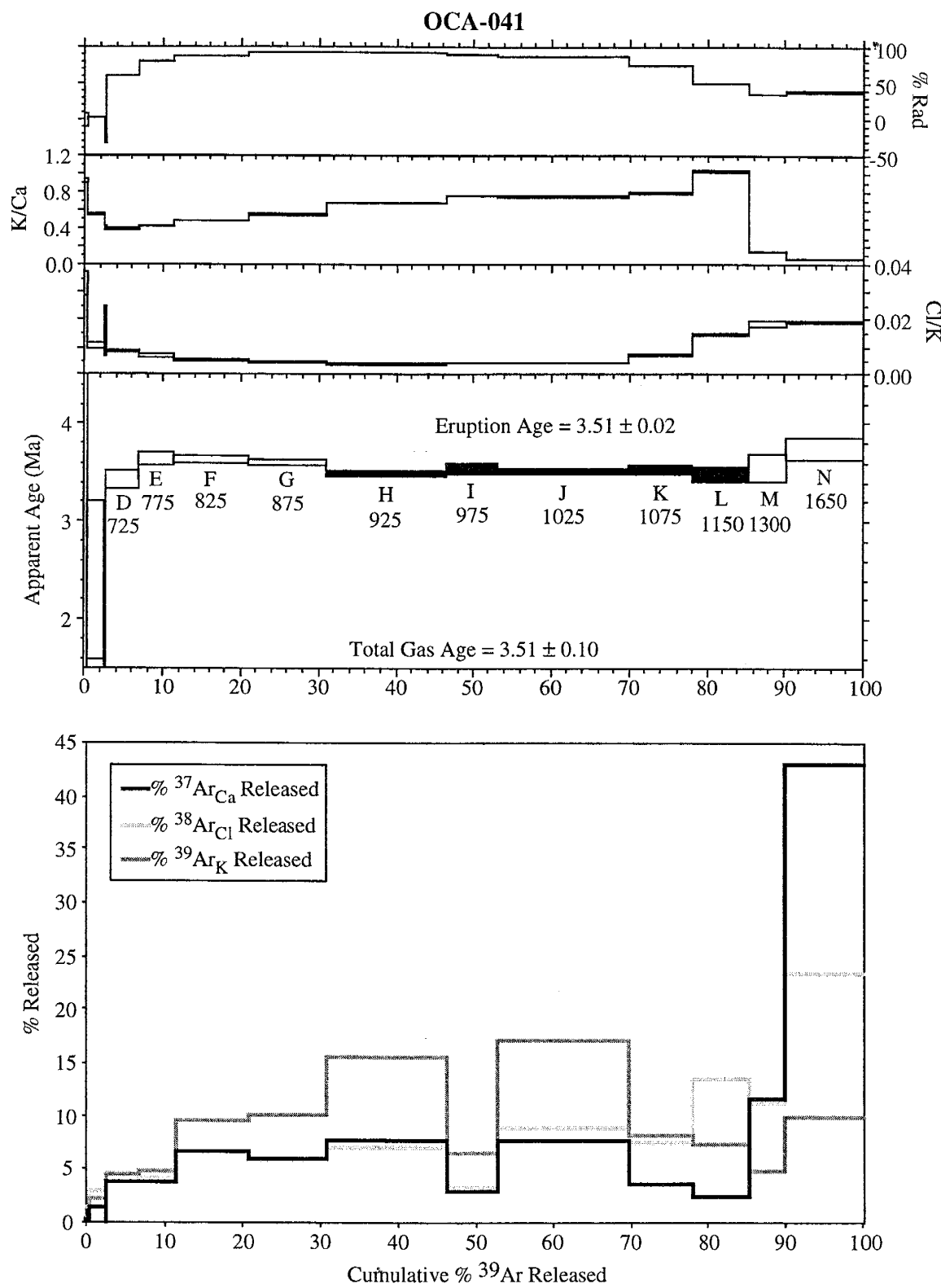


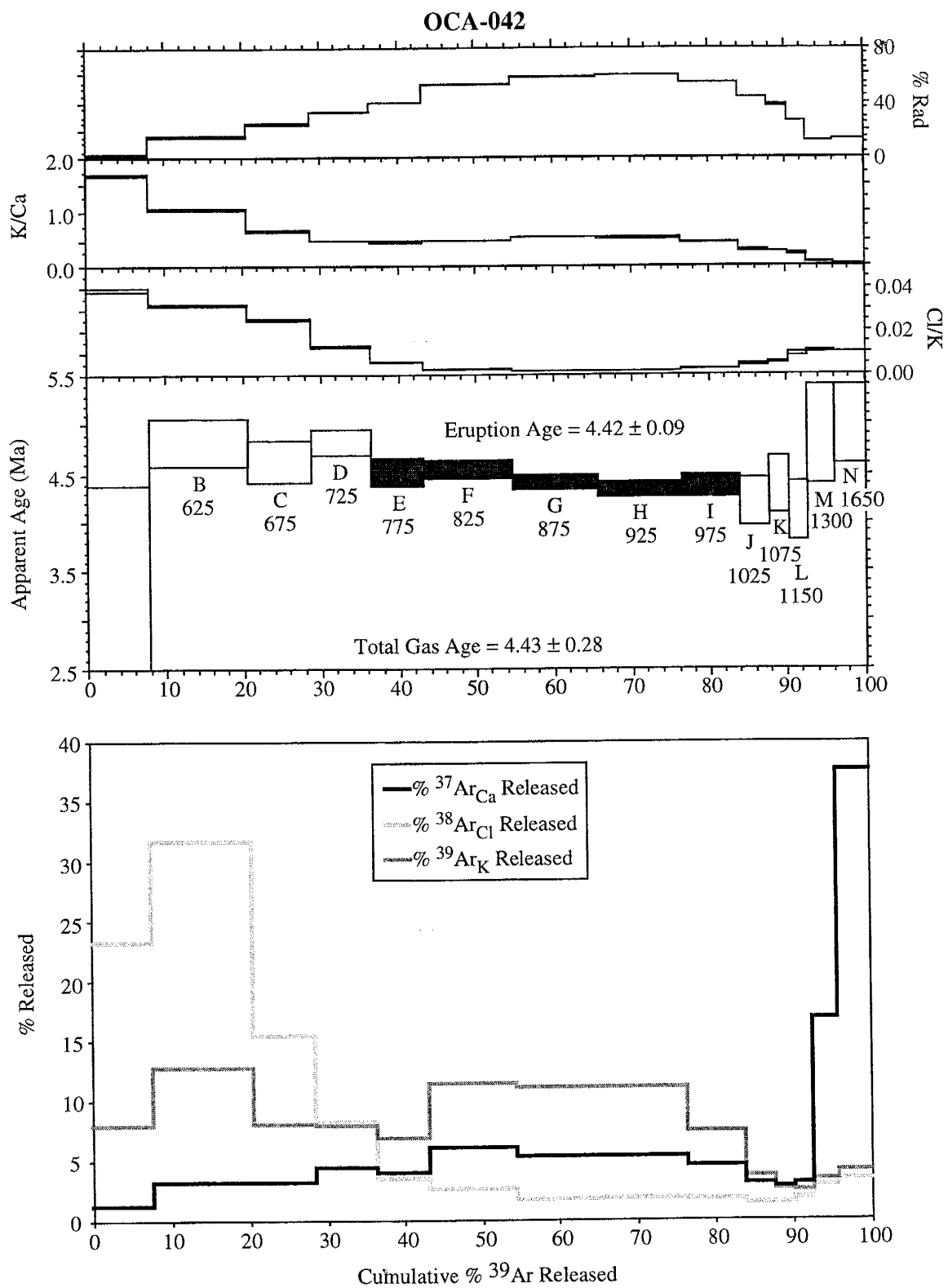


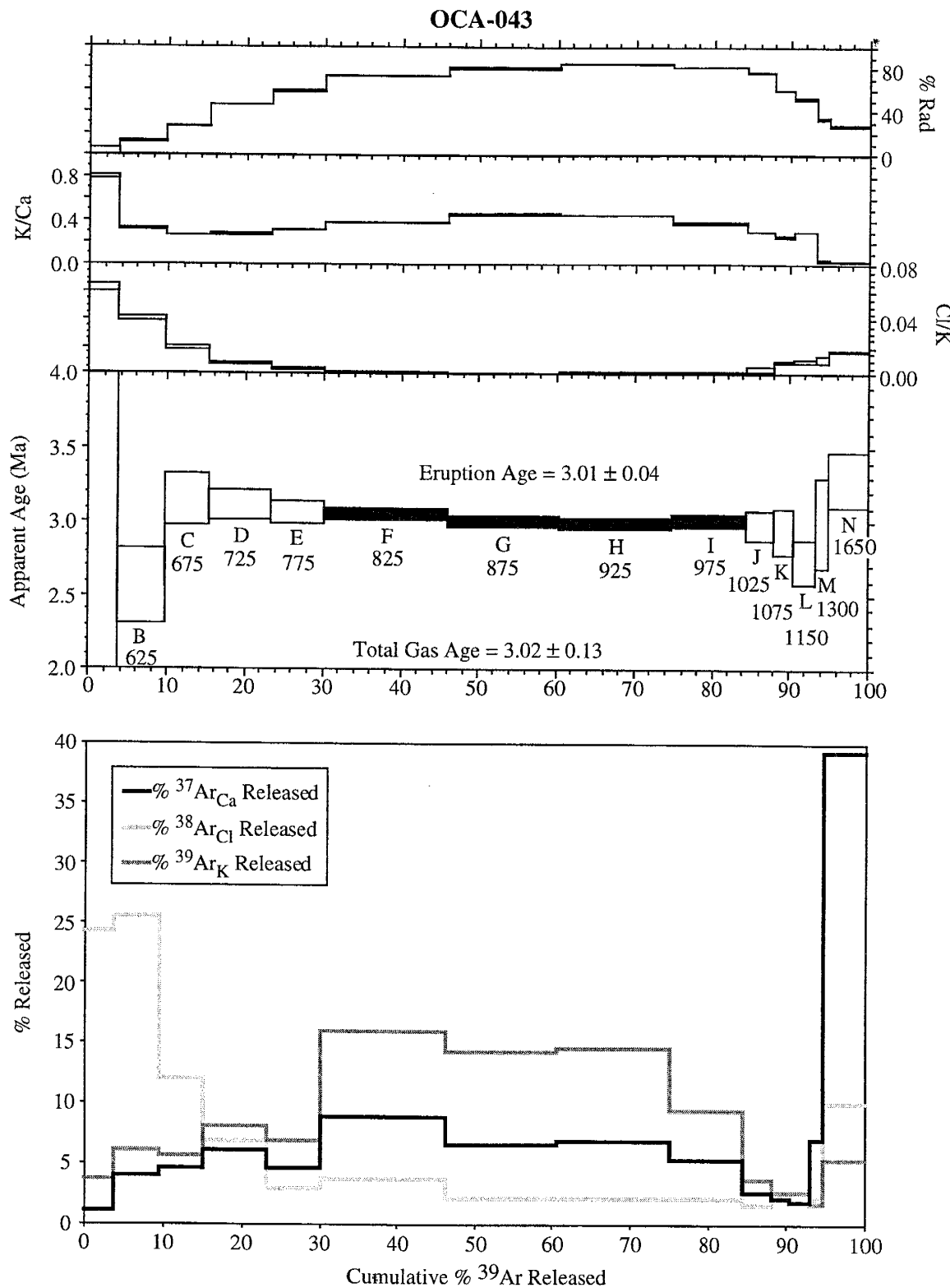


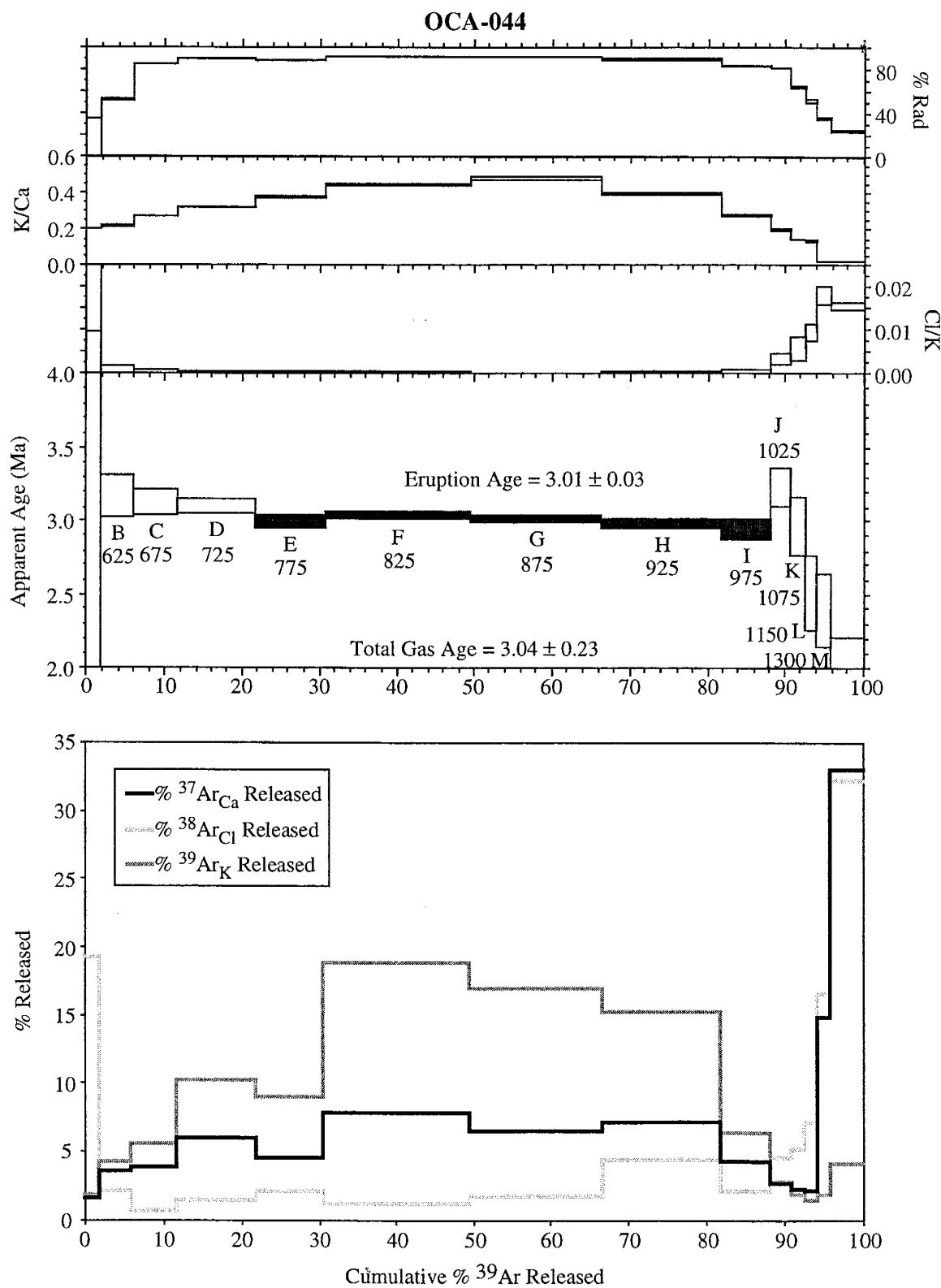


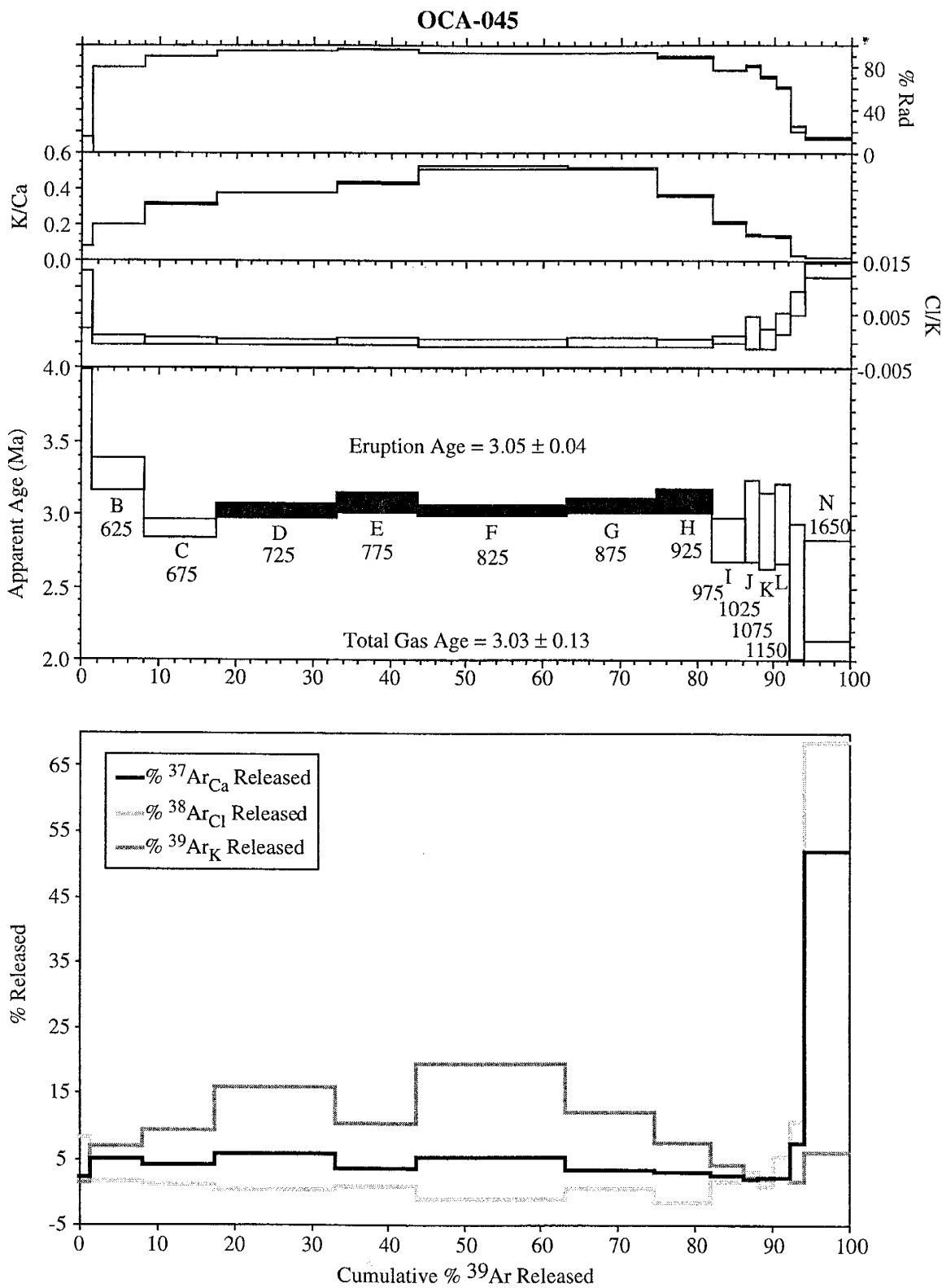


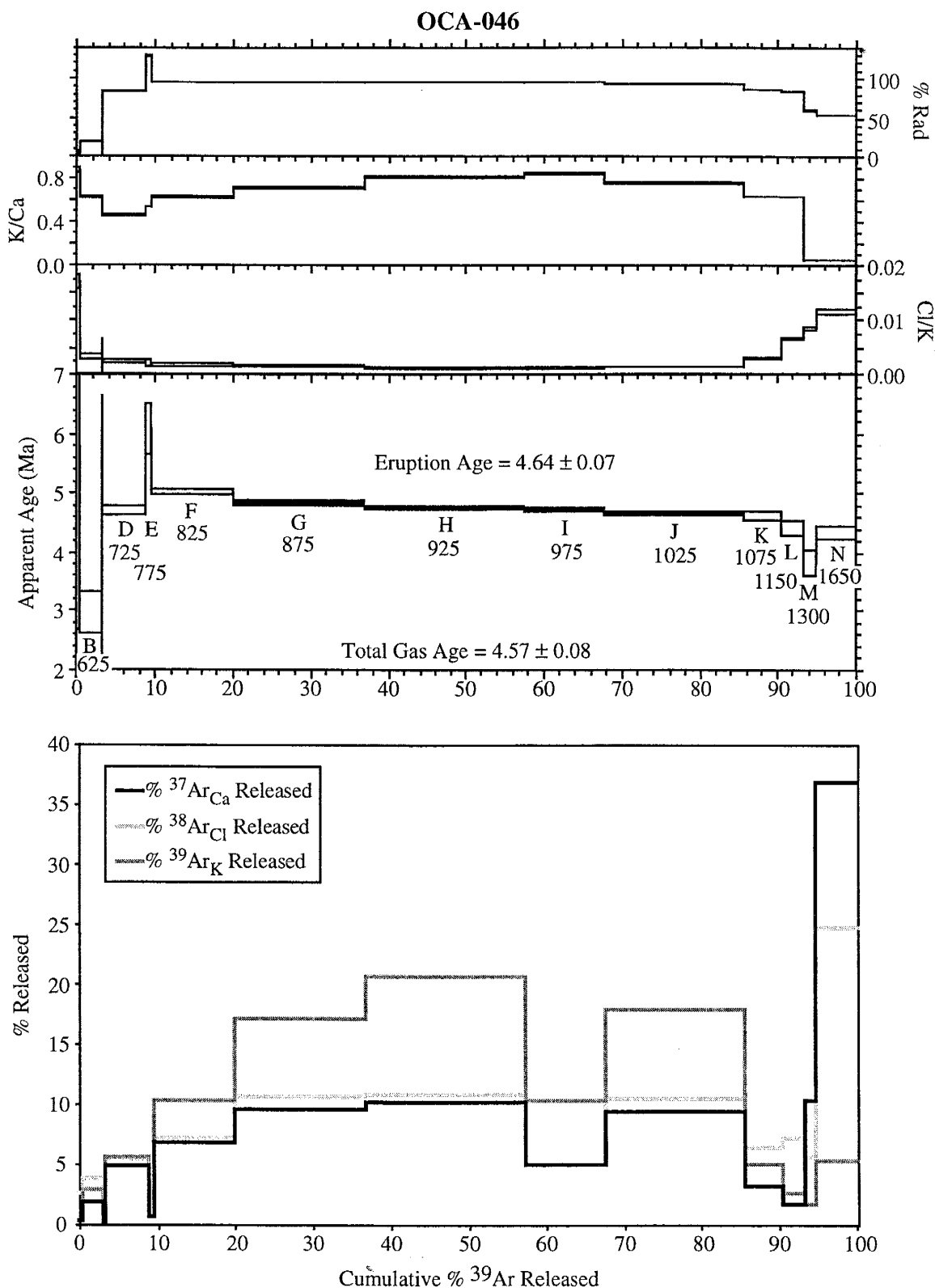


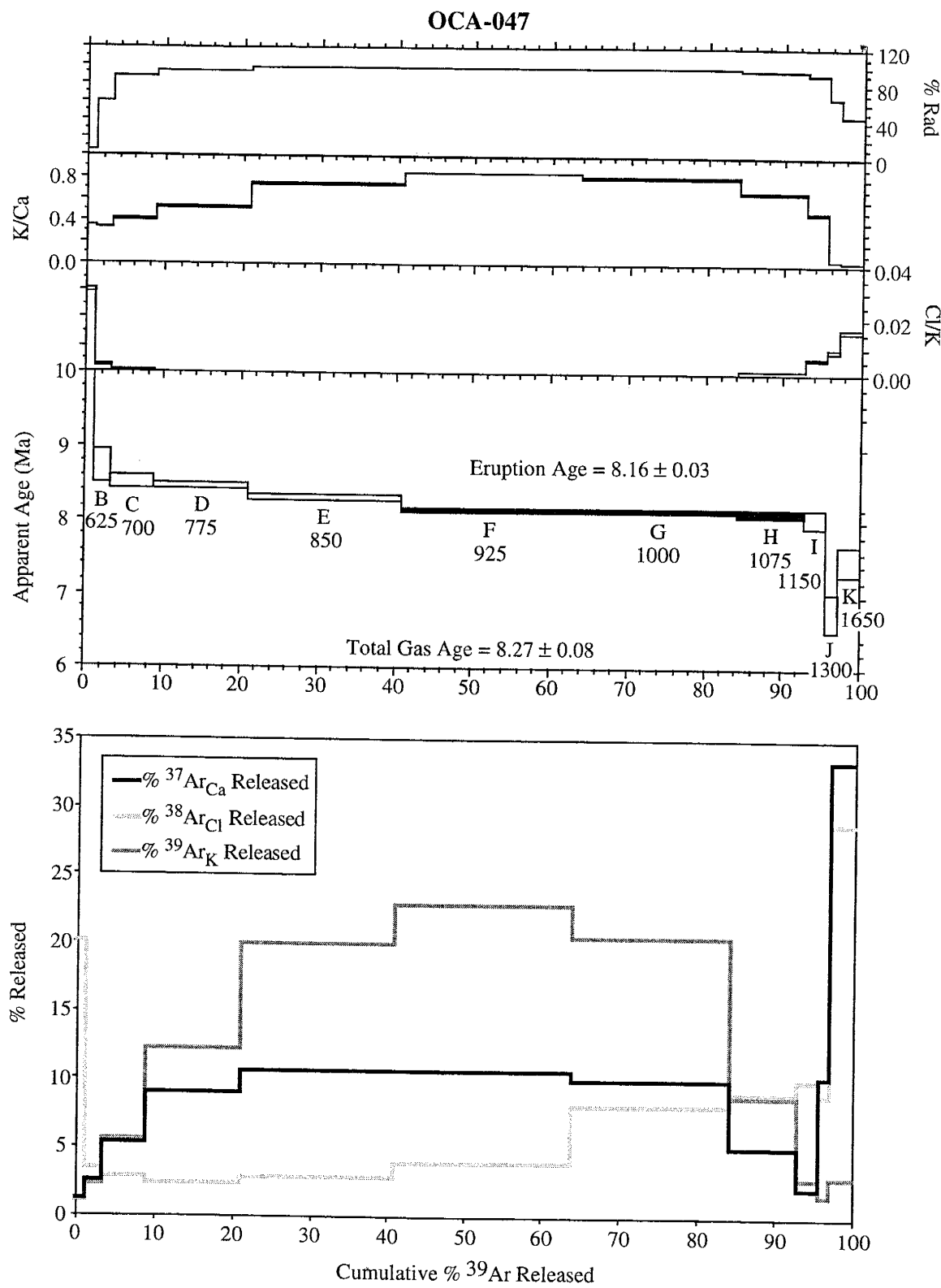


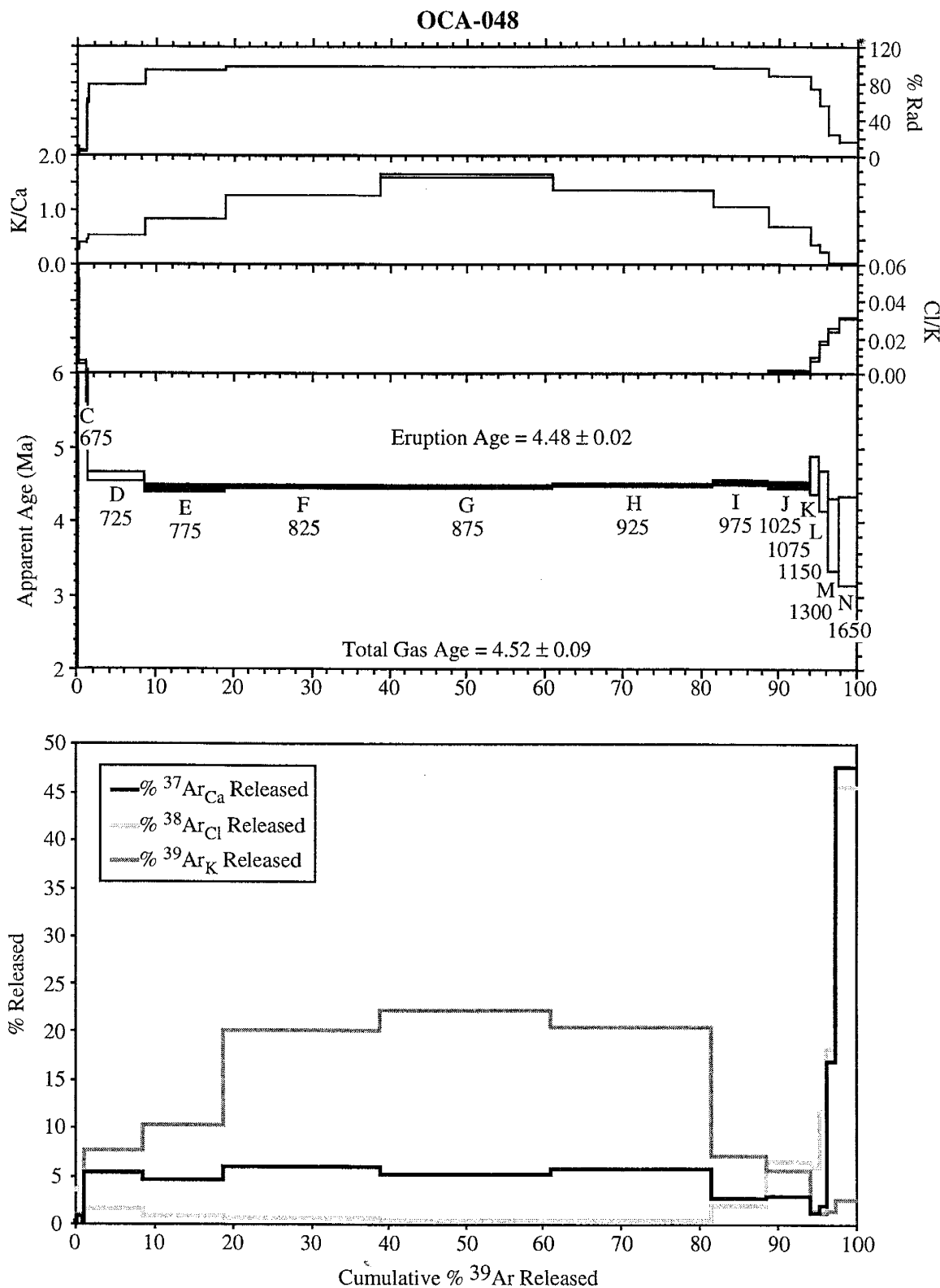


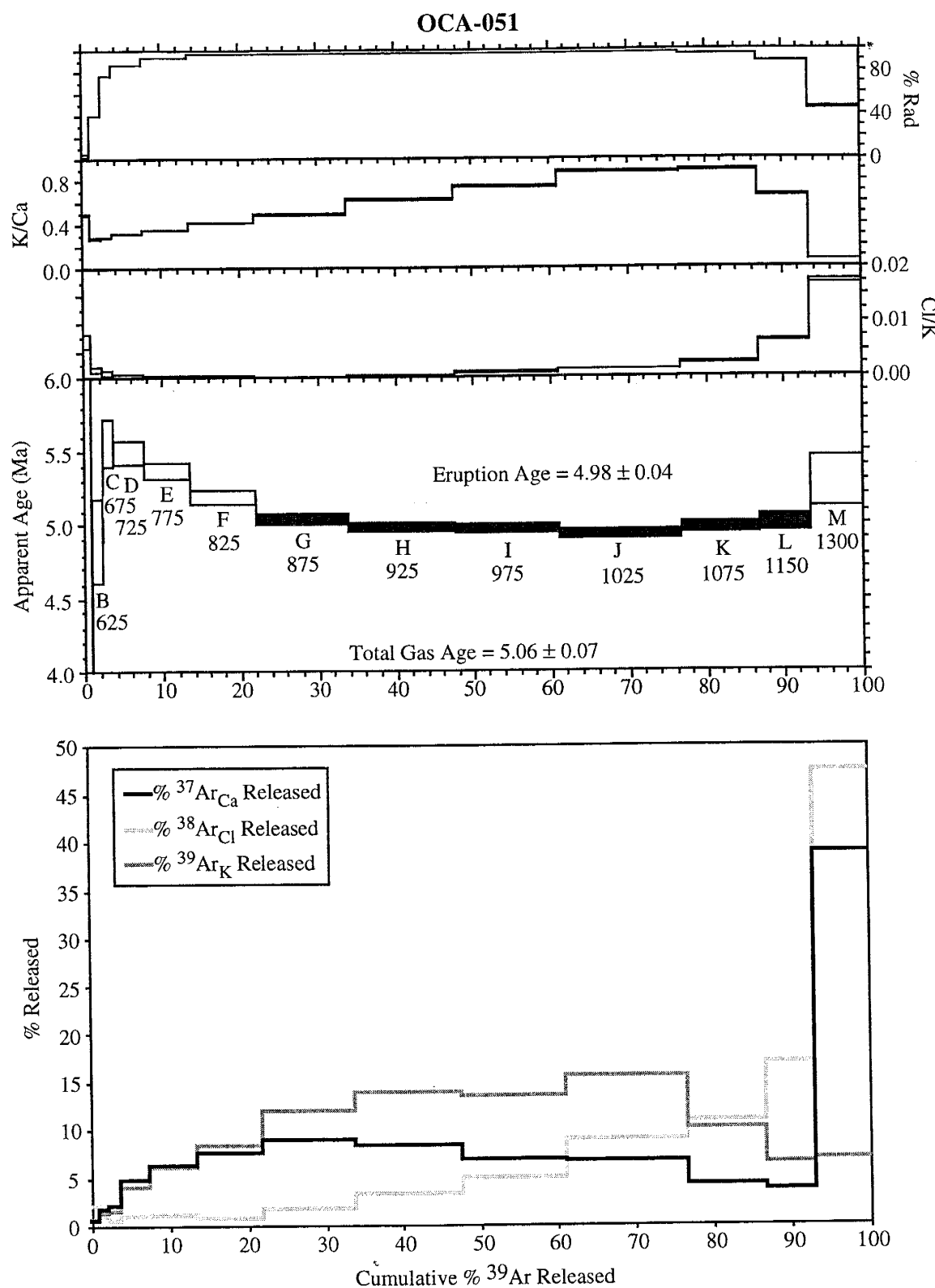


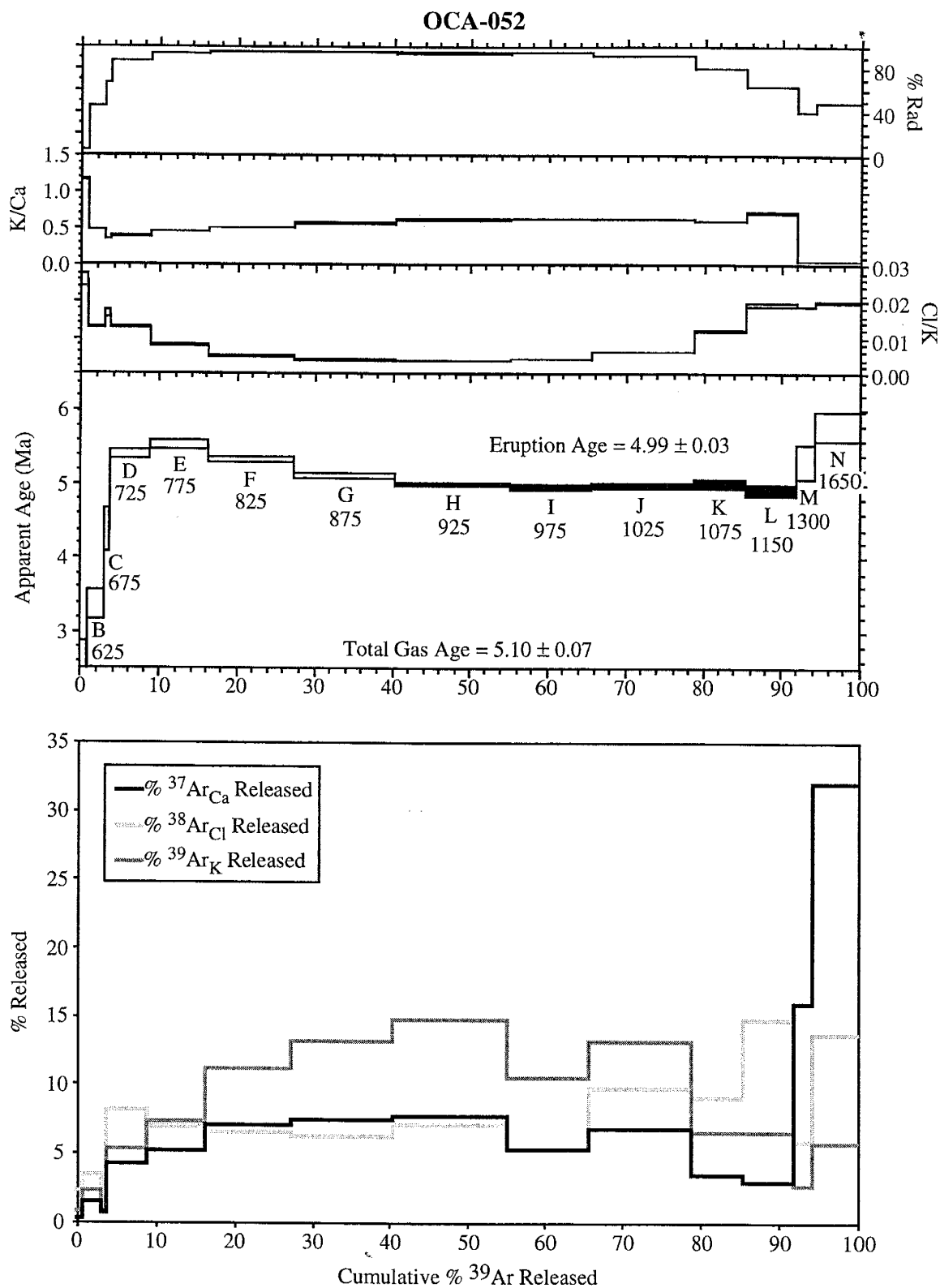


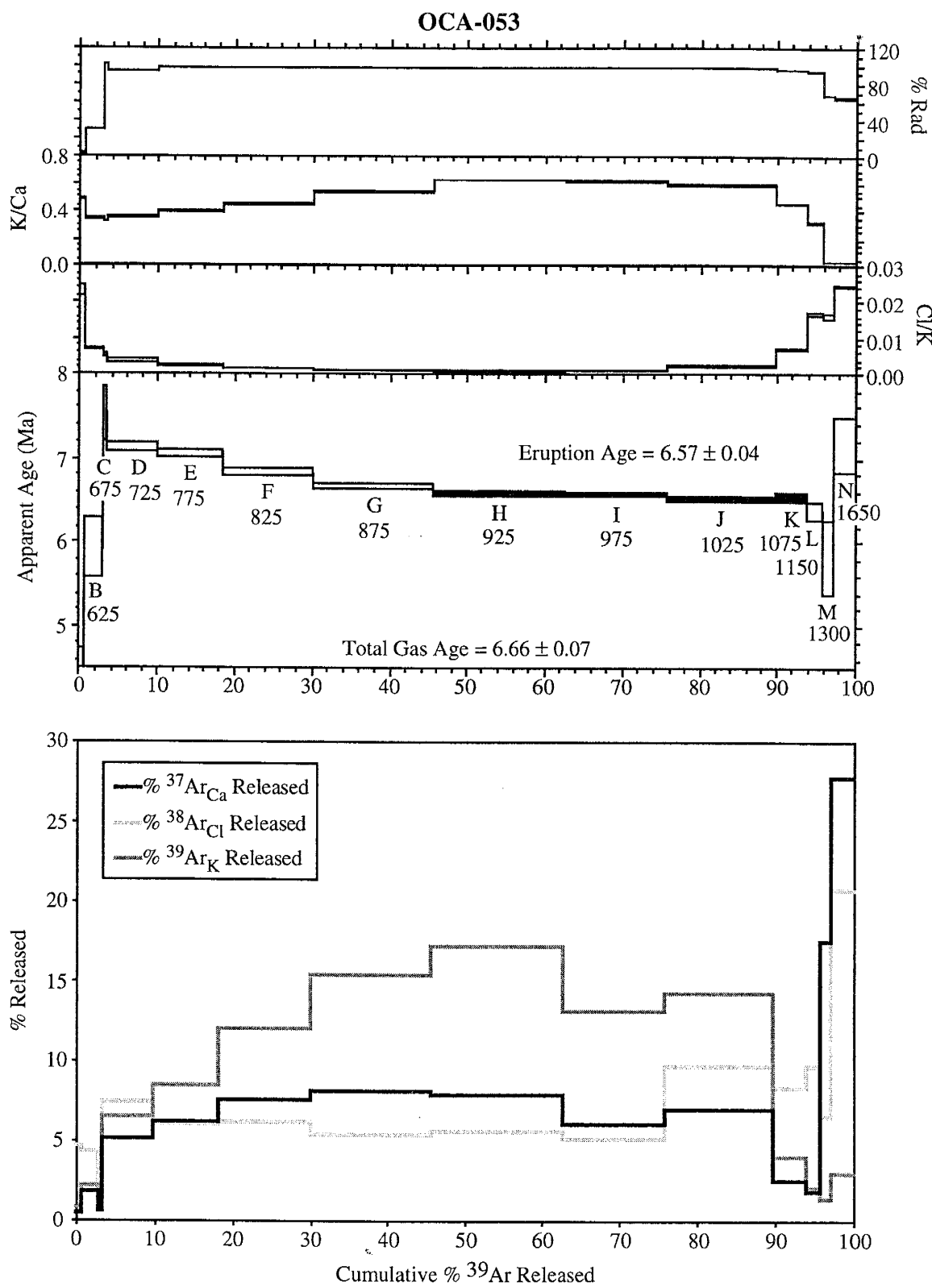


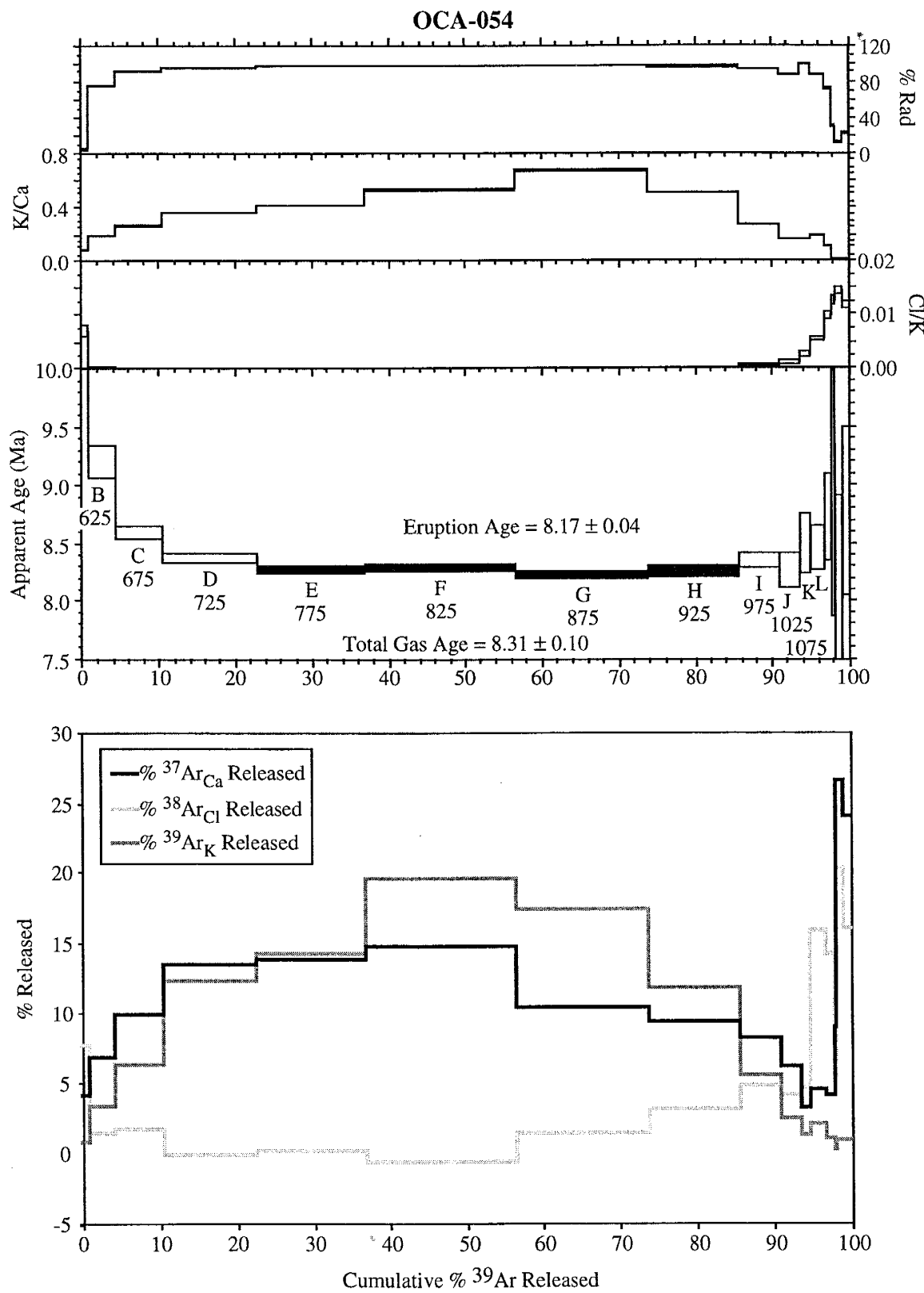


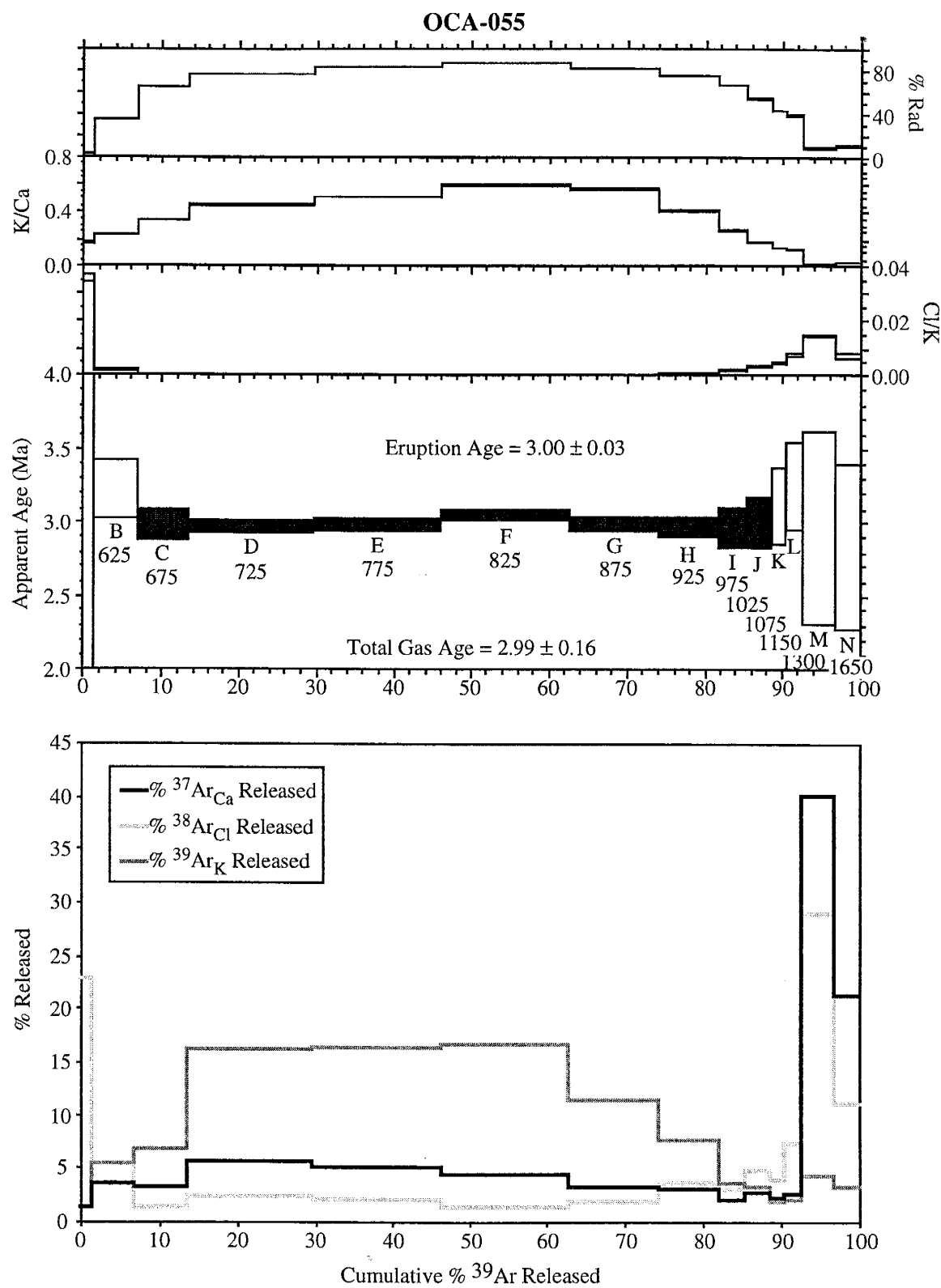


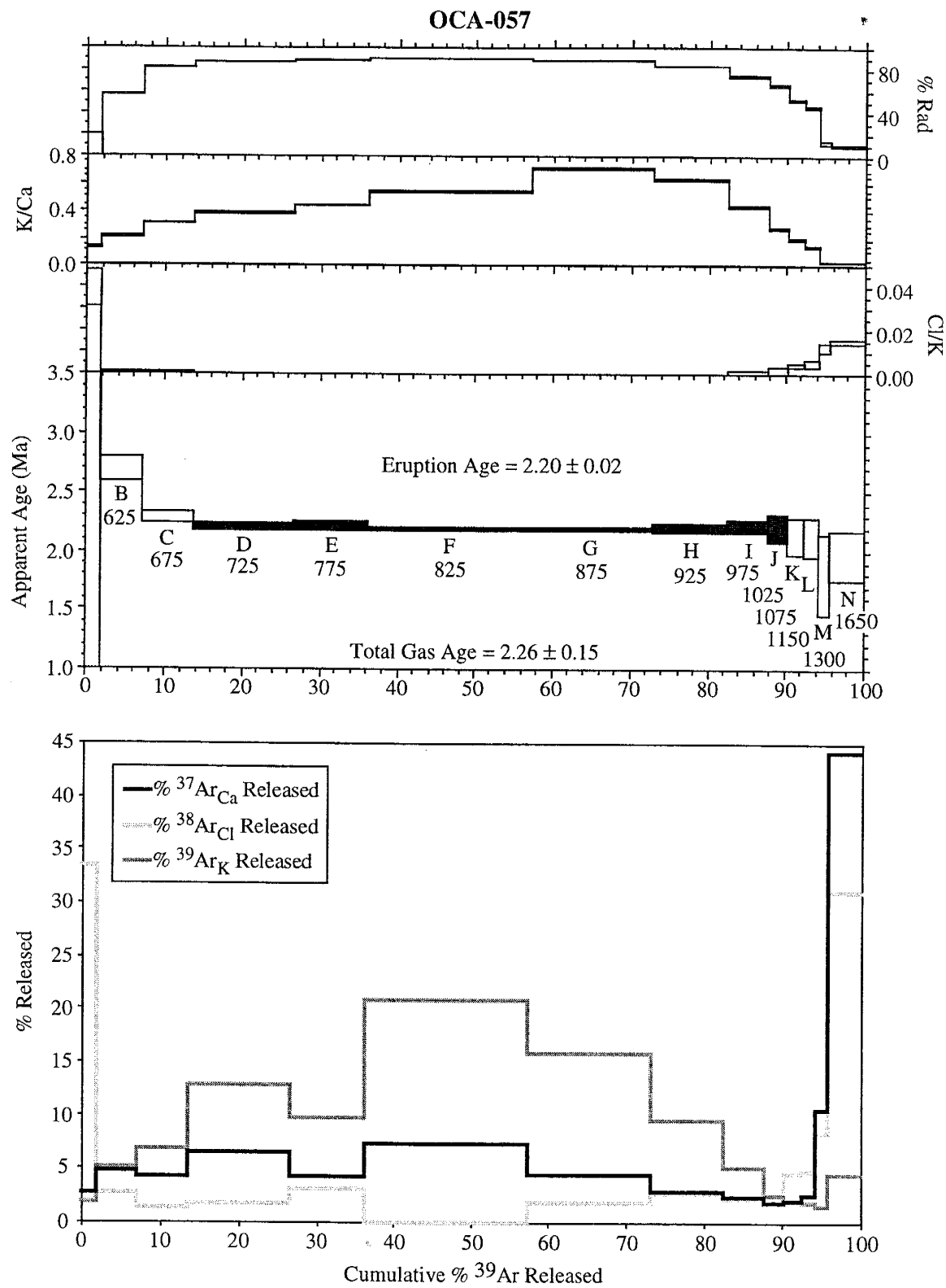


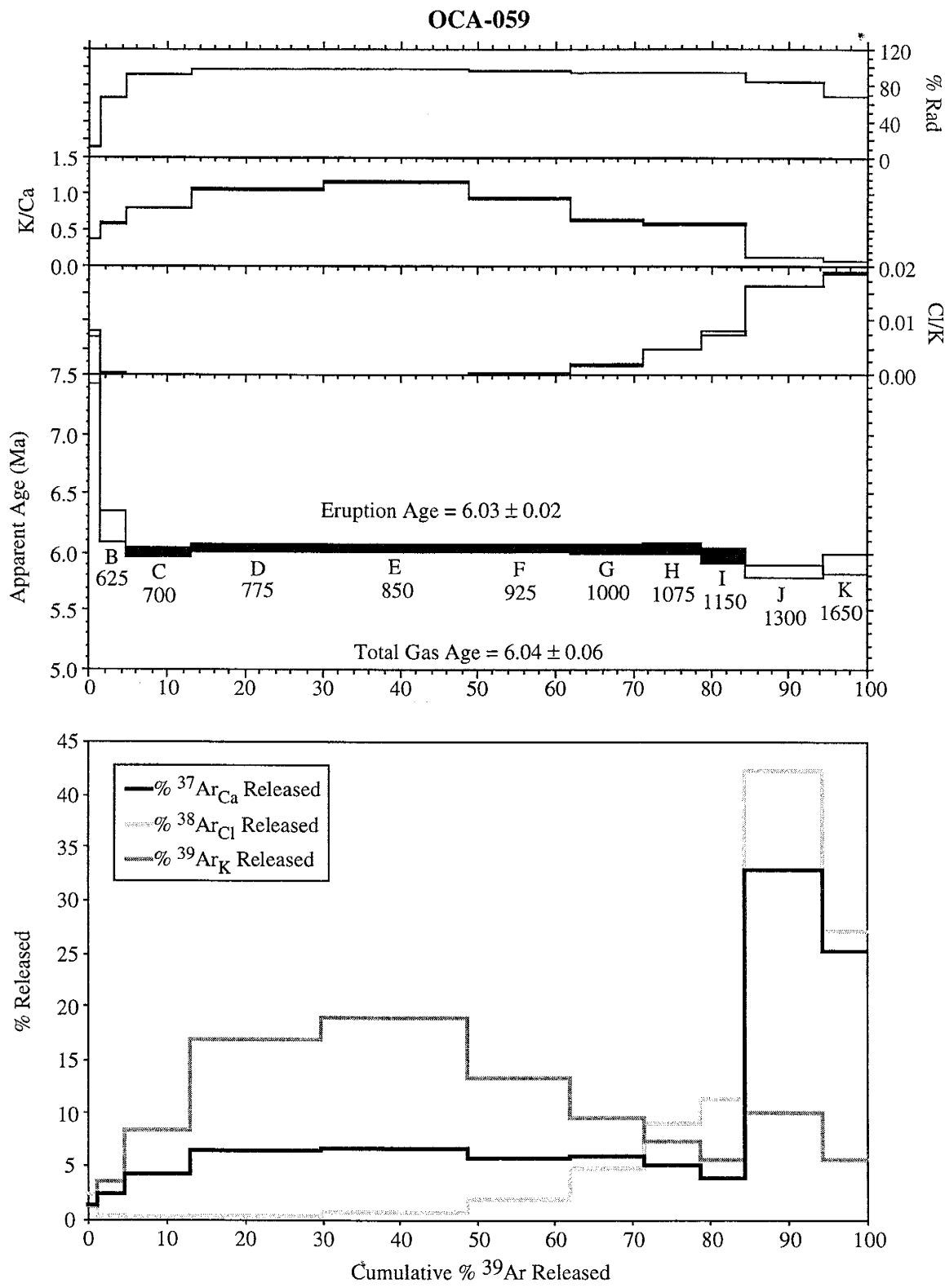


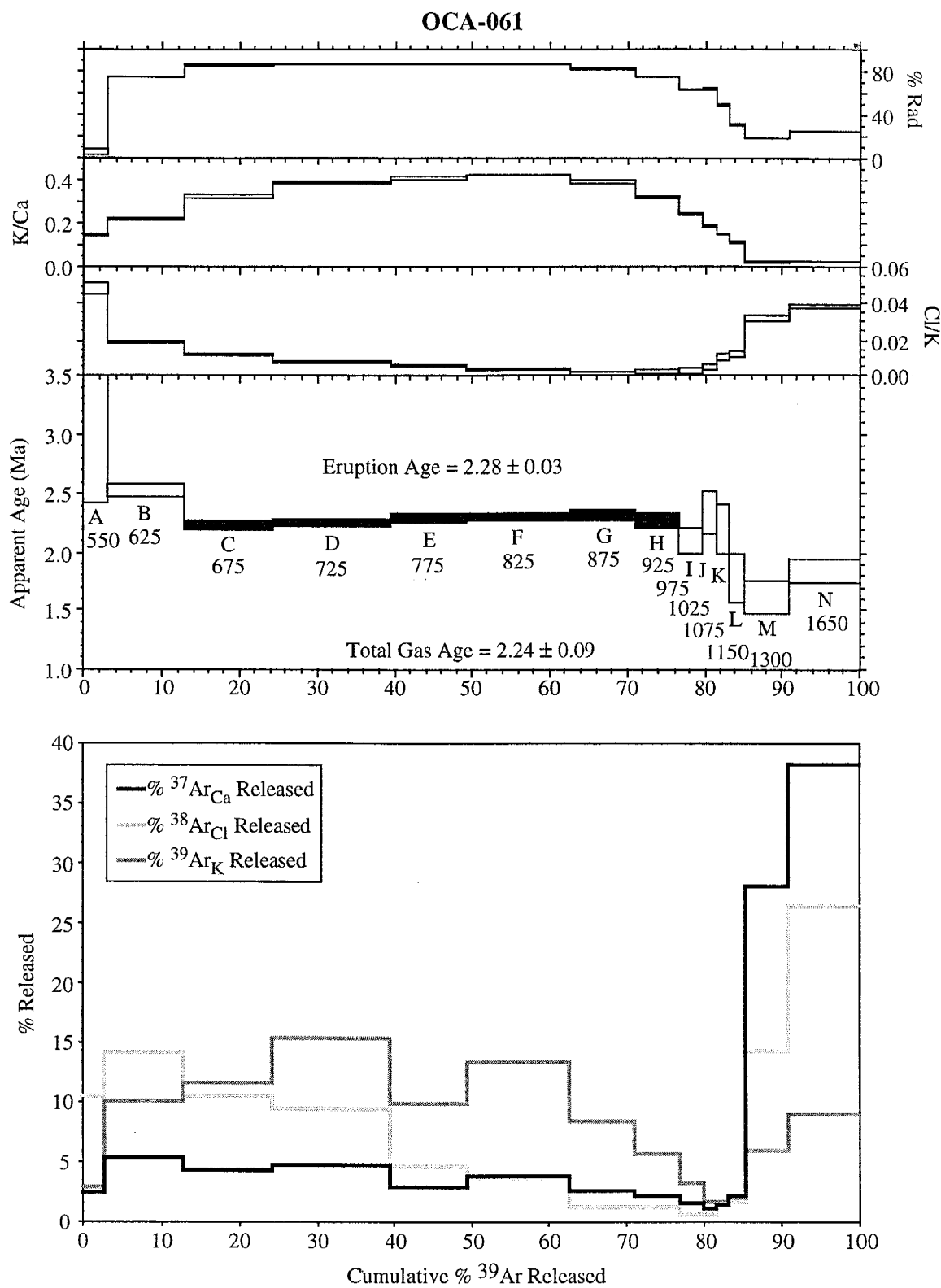


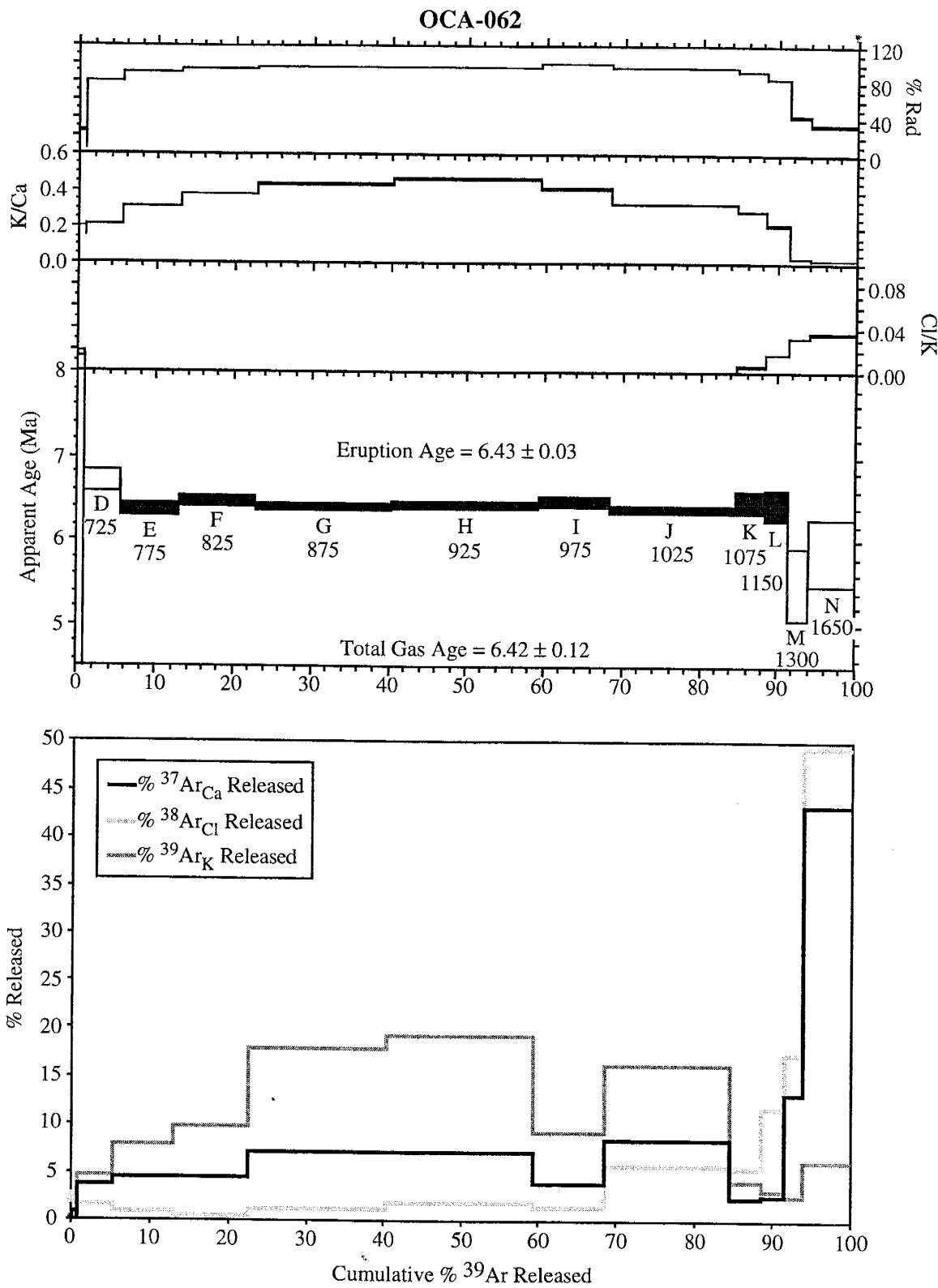


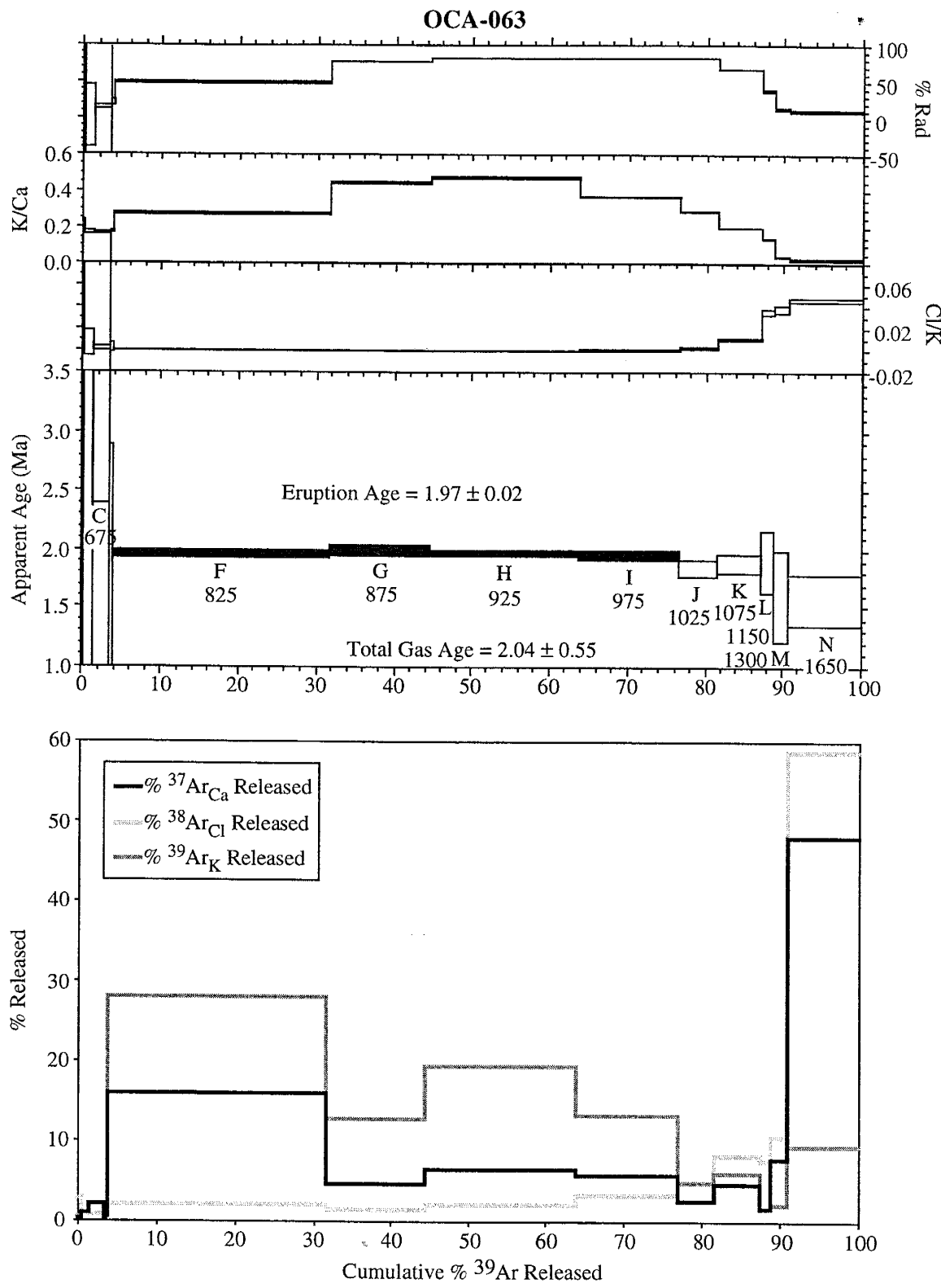


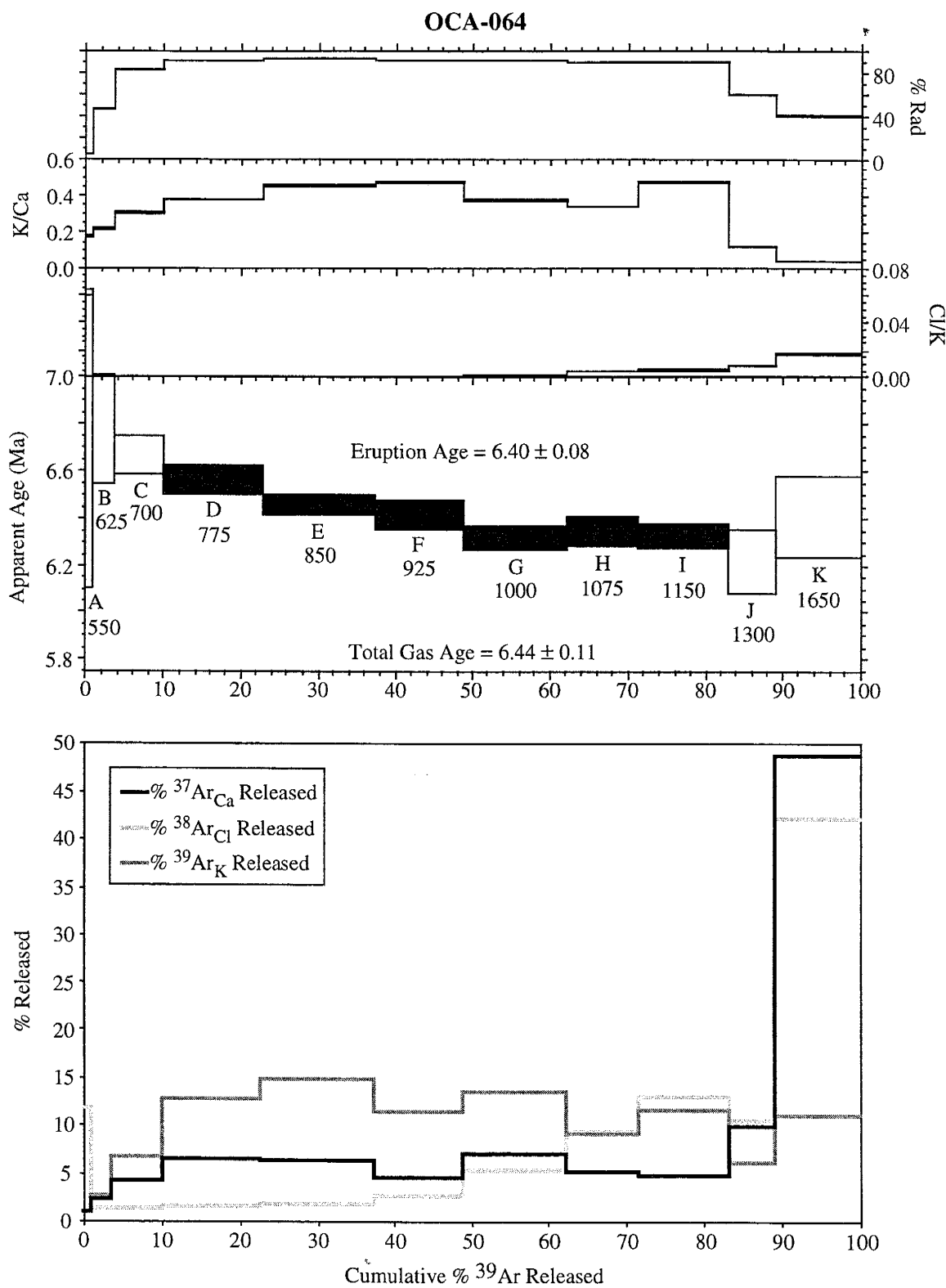


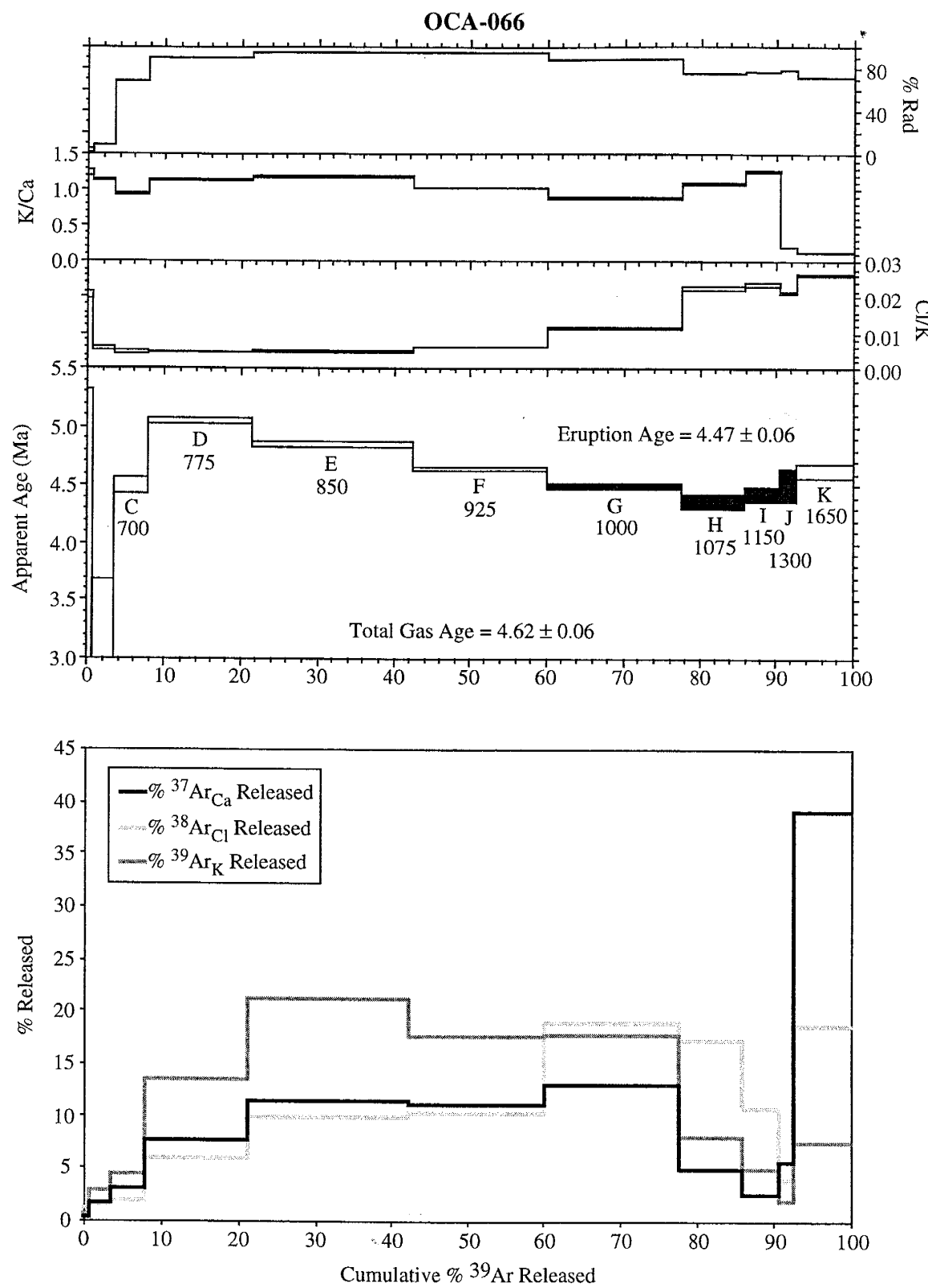


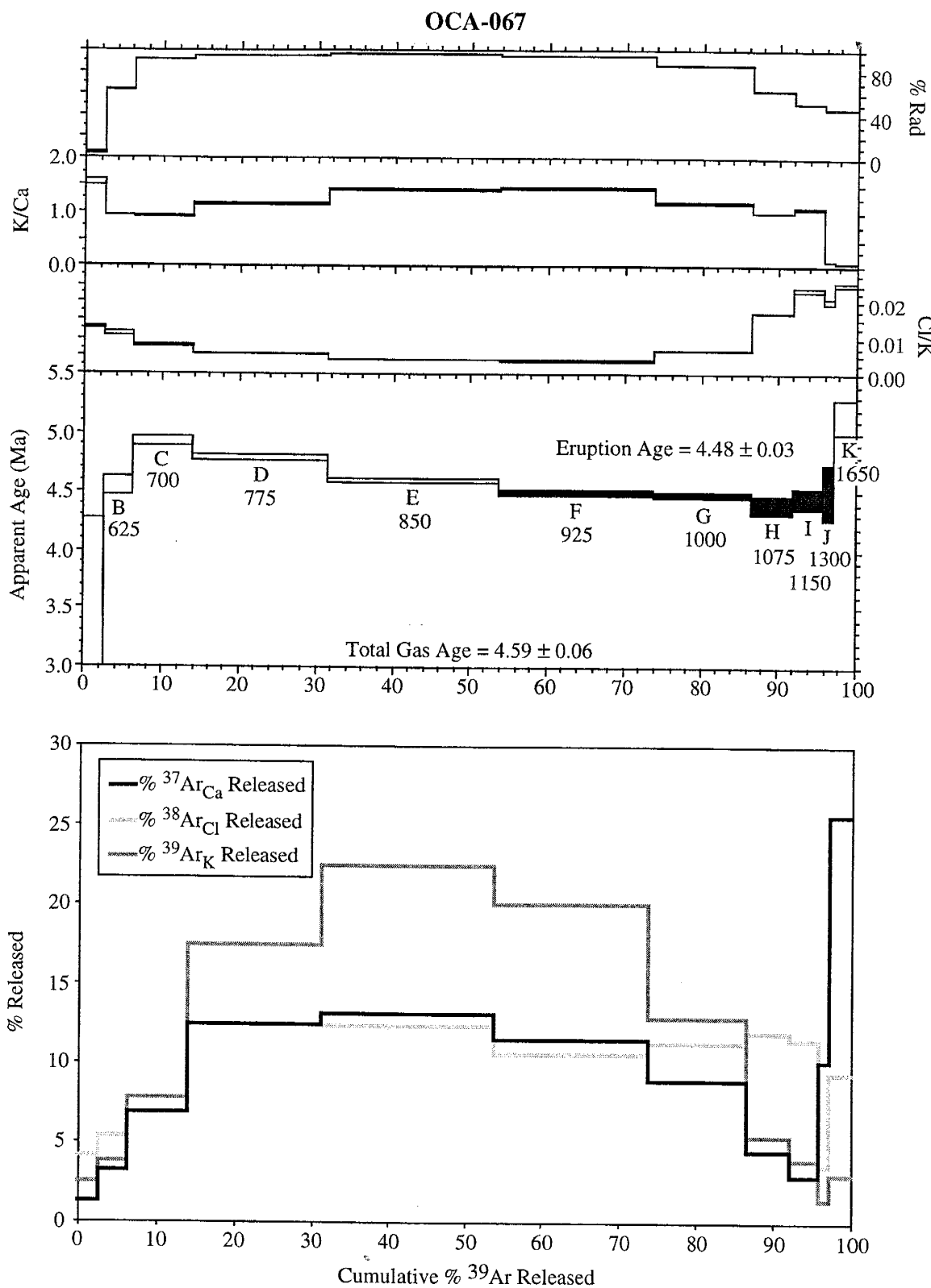


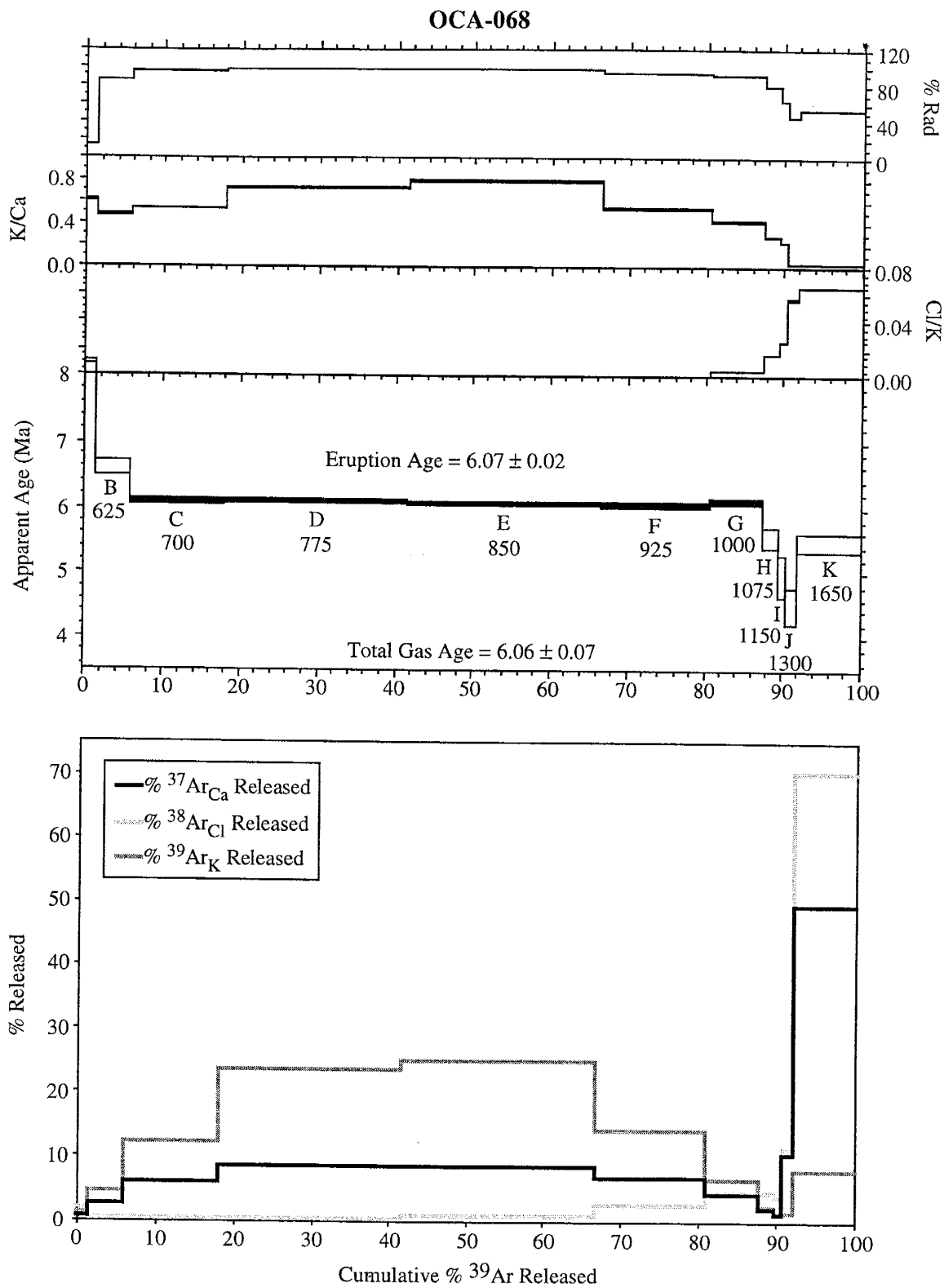


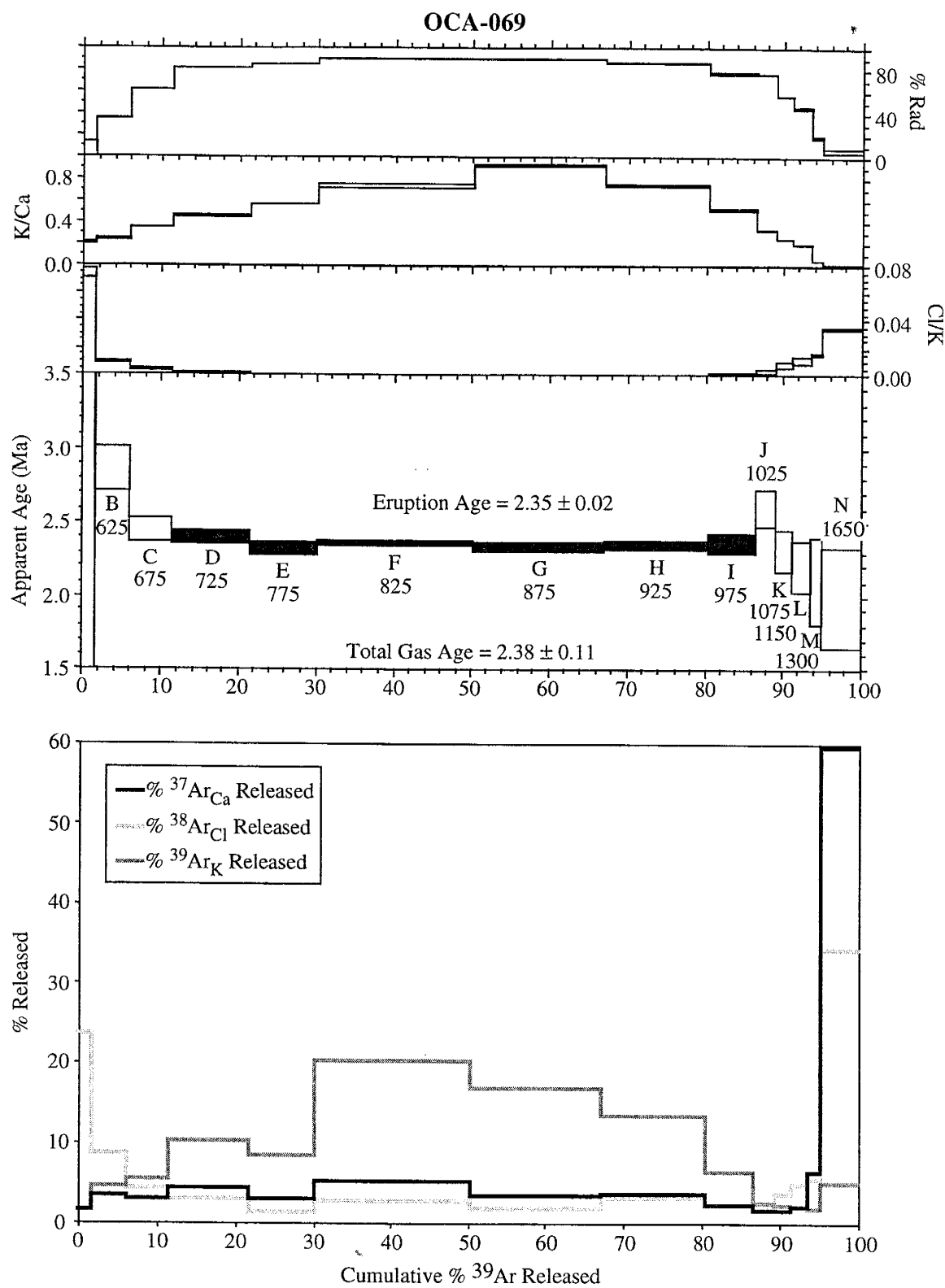


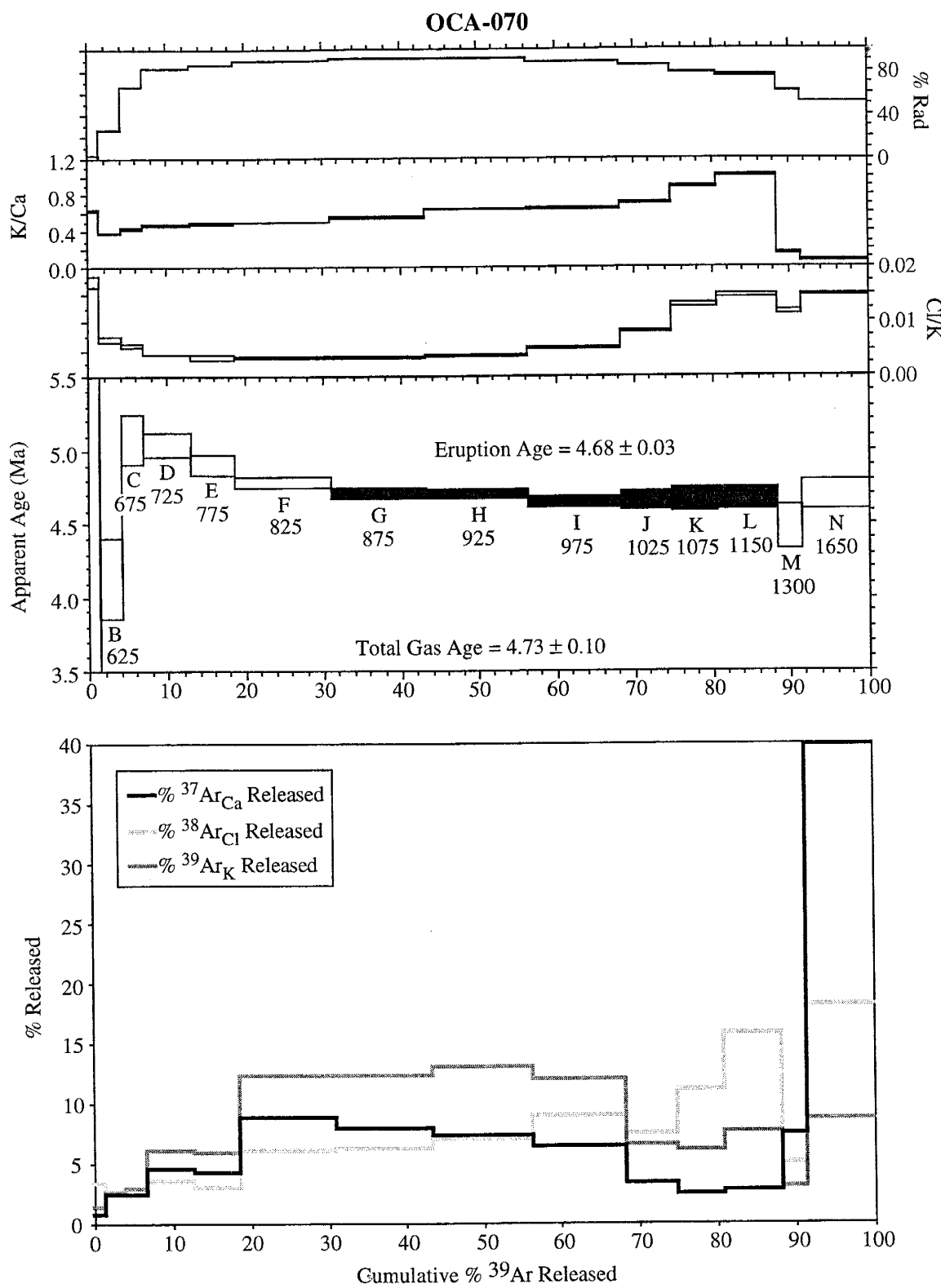


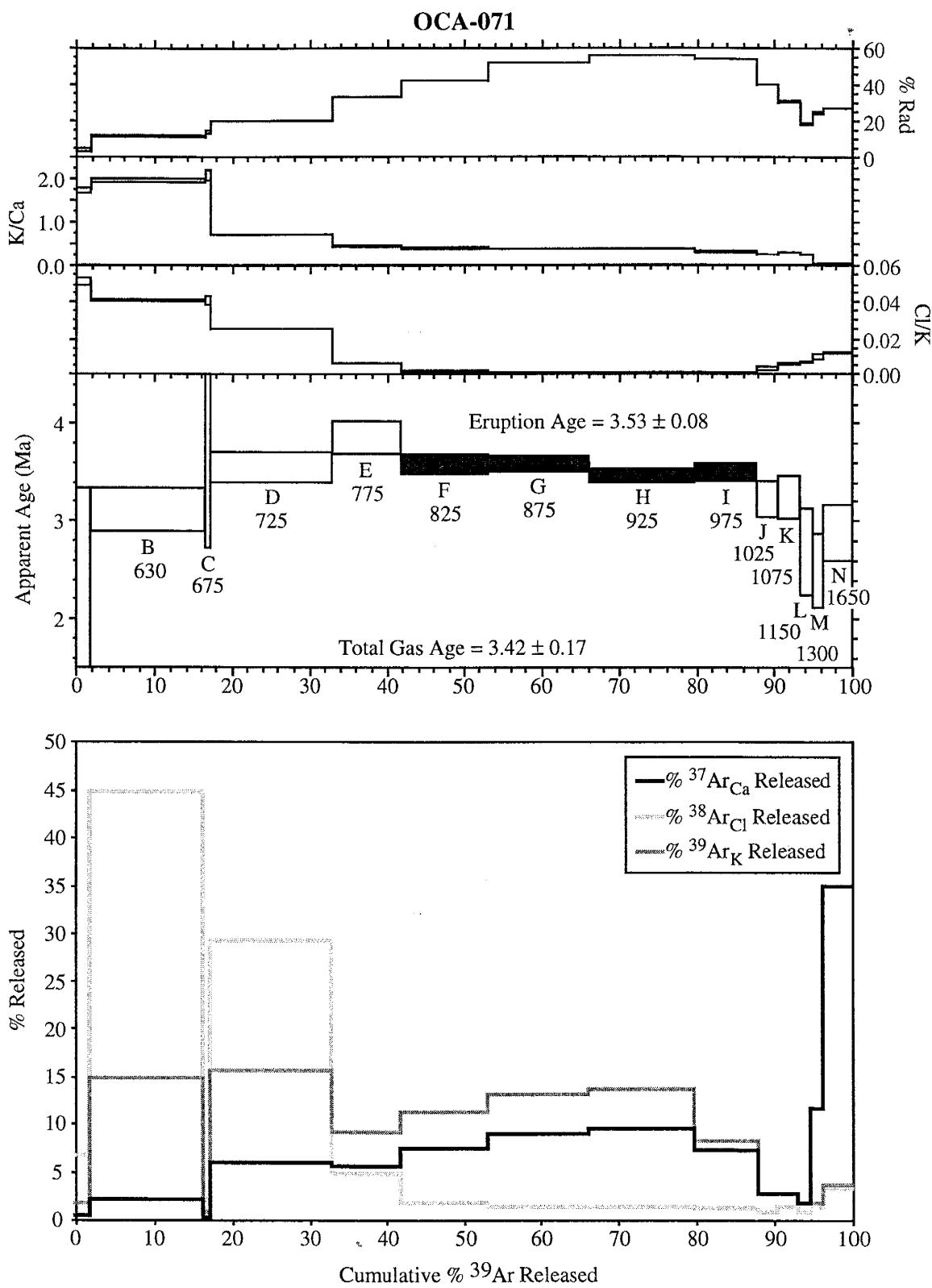


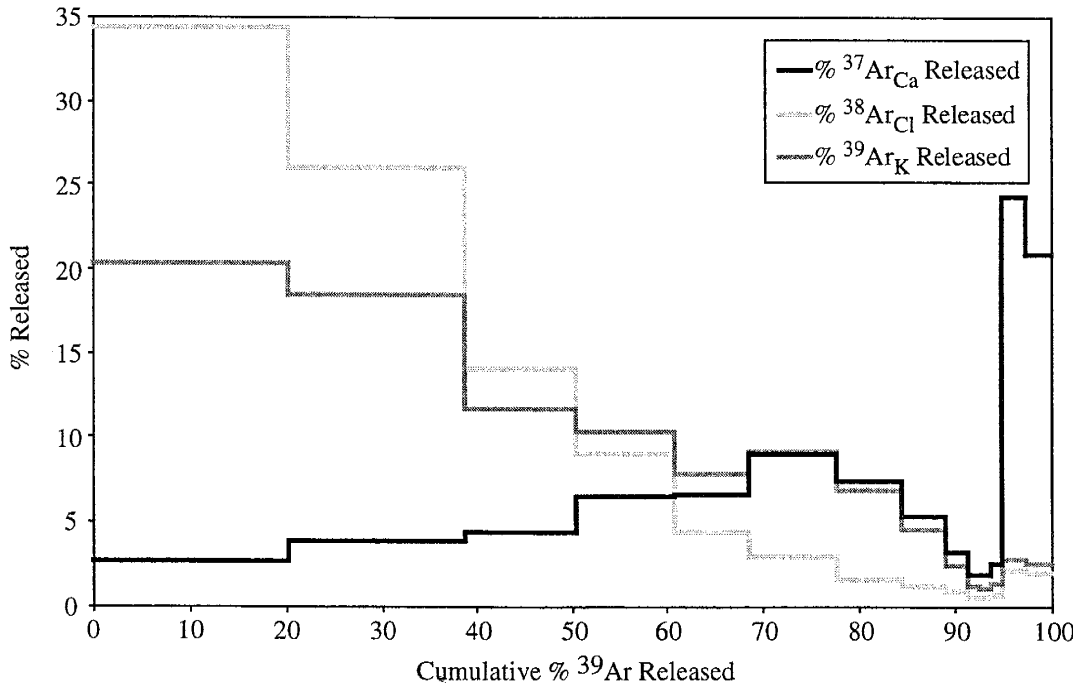
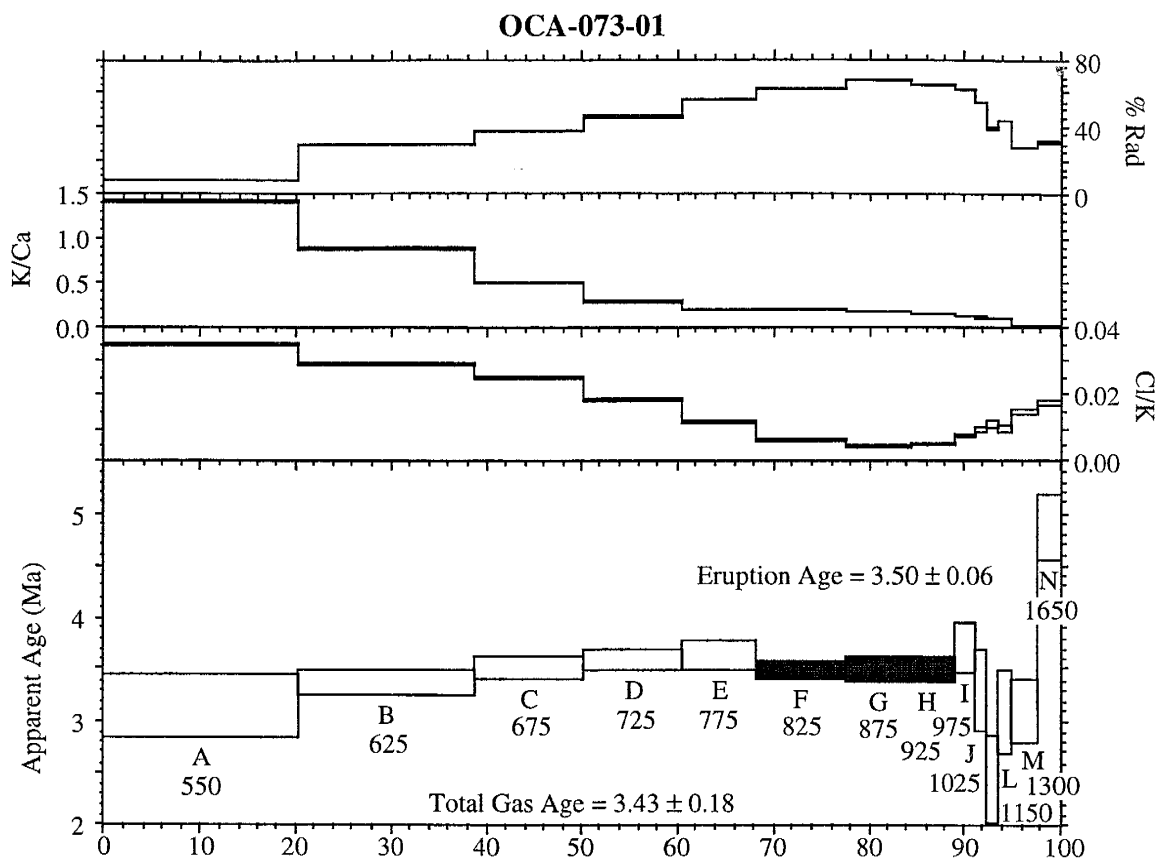


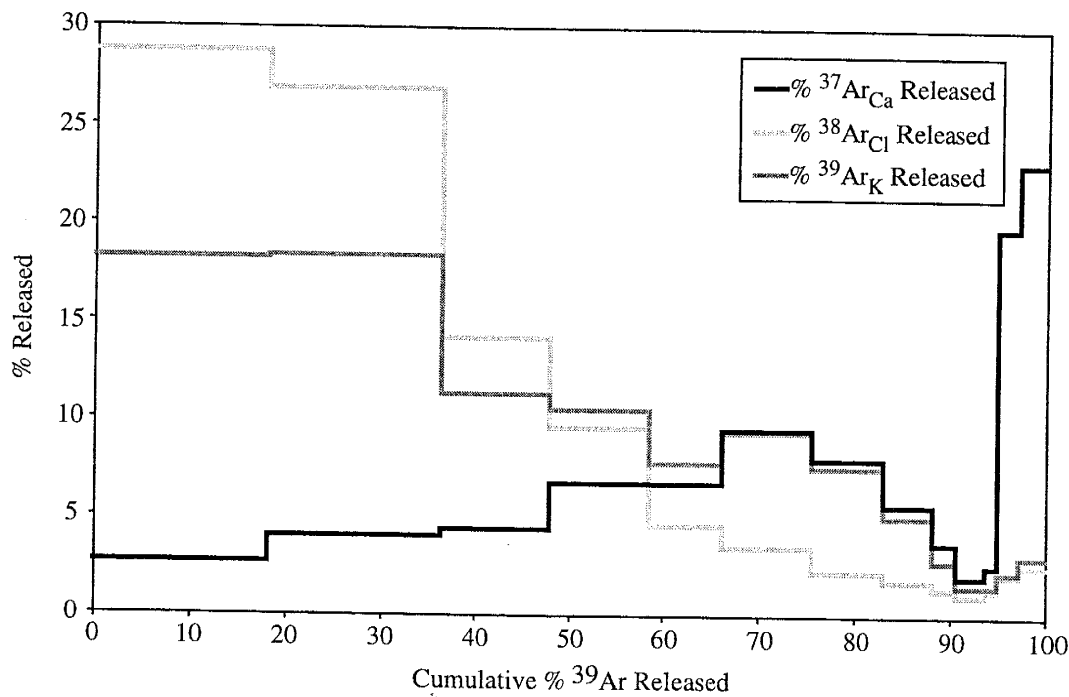
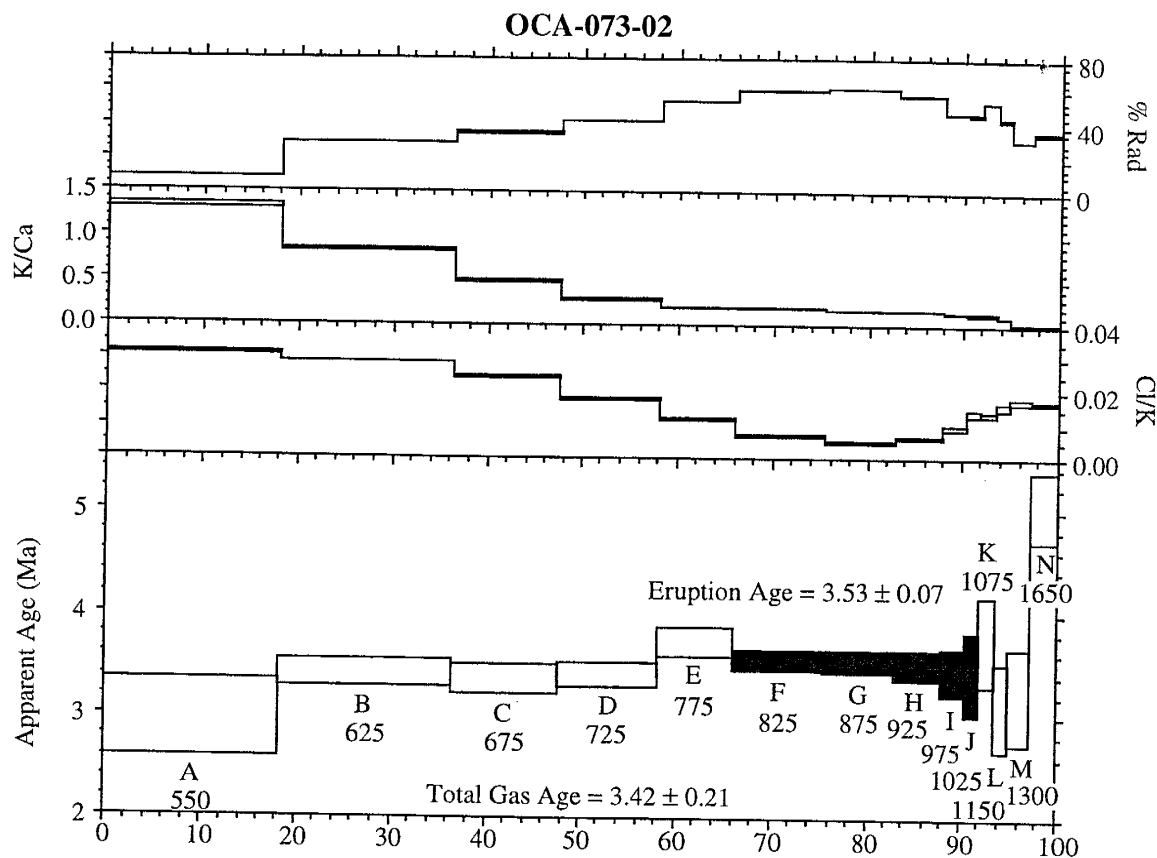


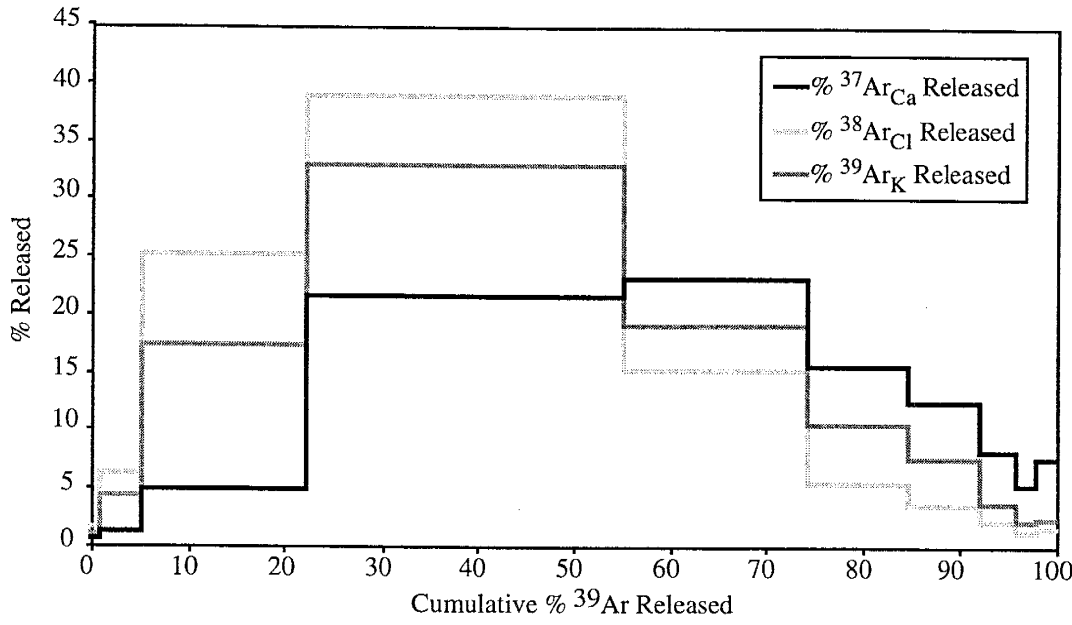
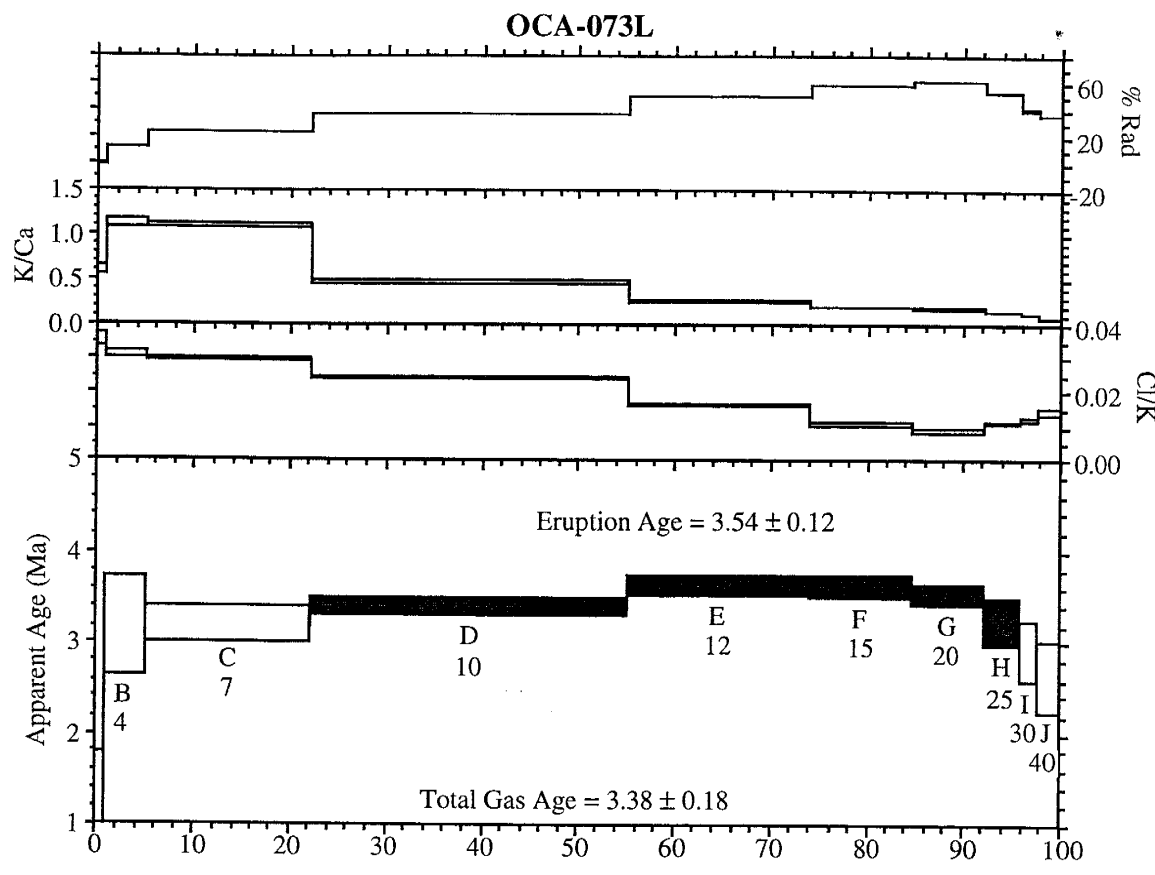


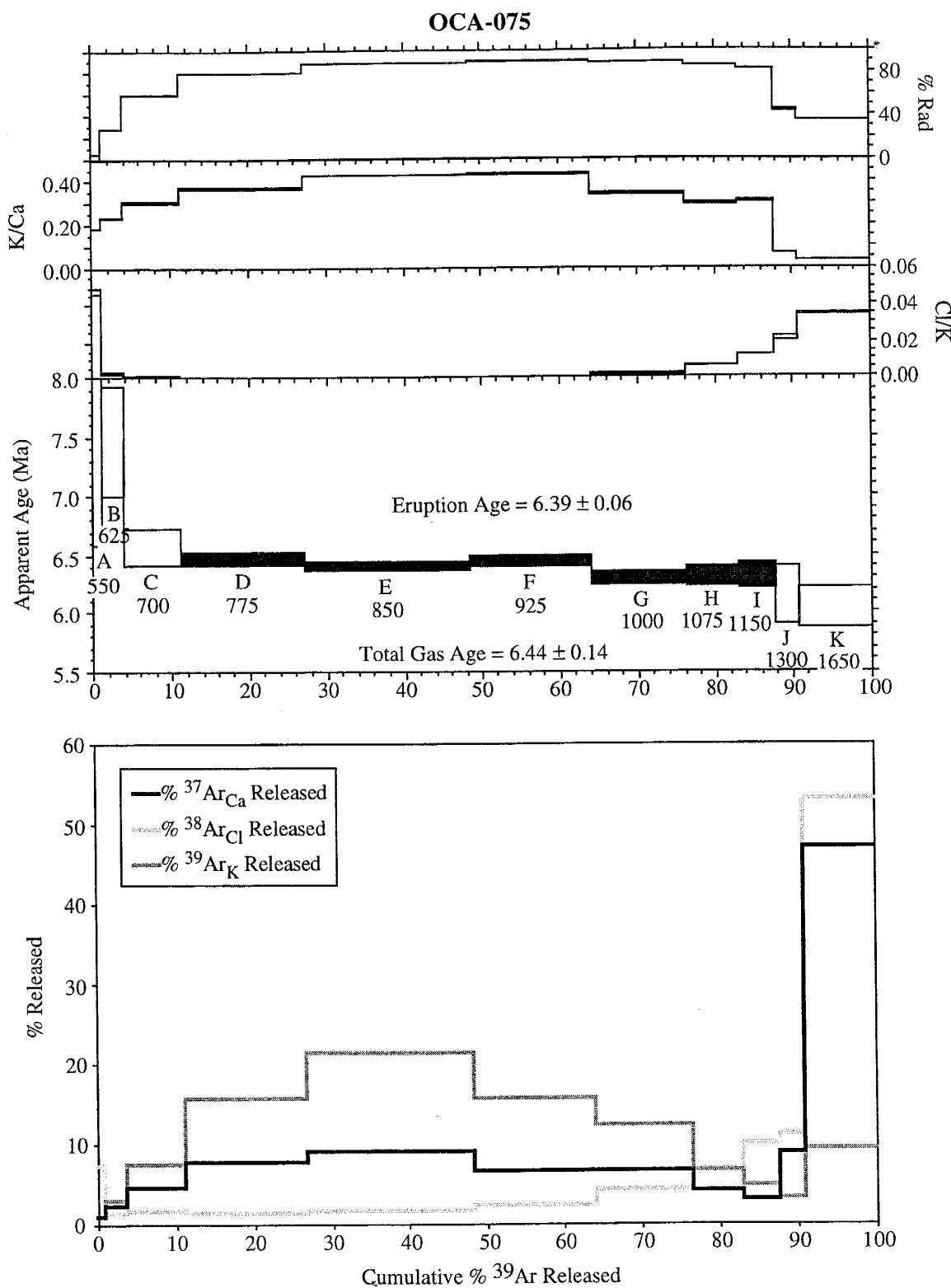


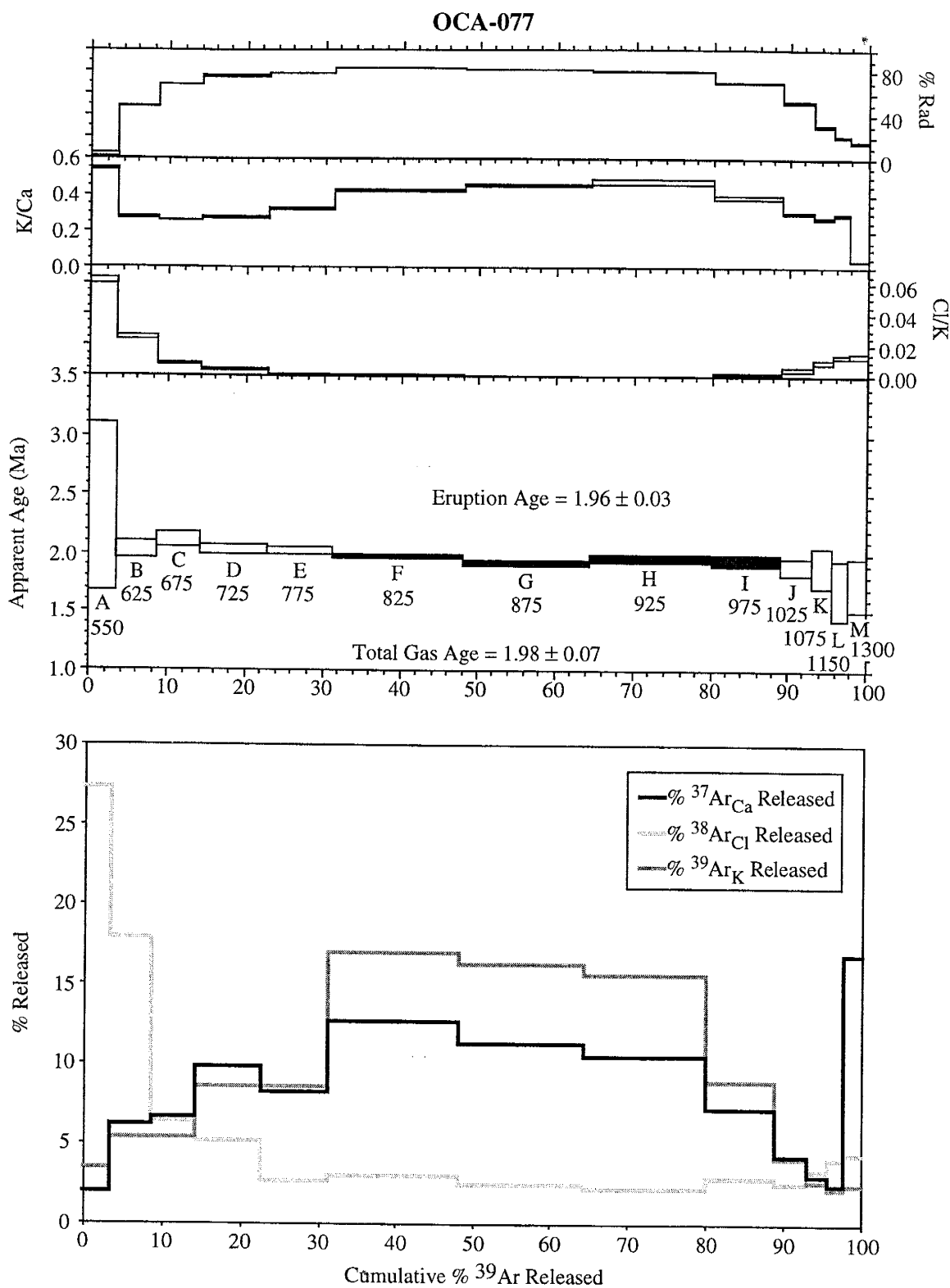


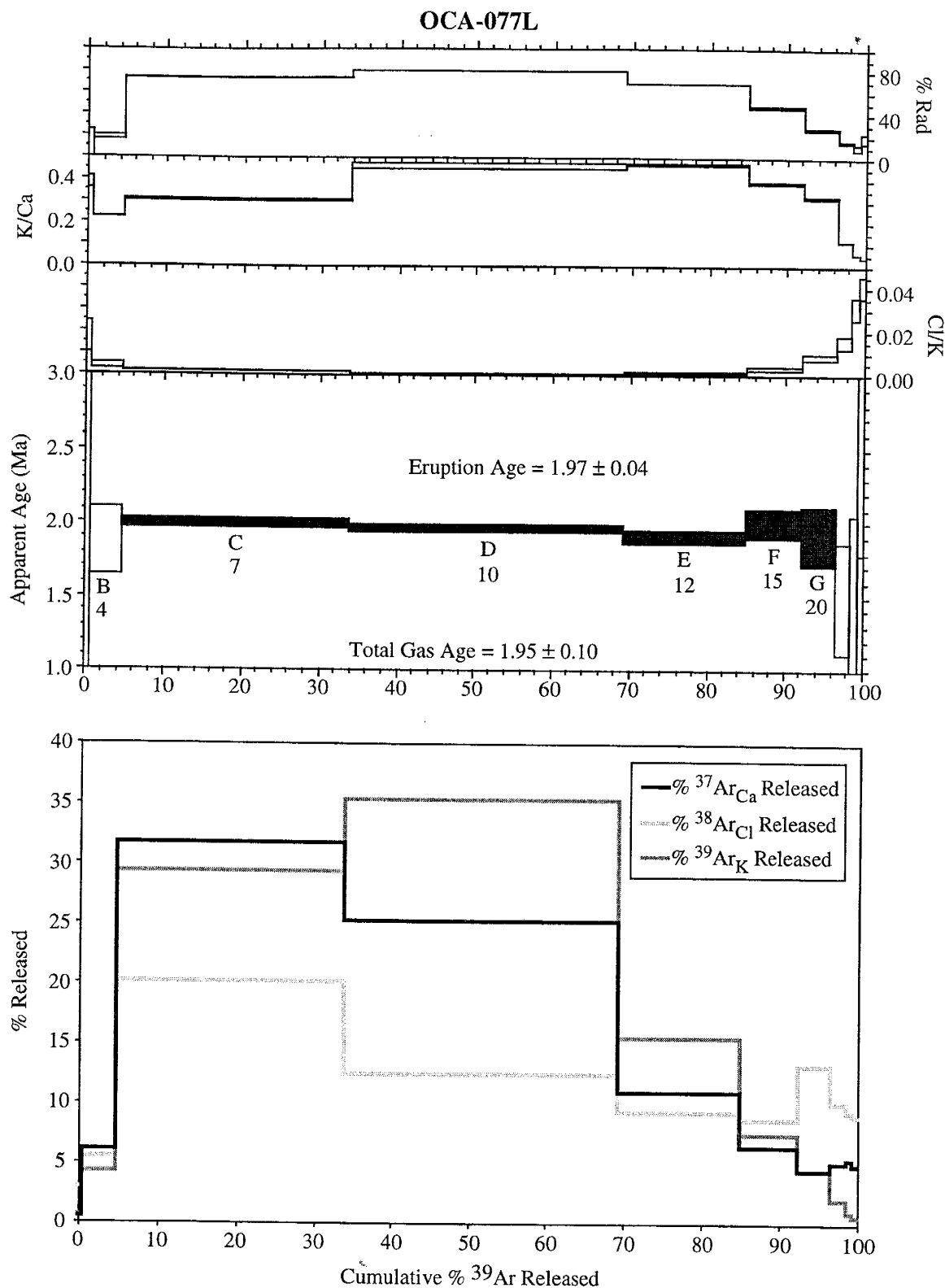




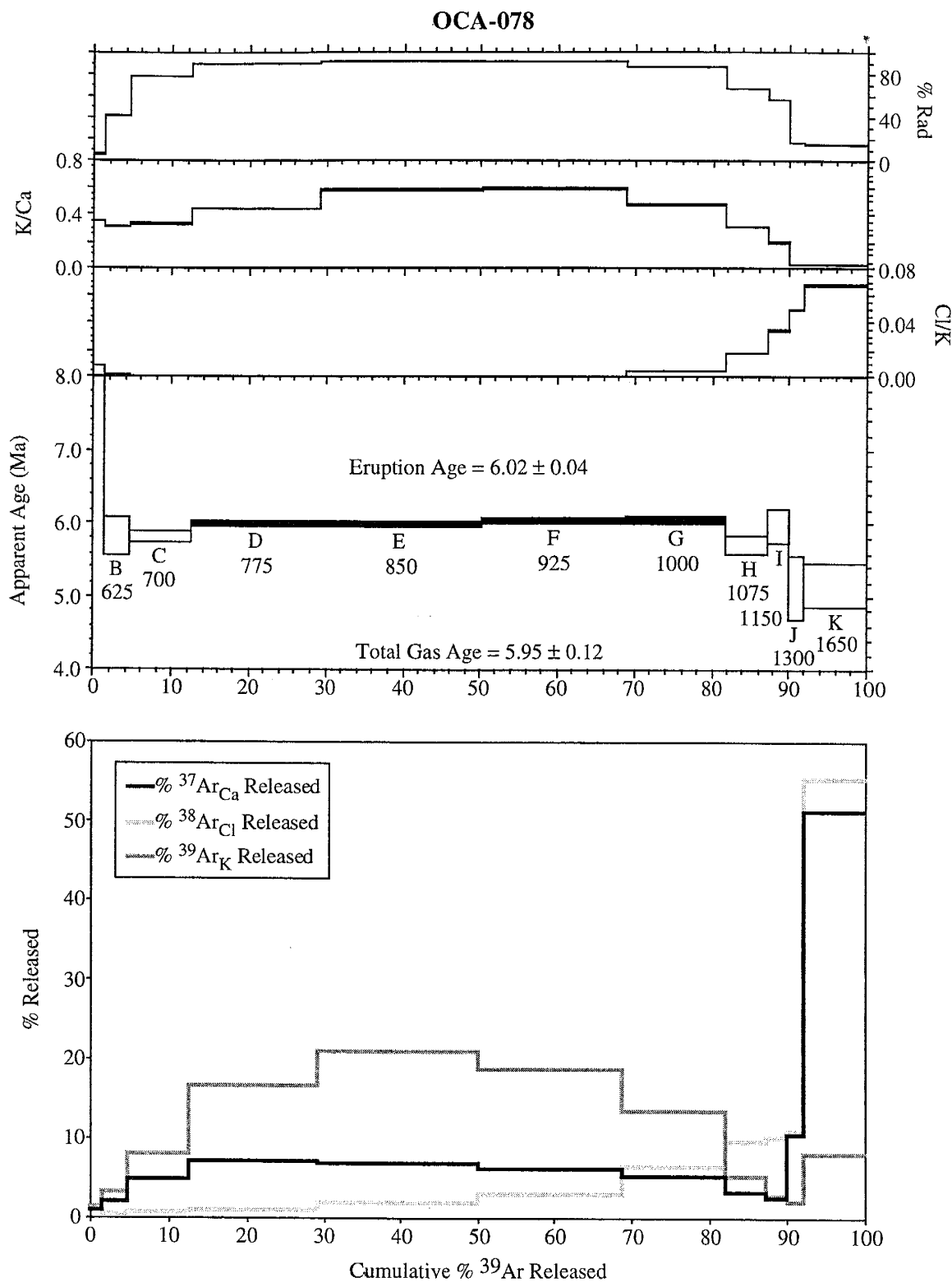


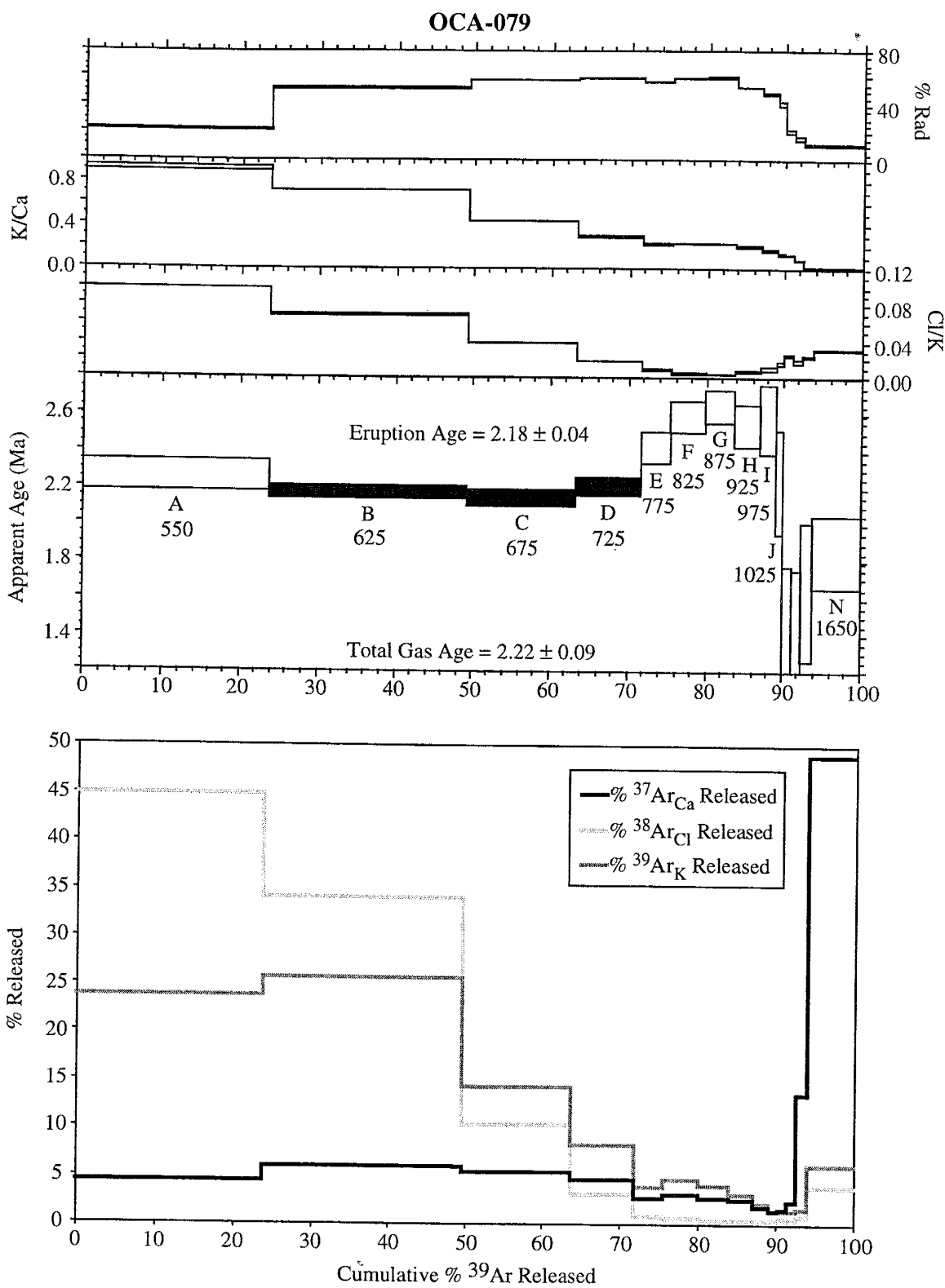


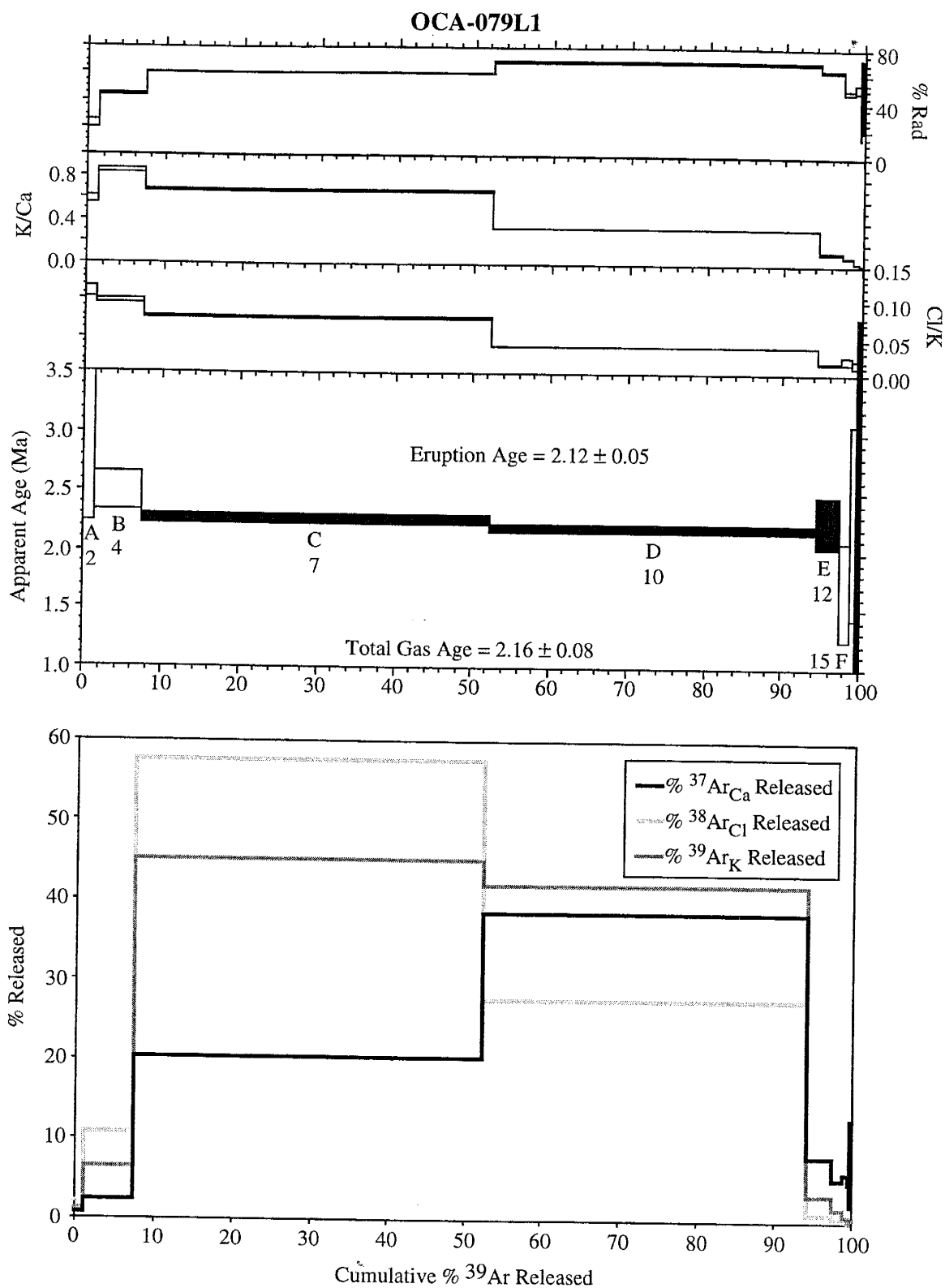


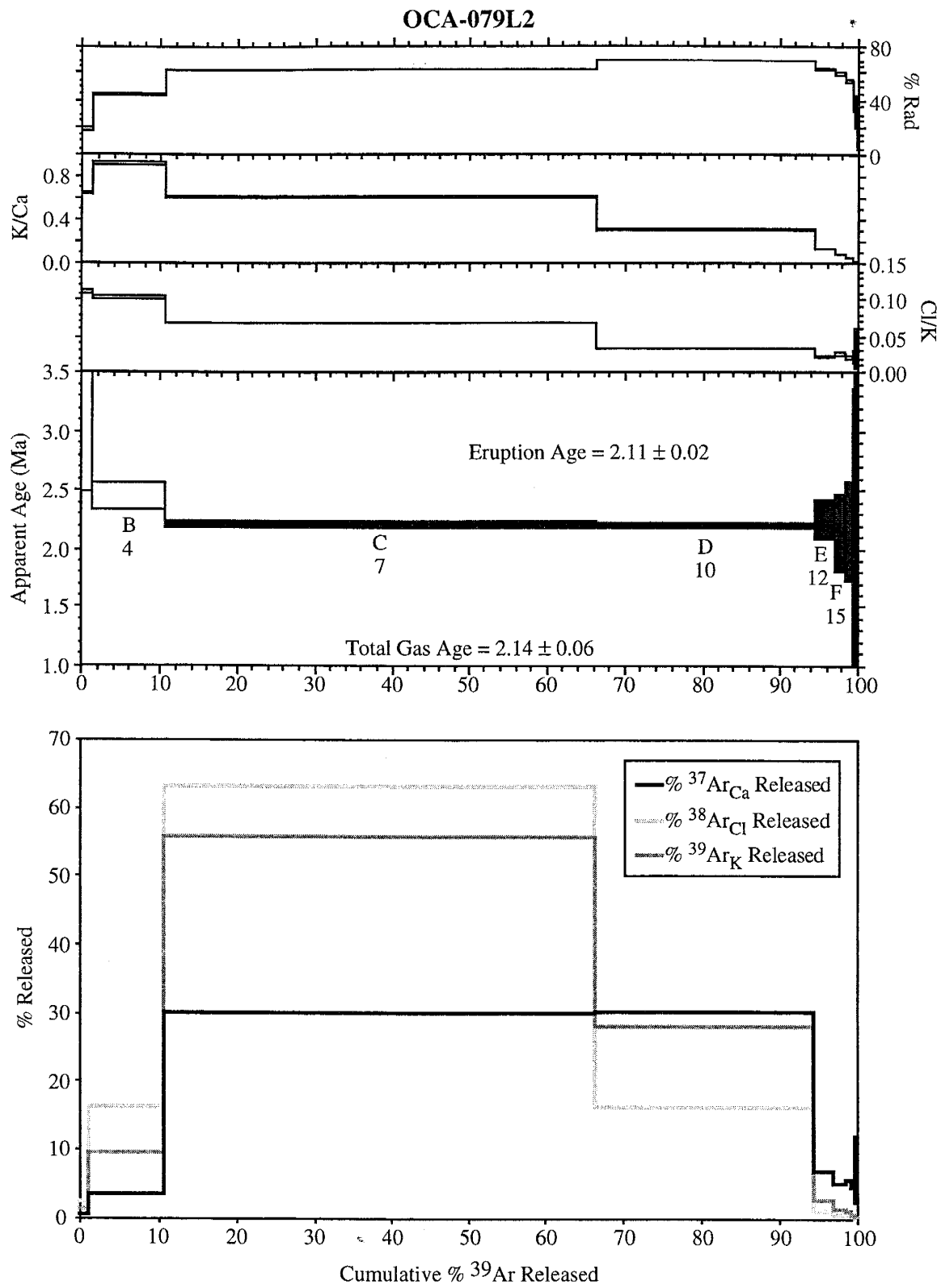


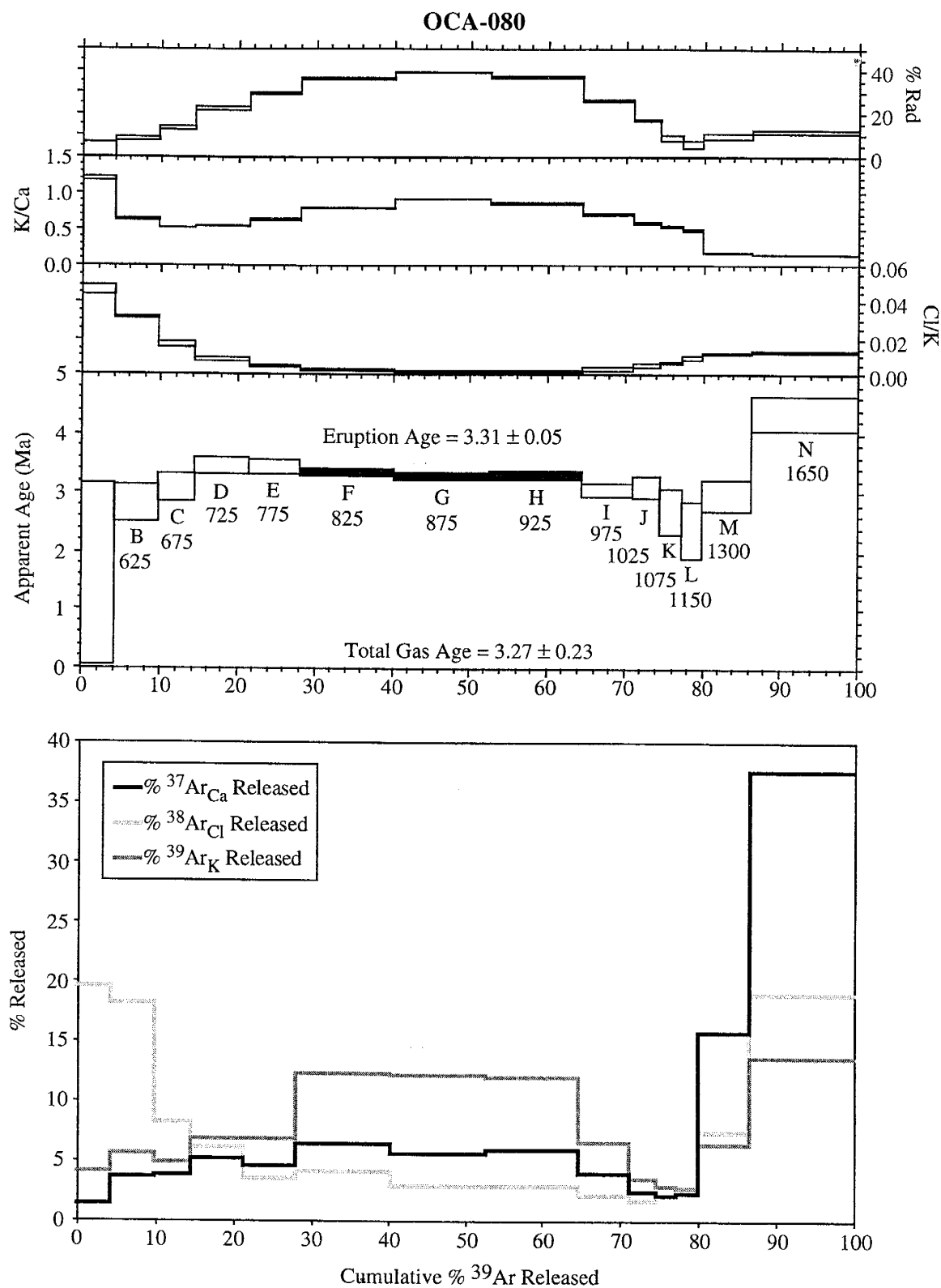
B-78

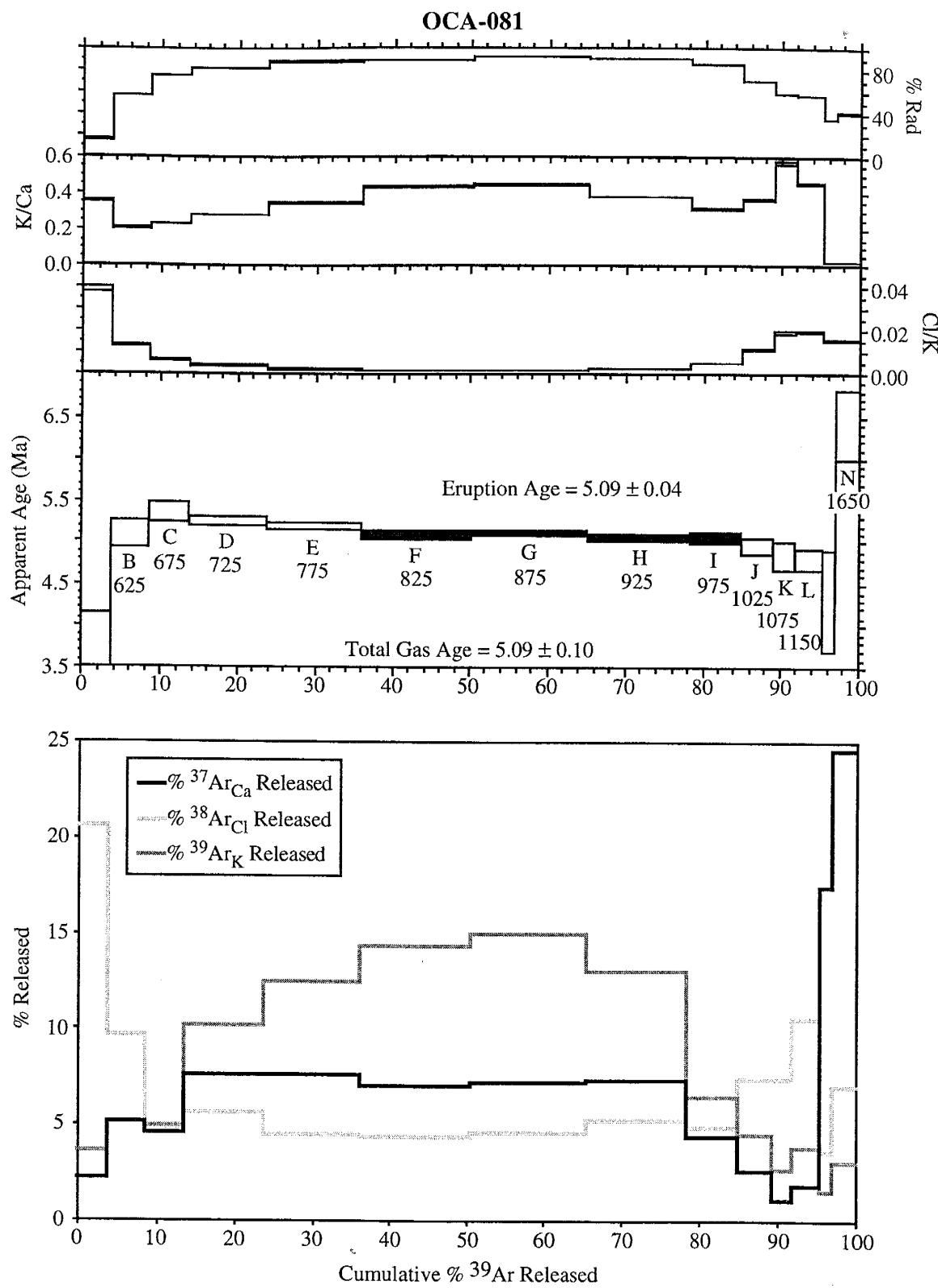


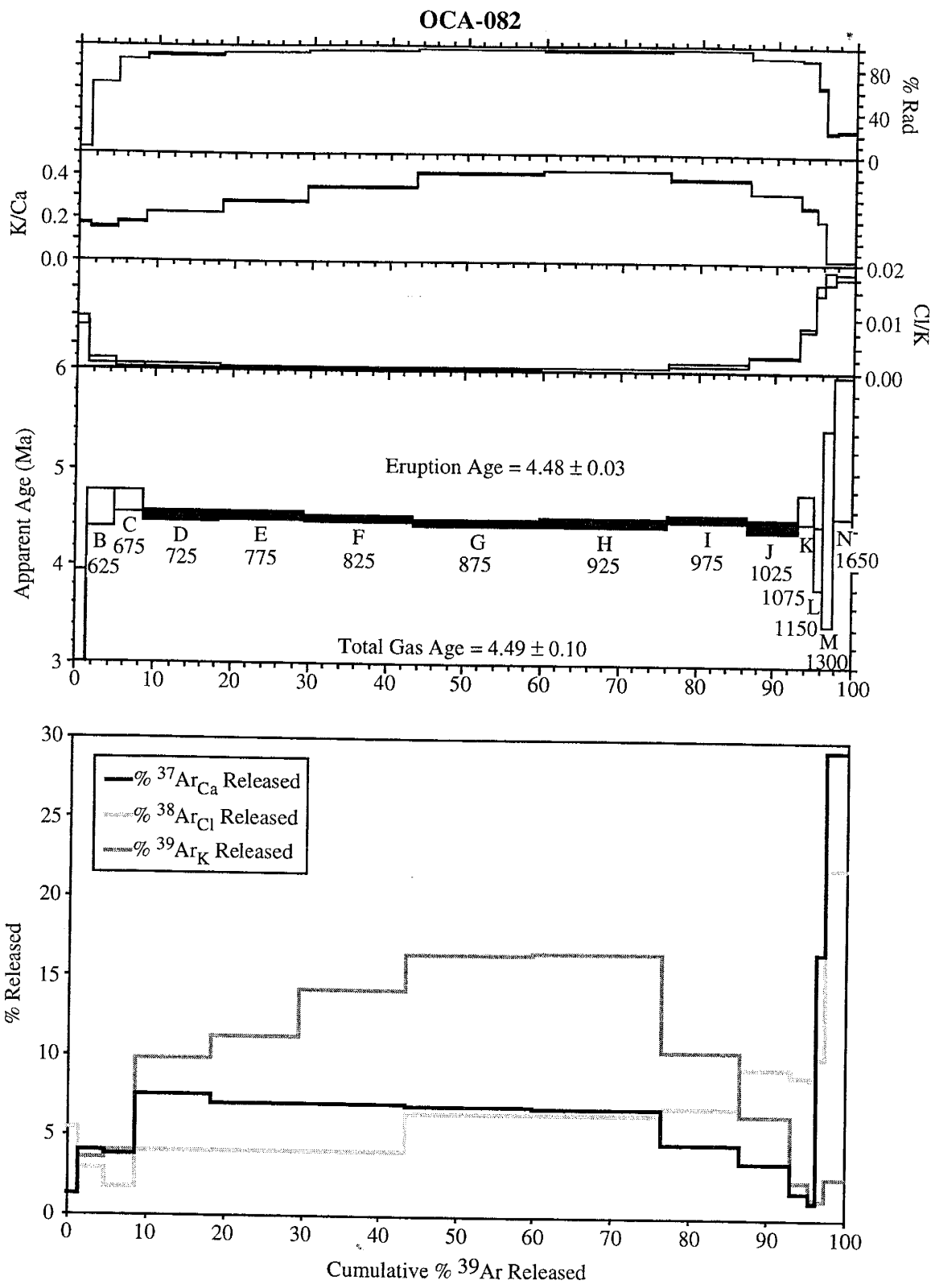


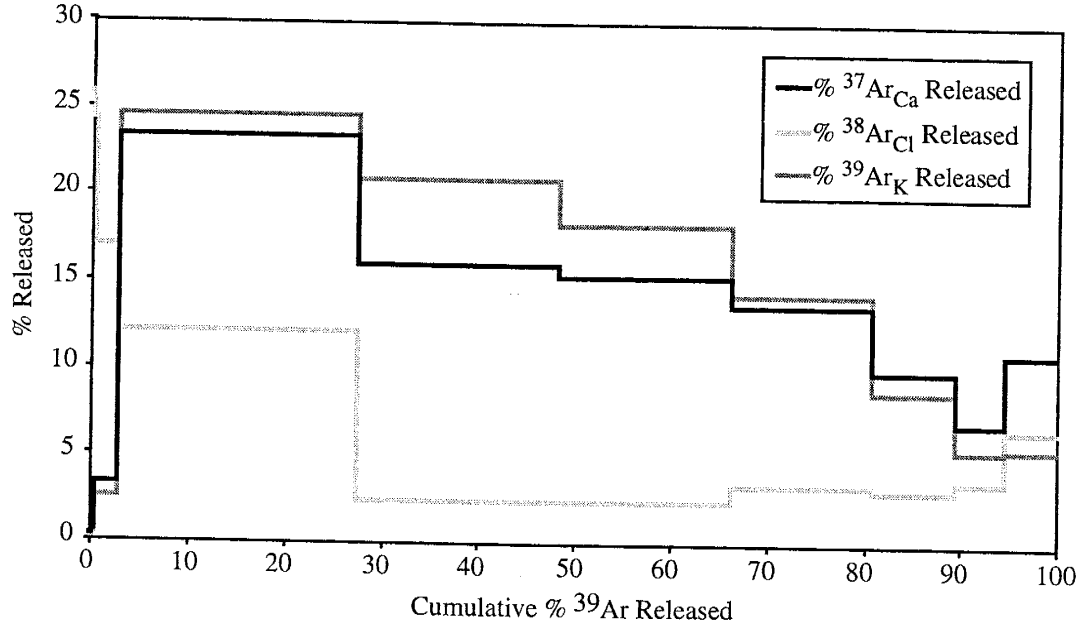
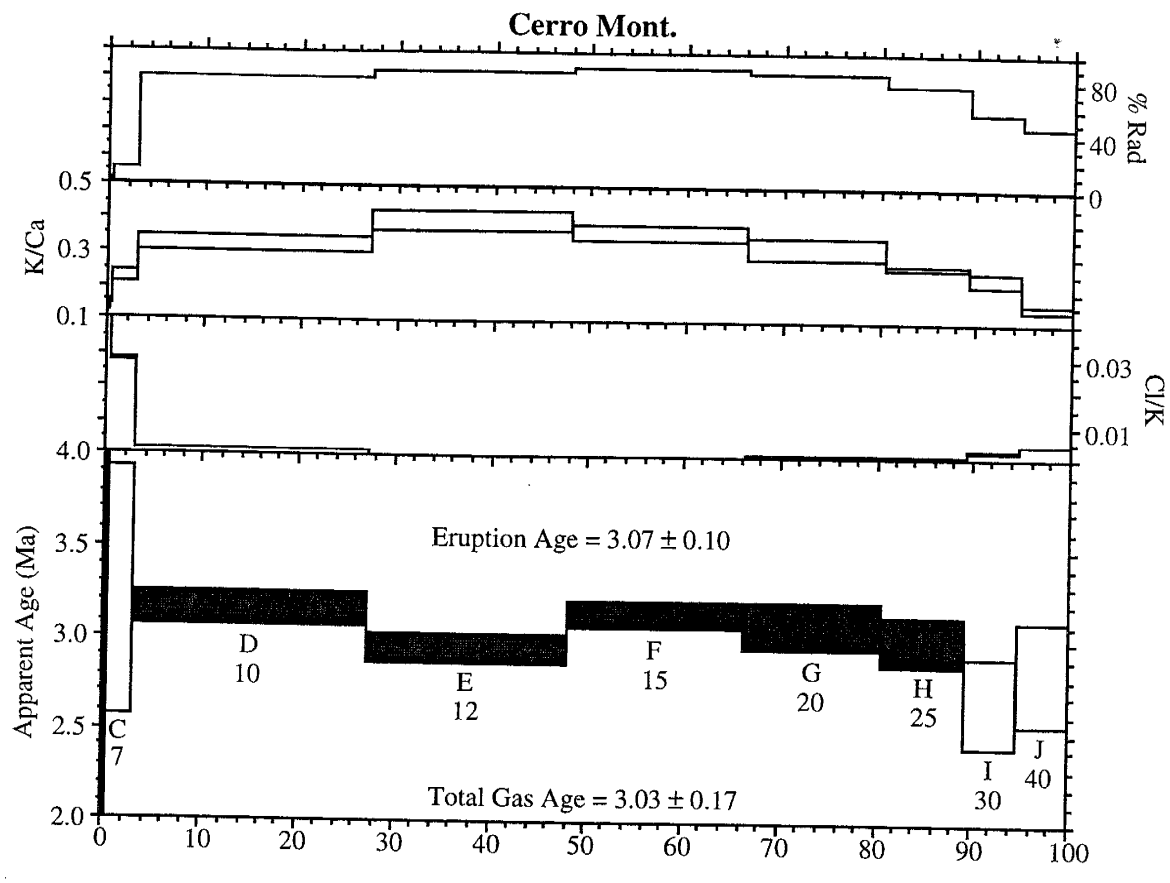












Appendix C: Values Used In The Calculation Of Volumes Erupted

Appendix C contains the values used to calculate the volume erupted for each flow unit. The areas of individual flows were calculated using the program ArcView 3.2. Where younger flows overlie older flows, the area of the older flows underlying the younger flows were included in the calculation as well as an estimate of the amount eroded. For a given flow unit, the areas of each flow were added together. The areas of each flow unit were then converted to a percent of the total area. Volume estimates were calculated by multiplying the area % of each flow unit by the total volume erupted, 90 km³ (from Neilsen and Dungan, 1985).

Appendix C: Values Used In The Calculation of Volumes Erupted

Flow unit (Ma)	Area (km ²)	Volume (km ³)	Vol. % Erupted
0.67-0.95	42.23	2.0	2.2
1.55-1.59	146.85	6.8	7.6
1.78-1.82	3.39	0.2	0.2
1.93-1.99	35.05	1.6	1.8
2.18-2.59	92.41	4.3	4.8
2.85-3.36	772.69	36	39.7
3.48-3.54	60.29	2.8	3.1
4.35-5.13	613.36	28	31.5
5.62-5.77	24.85	1.2	1.3
6.01-6.07	56.01	2.6	2.9
6.34-6.61	52.44	2.4	2.7
7.05-7.11	3.08	0.1	0.2
8.13-8.21	41.46	1.9	2.1

Appendix D: Values Used In Erosion Rate Calculations

Appendix D contains the elevation and ages used in the erosion rate calculations. The minimum erosion rates were calculated by dividing the elevation difference between two mesas, or a mesa and the present day valley bottom elevation adjacent to the mesa, by their age difference. The elevations were estimated off of 7.5 min topographic maps with 20 ft contour intervals. The elevations were then converted to meters. Valley bottom elevations were chosen by the lowest point within the valley adjacent to where the mesa elevation was determined. The analytical uncertainty of the eruption ages were not used in the calculations. Several ages and elevations exist for Charette Mesa, therefore, the elevation and ages for samples closest to the area of interest were used in the calculation. The median of the eruption ages for samples OCA-008 and OCA-009 were used for the eruption age of Charette Mesa in the Las Mesas Del Conjelon area. On Figure 18, the lines between the calculated erosion rates and the map point to the general area where the elevations were measured.

Appendix D: Values Used in Erosion Rate Calculations

Locations	Elevation (m)	Δ Elevation (m)	Age (Ma)	Δ Age (Ma)	Erosion Rate (m/Ma)
Urraca Mesa - Present	2539-2134	405	4.51-0	4.51	90
Rayado Mesa - Present	2256-1905	351	4.42-0	4.42	79
Apache (West) Mesa - Apache Mesa	2347-2210	137	5.72-4.59	1.13	121
Apache Mesa - Rivera Mesa	2210-2103	107	4.59-3.51	1.08	99
Apache Mesa - Charette Mesa	2210-2054	156	4.59-3.20	1.39	112
Charette Mesa - Present	2054-1905	149	3.20-0	3.20	47
Rivera Mesa - Present	2103-1905	198	3.51-0	3.51	56
Las Mesas Del Conjelon - Charette Mesa	2103-1920	183	6.04-2.94	3.10	59
Charette Mesa - OCA-057 Mesa	1932-1902	30	2.94-2.20	0.74	41
OCA-057 Mesa - Present	1902-1881	21	2.20-0	2.20	10
OCA-61 Mesa - Present	1890-1872	18	2.26-0	2.26	8
Black Mesa - OCA-033 Mesa	2286-2249	37	4.60-2.31	2.29	16
OCA-033 Mesa - Present	2249-2233	16	2.31-0	2.31	7

This Thesis is accepted on behalf of the faculty
of the Institute by the following committee:

William C McIntosh
Academic Adviser

William C McIntosh
Research Advisor

Philip R Kyle
Committee Member

John D. W.
Committee Member

Mark Chapman
Committee Member

8/24/00
Date